SAPIENZA
UNIVERSITÀ DI ROMA

Ph.D. PROGRAM IN PHARMACEUTICAL SCIENCES

XXXVI Cycle

Liposomes as a versatile tool for the delivery of natural antimicrobials

PhD Candidate
Giuliana Prevete

Tutor
Prof. Claudio Villani

Supervisor
Dr. Marco Mazzonna

Coordinator
Prof. Franco Mazzei

Academic year 2022/2023

TABLE OF CONTENTS

ABSTRACT

Antibiotics are indispensable pharmaceuticals to treat bacterial infections. However, they have been overused in clinic, agriculture and animal production setting, generating a strong selection pressure over bacterial species. This has led to the emergence and dissemination of antimicrobial resistant strains among humans, animals and the environment, culminating in the rise of the global health problem of antibiotic resistance, which requires immediate and urgent actions to be fought. Consequently, significant funding has been allocated for the development of new and effective strategies to expand the panel of therapeutic tools already available. Nevertheless, the development of new antibiotic drugs is a laborious process which cannot keep up with the rising rate of drug resistant bacteria.

In this perspective, an appealing alternative to the discovery of new therapies could be the use of bioactive compounds derived from biomass waste, thus representing an example of circular economy in which biomass waste are converted in valuable products, minimizing waste production. Among all bioactive compounds recoverable, polyphenols exhibit beneficial effects on human well-being, such as antimicrobial activity against both *Gram*-positive and *Gram*-negative bacteria.

Nevertheless, in some cases the polyphenols potential therapeutic use is limited by their adverse pharmacokinetic features resulting in a very low absorption rate after systemic administration in human body. To overcome these limitations, many engineered nanoparticles can be applied as drug delivery systems due to the possibility of engineering them for multiple purposes. Among all the nanoparticles developed in the last decades, liposomes are the most widely used drug delivery systems thanks to their versatility, low toxicity, biocompatibility and biodegradability.

In this scenario, this work of thesis aimed to develop liposomes as delivery systems of natural antimicrobial polyphenols, both as single biocompound and as phytocomplexes, thus improving their pharmacokinetic profiles and enhancing their activity against target bacteria examined.

Polyphenols investigated in this thesis were obtained from agri-food by-products and waste, such as olive leaves and orange peels.

Liposomes were formulated with natural phosphocholines (DMPC, DPPC, DOPC) and cholesterol, in presence or absence of synthetic cationic amphiphiles, which should enhance the interaction between liposomes developed and target bacteria strains.

In particular, two different cationic amphiphiles were used: 1) a galactosylated amphiphile (GLT1) characterized by the presence of a galactose residue, which should enhance the interactions toward lectins and sugar-protein transporters expressed on bacterial membrane; 2) the *allyl-hexadecyl-*

dimethyl-ammonium iodide, characterized by a polar head composed by a quaternary nitrogen and a hydrophobic alkyl chain, which should be able to enhance the electrostatic interaction between cationic liposomes and negatively charged bacteria.

The overall composition of the formulations was modulated to obtain vesicles with dimensions around 100 nm, a good polydispersity index related to the homogeneity of the systems, variable ζ-potential values, good stability with respect to aggregation phenomena and optimal entrapment efficiencies of polyphenols inside the liposomes.

The antimicrobial activity of polyphenols, free and entrapped in liposomes, was examined *in vitro* against different bacteria pathogens, both *Gram*-positive and *Gram*-negative strains, such as *Staphylococcus aureus*, *Enterococcus faecalis*, *Bacillus subtilis*, *Escherichia coli*, *Pseudomonas aeruginosa* and *Klebsiella oxytoca*.

1. Introduction

1.1 Antimicrobial Resistance: the "Silent Pandemic" of 21st century

Since their discovery, antibiotics have been one of the most effective drug treatments in medical history. Their introduction has helped to manage and greatly reduce mortality rate caused by infectious diseases, previously the leading cause of death in humans.[1] From the discovery of penicillin by Alexander Fleming in 1929, human life expectancy has increased by an average of 23 years thanks to the "golden era" of antibiotics,[2] which led to the development of more than 150 drugs. However, because of the inadequate regulations, usage imprecisions, awareness deficiency in best practices and inept therapeutic use, antimicrobials have been overused in clinic, agriculture and animal production setting, generating a strong selection pressure over bacteria species. This has led to the emergence and spread of antimicrobial resistant strains among humans, animals and the environment, culminating in the increase of the global health problem of antimicrobial resistance (AMR).

For instance, the agri-food field alone has a consistent contribution to the spread of AMR because of a massive use of antibiotics in livestock production for the treatment of disease and to promote the growth of animals,[3] as well as for the prophylactic treatment of fruit trees[4] and for the management of infectious disease in aquaculture.[5] In each of these situations the antibiotics effect is extended beyond the site of use: antimicrobials applied in animal farming operations leach into waterways and groundwater; antibiotics sprayed on plants can drift aerially; in many aquaculture settings antibiotics diffuse into the water surrounding the pens (**Figure 1**).

Figure 1. How Antimicrobial Resistance spreads.

AMR currently represents one of the major global public health threats of the 21st century due to the rapid growth of AMR infections rate and the lack of new antimicrobial medications being introduced to counteract this issue.[6,7] AMR is widely referred to as the "Silent Pandemic" and cannot be considered a future situation but a problem for which immediate and urgent actions are needed.[8] In fact, without preventative measures, it is estimated that by 2050 AMR could probably become the world's primary cause of death with the forecast of 10 million deaths per year.[9]

In response to AMR, several global health organizations and governments have taken action to combat this issue according to a unified global approach. "*One Health*" (**Figure 2**) is a multisectoral approach elaborated and proposed by World Health Organization (WHO) in collaboration with the Food and Agriculture Organization (FAO) and the World Organization of Animal Health (WOAH), embracing the concept that there is a clear connection between the health of both humans and animals and the shared surrounding environment,[10] with the aim to ensure effective actions from all sectors in reducing the risks of AMR.

Currently, the main coordinated activities proposed consist only in the prudent use of antibiotics under the guidelines of antimicrobial stewardship, in collecting epidemiological data and in minimizing the use of antibiotics in food animals and personal hygiene.[11] Success will involve individuals, communities and nations, all working together to ensure that the world continues to possess a sufficient armamentarium of effective antimicrobials that can sustain human and animal health, both now and in the future.[12]

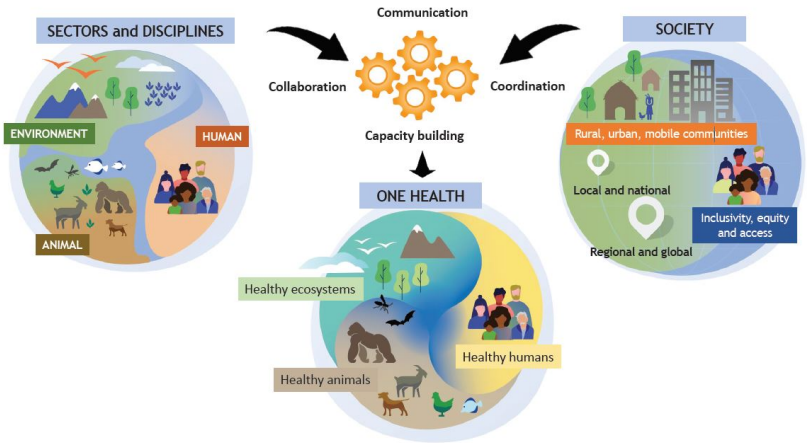

Figure 2. *One Health* multisectoral approach to fight Antimicrobial Resistance.

1.2. Mechanisms of antimicrobial resistance

Bacteria have demonstrated a great flexibility because of their genomic plasticity and capacity to exchange genetic information among very different species, providing them an endless adaptability. Thus, it should not be strange that these microorganisms have developed mechanisms to resist any weapon that humans develop against them: microorganisms adapt to antibiotics as easily as they adapt to a new environmental change.[13]

The antimicrobial resistance induced by bacteria can be broadly classified as[14]:

1. *Intrinsic resistance*. Specific bacterial genera or species have unique structural/functional characteristics providing resistance to certain antibiotics through the reduced outer membrane permeability, the activity of efflux pumps or the production of antibiotic-inactivating enzymes.[15]
2. *Acquired resistance*. Bacteria can develop resistance against antibiotics by receiving genetic code from other bacterial strains according to transformation, transposition and conjugation processes. The acquisition may be temporary or permanent.[16]

The main mechanisms of antimicrobial resistance, intrinsic or acquired, can be summarized into four categories (**Figure 3**):

a) *Limiting uptake of drug*. There is a natural difference in the ability of *Gram*-positive and *Gram*-negative bacteria to limit the uptake of antimicrobial agents. Bacterial lipopolysaccharide (LPS) is the major outer surface membrane components in all *Gram*-negative bacteria, whose structure and function provides a barrier to certain types of molecules, giving them an innate resistance to a large group of antimicrobial agents.[17] On the other hand, although *Gram*-positive bacteria do not possess an outer membrane and restricting drug access is not as prevalent, however some of these strains, such as *Staphylococcus aureus*, have recently developed resistance through the production of a thickened cell wall which makes difficult for the drug to enter the cell.[18]

b) *Drug target mutation*. There are multiple components in bacteria cell that may be targets of antimicrobial agents, which can be modified by bacteria themselves to enable resistance to those drugs. For example, one mechanism of resistance to the β-lactam antibiotics, used

almost exclusively by *Gram*-positive bacteria, is via alterations in the structure and/or number of penicillin-binding proteins which decrease or totally inhibit the drug binding.[19] Instead, *Gram*-negative bacteria thanks to thick LPS layer have intrinsic resistance to all the drugs acting on the cell wall synthesis.[20] Resistance to drugs targeting the ribosomal subunits may occur via ribosomal mutation, ribosomal subunit methylation or ribosomal protection. These resistance mechanisms interfere with the drug ability to bind the ribosome and therefore preventing the alteration of bacteria protein synthesis induced by the drug .[21] About drugs able to target nucleic acid synthesis, resistance is via mutations in DNA gyrase (*Gram*-negative bacteria) or topoisomerase IV (*Gram*-positive bacteria), which decrease or eliminate the ability of drugs to bind these components.[22]

c) *Drug inactivation*. Bacteria can inactivate antibiotics by chemical degradation or by transfer of a chemical group to the drug. There are many transferases that have been identified in both *Gram*-positive and *Gram*-negative bacteria, which commonly transfer acetyl, phosphoryl or adenyl groups.

d) *Drug efflux*. Bacteria possess chromosomally encoded genes for efflux pumps. The efflux pumps function is primarily to rid the bacterial cell of toxic substances. They are classified based on structure and energy source used and are involved in the transport of substrates across the cytoplasmatic membrane.[23,24] Most of efflux pumps are expressed constitutively, while other are induced or overexpressed under environmental stimuli or when a suitable substrate is present, such as after the administration of an antimicrobial drug.

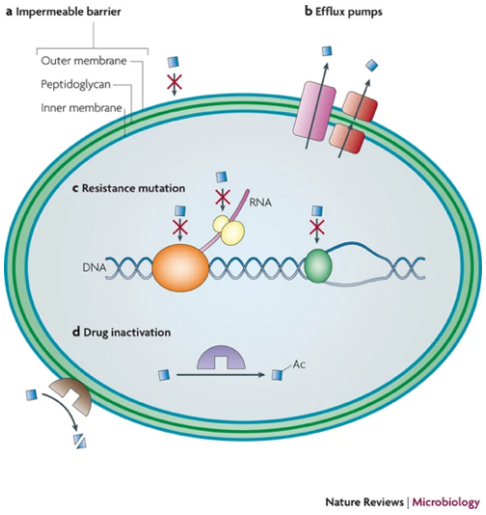

Figure 3. General mechanisms of Antimicrobial Resistance.

1.3. Planktonic and biofilm forming bacteria

The emergence, spread and dissemination of the global phenomenon of AMR must be ascribed to bacteria existing both as free-floating planktonic cells and clusters of bacteria forming biofilm. In particular, bacteria inside biofilm are at least 500 times much more resistance to antimicrobial agents than planktonic forms, since bacteria that are susceptible to antibiotics can develop resistance after forming biofilm.[25]

Bacterial biofilm can be described as a microbially derived sessile community characterized by cells which are irreversibly attached to a surface or to each other and are inserted in a matrix of extracellular polymeric substances (EPS), produced by bacteria themselves, exhibiting an altered phenotype in terms of growth rate and gene transcription.

The cellular biodiversity of bacteria within a biofilm is a crucial aspect making the pharmacological treatment too complicated in case of infection. In fact, in the innermost area of bacterial biofilm, where oxygen levels are very low and nutrients less available, are placed only the microorganisms able to survive in those stressful conditions, whilst in the external area are located bacterial species with different genotypic and phenotypic characteristics. Moreover, inside a biofilm are present the so-called "persister cells" with a down-regulated metabolic activity, these, despite being sensitive to antibiotics, are not reachable by the immune system cells and antimicrobials because enclosed in the deepest layers.[26]

Therefore, this multicellular environment is beneficial for bacteria survival for extended periods and is considered a self-defense measure to safeguard themselves against unfavorable conditions, thus conferring to the embedded cells unique properties not identified in planktonic cells.

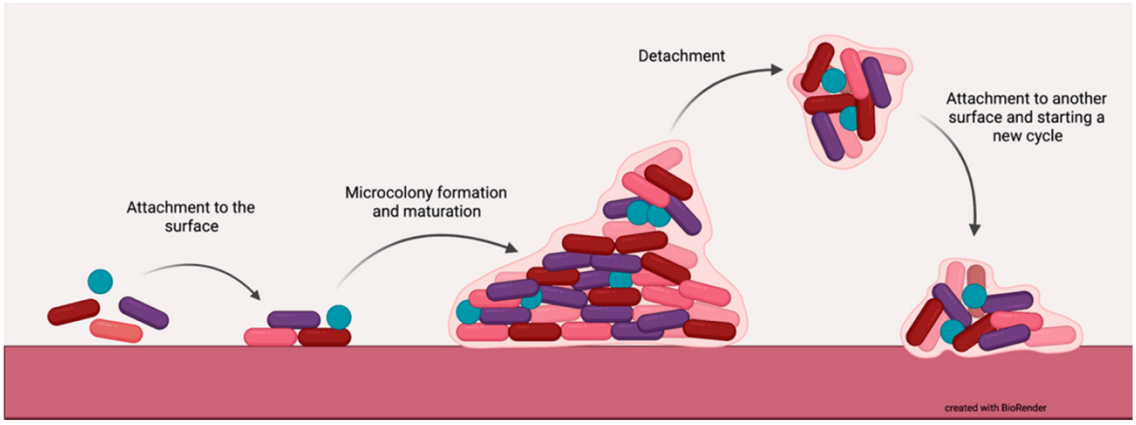

Figure 4. Cycle of biofilm formation.

Initial steps towards biofilm formation (**Figure 4**) involve bacteria attachment to surfaces, both living and non-living, including tissues, industrial surfaces and artificial devices (such as catheters, implants, cardiac valves, dental materials, contact lenses), using their flagella, pili or fimbriae (motile bacteria), or according to a passive process induced by electrostatic interactions or Van der Walls forces (non-motile bacteria).[27]

The further proliferation involves the production of various virulence factors making possible bacterial division, cellular proliferation, and production of extracellular matrix (ECM), in which bacteria are embedded.

ECM is composed of proteins, cellulose, alginates, extracellular teichoic acid, poly-*N*-acetyl glucosamine, lipids, nucleic acids, phospholipids, polysaccharides and extracellular DNA,[28] furthermore ECM is characterized by channels carrying water, nutrients, wastes and signal molecules within the whole structure, thus ensuring survival even of external cells.[29] The extracellular matrix is considered a mobile structure in which bacteria float; it is characterized by different viscosity areas able to rearrange in response to external stimuli such as the administration of an antibiotic. Consequently, the diffusion of antibiotics or other solutes can be slowed down in accordance with a mechanism called diffusion-reaction inhibition,[30] which can involve enzymatic degradation, oxidation and chelation reactions, thus enhancing the development of resistance to the antimicrobial agent used.

Moreover, within ECM, bacteria produce signal molecules called *autoinducers* able to promote the Quorum Sensing,[31] a communication tool used among bacteria cells to regulate all steps involved in biofilm formation, which allow the differentiation of the cells forming biofilm and carry out defense mechanisms with the aim to reduce, first and foremost, the antibiotics efficiency by providing an obstacle to drug diffusion, acting as a storage for enzymes involved in drugs degradation and bolstering the cellular structure. In detail, *Gram*-positive quorum sensing bacteria use peptides as autoinducers, whereas in *Gram* negative bacteria the most common autoinducers are *N*-acyl-homoserine lactones (AHLs).

Furthermore, biofilm bacteria can disperse over far distances as a result of isolation of new cells from growing ones, or reduction of biofilm mass, or quorum sensing and triggering induced by insufficient nutrient levels.[32] In particular, the detached cells can return to a planktonic form, by the expression of planktonic genes, or can colonize new surfaces and restart biofilm formation.

1.4. From waste to health: agri-food wastes as source of natural antimicrobial

Although the antibiotics discovery was a defining moment in the history of mankind that revolutionized medicine and saved countless lives, unfortunately these “magic bullets” have been accompanied by the emerging of resistant strains pathogens.[33]

As mentioned before, measures are urgently needed to control and overcome antibiotic resistance and to avoid a worldwide clinical collapse. Significant funding has been allocated for the development of new and effective strategies against multidrug resistant bacteria expanding the panel of potential therapeutical tools.[34] However, pharmaceutical synthetic compounds can have contraindications and side effects, leading to the appearance of new health alterations, moreover they can lead anyway to the appearance of new resistance bacterial strains. Besides, the research and the development of new antibiotic agents is a laborious process, which cannot keep up with rising rate of drug resistance and requires streamlining and accelerating the approval process for new drug products.[33]

Therefore, in recent years medicinal research has shown great interest in identifying new alternatives to the preparation of drugs that do not affect health, which can be represented by bioactive compounds coming from plants, fruits and functional foods.[35]

In this perspective, agri-food industry generates a large amount of waste (peels, seeds, shells, pomace and leaves) containing valuable compounds such as phenols, peptides, carotenoids, anthocyanins and fatty acids, fibers and enzymes which can be employed to produce functional foods or drugs useful in the treatment of various human ailments, including cancer, malaria, inflammatory diseases and microbial infections.[36]

According to Van der Werf and Gilliland, every year 198.9 kg of food losses and food waste are produced per capita in developed countries,[37] with a significant impact on biodiversity, human health and climate change.[38] For the proper management of these by-products, it is necessary a decisive change in the current economic model. In fact, although the actual linear economy model has allowed rapid industrial and cultural development, its extracting, consuming and disposal structure negatively impacts the availability of natural resources that supply the increasing world population, then generating large amount of waste.[39] In contraposition, during the last decades the circular economy model has been developed to address the utilization of agricultural wastes, by-products and co-products using innovative technologies and profitable business practices. The circular economy has been recommended as an alternative and more sustainable method to overcome the present model of extraction, production and consumption towards a system of

prevention, reuse and recovery of natural resources.[40] Therefore, the circular economy can be defined as a production and consumption model, which involves sharing, renting, reusing, repairing, renovating and recycling existing materials and products for as long as possible.[41,42]

This model aims to reduce waste to a minimum, transforming by-products into raw materials from which to produce new products with high health benefits and added value.[43]

1.5. Phenolic phytochemicals as an invaluable resource of antimicrobial agents

Among all bioactive compounds identified and recoverable from agri-food by-products and waste, polyphenols have gained pivotal attention thanks to their exhibited beneficial effects on well-being. Natural phenols are a wide group of molecules particularly present in the plant kingdom (over 8000 described so far),[44] which, in addition to their role in plant physiology regarding pigmentation, growth, reproduction and resistance to pathogens, play a key role in the Mediterranean diet and show significant biological activities ranging from antioxidant to antiproliferative properties.[45]

Polyphenols are considered one of the most important secondary metabolites categories produced by plants as a defense mechanism in specific conditions (pests, pathogens, herbivores), their amount can vary depending on the role they play in the plant and according to the conditions of plant growth such as temperature, soil properties, light and irrigation.[46,47]

Chemically, the structure of phenolic compounds varies widely but it is characterized as a common feature by the presence of one (simple phenol) or more (polyphenol) hydroxyl substituents attached directly to one or more aromatic rings.

Plant polyphenols are mainly classified into five different classes based on the structure of their molecular skeleton (**Figure 5**): phenolic acids, coumarins, stilbenes, flavonoids and lignans,[48,49] which can be often found in nature in glycosylated, esterified or condensed forms.

Plant polyphenols are present in fruits, vegetables and seeds that we consume daily (**Figure 5**), in particular: phenolic acids and coumarins are commonly found in coffee, turmeric, cinnamon, pomegranate, berries, nuts, tea and tropical fruits; stilbenes are mostly present in grapes and red wine, chocolate, nuts, blueberries and cabbage; the richest dietary source of lignans are flax seed, sesame seeds, cereals, legumes and berries; flavonoids are present in apples, buckwheat, tea, mango, carrots, kale, citrus fruits, aromatic plants, legumes, and in all the purple-blue-red colored fruits and flowers.[50,51]

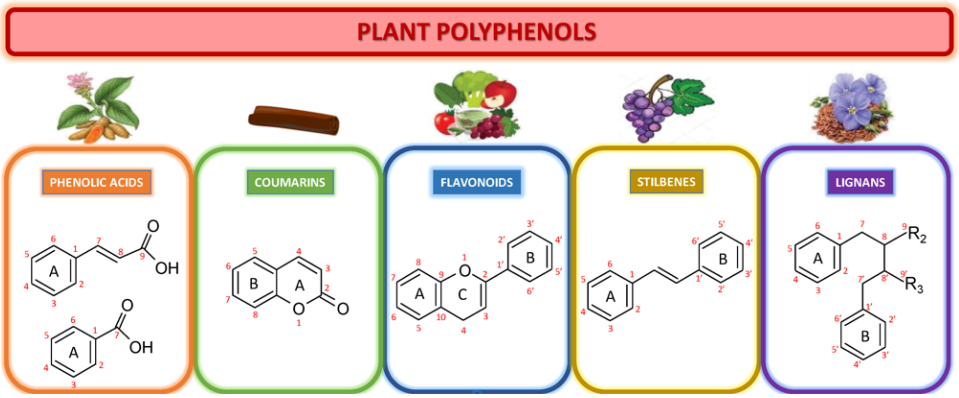

Figure 5. Plant polyphenols classification based on the structure of their molecular skeleton.

Extraction is a key step in the recovery of polyphenols as bioactive compounds from fruit and vegetables by-products, which can be achieved by different methodologies.

Traditional extraction techniques involve the use of a liquid for the extraction of solid or liquid matrices simply by means of solvent application and leaching. Soxhlet extraction, percolation and maceration have been utilized for more than a century for the isolation of polyphenols and have been acknowledged for long time in terms of convenience and productivity.[52] However, certain disadvantages pertaining to traditional extraction techniques render their application quite uneconomical due to excessive consumption of time, energy and extracting solvents when compared to alternative modern techniques. These underlying drawbacks have triggered research to explore more cost-effective and greener techniques for the extraction of polyphenols from a wide range of plant matrices and their by-products.[53]

Supercritical fluid extraction, microwave-assisted extraction, ultrasound-assisted extraction, ultrasound-microwave-assisted extraction and subcritical water extraction are the most widely modern green techniques used for preparing products with high amounts of polyphenols.[54] These techniques, in addition to being straightforward to apply, are characterized by short extraction times, reduced consumption of organic solvents, minimal environmental impact and low toxic waste yield.

Among all these innovative green methods, ultrasound-assisted extraction (UAE) showed many advantages such as less time and low energy required, extraction at low temperature, retention of the quality of the extract, versatility, simplicity, safety, rapidity, eco-friendliness and cost-effectiveness. UAE of bioactive compounds from fruit and vegetables waste and by-products is based on the use of high intensity sound waves, in particular ultrasounds cause disruption in the plant tissue through physical forces developed during acoustic cavitation and helps in release of extractable components in the solvent in very less time by enhancing the mass transport phenomena.[55]

1.5.1. Antibacterial mechanisms of polyphenols

Polyphenols act against bacteria on a multitude of molecular target through several mechanisms (**Figure 6**).[56]

They can directly bind and damage bacterial cell membrane, even if its complex multilayered structure protect bacteria against environmental factors. The cell walls of *Gram*-positive and *Gram*-negative bacteria are different. In *Gram*-negative bacteria the cell wall comprises an outer membrane, made up of protein, phospholipid bilayer and lipopolysaccharides, and a thin layer of peptidoglycan. In contrast, *Gram*-positive bacteria cell wall lacks an outer membrane, while contains lipoteichoic acid and a thick layer of peptidoglycan. In both cases, bacteria cell walls have been stated to play an imperative role in osmotic protection, therefore any damage on it reduces their tolerance to low osmotic pressure and high ionic strength. In this perspective, *Gram*-positive bacteria are the most sensitive to phenolic compounds, because of the lack of the outer membrane, whilst the presence of the outer membrane and a higher level of phospholipids make *Gram*-negative bacteria less susceptible.[57]

It has been reported that polyphenols may also interact with phospholipids or protein inside the lipid bilayer, thus destroying membrane integrity and permeability, whit a consequential alteration of its fluidity and ion transport process, finally inducing the leakage of cellular contents, including DNA.

Moreover, phenolic compounds have an impact on bacteria DNA synthesis and regulation, in fact the planarity and the hydrophobic core of polyphenols mean that they can penetrate the DNA helix during the replication, recombination, repair and transcription processes. The phenolic hydroxyl groups allow these molecules to form hydrogen bonds with the nucleic acid bases modifying the secondary structure and morphology of DNA; in addition, phenolic compounds can inhibit enzymes involved in the DNA synthetic pathways through several mechanisms, based on the structure of the single polyphenols considered and on the bacterial species involved.[58]

Furthermore, bacterial enzymatic activity is affected by phenolic compounds via protein-phenol interactions, which can occur through covalent or noncovalent bonds depending on the structural properties of proteins (i.e., hydrophobicity, molecular weight, conformational configuration, amino acids composition and sequence); this inhibition can involve hydrolase, oxidoreductase, lyase and transferase enzymes.

Finally, phenols are also able to inhibit bacteria gene expression, often related to virulence factors produced by pathogenic bacteria, thus inducing a down-regulation of genes responsible for invasion of host cells, bacteria mobility and their intracellular survival.[59]

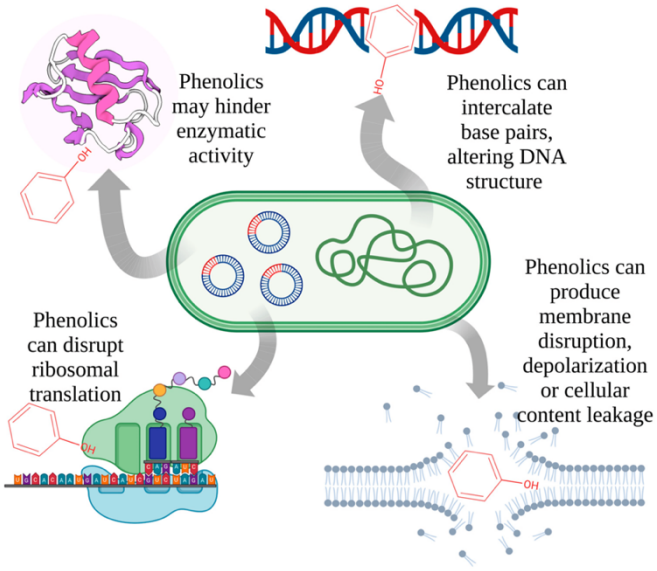

Figure 6. Antibacterial mechanisms of action of phenolic compounds.

1.5.2. Polyphenols physicochemical limitations and new therapeutic strategies

Although the positive effects of phenolic phytochemicals on human health have been confirmed by a variety of study reported in the literature, their use in humans is limited by many physicochemical factors, which affect their absorption and consequently lead to the use of high doses to obtain significant beneficial effects.

In particular, the characteristic low absorption rate of polyphenols is mainly related to:

- *Low solubility*. Depending on their chemical structure, polyphenols are characterized by a different degree of solubility in water. Plant polyphenols are often characterized by large lipophilic portion in their molecular structure, which makes their solubility very low in aqueous media and consequently in biological fluids.[60] In particular, molecules with high molecular weight are usually not well dissolved in water.

- *Poor stability*. The poor stability of polyphenols in the gastrointestinal tract plays an important role in their low absorption rate and distribution until reaching target sites. When polyphenols-based products are administrated, they pass through mouth, stomach, and small intestine, before passing to the bloodstream. During their route through the gastrointestinal tract, polyphenols are subjected to large pH variation, which could degrade them.[61]
- *Low permeation*. The small intestine is a special site for the absorption of polyphenols. However, no specific receptors have been found on the surface of small intestine epithelial cells to carry polyphenols into cells and then into the bloodstream. Therefore, the mechanism for polyphenols transport across epithelium is principally based on passive diffusion, including paracellular and transcellular diffusions. Once polyphenols are transcellularly diffused into epithelia cells, active efflux process takes place to excrete them back to lumen (**Figure 7**).

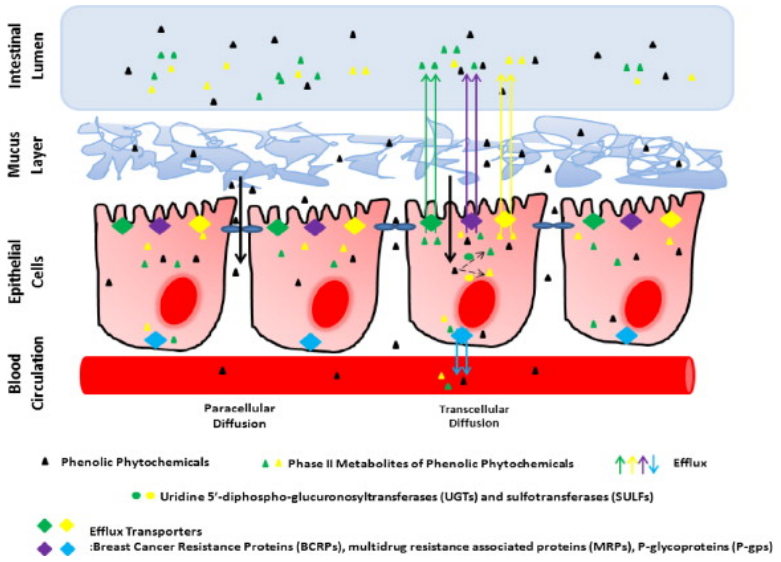

Figure 7. Passive diffusion, metabolism and active efflux of phenolic compounds.

- *Extensive metabolic reactions*. Some natural compounds tend to be biologically unstable and prone to degradation to form phase II metabolites, which are also recognized by efflux transporters that pump back them to lumen where they are excreted or further degraded.[62]

These limitations can be overcome by the use of nanotechnologies, to this purpose many nanocarriers have been developed to improve bioavailability of polyphenols, prevent degradation caused by environment conditions such as pH, enzymatic activity, presence of oxygen, and avoid interactions with other components in the human body, thus reducing the possibility of systemic side effects.

1.6. Nanoparticles for the delivery of polyphenols

Nanoparticles (NPs) are a widely used tool in medicine for drug delivery, thanks to their ability to distribute in human body and the possibility of engineering them based on the goal to be achieved.

An ideal drug delivery nanosystem should have the following features:[63-65]

- Non-toxic, biodegradable and biocompatible.
- Particle size around 100 nm (except for transport through monocytes and macrophages).
- Ability to encapsulate small molecules, proteins, peptides or nucleic acids.
- Stability in bloodstream (absence of aggregation or dissociation).
- Controlled release of drug entrapped at the target site.
- Protection of drug from the external environment.

To this purpose, nanoparticles can be adjusted in terms of size, surface charge and shape (NPs can be spherical, hexagonal, cubic, etc.) to improve the interaction with the target biological environment.

At the present, delivery systems such as phytosomes®, liposomes, protein-based nanoparticles, polymeric nanoparticles, metal nanoparticles, dendrimers, micelles, and emulsions have emerged as attractive options for controlled delivery of bioactive molecules (**Figure 8**).[66]

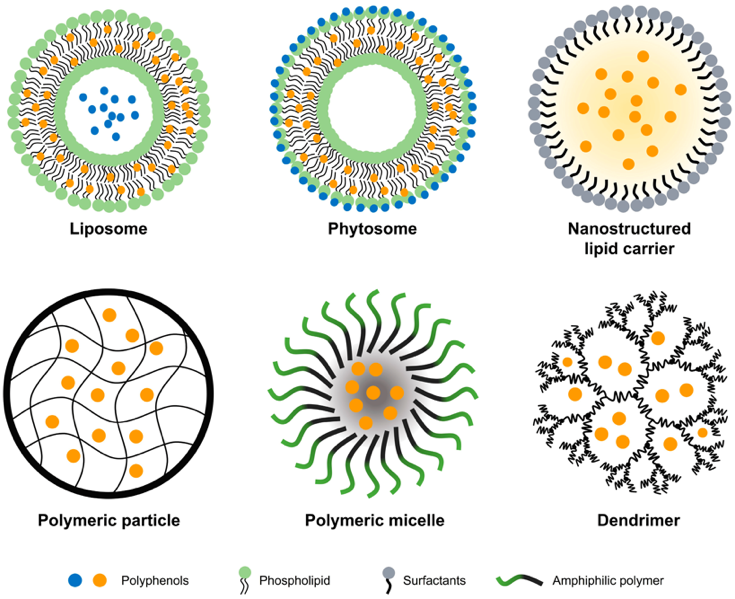

Figure 8. Representative drug delivery systems for polyphenols.[67]

- *Phytosome®.* Phytosomes were developed in the late 1980s with the aim to increase the bioavailability of drugs by complexing them to phospholipids obtaining a relatively stable complex formed by electrostatic interaction between phospholipids (manly phosphatidylcholine) and conveyed biomolecules. This electrostatic effect mainly includes ion-dipole, dipole-dipole and hydrogen bonding.[68] Phospholipid complexes are often more bioavailable than the biomolecule alone, due to the presence of phosphatidylcholines which are the major components of cell membranes, thus enhancing the ability of the biomolecule to circulate in the body.[69]

- *Liposomes*. Liposomes are (phospho)lipid-based vesicles composed of one or more lipid bilayers enclosing inner aqueous compartment(s). Such a structure facilitates encapsulation of a wide variety of drugs and active ingredients: hydrophilic compounds are entrapped into the inner water space; lipophilic compounds are encapsulated inside the lipid bilayer and amphiphilic compound between these two regions. Liposomes are characterized by their lipid composition, morphology, particle size, surface properties and membrane rigidity/elasticity, determining their stability and interaction with the biological targets. For all these features, liposomes are widely used for polyphenols entrapment compared to other nanoparticles developed.[70]

- *Protein-based nanoparticles*. Among all the proteins employable for developing nanoparticles systems, gelatin is a water-soluble protein widely used in medicine, cosmetics and food,[71] obtained by collagen hydrolysis in acid or alkaline conditions.[72] If the acid conditions are used to hydrolyze egg collagen, the gelatin A is obtained with an isoelectric point of about 9. On the opposite, in alkaline conditions gelatin B is produced with an isoelectric point of about 5.[73] Gelatin is a polyamphoteric electrolyte characterized by the presence of hydrophobic groups, which enable it to be coupled with many crosslinking agents and ligands; it is cheap, easily obtainable and has good biocompatibility and biodegradability. Moreover, gelatin nanoparticles surface can be modified with the aim of increasing their stability and controlling the release of loaded biomolecules.[74]

- *Polimeric nanoparticles.* Chitosan is a semi-synthetic polysaccharide obtained by the deacetylation of chitin, the only alkaline polysaccharide widely present in nature. It has

received increasing attention due to its good biocompatibility, degradability, non-antigenicity, high permeability, non-toxic and good-film forming properties.[75] In addition, it shows adhesive properties and can reversibly open the tight junctions between epithelial cells, thereby promoting paracellular transport between cells.[76] Chitosan has been used as carrier in drug delivery due to its ability to increase the functional activity and oral availability of the encapsulated active substances. Moreover, properties required for some specific applications can be obtained through appropriate structural modifications.

- *Micelles.* Micelles are colloidal systems that form in aqueous solution by spontaneous association of amphiphilic molecules. Their hydrophobic core can be used to encapsulate water-insoluble biomolecules, while the hydrophilic corona, protecting the core, can prevent its removal by the reticuloendothelial system, increasing its circulation time and avoiding interactions between biomolecules and blood components.[77] A large number of research results have shown that many biological activities of bioactive molecules are fully maintained after encapsulation in micelles.[78]

- *Emulsions*. Emulsions are a class of disperse systems consisting of two immiscible liquids, where liquid droplets (the disperse phase) are dispersed in a liquid medium (the continuous phase).[79] According to their size, they can be divided into micro- (10-100 nm), nano- (100-1000 nm) and macro-emulsions (0.5-100 mm). In detail, nanoemulsions have been used to encapsulate a variety of biocompounds due to their small size, large surface area, high optical clarity, good stability and ability to improve drug bioavailability.[80] Although nanoemulsions have significant advantages, they are unstable at low pH, and their small size and liquid nature make the release of conveyed molecules difficult to control.

- *Metal nanoparticles*. Inorganic nanoparticles are suitable for drug delivery thanks to their good controllability of size and shape, large specific surface area, and imaging potential. They are composed of pure metals such as gold, silver or platinum, with a size between 1-100 nm and a variety of shape such as ball, bar and cage. Metal nanoparticles are non-toxic, biocompatible and their surface can be easily functionalized.[81]

- *Dendrimers*. A dendrimer is a monodisperse, three-dimensional, hyper-branched radial symmetric polymer with host-guest capabilities.[82] Its core structure is a cavity that can contain biologically active components, and the branches can be functionalized or complexed with other compounds. These nanoparticles were found to have no toxicity towards normal cells and can simply pass through biological barriers.

1.7. Liposomes

Among the nanoparticles delivery systems described above, liposomes are probably the most versatile and efficient ones for the encapsulation of polyphenols.

Liposomes were discovered in the 1960s by Alec D. Bangham at the University of Cambridge,[83] who was investigating the role of phospholipids in the blood clotting process and highlighted how lipids in contact with water spontaneously form spherical particles due to their amphiphilic nature.

Firstly, Bangham reported the usefulness of liposomes as biomembrane model systems because of their structural similarity with cell membrane, to study fundamental membrane processes such as permeation, adhesion and fusion.[84] In 1971, Gregoriadis et al.[85] understood the potential of using liposomes as delivery systems of bioactive substances, thereafter liposomes have demonstrated their outstanding role in the field of drug delivery. In this perspective, in 1990 the first injectable drug-amphotericin B liposome (AmBi®some®) was available in Europe and in 1995 Doxil® (a doxorubicin liposome formulation) was the first anticancer FDA-approved nano-drug.[86]

Liposomes (**Figure 9**) are small lipid-based vesicles composed of naturally occurring and/or synthetic phospholipids, which self-enclose in water to form spheres of lipid bilayers with an internal aqueous core. This minimizes the contact between the hydrophobic fatty acid chains of phospholipids and the hydrophilic aqueous environment, resulting in a thermodynamically favorable formation further enhanced by hydrogen bonding, van der Walls forces and other electrostatic interactions.[87,88]

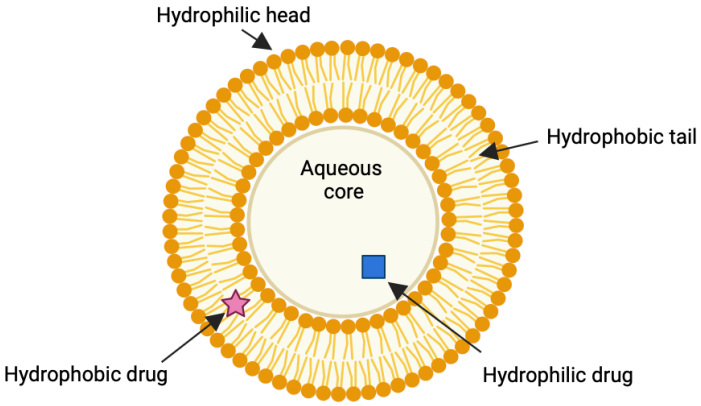

Figure 9. Graphical representation of liposome structure (created with BioRender.com).

Generally, liposomes are classified based on size and number of lamellae (the number of concentric lipid bilayers) into (**Figure 10**):

- SUVs (*small unilamellar vesicles*): consisting of a single lipid bilayer with dimensions in the range of 20-100 nm, thermodynamically unstable.
- LUVs (*large unilamellar vesicles*): consisting of a single lipid bilayer characterized by diameter higher than 100 nm.
- GUVs (*giant unilamellar vesicles*): characterized by a single lipid bilayer with dimensions higher than 1000 nm.
- OLVs (*oligolamellar vesicle*): composed of few concentric lamellae and diameter varying between 0.1-1 μm.
- MLVs (*multilamellar vesicles*): formed by multiple bilayers with a size range between 0.1 and 0.5 μm.
- MVVs (*multivesicular vesicles*): composed by multiple vesicles with size higher than 10 μm.

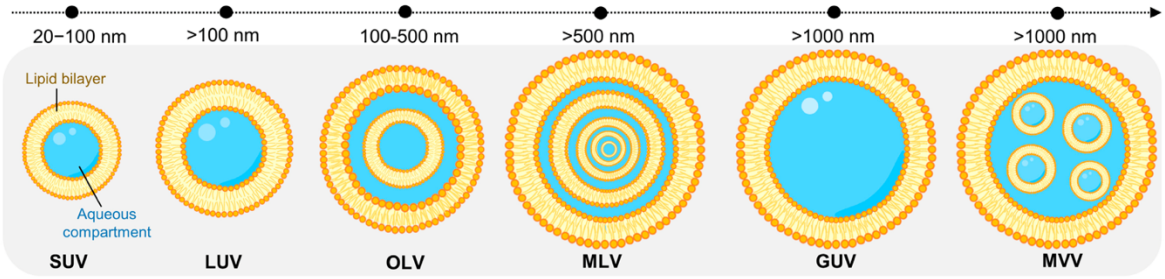

Figure 10. Visual representation of the different classes of liposomes base on size and lamellarity. SUV: small unilamellar vesicles; LUV: large unilamellar vesicles; OLV: oligolamellar vesicles; MLV: multilamellar vesicles; GUV: giant unilamellar vesicles; MVV: multivesicular vesicles.[89]

Due to their unique physicochemical features, liposomes are useful drug delivery systems for carrying hydrophilic (in the aqueous core), lipophilic (inside the lipid bilayer) and amphiphilic (partitioned at the surface of the bilayers) drugs.[90] The lipophilic drugs become highly embedded in the lipid bilayers when liposomes self-assemble. Instead, the hydrophilic drugs may not be incorporated with high efficiency because the volume of hydration is larger on the outside of the liposomes rather than the core, with its limited aqueous volume, therefore appropriate encapsulation methods must be adopted (i.e., microfluidic methods). As a result of such variations, it is imperative to understand the physicochemical properties of the drug and the lipids to improve the drug loading in liposomes.[91]

The solubility and *in vivo* fate of entrapped compounds depend on the liposomes employed. However, generally advantages deriving from liposomal encapsulation include: improvement of

drugs solubility; prevention of chemical and biological degradation of molecules under storage conditions and during patient administration; reduction of non-specific side effects and toxicity of encapsulated drugs; improvement of drug efficiency and therapeutic index; targeting since liposomes can be chemically modified with attached specific surface ligands; compatibility because composed of biodegradable and nontoxic materials.[92-94]

For all these aspects, liposomes are undoubtedly the most studied and investigated nanocarriers for targeted drug delivery with many successful applications and clinical trials.[95-100]

One of the main parameters characterizing liposomes is the transition temperature (T_m), whereby phospholipids shift from the solid-gel phase to the liquid-crystalline phase (**Figure 11**).[101]

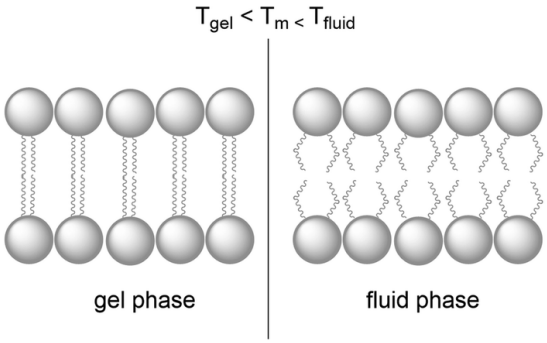

Figure 11. A lipid bilayer changes from the rigid gel phase (left) to the mobile fluid phase (right) above the transition temperature (T_m) of the lipid.[102]

In detail, below the T_m lipids are in the gel phase, a solid-like state in which the movements of lipids inside the bilayer are very slow, whereas at temperature higher than T_m lipids are in a liquid-crystal phase in which the mobility of lipids is much higher and the thickness of lipid bilayer decreases. Therefore, the fluid state of lipids is more permeable and can be exploited to encapsulate drugs during liposomes production. At body temperature ($T \approx 37°C$) a fluid state will make the liposomes leaky, and the encapsulated drugs are likely to escape before reaching the site of action. Thus, choosing phospholipids with gel states at physiological conditions is often desirable to stabilize liposomes. Each lipid or mixture of lipids has a characteristic T_m depending on the length of the fatty acid chains, the number of unsaturations and the nature of the polar heads, which define the fluidity and permeability of the final lipid bilayer. Typically, T_m increases with the length of alkyl chains while decreases with increasing unsaturation. Thus, bilayer composed by phospholipids with long and saturated hydrocarbon chains are stiffer and less permeable than bilayers composed by phospholipids with shorter and unsaturated chains.[91]

Phospholipids have an intrinsic natural flip-flop or rotational freedom, which also promotes leakiness of encapsulated drugs. To stabilize the lipid bilayer, cholesterol is generally added in different concentrations to the formulations to have beneficial effects on the capacity of liposomes to encapsulate and retain a drug.[103,105] Inside lipid bilayers, cholesterol arranges along the phospholipid aliphatic chains, exposing its hydroxyl group to the hydrophilic region and its condensed aliphatic rings, characterized by a flat and rigid structure, parallel to the fatty acid chains thanks to hydrophobic interactions. Therefore, the inclusion of cholesterol in the mixture enhances the stability of the lipid bilayer through the so-called "*bilayer-tightening effect*", inducing a dense packing and increasing the orientation order of lipid chains. This leads to a more compact structure with reduced permeability to water-soluble molecules and increased rigidity.[105,106]

The charge of liposomes can play an important role in the fate of liposomes during the storage and after administration.[107,108] Liposomes can be either negatively, neutrally or positively charged depending on the additives in their composition. This may affect liposomes stability, pharmacokinetic, biodistribution and cellular uptake. Charged liposomes exhibit electrostatic repulsion and consequently do not aggregate quickly in storage condition. Moreover, the charge of liposomes also affects their biological responses. For instance, the negatively charged liposomes are recognized by macrophages and enter the cell through endocytosis at a higher rate than neutral ones, resulting in shorter circulation time. On the other hand, since cell membranes are negatively charged, the presence of cationic amphiphiles in liposomes increases cell-liposome interaction and internalization[109] due to electrostatic interactions, which result in the uptake by phagocytic system.[110-112]

1.7.1. Liposomes functionalization for targeted delivery

Undoubtedly, the perfect antimicrobial treatment should preferentially allow elimination of the infectious agent without affecting the essential microbiota or non-pathogenic cells. Considering the available antimicrobial sources, this goal is far from being achievable for bacterial infections. A more realistic approach is the development of antibiotic-loaded vehicles able to directly target a specific site, such as selective tissue, organ or eventually a strictly defined pathogenic bacteria.[113]

In this regard, liposomes offer outstanding possibilities, because they can be designed to target bacterial infections through non-specific or specific approaches:

- *Non-specific approaches*. Preferential accumulation at infected sites and direct interaction with bacteria can be achieved by modifying some physicochemical features of liposomes, in particular their surface charge.[114] Since pathogenic bacteria possess, under physiological conditions, a negatively charged cell wall, positively charged liposomes are able to target bacteria by electrostatic interactions.[115] Liposomes can also be designed to liberate the entrapped compound in response to a variation of pH or temperature. pH-responsive liposomes are able to change their conformation and chemical properties in response to acidic pH, allowing the target and the accumulation at infectious biofilms characterized by acidic pH.[116] Instead, temperature-sensitive liposomes are able to release the drug loaded in response to local heating, when temperature is above the transition temperature of the lipid bilayer.[117]

- *Specific approaches.* To achieve a specific interaction, liposomes can be functionalized with targeting ligands at their surface, such as proteins, carbohydrates, aptamers, antibodies or antibody fragments (**Figure 12**), which are recognized by particular surface receptors located at the target cells allowing a localized delivery of the delivered drug.[118] In this perspective, some sugar molecules can be used as a targeting ligand to functionalize liposomes, enhancing a specific interaction with bacteria cells towards lectins, a class of non-enzymatic proteins mostly located on bacterial cell membranes, able to recognize and bind selectively carbohydrates.[119] This may allow a reduction of the total dose required for the treatment, consequently decreasing drug accumulation at healthy tissues and the risk of dose-dependent toxicity. Therefore, this strategy is particularly interesting for antibiotics that have shown high side-effects and for the treatment of intracellular bacterial infections caused by resistant bacteria strains.

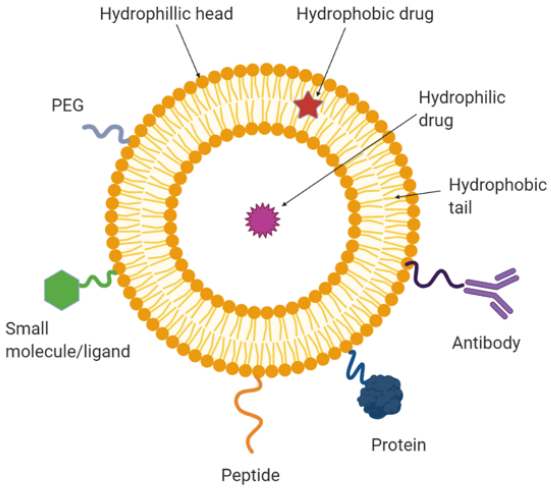

Figure 12. Liposome modification for targeted drug delivery (created with BioRender.com).

In both approaches, liposomal composition (surface charge and fluidity) and bacterial surface patterns (global surface charge, outer membrane proteins, hydrophobic properties, LPS structure) influence the affinity between liposomes and bacteria. Due to the similarity of the structure and composition of liposomes to bacterial membrane, they have unique capacity to interact with bacteria through fusion with their cell membrane, which could promote its structural breakdown and potentially reverse its low permeability, thus enabling high delivery of antibiotics into target bacteria and potentially overcoming antibiotic resistance mechanisms.[120]

1.8. References

[1] R.I. Aminov, A Brief History of the Antibiotic Era: Lessons Learned and Challenges for the Future, *Front Microbiol*, **2010**, *1* (134), 134.
https://doi.org/10.3389/fmicb.2010.00134

[2] M.I. Hutchings, A.W. Truman, B. Wilkinson, Antibiotics: Past, Present and Future. *Curr Opin Microbiol,* **2019**, *51* (1), 72.
https://doi.org/10.1016/j.mib.2019.10.008

[3] W. Witte, Medical consequences of antibiotic use in agriculture, *Science*, **1998**, *279*, 996.
https://doi.org/10.1126/science.279.5353.996.

[4] P. S. McManus, V. O. Stockwell, G. W. Sundin, A.L. Jones, Antibiotic use in plant agriculture, *Annu. Rev. Phytopathol*, **2002**, *40*, 443.
https://doi.org/10.1146/annurev.phyto.40.120301.093927

[5] F. C. Cabello, Heavy use of prophylactic antibiotics in aquaculture: a growing problem for human and animal health and for the environment, *Environ.* Microbiol, **2006**, *8*, 1137.
https://doi.org/10.1111/j.1462-2920.2006.01054.x

[6] M. Ferreira, M. Ogren, J. N. R. Dias, M. Silva, S. Gil, L. Tavares, F. Aires-da-Silva, M. M. Gaspar, S. I. Aguiar, Liposomes as Antibiotic Delivery Systems: A Promising Nanotechnological Strategy against Antimictobial Resistance, *Molecules*, **2021**, *26*, 2047.
https://doi.org/10.3390/molecules26072047

[7] F. Prestinaci, P. Pezzotti, A. Pantosti, Antimicrobial Resistance: a Global Multifaceted Phenomenon, *Pathog Glob Health*, **2015**, *109* (7), 309.
https://doi.org/10.1179/2047773215Y.0000000030

[8] R.C. Founou, A.J. Blocker, M. Noubom, C. Tsayem, S.P. Choukem, M.V. Dongen, et al. The COVID-19 Pandemic: a Threat to Antimicrobial Resistance Containment, *Future Sci*, **2021**, *7* (8), FSO736. https://doi.org/10.2144/fsoa-2021-0012.

[9] J. O'Neill, Review on Antimicrobial Resistance. Tackling Drug-Resistant Infections Globally, Government of the United Kingdom, **2016**.

[10] J.S. Mackenzie, M. Jeggo, The One Health Approach- Why is it so important?, *Trop. Med. Infect. Dis*, **2019**, *4*, 88.
https://doi.org/10.3390/tropicalmed1020088.

[11] M.A. Abushaheen, Muzaheed, A.J. Fatani, M. Alosaimi, W. Mansy, M. George, S. Acharya, S. Rathod, D.D. Divakar, C. Jhugroo, S. Vellappally, A.A. Khan, J. Shaik, P. Jhugroo, Antimicrobial resistance, mechanisms and its clinical significance, *Dis Mon*, **2020**, *66* (6), 100971. https://doi.org/10.1016/j.disamonth.2020.100971.

[12] K.W.K. Tang, B.C. Millar, J.E. Moore, Antimicrobial Resistance (AMR), *Br J Biomed Sci*, **2023**, *28* (80), 11387. https://doi.org/10.3389/bjbs.2023.11387.

[13] A.R. Rojas, J. Rodríguez-Beltrán, A. Couce, J. Blázquez, Antibiotics and antibiotic resistance: A bitter fight against evolution, *Int J Med Microbiol*, **2013**, *303* (6) ,293. https://doi.org/10.1016/j.ijmm.2013.02.004.

[14] E. van Duijkeren, A.K. Schink, M.C. Roberts, Y. Wang, S. Schwarz, Mechanisms of Bacterial Resistance to Antimicrobial Agents, *Microbiol Spectr*, **2018**, *6* (1), ARBA-0019-2017. https://doi.org/10.1128/microbiolspec.ARBA-0019-2017

[15] J.L. Martinez, General principles of antibiotic resistance in bacteria, *Drug Discov Today Technol*, **2014**, *11*, 33. https://doi.org/10.1016/j.ddtec.2014.02.001.

[16] J. Blázquez, A. Couce, J. Rodríguez-Beltrán, Antimicrobials as promoters of genetic variation, *Curr Opin Microbiol*, **2012**, *15* (5), 561. https://doi.org/10.1016/j.mib.2012.07.007

[17] J.M. Blair, G.E. Richmond, L.J. Piddock, Multidrug efflux pumps in Gram-negative bacteria and their role in antibiotic resistance, *Future Microbiol*, **2014**, *9* (10), 1165. https://doi.org/10.2217/fmb.14.66. PMID: 25405886.

[18] P.A. Lambert, Cellular impermeability and uptake of biocides and antibiotics in Gram-positive bacteria and mycobacteria, *J Appl Microbiol*, **2012**, *92*, 46. https://doi.org/10.1046/j.1365-2672.92.5s1.7.x

[19] W.C. Reygaert, Methicillin-resistant Staphylococcus aureus (MRSA): molecular aspects of antimicrobial resistance and virulence, *Clin Lab Sci*, **2009**, *22*, 115. https://doi.org/10.29074/ascls.22.2.115

[20] C.P. Randall, K.R. Mariner, I. Chopra, A.J. O'Neill, The target of daptomycin is absent from Escherichia coli and other gram-negative pathogens, *Antimicrob Agents Chemother*, **2013**, *57* (1), 637. https://doi.org/10.1128/AAC.02005-12.

[21] M.C. Roberts, Resistance to macrolide, lincosamide, streptogramin, ketolide, and oxazolidinone antibiotics, *Mol Biotechnol*, **2004**, *28* (1), 47.
https://doi.org/10.1385/MB:28:1:47.
[22] L.S. Redgrave, S.B. Sutton, M.A. Webber, L.J. Piddock, Fluoroquinolone resistance: mechanisms, impact on bacteria, and role in evolutionary success, *Trends Microbiol*, **2014**, *22* (8), 438.
https://doi.org/10.1016/j.tim.2014.04.007
[23] C. Kourtesi, A.R. Ball, Y.Y. Huang, S.M. Jachak, D.M. Vera, P. Khondkar, S. Gibbons, M.R. Hamblin, G.P. Tegos, Microbial efflux systems and inhibitors: approaches to drug discovery and the challenge of clinical implementation, *Open Microbiol J*, **2013**, *7*, 34.
https://doi.org/10.2174/1874285801307010034.
[24] D.I. Andersson, Persistence of antibiotic resistant bacteria, *Curr Opin Microbiol*, **2003**, *6* (5), 452.
htpps://doi.org/10.1016/j.mib.2003.09.001.
[25] Z. Sedarat, A.W. Taylor-Robinson, A Consideration of Antibacterial Agent Efficacies in the Treatment and Prevention of Formation of Staphylococcus aureus Biofilm, *J Microbiol Infec Dis*, **2019**, *9* (4), 167.
https://doi.org/10.5799/jmid.657903.
[26] K. Lewis, Persister cells, *Annu Rev Microbiol*, **2010**, *64*, 357.
https://doi.org/10.1146/annurev.micro.112408.134306
[27] S. McCarty, E. Woods, S. L. Percival, Biofilms in Infection Prevention and Control, 1st edition, Academic Press, **2014**, 143.
[28] D.E. Moormeier, K.W. Bayles, Staphylococcus aureus biofilm: a complex developmental organism, *Mol Microbiol*, **2017**, *104* (3), 365.
https://doi.org/10.1111/mmi.13634.
[29] B. Costerton, Microbial ecology comes of age and joins the general ecology community, *PNAS*, **2004**, *49*, 16983.
https://doi.org/10.1073/pnas.0407886101
[30] S. Daddi Oubekka, R. Briandet, M.P. Fontaine-Aupart, K. Steenkeste, Correlative time-resolved fluorescence microscopy to assess antibiotic diffusion-reaction in biofilms, *Antimicrob Agents Chemother*, **2012**, *56* (6), 3349.
https://doi.org/10.1128/AAC.00216-12

[31] G. Brackman, P. Cos, L. Maes, H.J. Nelis, T. Coenye, Quorum sensing inhibitors increase the susceptibility of bacterial biofilms to antibiotics in vitro and in vivo, *Antimicrob Agents Chemother*, **2011**, *55* (6), 2655.
https://doi.org/10.1128/AAC.00045-11.
[32] P. Speziale, G. Pietrocola, T.J. Foster, J.A. Geoghegan, Protein-based biofilm matrices in Staphylococci, *Front Cell Infect Microbiol*, **2014**, *10* (4), 171.
https://doi.org/10.3389/fcimb.2014.00171
[33] B. Aslam, W. Wang, M.I. Arshad, M. Khurshid, S. Muzammil, M.H. Rasool, M.A. Nisar, R.F. Alvi, M.A. Aslam, M.U. Qamar, M.K.F. Salamat, Z. Baloch, Antibiotic resistance: a rundown of a global crisis, *Infect Drug Resist*, **2018**, *11*, 1645.
https://doi.org/10.2147/IDR.S173867
[34] M.A. Mohamed, M. Nasr, W.F. Elkhatib, W.N. Eltayeb, A.A. Elshamy, G.S. El-Sayyad, Nanobiotic formulations as promising advances for combating MRSA resistance: susceptibilities and post-antibiotic effects of clindamycin, doxycycline, and linezolid, *RSC Adv*, **2021**, *11* (63), 39696. https://doi.org/10.1039/d1ra08639a
[35] J. Kardan Yamchi, M. Haeili, S. Gizaw Feyisa, H. Kazemian, A. Hashemi Shahraki, F. Zahednamazi, A.A. Imani Fooladi, M.M. Feizabadi, Evaluation of efflux pump gene expression among drug susceptible and drug resistant strains of Mycobacterium tuberculosis from Iran, *Infect Genet Evol*, **2015**, *36*, 23.
https://doi.org/10.1016/j.meegid.2015.08.036.
[36] A.S. Abdel-Razek, M.E. El-Naggar, A. Allam, O.M. Morsy, S.I. Othman, Microbial Natural Products in Drug Discovery, *Processes*, **2020**, *8*, 470.
https://doi.org/10.3390/pr8040470.
[37] P. van der Werf, J.A. Gilliland, A systematic review of food losses and food waste generation in developed countries, *Proceedings of the Institution of Civil Engineers – Waste and Resource Management*, **2017**, *170* (2), 66.
https://doi.org/10.1680/jwarm.16.00026
[38] C. Beretta, M. Stucki, S. Hellweg, Environmental impacts and hotspots of food losses: value chain analysis of Swiss food consumption, *Environ. Sci. Technol,* **2017**, *51* (19), 11165.
https://doi.org/10.1021/acs.est.6b06179.

[39] M. Pagotto, H. Anthony, Towards a Circular Economy on Australian Agri-food Industry: An Application of Input-Output Approaches for Analyzing Resource Efficiency and Competitiveness Potential, *J Ind Eco*, **2016**, *20* (5), 1176.
http://dx.doi.org/10.1111/jiec.12373
[40] B. Esposito, M. Sessa, D. Sica, O. Malandrino, Towards Circular Economy in the Agri-Food Sector. A Systematic Literature Review, *Sustainability,* **2020**, *12*, 7401.
https://doi.org/10.3390/su12187401
[41] M.Lieder, A. Rashid, Towards circular economy implementation: a comprehensive review in context of manufacturing industry, *J Cleaner Production*, **2016**, *115*, 36. https://doi.org/10.1016/j.jclepro.2015.12.042
[42] Ellen MacArthur Foundation. Towards the Circular Economy. Opportunities for the Consumer Goods Sector; EMF: Cowes, Island of Wight, UK, **2013**.
[43] L. Panzella, F. Moccia, R. Nasti, S. Marzorati, L. Verotta, A. Napolitano, Bioactive Phenolic Compounds From Agri-Food Wastes: An Update on Green and Sustainable Extraction Methodologies, *Front Nutr*, **2020**, *7* (7), 60.
https://doi.org/10.3389/fnut.2020.00060.
[44] M. Leri, M. Scuoto, M.L. Ontario, E.J. Calabrese, M. Bucciantini, M. Stefani, Healthy Effects of Plants Polyphenols: Molecular Mechanisms, *Int. J. Mol. Sci*, **2020**, *21*, 1250. https://doi.org/10.3390/ijms21041250
[45] A. Rana, M. Samtiya, T. Dhewa, V. Mishra, R.E. Aluko, Health benefits of polyphenols: A concise review, *J Food Biochem*, **2022**, *46* (10), 14264.
https://doi.org/10.1111/jfbc.14264.
[46] L.A. de la Rosa, J.O. Moreno-Escamilla, J. Rodrigo-García, E. Alvarez-Parrilla, Phenolic Compounds. In Postharvest Physiology and Biochemistry of Fruits and Vegetables, 1st edition, Elsevier, **2019**; 253.
[47] N. Rispail, P. Morris, K.J. Webb, KPhenolic Compounds: Extraction and analysis, Springer, **2006**, 349.
[48] D.M. Pereira, P. Valentão, J.A. Pereira, P.B. Andrade, Phenolics: From Chemistry to Biology, *Molecules*, **2009**, *14* (6), 2202.
https://doi.org/10.3390/molecules14062202.
[49] A. Belscak-Cvitanovic, K. Durgo, A. Hudek, V. Bacun-Druzina, D. Komes, Overview of Polyphenols and Their Properties. In: Galanakis, C.M., Ed., Polyphenols: Properties, Recovery, and Applications,

Woodhead Publishing, **2018,** *3*.
https://doi.org/10.1016/B978-0-12-813572-3.00001-4
[50] R. Tsao, Chemistry and biochemistry of dietary polyphenols, *Nutrients*, **2010**, *2* (12), 1231.
https://doi.org/10.3390/nu2121231.
[51] M. D'Archivio, C. Filesi, R. Di Benedetto, R. Gargiulo, C. Giovannini, R. Masella, Polyphenols, dietary sources and bioavailability, *Ann Ist Super Sanita*, **2007**, *43* (4), 348.
[52] C.D. Stalikas, Extraction, separation, and detection methods for phenolic acids and flavonoids, *J Sep Sci*, **2007**, *30* (18), 3268.
https://doi.org/10.1002/jssc.200700261.
[53] F. Chemat, M. A. Vian, G. Cravotto, Green extraction of natural products: concept and principles, *Int J Mol Sci*, **2012**, *13* (7), 8615.
https://doi.org/10.3390/ijms13078615
[54] M. Solana, I. Boschiero, S. Dall'Acqua, A. Bertucco, A comparison between supercritical fluid and pressurized liquid extraction methods for obtaining phenolic compounds from Asparagus officinalis L, *J Supercr Flu*, **2015**, *100*, 201.
https://doi.org/10.1016/j.supflu.2015.02.014
[55] M. Ashokkumar, Applications of ultrasound in food and bioprocessing, *Ultrason Sonochem*, **2015**, *25*, 17.
https://doi.org/10.1016/j.ultsonch.2014.08.012.
[56] M. Makarewicz, I. Drożdż, T. Tarko, A. Duda-Chodak, The Interactions between Polyphenols and Microorganisms, Especially Gut Microbiota, *Antioxidants*, **2021**, *10* (2),188.
https://doi.org/10.3390/antiox10020188.
[57] M. Efenberger-Szmechtyk, A. Nowak, A. Czyzowska, Plant extracts rich in polyphenols: Antibacterial agents and natural preservatives for meat and meat products, *Crit. Rev. Food Sc. Nutr,* **2021**, *61*, 149.
https://doi.org/10.1080/10408398.2020.1722060
[58] L. Guo, Q. Sun, S. Gong, X. Bi, W. Jiang, W. Xue, P. Fei, Antimicrobial Activity and Action Approach of the Olive Oil Polyphenol Extract Against Listeria monocytogenes, *Front. Microbiol*, **2019**, *10*, 1586.
https:/doi.org/10.3389/fmicb.2019.01586

[59] Z. Alvarado-Martinez, P. Bravo, N.F. Kennedy, M. Krishna, S. Hussain, A.C. Young, D. Biswas, Antimicrobial and Antivirulence Impacts of Phenolics on Salmonella Enterica Serovar Typhimurium, *Antibiotics*, **2020**, *9* (10), 668.
https://doi.org/10.3390/antibiotics9100668 ().
[60] Y. Shoji, H. Nakashima, Nutraceutics and delivery systems, *J Drug Target*, **2004**, *12* (6), 385.
https://doi.org/10.1080/10611860400003817.
[61] B. Hu, X. Liu, C. Zhang, X. Zeng, Food macromolecule based nanodelivery systems for enhancing the bioavailability of polyphenols, *J Food Drug Anal*, **2017**, *25* (1), 3.
https://doi.org/10.1016/j.jfda.2016.11.004
[62] S. Gao, M. Hu, Bioavailability Challenges Associated with Development of Anti-Cancer Phenolics, *Mini Rev Med Chem*, **2010**, *10* (6), 550.
https://dx.doi.org/10.2174/138955710791384081
[63] E. Blanco, H. Shen, M. Ferrari, Principles of nanoparticle design for overcoming biological barriers to drug delivery, *Nat Biotechnol*, **2015**, *33*, 941.
https://doi.org/10.1038/nbt.3330
[64] D.M. Teleanu, C. Chircov, A.M. Grumezescu, R.I. Teleanu, Neuronanomedicine: An up-to-date overview, *Pharmaceutic*, **2019**, *11* (3), 101.
https://doi.org/10.3390/pharmaceutics11030101
[65] N. Zahin, R. Anwar, D. Tewari, M.T. Kabir, A. Sajid, B. Mathew, M.S. Uddin, L. Aleya, M.M. Abdel-Daim, Nanoparticles and its biomedical applications in health and diseases: special focus on drug delivery, *Environ Sci Pollut Res Int*, **2020**, *27* (16), 19151.
https://doi.org/10.1007/s11356-019-05211-0
[66] A. A., Ajazuddin, R.J. Patel RJ, S. Saraf, Recent expansion of pharmaceutical nanotechnologies and targeting strategies in the field of phytopharmaceuticals for the delivery of herbal extracts and bioactives, *J Control Release*, **2016**, *10* (241), 110.
https://doi.org/10.1016/j.jconrel.2016.09.017.
[67] K.H. Kim, M.R. Ki, K.H. Min, S.P. Pack, Advanced Delivery System of Polyphenols for Effective Cancer Prevention and Therapy, *Antioxidants,* **2023**, *12* (5), 1048.
https://doi.org/10.3390/antiox12051048
[68] D. Bhingardeve, S. S. Patil, R. Patil, Phytosome-Valuable Phyto-Phospholipid Carriers, J Curr Phar Res, **2014**, *5* (1), 1386.
https://doi.org/10.33786/JCPR.2014.V05I01.008

[69] R. Rossi, F. Basilico, G. Rossoni, A. Riva, P. Morazzoni, P. Mauri, Liquid chromatography/atmospheric pressure chemical ionization ion trap mass spectrometry of bilobalide in plasma and brain of rats after oral administration of its phospholipidic complex, *J Pharm Biomed Anal*, **2009**, *50* (2), 224.
https://doi.org/10.1016/j.jpba.2009.04.026
[70] T. Lian, R.J. Ho, Trends and developments in liposome drug delivery systems, *J Pharm Sci*, **2001**, *90* (6), 667.
https://doi.org/10.1002/jps.1023.
[71] A.O. Elzoghby, W.M. Samy, N.A. Elgindy, Protein-based nanocarriers as promising drug and gene delivery systems, *J Control Release*, **2012**, *161* (1), 38.
https://doi.org/10.1016/j.jconrel.2012.04.036.
[72] M. Foox, M. Zilberman, Drug delivery from gelatin-based systems, *Expert Opin Drug Deliv*, **2015**, *12* (9), 1547.
https://doi.org/10.1517/17425247.2015.1037272
[73] N. Sahoo, R.K. Sahoo, N. Biswas, A. Guha, K. Kuotsu, Recent advancement of gelatin nanoparticles in drug and vaccine delivery, *Int J Biol Macromol*, **2015**, *81*, 317.
https://doi.org/10.1016/j.ijbiomac.2015.08.006.
[74] T.G. Shutava, S.S. Balkundi, P. Vangala, J.J. Steffan, R.L. Bigelow, J.A. Cardelli, D.P. O'Neal, Y.M. Lvov, Layer-by-Layer-Coated Gelatin Nanoparticles as a Vehicle for Delivery of Natural Polyphenols, *ACS Nano*, **2009**, *3* (7), 1877.
https://doi.org/10.1021/nn900451a.
[75] A. Elgadir, M.S. Uddin, S. Ferdosh, A. Adam, A.J.K. Chowdhury, M.Z.I. Sarker, Impact of chitosan composites and chitosan nanoparticle composites on various drug delivery systems: A review, *J Food Drug Anal*, **2015**, *23* (4), 619.
https://doi.org/10.1016/j.jfda.2014.10.008
[76] T.M. Ways, W.M. Lau, V.V. Khutoryanskiy, Chitosan and Its Derivatives for Application in Mucoadhesive Drug Delivery Systems, *Polymers*, **2018**, *10* (3), 267.
https://doi.org/10.3390/polym10030267.
[77] A. Najmeh, M. Nosrat, M.G. Mohsen; G. Atefeh, Advances in nanomicelles for sustained drug delivery, *J Ind Eng Chem*, **2017**, *55*, 21.
https://doi.org/10.1016/j.jiec.2017.06.050,

[78] L.J. Carlson, B. Cote, A. W.G. Alani, D. A. Rao, Polymeric Micellar Co-delivery of Resveratrol and Curcumin to Mitigate In Vitro Doxorubicin-Induced Cardiotoxicity, *J Pharm Sci*, **2014**, *103* (8), 2315. https://doi.org/10.1002/jps.24042

[79] A. Elham, M. Yahya, J. Seid, G. Mohammad, A. Mehran, Optimization of Folic Acid Nano-emulsification and Encapsulation by Maltodextrin-Whey Protein Double Emulsions, *Int J Bio Macromol, **2016***, 86, 197.

Htpps://doi.org/10.1016/j.ijbiomac.2016.01.064

[80] H. Yu, Q. Huang, Improving the oral bioavailability of curcumin using novel organogel-based nanoemulsions, *J Agric Food Chem*, **2012**, *60* (21), 5373.

Htpps://doi.org/10.1021/jf300609p.

[81] T. V. Verissimo, N.T. Santos, J. R. Silva, Ri. B. Azevedo, A. J. Gomes, C. N. Lunardi, In vitro cytotoxicity and phototoxicity of surface-modified gold nanoparticles associated with neutral red as a potential drug delivery system in phototherapy, *Mater Sci and Eng C Mater Biol Appl*, **2016**, *65*, 199.

https://doi.org/10.1016/j.msec.2016.04.030.

[82] E. Abbasi, S.F. Aval, A. Akbarzadeh, M. Milani, H.T. Nasrabadi, S.W. Joo, Y. Hanifehpour, K. Nejati-Koshki, R. Pashaei-Asl, Dendrimers: synthesis, applications, and properties, *Nanoscale Res Let,* **2014**, *9* (1), 247.

https://doi.org/10.1186/1556-276X-9-247.

[83] A.D. Bangham, M.M. Standish, J.C. Watkins, Diffusion of univalent ions across the lamellae of swollen phospholipids, *J Mol Biol*, **1965**, *13*, 238.

https://doi.org/10.1016/S0022-2836(65)80093-6

[84] A.D. Bangham, M.M. Standish, J.C. Watkins, G. Weissmann, The diffusion of ions from a phospholipid model membrane system, *Protoplasma*, **1967**, *63* (1),183.

[85] G. Gregoriadis, P.D. Leathwood, B.E. Ryman, Enzyme entrapment in liposomes, *FEBS Lett*, *1975*, *14*, 95.

https://doi.org/10.1016/0014-5793(71)80109-6

[86] I.M. Hann, H.G. Prentice, Lipid-based amphotericin B: a review of the last 10 years of *use, Int J Antimicrob Agents*, **2001**, *17*, 161.

https://doi.org/10.1016/S0924-8579(00)00341-1

[87] J.N. Israelachvili, S. Marcelja, R.G. Horn, Physical principles of membrane organization, *Q Rev Biophys*, **1980**, *13* (2), 121.

https://doi.org/10.1017/s0033583500001645

[88] D.D. Lasic, Novel applications of liposomes*, Trends Biotechnol*, **1998**, *16* (7), 307. https://doi.org/10.1016/s0167-7799(98)01220-7.

[89] H. Luiz, J. Oliveira Pinho, M.M. Gaspar, MAdvancing Medicine with Lipid-Based Nanosystems—The Successful Case of Liposomes, *Biomedicines,* **2023**, *11*, 435. https://doi.org/10.3390/biomedicines11020435

[90] V.P. Torchilin, Recent advances with liposomes as pharmaceutical carriers, *Nat Rev Drug Discov,* **2005**, *4* (2), 145.

htpps://doi.org/10.1038/nrd1632.

[91] B.S. Pattni, V.V. Chupin, V.P. Torchilin, New Developments in Liposomal Drug Delivery, *Chem Rev*, **2015**, *14*, 10938.

https://doi.org/10.1021/acs.chemrev.5b00046

[92] T.M. Allen, P.R. Cullis, Liposomal drug delivery systems: From concept to clinical applications, *Adv Drug Deliv Rev*, **2013**, *65*, 36.

https://doi.org/10.1016/J.ADDR.2012.09.037

[93] Z. Drulis-Kawa, A. Dorotkiewicz-Jach, Liposomes as delivery systems for antibiotics, *Int J Pharm*, **2010**, *387*, 187.

https://doi.org/10.1016/J.IJPHARM.2009.11.033

[94] M. Li, C. Du, N. Guo, Y. Teng, X. Meng, H. Sun, S. Li, P. Yu, H. Galons, Composition design and medical application of liposomes, *Eur J Med Chem*, **2019**, *164*, 640. https://doi.org/10.1016/J.EJMECH.2019.01.007

[95] Barenholz Y. Doxil®-the first FDA-approved nano-drug: lessons learned, *J Control Release*, **2012**, *10*, 117.

https://doi.org/10.1016/j.jconrel.2012.03.020.

[96] K.V. Clemons, D.A. Stevens, Comparative efficacies of four amphotericin B formulations--Fungizone, amphotec (Amphocil), AmBisome, and Abelcet--against systemic murine aspergillosis. *Antimicrob Agents Chemother*, **2004**, *48* (3), 1047.

https://doi.org/10.1128/AAC.48.3.1047-1050.2004

[97] B. Carvalho, L.M. Roland, L.F. Chu, V.A. Campitelli, E.T. Riley, Single-dose, extended-release epidural morphine (DepoDur) compared to conventional epidural morphine for post-cesarean pain, *Anesth Analg*, **2007**, *105* (1), 176.

https://doi.org/10.1213/01.ane.0000265533.13477.26

[98] M.W. Saif, MM-398 achieves primary endpoint of overall survival in phase III study in patients with gemcitabine refractory metastatic pancreatic cancer, *JOP*, **2014**, *27*, 278. https://doi.org/10.6092/1590-8577/2507.

[99] F.S. Farhat, S. Temraz, J. Kattan, K. Ibrahim, N. Bitar, N. Haddad, R. Jalloul, H.A. Hatoum, G. Nsouli, A. Shamseddine, A phase II study of lipoplatin (liposomal cisplatin)/vinorelbine combination in HER-2/neu-negative metastatic breast cancer, *Clin Breast Cancer,* **2011**, *11*, 384. https://doi.org/10.1016/j.clbc.2011.08.005

[100] Y.L Wu, K. Park, R.A. Soo, Y. Sun, K. Tyroller, D. Wages, G. Ely, J.C. Yang, T. Mok, INSPIRE: A phase III study of the BLP25 liposome vaccine (L-BLP25) in Asian patients with unresectable stage III non-small cell lung cancer, *BMC Cancer*, **2011**, *7* (11), 430. https://doi.org/10.1186/1471-2407-11-430

[101] J. Li, X. Wang, T. Zhang, C. Wang, Z. Huang, X. Luo, Y. Deng, A review on phospholipids and their main applications in drug delivery systems, *Asian J Pharm Sci*, **2015**, *10*, 81. https://doi.org/10.1016/j.ajps.2014.09.004

[102] A. Pannwitz, D.M. Klein, S. Rodriguez-Jimenez, C. Casadevall, H. Song, E. Reisner, L. Hammarstrom, S. Bonnet, Roadmap towards solar fuel synthesis at the water interface of liposomes membranes, *Chem. Soc. Rev.*, **2021**, *50*, 4833. https://doi.org/10.1039/D0CS00737D

[103] S. Vemuri, C.T. Rhodes, Preparation and characterization of liposomes as therapeutic delivery systems: a review, *Pharm Acta Helv*, **1995**, *70* (2), 95. https://doi.org/10.1016/0031-6865(95)00010-7.

[104] B. de Kruyff, R.A. Demel, L.L. van Deenen, The effect of cholesterol and epicholesterol incorporation on the permeability and on the phase transition of intact Acholeplasma laidlawii cell membranes and derived liposomes, *Biochim Biophys Acta*, **1972**, *17*. https://doi.org/10.1016/0005-2736(72)90032-6.

[105] J.N. Israelachvili, D.J. Mitchell, A model for the packing of lipids in bilayer membranes, *Biochimica et Biophysica Acta (BBA) – Biomembranes*, **1975**, *389*, 13. https://doi.org/10.1016/0005-2736(75)90381-8

[106] G. Bozzuto, A. Molinari, Liposomes as nanomedical devices, *Int J Nanomedicine*, **2015**, *10*, 975. https://doi.org/10.2147/IJN.S68861

[107] R.L. Juliano, D. Stamp, The effect of particle size and charge on the clearance rates of liposomes and liposome encapsulated drugs, *Biochem Biophys Res Commun*, **1975**, *7*, 651.

https://doi.org/10.1016/s0006-291x(75)80433-5

[108] S.M. Johnson, The effect of charge and cholesterol on the size and thickness of sonicated phospholipid vesicles, *Biochim Biophys Acta*, **1973**, *25*, 27.

https://doi.org/10.1016/0005-2736(73)90022-9.

[109] C. R. Miller, B. Bondurant, S. D. McLean, K. A. McGovern, D. F. O'Brien, Liposomes-Cell Interaction in Vitro: Effect of Liposome Surface Charge on the Binding and Endocytosis of Conventional and Sterically Stabilized Liposomes, B*iochemistry*, **1998**, *37* (37), 12875.

https://doi.org/10.1021/bi980096y

[110] P. Yingchoncharoen, D.S. Kalinowski, D.R. Richardson, Lipid-based drug delivery systems in cancer therapy: What is available and what is yet to come, *Pharmacol Rev*, **2016**, *68*, 701. https://doi.org/10.1124/pr.115.012070

[111] C.R. Dass, P.F.M. Choong, Targeting of small molecule anticancer drugs to the tumour and its vasculature using cationic liposomes: Lessons from gene therapy, *Cancer Cell Int*, **2006**, *6* (17). https://doi.org/10.1186/1475-2867-6-17

[112] W. Chen, H. Li, Z. Liu, W. Yuan, Lipopolyplex for Therapeutic Gene Delivery and Its Application for the Treatment of Parkinson's Disease, *Front Aging Neurosci*, **2016**, *5* (8), 68.

https://doi.org/10.3389/fnagi.2016.00068.

[113] Z. Drulis-Kawa, A. Dorotkiewicz-Jach, Liposomes as delivery systems for antibiotics, *Int J Pharma*, **2010**, *387* (1), 187.

https://doi.org/10.1016/j.ijpharm.2009.11.033

[114] W. Doroszkiewicz, The interaction between Pseudomonas aeruginosa cells and cationic PC:Chol:DOTAP liposomal vesicles versus outer-membrane structure and envelope properties of bacterial cell, *Int* l *J Pharma*, **2009**, *367*, 211.

https://doi.org/10.1016/j.ijpharm.2008.09.043

[115] W. Da-Yuan, H.C. van der Mei, R. Yijin, J. Busscher Henk, S. Linqi; Lipid-Based Antimicrobial Delivery-Systems for the Treatment of Bacterial Infections, *Front Chem*, **2020**, *7*, 2296.

https://doi.org/10.3389/fchem.2019.00872

[116] B. Kneidl, M. Peller, G. Winter, L.H. Lindner, M. Hossann, Thermosensitive liposomal drug delivery systems: state of the art review, *Int J Nanomedicine*, **2014**, *16* (9), 4387.

https://doi.org/10.2147/IJN.S49297.

[117] M. Alhariri, A. Azghani, A. Omri, Liposomal antibiotics for the treatment of infectious diseases, *Expert Opin Drug Deliv***, 2013**, *10* (11), 1515.

https://doi.org/10.1517/17425247.2013.822860.

[118] A. Mauceri, L. Giansanti, G. Bozzuto, M. Condello, A. Molinari, L. Galantini, A. Piozzi, G. Mancini, Structurally related glucosylated liposomes: Correlation of physicochemical and biological features, *Biochim Biophys Acta Biomembr*, **2019**, *1* (8),1468.
https://doi.org/10.1016/j.bbamem.2019.06.003.

[119] D. Nicolosi, M. Scalia, V.M. Nicolosi, R. Pignatello, Encapsulation in fusogenic liposomes broadens the spectrum of action of vancomycin against Gram-negative bacteria, *Int J Antimicrob Agents*, **2010**, *35* (6), 553.
https://doi.org/10.1016/j.ijantimicag.2010.01.015.

[120] M. Ferreira, M. Ogren M, J.N.R. Dias, M. Silva, S. Gil, L. Tavares, F. Aires-da-Silva, M.M. Gaspar, S.I. Aguiar, Liposomes as Antibiotic Delivery Systems: A Promising Nanotechnological Strategy against Antimicrobial Resistance, *Molecule*s, **202,** *2* (7), 2047.
https://doi.org/10.3390/molecules26072047.

2. Aim of the thesis

The pharmacological treatment of drug-resistant bacteria infections, caused by both planktonic and biofilm forming bacteria, is one of the main challenges of the 21st century.

It is well known that the research and the development of new antibiotic agents is a laborious process, which consequently cannot keep up with rising rate of drug resistance. Therefore, an appealing alternative to the discovery of new drugs could be represented by the use of natural antimicrobials derived from plant matrixes.

In this regard, the biological activities of plant extracts have been widely attributed to the presence of different biomolecules known to elicit therapeutic effects. Among all these compounds, plant polyphenols exhibit a wide range of biological effects, including antimicrobial activity against *Gram*-positive and *Gram*-negative bacteria, either as single biocompound or as phytocomplexes, exploiting, in this latter case, the synergistic action of the numerous biomolecules present.

However, despite the positive effects on human well-being, the use of polyphenols is limited because of their low solubility, poor stability, extensive metabolic degradation and rapid elimination, culminating in low bioavailability after any systemic administration.

To overcome all these limitations, polyphenols can be encapsulated in liposomes, which are probably the most widely studied and well-investigated nanocarriers for targeted drug delivery, thanks to all their unique physicochemical features.

The work described in this thesis aims to investigate the *in vitro* antimicrobial activity of plant derived polyphenols examining the effect of the encapsulation in liposomes on their activity.

In the perspective of a circular economy, plant extracts rich in polyphenols have been obtained through the recovery and reuse of agri-food by-products and waste, such as olive leaves and orange peels. The antimicrobial experiments have been conducted on the phytocomplexes in their entirety and evaluating the contribution of single polyphenols.

Polyphenols have been embedded in liposomes to improve their pharmacokinetic limitations; moreover, liposomes have been functionalized to enhance the interaction on the selected target bacteria.

Different types of amphiphiles (**Chart 1**) have been exploited in the production of liposomes investigated in this thesis, in particular:

- Natural lipids derived from phosphatidylcholine esterified with different acyl chains, namely 1,2-dioleoyl-*sn*-glycero-3-phosphocholine (C18:1 DOPC), 1,2-dipalmitoyl-*sn*-glycero-3-phosphocholine (C16:0 DPPC) and 1,2-dimyristoyl-*sn*-glycero-3-phosphocholine (C14:0 DMPC).
- A synthetic galactosylated amphiphile, GLT1, characterized by a hydrophobic chain, a polar head functionalized with a galactose residue and a hydrophilic spacer composed by a polyethylene glycol chain, an azido group and a quaternary nitrogen. The positive charge and the sugar moiety of this amphiphile should enhance the interaction between liposomes and bacteria cells.
- A synthetic cationic amphiphile, namely allyl-hexadecyl-dimethyl-ammonium iodide (LIPCAT), characterized by a polar head composed by a quaternary nitrogen and a hydrophobic alkyl chain, which should be able to enhance the electrostatic interaction between cationic liposomes and negatively charged bacteria.

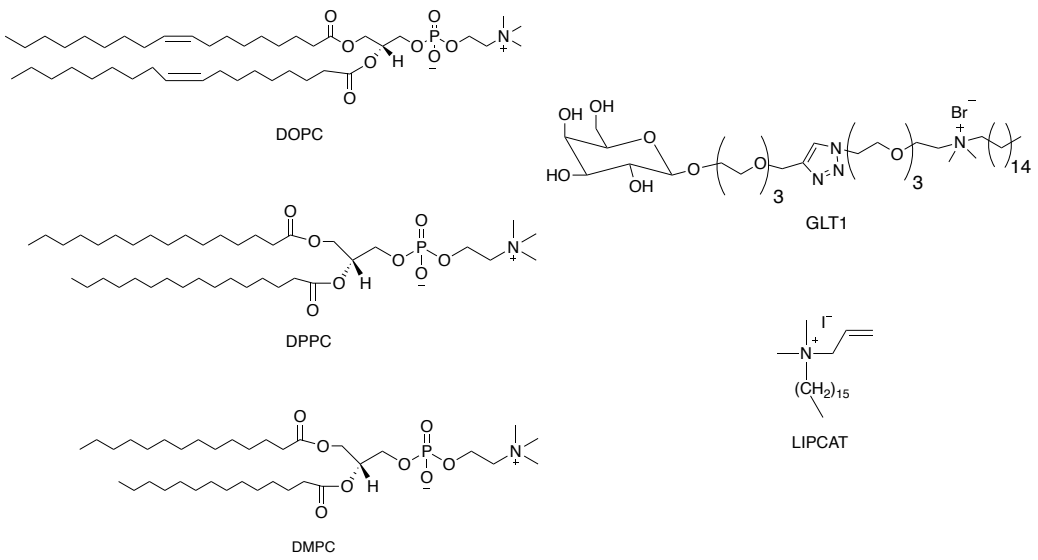

Chart 1. Amphiphilic components used in liposome formulations.

The antimicrobial activity of polyphenols free and entrapped in liposomes has been evaluated *in vitro* against different bacteria pathogens such as *Staphylococcus aureus*, *Enterococcus faecalis*, *Bacillus subtilis*, *Escherichia coli*, *Pseudomonas aeruginosa* and *Klebsiella oxytoca*. All these bacterial strains can be resistant to more than one antibiotic and are able to develop biofilms; moreover, they are responsible for many infections in hospital and community environments that are associated with high mortality rates.[1-5]

2.1. References

[1] H. Boucher, L. G. Miller, R. R. Razonable, Serious Infections Caused by Methicillin-Resistant *Staphylococcus aureus* Clinical Infectious Diseases, *Clin Microbiol Rev*, **2010**, *51*, 603. https://doi.org/10.1128/CMR.00134-14

[2] J.A.T. Sandoe, I.R. Witherden, J.H. Cove, J. Heritage, M.H. Wilcox, Correlation between enterococcal biofilm formation in vitro and medical-device-related infection potential in vivo, J *Med Microbiol*, **2003**, *52* (7), 547.
https://doi.org/10.1099/jmm.0.05201-0

[3] L.S. Cairns, L. Hobley, N.R. Stanley-Wall, Biofilm formation by Bacillus subtilis: new insights into regulatory strategies and assembly mechanisms, *Mol Microbiol*, **2014**, *93* (4), 587.
https://doi.org/10.1111/mmi.12697

[4] H.S. Cho, J.H. Lee, S.Y. Ryu, S.W. Joo, M.H. Cho, J. Lee, Inhibition of Pseudomonas aeruginosa and Escherichia coli O157:H7 biofilm formation by plant metabolite ε-viniferin, *J Agric Food Chem*, **2013**, *61* (29), 7120.
https://doi.org/10.1021/jf4009313

[5] L. Singh, M.P. Cariappa, M. Kaur, Klebsiella oxytoca: An emerging pathogen?, *Med J Armed Forces India*, **2016**, *72*(1), S59.
https://doi.org/10.1016/j.mjafi.2016.05.002

3. Bacteriostatic and anti-biofilm activity of *trans*-resveratrol free and loaded in liposomes on *S. aureus* strains

3.1. Introduction

Trans-resveratrol (3,5,4'-trihydroxystilbene, RSV) is a stilbenoid polyphenol produced as a secondary metabolite by many plants to fight external attacks by pathogens. It is especially present in red wine, soybeans, grapes, peanuts, mulberries, blueberries and pomegranates.[1] *Trans*-resveratrol is the most pharmacologically active form, but it can be converted into the less active *cis* isomer by UV-light irradiation or direct sunlight.[2]

RSV has a wide spectrum of antimicrobial activities against many *Gram*-positive and *Gram*-negative bacterial strains. In particular, this polyphenol exhibits antimicrobial and anti-biofilm activity on several *S. aureus* strains, both resistant and non-resistant to diverse antibiotics.[1,3-5]

RSV antimicrobial action seems to be related to its ability to interfere with the bacteria cell cycle,[4,6] though the mechanism of bacterial growth inhibition is not yet fully understood.[1]

Although it seems well-established that the antimicrobial action of RSV on *S. aureus* is bacteriostatic and not bactericidal, discordant results are reported in the literature, even on the same bacterial strain. In fact, not only different *Minimum Inhibitory Concentration* (MIC) values are reported, but in some experiments no antibacterial activity is even found.

Regarding the anti-biofilm activity, we are faced with the same scenario: some authors report that RSV does not inhibit *S. aureus* biofilm formation,[5,7] others report that it reduces the ability of *S. aureus* to form biofilm by disruption of mature biofilms.[8,9]

Also, in the case of biofilm, it is unclear whether the RSV anti-biofilm activity is related to its anti-adhesive or antibacterial properties. These discrepancies may be due to the different solubility of RSV in the media used for experimental treatments and to the different working culture broths (Mueller-Hinton and Luria-Bertani, respectively).

Furthermore, the experimental data reported in the literature show RSV antimicrobial properties at concentrations that are higher than those obtainable in plasma following oral administration, as a consequence of the low bioavailability and high biodegradability of RSV.[10-12]

Therefore, there is a limit to the treatment of infections by RSV dictated by the bioavailability of the drug itself.[11] In order to increase RSV bioavailability, and thus to give a future perspective to the positive results of the *in vitro* studies, it is necessary to turn to nanotechnology, which provides the techniques for developing suitable nanosystems for RSV delivery. In this context, liposomes have

been widely demonstrated to improve the antimicrobial efficacy of many drugs against *S. aureus* and MRSA and remain one of the most promising delivery systems even for combination therapies.[13]

In this chapter, we investigated the effective bacteriostatic and antibiofilm activity of RSV on two strains of *S. aureus*, wild type (ATCC 25923) and methicillin resistant (ATCC 33591), paying particular attention to the benefits brought by liposomal delivery on the antimicrobial properties of RSV. In fact, given the poor solubility of RSV in biological fluids, it is important to study the physicochemical properties and the actual biological effects of the liposome formulation, that may differ from that of free RSV: liposomes can enhance or reduce the biological effect or even give rise to a new activity. To this purpose, RSV was embedded in liposomes formulated with a natural phospholipid (1,2-dioleoyl-*sn*-glycero-3-phosphocholine, DOPC) and cholesterol (Chol), in the presence and in the absence of a cationic galactosylated amphiphile, GLT1, that has been already proven to enhance RSV-loaded liposome activity in demolition experiments of mature MRSA biofilm[9] (**Chart 1**).

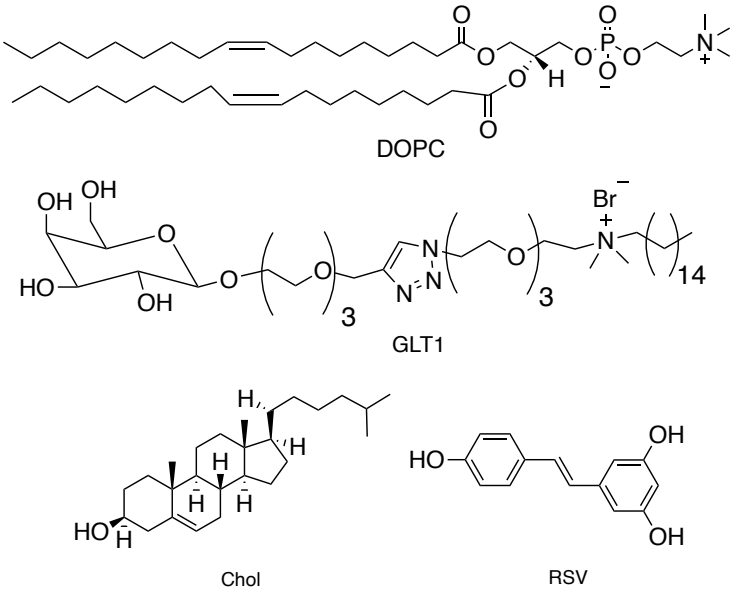

Chart 1. Molecular structures of liposome components (DOPC, Chol and GLT1) and *trans*-resveratrol (RSV)

The colloidal stability of liposomes was monitored over time by Dynamic Light Scattering (DLS) and Dynamic Electrophoretic Light Scattering (DELS) measurements, while the interaction between liposomes and both bacteria pathogens was investigated by DELS measurements to reveal any preferential interaction of the galactosylated cationic liposomes with the bacterial surface. The entrapment efficiency and the release profile of RSV *in vitro* were evaluated by UPLC analysis.

The antibiofilm activity of RSV, free and liposome-loaded, was investigated against *S. aureus* wild type strain, according to a mature biofilm experimental model assessed in a previous study on MRSA.[9] Furthermore, the antibiofilm properties were investigated by analyzing the antiadhesive effects induced by liposome-loaded RSV or free RSV, against both bacteria pathogens.

Finally, due to the discordant data reported in the literature, we also estimated the bacteriostatic effect induced by RSV, free or embedded in liposome, on both bacteria strains; moreover, to clarify whether the antimicrobial effect might have been associated to damages to the bacterial cell wall, we stained the bacteria with propidium iodide in the presence of RSV.

3.2. Results and Discussion

3.2.1. Synthesis of the galactosylated amphiphile GLT1

The galactosylated amphiphile **GLT1** has been synthesized to be included in liposomal formulations for the delivery of RSV with the aim to target bacteria cells involved in our study.

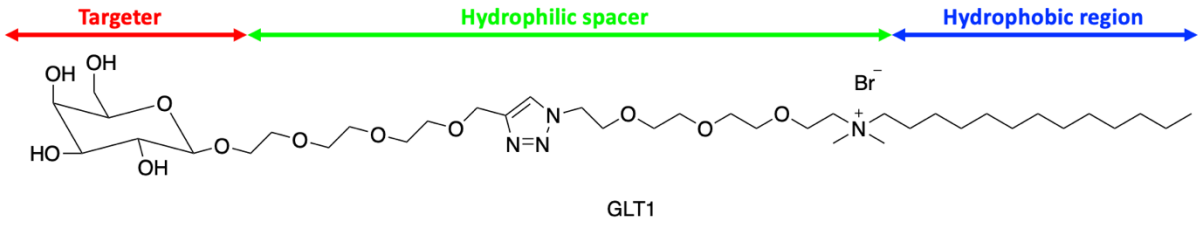

GLT1

Figure 1. Molecular structure of galactosylated amphiphile GLT1.

The structure of galactosylated amphiphile **GLT1** (**Figure 1**) features:

- a sugar moiety of galactose, which should be able to improve the interaction between liposomes and bacteria due to specific lectins and sugar protein transporters expressed on bacteria cellular membrane.[14-16]
- a hydrophilic spacer composed by a polyethylene glycol chain, an azido group and a quaternary nitrogen, which should guarantee a good exposure of the galactose residue on the external liposomal surface.
- a hexadecyl hydrophobic chain, which promotes the inclusion of GLT1 into the liposome lipid bilayer.

GLT1 has been synthesized according to a synthetic pathway (**Scheme 1**) reported in the literature and developed by the group where this thesis was carried out.[17]

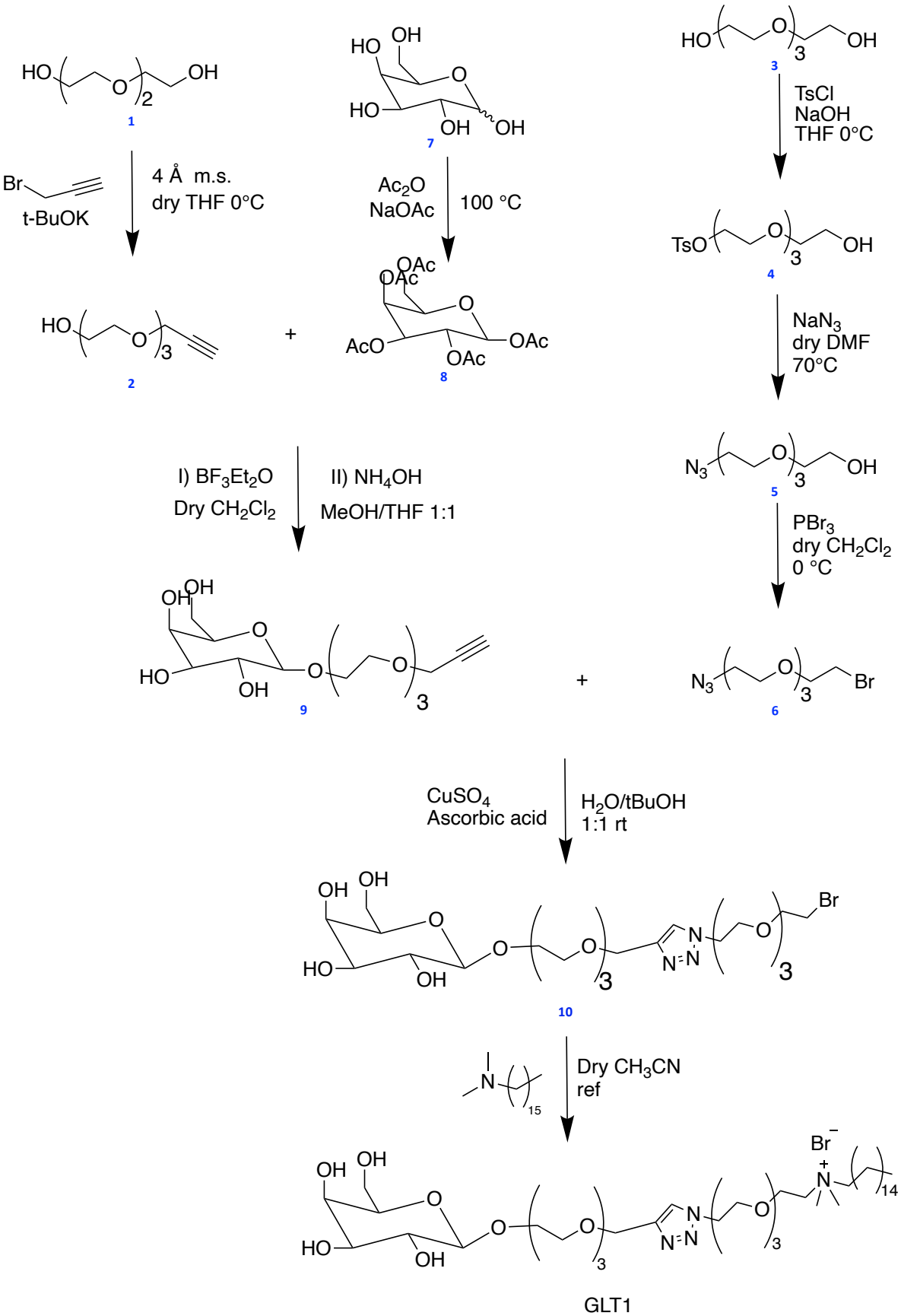

Scheme 1. Synthetic route for GLT1 preparation.

The key step of the synthetic pathway is a Cu(I)-catalyzed azide–alkyne 1,3-dipolar cycloaddition between compound **6** and **9** to selectively obtain the 1-4 regioisomer compound **10.**

Compound **6** was synthesized following a three steps reaction: monotosylation of tetraethylene glycol, azidation of monotosylated tetraethylenglycol and bromuration of the azido-compound.

The galactosylated compound **9** characterized by the terminal alkyne group was obtained by glycosylation of the peracetylated sugar **8** with propargylated triethylene glycol **2.** This latter was synthesized by selective mono-propargylation of triethylene glycol.

The peracetylated sugar **8** was prepared by peracetylation of D-galactopyranoside **7** with acetic anhydride, both α and β anomers were obtained, then the β anomer was exclusively isolated by crystallization in ethanol.

Finally, GLT1 was obtained by alkylation of *N*,*N*-dimethyl-hexadecyl-amine with compound **10**.

3.2.2. Liposomes preparation

Liposome as delivery systems of RSV were formulated with a natural unsaturated phospholipid (DOPC) and cholesterol (Chol), in presence or absence of the cationic galactosylated amphiphile GLT1 previously synthetized (**Chart 1**). Moreover, empty liposomes, both neutral and galactosylated were also prepared as reference samples.

The inclusion of cholesterol in the lipid mixture enhances the stability of the lipid bilayer through the *bilayer-tightening effect* inducing a dense packing and increasing the orientation order of lipid chains. This leads to a more compact structure with reduced permeability to water soluble molecules and increased retention of the entrapped drugs.[18] Furthermore, cholesterol was added to all the formulations to improve the lipid bilayer stability mostly in presence of GLT1 because of its detergent properties and ability to the destabilize the lipid bilayer leading to the formation of micellar aggregates rather than liposomes.[19]

The presence of GLT1 as cationic amphiphile in the lipid bilayer should enhance interactions with the bacterial cells in two ways: from one hand the cationic charge allows an electrostatic interaction with the negatively charged bacterial membrane, from the other the galactosylated moiety should improve the interaction due to specific lectins and sugar protein transporters expressed on bacteria cellular membrane.[15,20]

Liposomes 20 mM in total lipid concentration were prepared in PBS (150 mM) by the thin lipid film hydration method, coupled with the freeze-thaw protocol and followed by an extrusion process, thus obtaining unilamellar vesicles with dimensions around 100 nm. RSV was entrapped by passive

loading in the lipid bilayer, samples containing RSV were sonicated at 40 W (10 cycles of 10 s) using a probe sonicator before freeze-thaw cycles, to break RSV aggregates in aqueous solutions and enhance its entrapment in the lipid bilayer.[21]

Finally, unentrapped RSV was removed by dialysis after the extrusion step.

3.2.3. Liposomes physicochemical characterization

For all liposomes the values of hydrodynamic diameter (D_h), polydispersity index (PDI), ζ-potential and RSV Entrapment Efficiency (EE%) were investigated.

The results reported in **Table 1** are consistent with those reported in the literature,[9] demonstrating reproducibility and reliability of the experimental procedures.

Table 1. Physicochemical features of empty and loaded liposomes (20 mM in total lipids) in PBS (pH 7.4)

Formulation	Composition	D_h (nm)	PDI	ζ-potential (mV)	EE (%)	RSV (mM)
L	DOPC/Chol 8.0:2.0	108 ± 2	0.09 ± 0.01	-1 ± 1	-	-
LR	DOPC/Chol/RSV* 8.0:2.0:2.5	99 ± 1	0.11 ± 0.01	-3 ± 2	71 ± 3	1.78 ± 0.08
LG	DOPC/Chol/GLT1 7.5:2.0:0.5	95 ± 3	0.08 ± 0.01	18 ± 1	-	-
LGR	DOPC/Chol/GLT1/RSV* 7.5:2.0:0.5:2.5	97 ± 2	0.10 ± 0.01	18 ± 1	88 ± 2	2.11 ± 0.13

*[RSV]/[lipids] ratio at the beginning of the preparation is 1/8

Liposomes particle size distribution and polydispersity index were investigated by dynamic light scattering (DLS) measurements. Results reported in **Table 1** show a narrow size distribution for all liposomes, with a diameter between 95 nm and 108 nm and a low PDI (0.08-0.11), according to the extrusion protocol adopted. It is worth to note the slight reduction in size for galactosylated formulations (LG and LGR) compared to the neutral ones (L and LR). This evidence could be related to the arrangement of GLT1 within the DOPC/Chol bilayer due to the larger interfacial area of GLT1 with respect to DOPC, which could force the aggregates to adopt a stronger curvature resulting in smaller diameters.[17,19]

To investigate the surface charge of liposomes, ζ-potential values were determined by Dielectrophoretic Light Scattering (DELS) measurements, using the phase analysis light scattering (PALS). According to the results reported in **Table 1**, DOPC/Chol empty liposomes feature negative

ζ-potential value due to the exposure of the phosphocholine phosphate groups. In presence of RSV, a slight decrease of ζ-potential value was recorded probably due to the localization of RSV in tight packed membranes at the membrane surface rather than the inner region, suggesting the affinity of RSV hydroxyl groups for lipid headgroups by replacing of water molecules localized at the hydrophilic and hydrophobic interface.[22] Moreover, at pH 7.4 in mixed membranes a small percentage of RSV is ionized and the negatively charged groups are oriented towards the interface making the ζ-potential more negative.[23] On the other hand, DOPC/Chol/GLT1 liposomes highlighted a positive and quite high ζ-potential value both in presence and in absence of RSV. This evidence may be related to some reasons: the deeper position of RSV inside the functionalized lipid bilayer due to a possible interaction between RSV and the galactosylated amphiphile resulting in a lower degree of dissociation,[24] and a higher hydration of the bilayer because of the presence of the polyoxyethylenic spacer.

The loaded RSV content in liposomes (EE%) was evaluated by UPLC measurements. According to the results reported in **Table 1**, galactosylated liposomes entrapped a higher amount of RSV compared to DOPC/Chol based liposomes. The ability of cationic liposomes to entrap higher amount of RSV may be related to the interaction between RSV and quaternary ammonium group of the galactosylated lipid.[24]

3.2.3.1. Stability studies

To investigate the stability over time of neutral and galactosylated liposomes, both empty and RSV-loaded, samples were stored at room temperature and in the dark protected from light sources to avoid the isomerization of *trans*-resveratrol in the less active *cis* isomer.

The physical stability of liposomes was investigated following particles hydrodynamic diameter, PDI and ζ-potential values at different times, up to 14 days of storage, with the aim to highlight any aggregation phenomena. All data collected are reported in **Figure 2.**

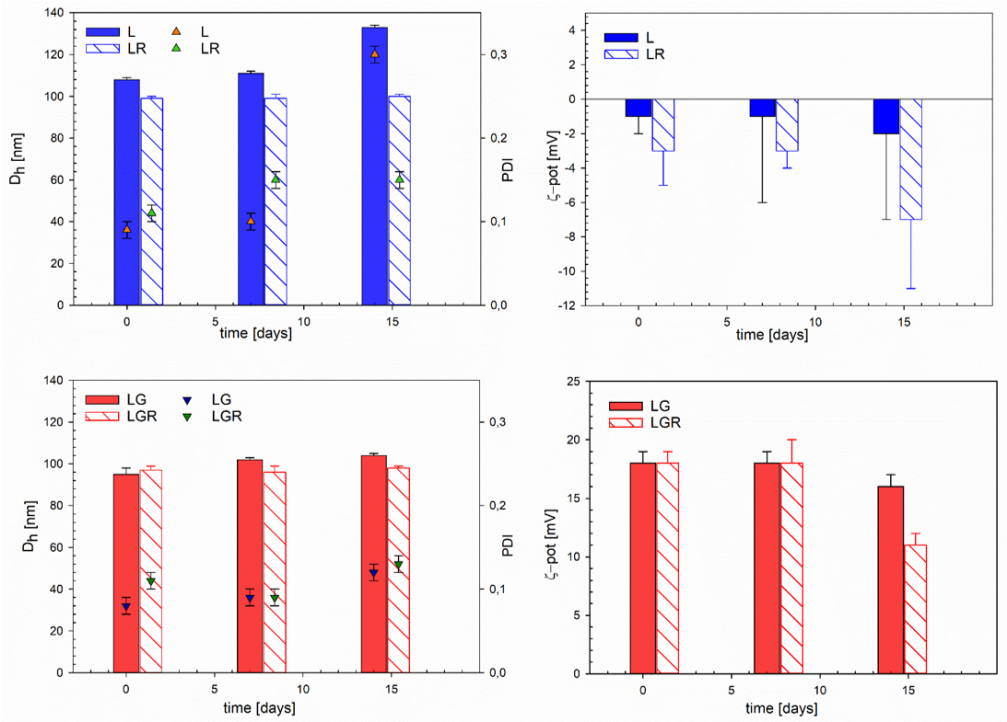

Figure 2. Colloidal properties upon time of liposomes (1 mM in total lipids) in PBS. D_h and PDI are the hydrodynamic diameter and the polydispersity index, respectively, calculated by the cumulants method; ζ-pot is the ζ-potential determined using the phase analysis light scattering. Solid bars correspond to RSV-loaded liposomes, stripped bars to the empty ones. The error bars associated to D_h, PDI, ζ-pots are the standard deviations of three repeated measurements on three different samples.

The formulations are stable for two weeks during storage, without any significant changes in size and PDI, except for LGR liposomes for which a decrease in ζ-potential was observed. This effect may be due to the migration of RSV towards the surface, which represents a more hydrated environment: in these conditions, RSV can partially undergo ionization, with the negatively charged hydroxyl group oriented towards the lipid water interface, thus making the potential less positive.[25]

3.2.3.2. *In vitro* release study

With the goal of evaluating the release profiles of RSV from neutral and galactosylated liposomes, an *in vitro* release study was performed by dialysis method. Samples were examined by UPLC analysis to determine the % leakage of RSV over time monitored for a period of 24 h.

Figure 3 shows the amount of RSV released from DOPC/Chol and DOPC/Chol/GLT1 liposomes. The % leakage of RSV from DOPC/Chol liposomes was higher than that recorded for galactosylated liposomes. This result could be related to the possible interaction between RSV and the galactosylated amphiphile as discussed above,[24,26] resulting in the reduction of drug release rate compared to the data collected from the release study of RSV from DOPC/Chol liposomes. However,

both release curves highlighted a quite similar trend characterized by a quick release during the first 7 h followed by a gradual slow release until 24 h. A final RSV leakage of ~ 60% and ~ 40% from DOPC/Chol and DOPC/Chol/GLT1 liposomes was observed respectively.

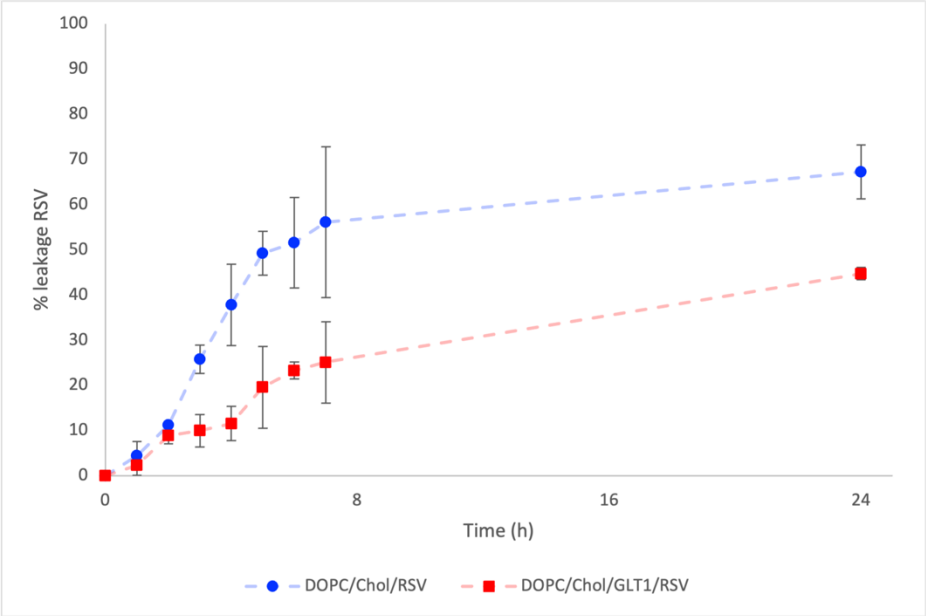

Figure 3. Leakage of RSV up to 24 h from DOPC/Chol liposomes (blue circle) and DOPC/Chol/GLT1 liposomes (red square).

3.2.4. Liposomes-bacteria interaction

The electrostatic interaction of neutral and cationic galactosylated liposomes with bacteria was investigated by ζ-potential measurements to highlight the formulation able to interact more efficiently with bacteria cells involved in the study. To this purpose, ζ-potential is considered as a simple and powerful tool thanks to the different ζ-potential values that bacteria and liposomes feature, which are determined by both surface charge and ions associated to the surface.[27] Indeed, bacteria always display a negative ζ-potential value, while liposomes show variable values depending on the lipidic components involved. Neutral liposomes composed of DOPC and Chol are characterized by a slightly negative ζ-potential, while cationic galactosylated liposomes composed of DOPC, Chol and GLT1 show positive values. The interaction between bacteria and liposomes results in different ζ-potential values compared to that of bacteria and liposomes before mixing.

All the experiments were carried out keeping the bacteria concentration at 10^5 CFU/mL and varying liposomal concentrations from 0.1 mM to 1 mM in total lipids. In this concentration range, the number of liposomes present in the solution is between 10^{11} - 10^{12} liposomes/mL,[28] always larger than the one of bacteria. Thus, in the absence of specific interactions, the ζ-potential value of the

mixture will reflect the ζ-potential of liposomes. The results of ζ-potential measurements are reported in **Figure 4**; ζ-potential values of liposomes alone as a function of concentration are also reported as a reference. As expected, both *S. aureus* wild type and MRSA showed a negative ζ-potential value around -4 mV and -7 mV respectively.

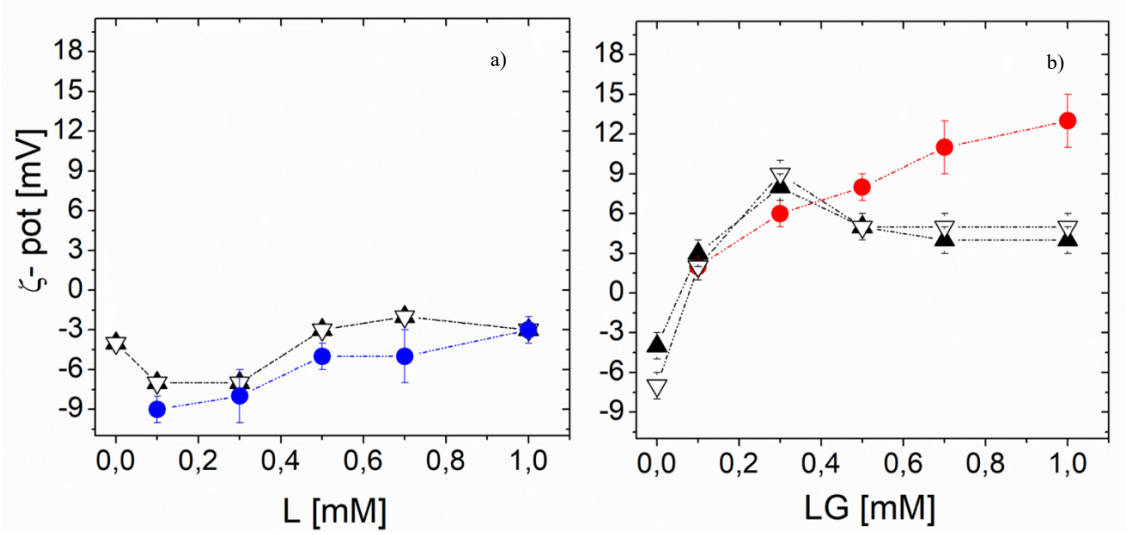

Figure 4. ζ-potential values of a 10^5 CFU/mL dispersion of bacteria in PBS 15 mM as a function of added liposome concentration.
a) blue dots: L (DOPC/Chol) liposomes alone; black triangle = ζ-potential values of *S. aureus* wild type strain in the presence of L liposomes; white triangle = ζ-potential values of MRSA strain in the presence of L liposomes.
b) red dots: LG (DOPC/Chol/GLT1) liposomes; black triangle = ζ-potential values of *S. aureus* wild type strain in the presence of LG liposomes; white triangle = ζ-potential values of MRSA strain in the presence of LG liposomes

After addiction of low concentration of DOPC/Chol liposomes the ζ-potential of the mixed liposome-bacteria suspension is slightly decreased, probably due to the mixing of liposomes and less negative bacteria, both for *S. aureus* wild type and MRSA. In fact, the behavior of mixed bacteria-liposomes suspensions is very similar to the one of liposomes alone, thus suggesting that the main contribution to the measured value of ζ-potential stems from neutral liposomes, which do not interact with bacteria and remain un-associated. At 1 mM no difference in ζ-potential can be observe, because of the large excess of liposomes in the suspension. On the contrary, for DOPC/Chol/GLT1 formulation, while in absence of bacteria the ζ-potential of the reference liposomal suspension increases with concentration, the very different trend measured in the mixed liposome-bacteria suspension suggest the presence of interaction between bacteria and cationic galactosylated liposomes. The electrostatic interaction between galactosylated liposomes and negatively charged bacteria is evident in the progressive reduction of the measured value of ζ-potential, which reaches a maximum close to 0.3 mM in total lipids, then decreases again for both

the bacteria strains. Above 0.3 mM, a saturation in liposome-bacteria interaction probably occurs and liposomes are mostly associated, so that a further liposomes addition does not promote any variation in the measure value. The observed slight decrease above 0.3 mM could be attribute to screening effect.

3.2.5. Antimicrobial properties of RSV

3.2.5.1. Antibiofilm RSV activity on *S. aureus* wild type

To assess whether RSV, free or delivered by liposomes, has a different efficacy in reducing biofilm on two different *S. aureus* strains, wild type or methicillin resistant one (MRSA), the biofilm reduction induced by RSV was evaluated on *S. aureus* wild type strain, following the same protocol described for MRSA biofilm and reported in the literature.[9]

Firstly, RSV antibiofilm activity was evaluated at different concentrations, ranging from 25 μg/mL to 200 μg/mL, determining the biofilm reduction by Crystal Violet (CV) assay.

Figure 5 shows the CV absorbance related to *S. aureus* wild type biofilm demolition in the presence of RSV, free or liposome-embedded, at the concentration that gave the highest biofilm reduction (50 μg/mL).

A higher value of absorbance indicates a higher amount of biofilm and, thus, a lower demolition capacity of the systems investigated. The CV absorbance obtained for untreated mature biofilm was used as reference. The experimental data demonstrate that empty liposomes, L and LG formulations, display only a slight reduction of biofilm, which is not statistically significant. Instead, free RSV induces a biofilm reduction of about 38% with respect to untreated biofilm ($p<0.05$), confirming its ability to inhibit biofilm formation.

The ability of free RSV to destroy mature *S. aureus* wild type biofilm increases when encapsulated in galactosylated LG liposomes. In fact, LG-RSV resulted to be more effective than L-RSV formulation. In detail, LG-RSV liposomes reduce biofilm formation of *S. aureus* wild type to about half the value of untreated bacteria (representing 54% of untreated cells ($p<0.01$)), while L-RSV liposomes has an even slightly lower biofilm-reduction capacity (34%, $p<0.05$) than that of free RSV. These results are consistent with those obtained by S. Aiello et al. for MRSA: also in that case, the galactosylated liposomal formulation LG-RSV displayed a good demolition capacity against mature MRSA biofilm, compared to other liposomal formulations and free RSV.[9]

For this reason, the galactosylated formulation LG-RSV was selected to carry out more in-depth investigations on its antibacterial properties against the two *S. aureus* strains.

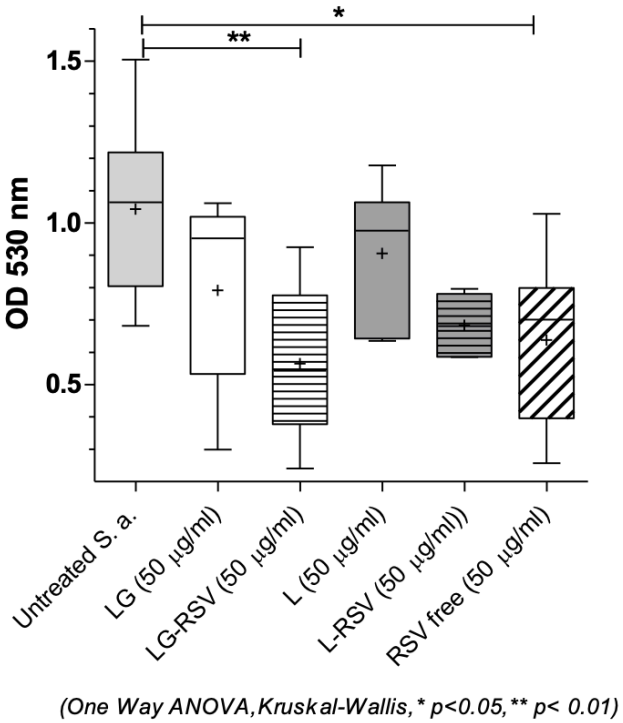

Figure 5. Anti-biofilm activity of RSV, free and liposome-loaded, on *S. aureus* wild type mature biofilm. A statistically difference was found only in the comparison between untreated bacteria and LG-RSV-treated (** indicates p<0.01), and between untreated and free RSV-treated ones (*p<0.05). + Symbol indicates the mean value of each series.

3.2.5.2. Anti-adherence activity of RSV on *S. aureus* wild type and MRSA

To assess whether the observed anti-biofilm effect could be ascribed to the anti-adherence or bacterial growth inhibiting properties of RSV, we performed a Zone of Inhibition (ZOI) agar-based assay.[29] This assay allowed to measure the adherence inhibition halos diameter induced by LG-RSV liposomes after overnight bacterial incubation on MH agar plates.

Figure 6 shows that LG-RSV liposomes (10 μL per plate of 1.5 μg/mL RSV loaded in LG liposomes) were able to induce a clear anti-adherence effect on both bacterial strains, which was slightly higher in *S. aureus* wild type than in MRSA (mean inhibition halos diameter was 21 mm for *S. aureus* vs 15.5 mm for MRSA, in two experiments). On the contrary free RSV induced only a faint inhibition halo. It is also worth noting that empty LG liposomes did not induce any inhibition in adhesion to the medium agar.

In the literature, it was frequently found that a compound displaying anti-adherence activity is also able to effectively reduce the bacterial biofilm. Such a result was found by many authors, with many

bacterial species examined and by using natural products.[30-32] Therefore we could figure out that the biofilm initially formed in the presence of RSV encapsulated in LG liposomes might be less stable and more prone to demolition. Besides, our finding that the treatment with RSV loaded in LG liposomes is also able to reduce an already mature *S. aureus* biofilm, most probably because it affects the bacterial adherence to the substrate, likely enforces this working hypothesis.

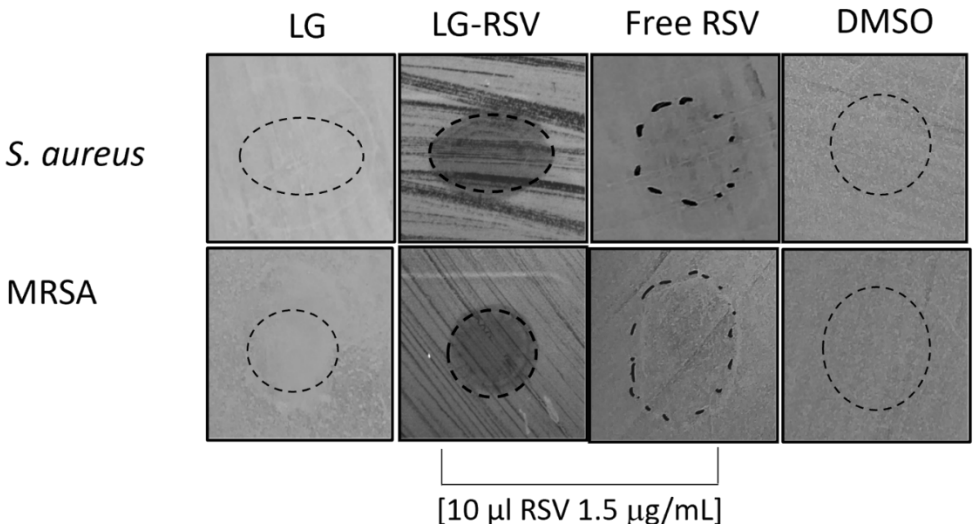

Figure 6. Anti-adherence properties of RSV, free and loaded in liposomes, on *S. aureus* wild type and MRSA bacteria. Empty LG liposomes and DMSO did not induce any visible inhibition halos.

3.2.5.3. MIC determination on *S. aureus* widl type and MRSA

Considering the results obtained on the biofilm, we aimed to verify whether the encapsulation of RSV could improve not only the anti-adherence capacity but also its inhibiting activity on bacterial growth.

In these experiments, unlike previous ones, none of the formulated LG-RSV concentration assayed induced any inhibiting effect on both bacterial strains growth, while free RSV displayed a bacteriostatic activity on both strains (**Figure 7** shows a representative one of the three experiments performed).

This result could be due to the slow release of RSV by LG liposomes in the bacteria culture, resulting in a failure to achieve an effective concentration, as compared with that of free RSV, which is administrated all at once in the well.

Furthermore, it is worth to note that free RSV minimal concentration able to inhibit bacterial growth was lower for MRSA (MIC value = 100 µg/mL) with respect to *S. aureus* wild type (MIC value = 200

μg/mL) as reported in **Table 2**. This evidence may be ascribed to the lower fitness of MRSA in normal conditions of growth resulting in a lower MIC value measured.[32]

Table 2. Determination of MIC value for RSV, both free and loaded in LG liposomes (LG-RSV).

	MIC value (μg/mL)	
Bacterial Strain	LG-RSV	RSV
S. *aureus* wild type (ATCC 25923)	n.a.	200
MRSA (ATCC 33591)	n.a.	100

n.a.: no activity

The different susceptibility of the two strains to free RSV was confirmed also by the respective CFU counts of the samples that we found inhibited by 200 μg/mL RSV. After another 24 h of growth on MH agar plates, the CFU count of these transparent wells showed roughly a ration of 10-fold less MRSA compared to S. *aureus* colonies (**Figure 7**).

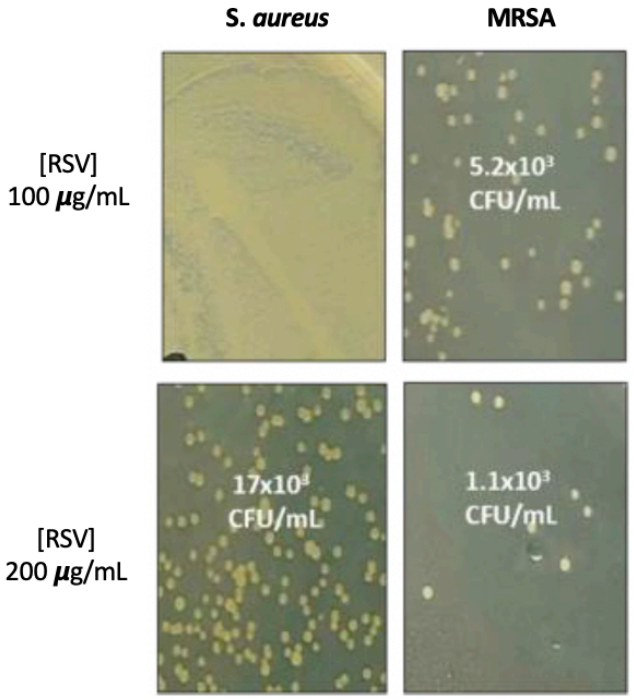

Figure 7. MH agar plates after treatment with RSV. The plates show that the number of MRSA CFUs after treatment with 100 μg/mL RSV, is roughly 3-fold lower (mean CFU count 5.2 x 10^3/mL) than the correspondent S. *aureus* CFUs (mean CFU count 17 x 10^3/mL) after treatment with 200 μg/mL RSV. the MRSA strains, treated with the latter amount, resulted in roughly 10-fold less CFUs (1.1 x 10^3/mL) as compared to S. *aureus*.

However, the question remains as to why RSV loaded in LG liposomes inhibits biofilm better than free RSV, while it is not able to inhibit the planktonic bacteria like, instead, free RSV does. Most antibiotics are developed and tested against bacteria in the planktonic state, on which they are

effective, while they are ineffective against bacterial biofilms. This highlights the importance of investigating the anti-biofilm activity of candidate antibacterial agents, rather than extrapolating from the results of planktonic assays. According to our results, as previously discussed, RSV loaded in LG liposomes behaves exactly the opposite: it reduces S. *aureus* wild type and MRSA mature biofilm but does not inhibit their planktonic growth. To clarify this finding, it would be necessary to investigate the cell wall phenotype and the ultrastructure differences existing between planktonic and biofilm staphylococci, and on the RSV interaction with these two different types of cells wall structure.

3.2.5.4. Cell wall damage induced by RSV on *S. aureus* wild type and MRSA

With the aim to find a possible explanation of the anti-adherence and anti-biofilm effects induced by RSV, both free and loaded in liposomes, as previously discussed, we investigated the ability of free RSV to induce a damage to the bacterial cell wall.

To this purpose, after overnight incubation with free RSV on a chamber slide, *S. aureus* wild type and MRSA were stained with the non-viable dye propidium iodide (PI) which enters only in cells with damage cells.

Based on the results of MIC determination, we treated MRSA strain with a free RSV solution at half the concentration used for *S. aureus* wild type (100 and 200 μg/mL, respectively for MRSA and S. aureus) and analyzed the slide with a Confocal Microscope.

Figure 8a and **8b** displays that RSV-treated bacteria resulted all positive for PI staining, being the untreated controls positive approximately for a 10-20% out of the total bacterial in the wells. This staining possibly suggest that RSV induces in the bacteria cell wall breaks or pores formation, through which the fluorochrome PI may enter.

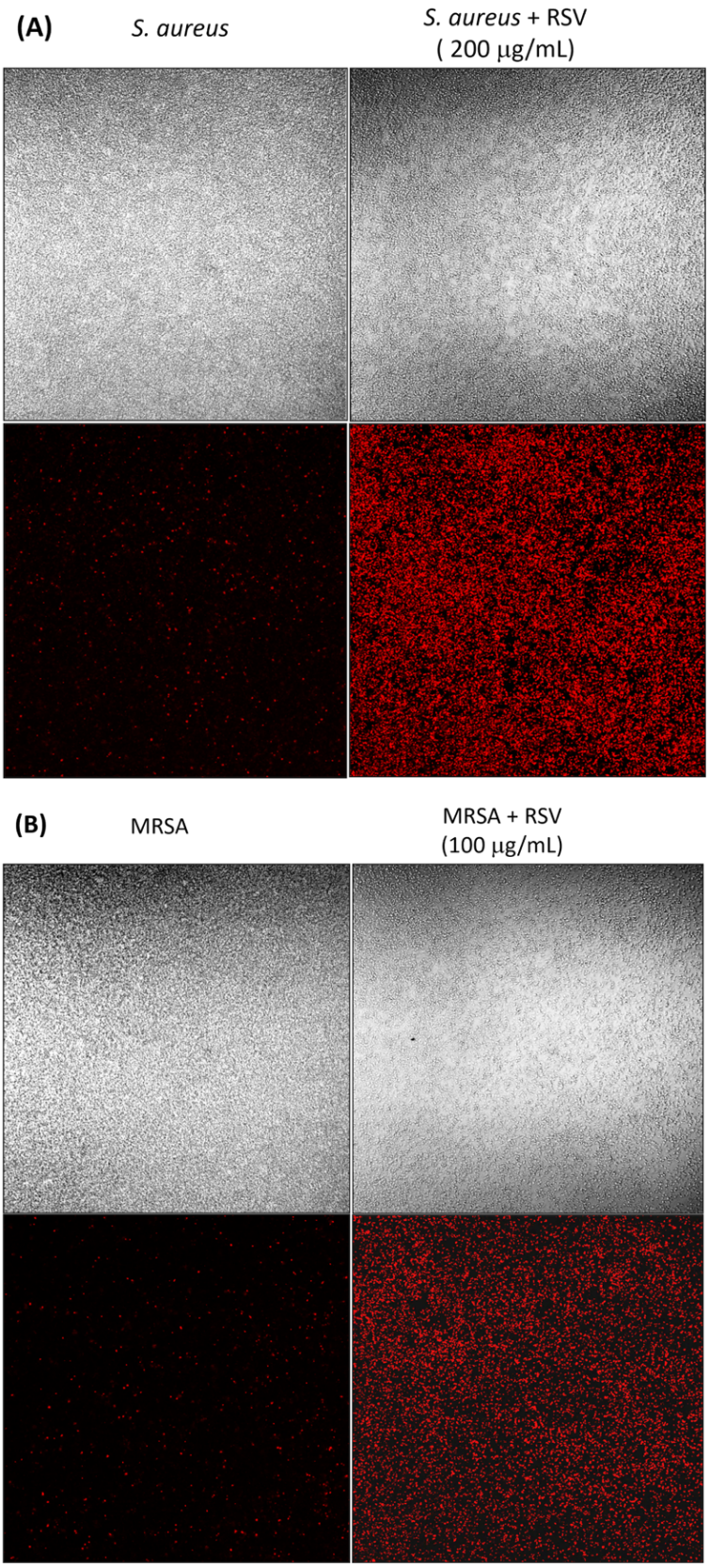

Figure 8. Propidium iodide staining of *S. aureus* wild type (A) and MRSA (B) bacteria after 16 h of incubation with free RSV (200 μg/mL for *S. aureus* wild type, 100 μg/mL for MRSA) to assess the possible cell wall damage induced by RSV. The phase contrast picture (at 40X magnification) is reported in each of the two upper panels, while the PI staining is shown in the lower ones.

To assess whether the positive staining was associated to bacterial cells death, after the microscope analysis, we plated aliquots of the bacteria on fresh MH agar plates. The CFU determination (**Figure 9**) correctly reflect the bacterial number observed in the relative wells (**Figure 8** upper panel, phase contrast) of the slide, and shows for *S. aureus* wild type a roughly three-fold (p=0.02) and for MRSA (p=0.012) a five-fold reduction of live bacteria, as compared to the untreated ones.

This is a confirmation of the growth inhibiting properties of RSV and the capacity of this stilbenoid polyphenol to affect the bacteria cell wall integrity.

However, it is worth noting that these cell wall breaks do not prevent RSV-treated bacteria to grow when transferred on fresh medium, possibly being a reversible, or transient, phenomenon.

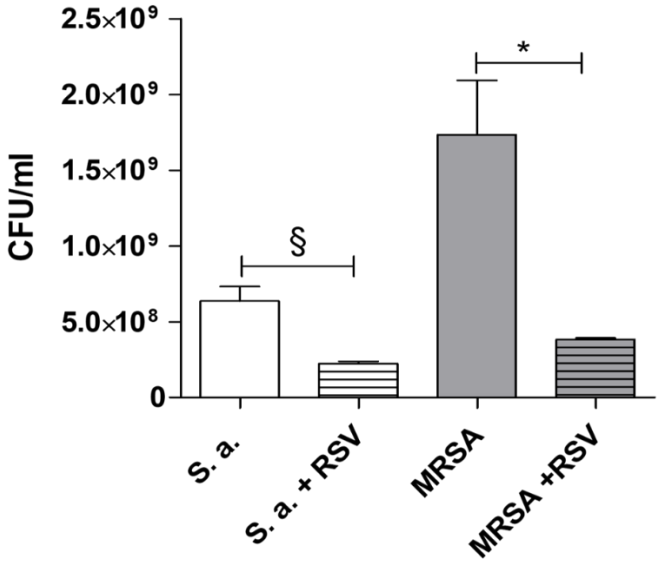

(Mann Whitney test, § p=0.02; * p=0.012)

% Positive IP	ca 20	100	ca 10	100
[free RSV]	0	200 µg/mL	0	100 µg/mL

Figure 9. Determination of *S. aureus* wild type and MRSA CFU after 16h RSV treatment.

3.3. Conclusions

The investigation presented in this chapter is useful to elucidate the antibacterial activity of RSV, both free and delivered in cationic galactosylated liposomes, on two strain of *S. aureus*, wild type (ATCC 25923) and methicillin-resistant (MRSA, ATCC 33591). In particular, we confirmed that free RSV has weak antiadhesive activity and good bacteriostatic activity and that these activities are presumably related to its ability to form pores in bacteria cell wall. However, the presence of such pores does not impair the ability of bacteria to replicate in the absence of RSV.

Regarding the biological activity of RSV encapsulated in functionalized liposomes, we demonstrated that the inclusion of RSV in LG liposomes greatly amplifies the antiadhesive (against both strains, *S. aureus* wild type and MRSA) and antibiofilm (on *S. aureus* wild type) properties while completely knocking down the bacteriostatic ones.

We can reasonable assume that, to exert its antibacterial activity, RSV must interact directly with the bacteria wall, and this is not possible if it is included in liposomes. However, given the poor solubility of RSV in biological fluids, we believe that RSV-loaded liposomes are good candidate as an adjuvant in biofilm-associated antibacterial therapies, thanks to their good antiadhesive activity.

3.4. Experimental Materials and Methods

3.4.1. Materials

All reagents used for the preparation of GLT1 such as *tert*-butanol (*t*-BuOH), potassium *tert*-butoxide (*t*-BuOK), tetrahydrofuran (THF), ethyl acetate (EtOAc), tetraethylene glycol, acetic anhydride (Ac_2O), sodium acetate (NaOAc), β-D-galactopyranoside, *p*-toluenesulfonyl chloride (TsCl), dichloromethane (CH_2Cl_2), sodium hydroxide (NaOH), sodium azide (NaN_3), N,*N*-dimethylformamide (DMF), boron trifluoride diethyl etherate (BF_3Et_2O), ammonium hydroxide (NH_4OH), phosphorus (III) bromide (PBr_3), copper (II) sulfate pentahydrate ($CuSO_4 \cdot H_2O$), ascorbic acid and *N*,*N*-hexadecyl-dimethyl-amine were purchased from Sigma-Aldrich.

1,2-dioleoyl-*sn*-glycero-3-phosphocholine (DOPC) was purchased from Avanti Polar Lipids (Alabaster, AL, USA); phosphate-buffered saline (PBS, 150 mM; 10 mM phosphate buffer, 2.7 mM KCl, 137 mM NaCl, pH 7.4, at 25 °C), *trans*-resveratrol (purity 99%), *trans*-stilbene (purity 96%), cholesterol (purity 99%), crystal violet (tris(4-(dimethylamino)phenyl)methylium chloride, purity ≥ 90%), Dulbecco's Phospahte Buffer Saline (DPBS, 1X), propidium iodide solution (1.0 mg/mL in water) chloroform ($CHCl_3$, analytical grade), and cellulose dialysis membrane (D9527-100FT, molecular weight cut off = 14 kDa) were purchased from Sigma-Aldrich. Dialysis membrane was activated by washing the tubing under running water for 3-4 hour, treating the tubing with a 0.3% w/v solution of sodium sulfide at 80°C for 1 minute, washing with hot water (60°C) for 2 minutes, followed by acidification with a 0.2 % (v/v) solution of sulfuric acid and then rinsing with hot water to remove the acid.

Muller-Hinton (MH) broth and MH agar were purchased from Fisher Scientific (Milan, Italy).

Methanol (MeOH), ethanol (EtOH), acetonitrile (ACN) and water, all HPLC-grade, were purchased from VWR International s.r.l (Milan, Italy); formic acid was supplied by Carlo Erba (Milan, Italy).

3.4.2. Synthesis of galactosylated amphiphile GLT1

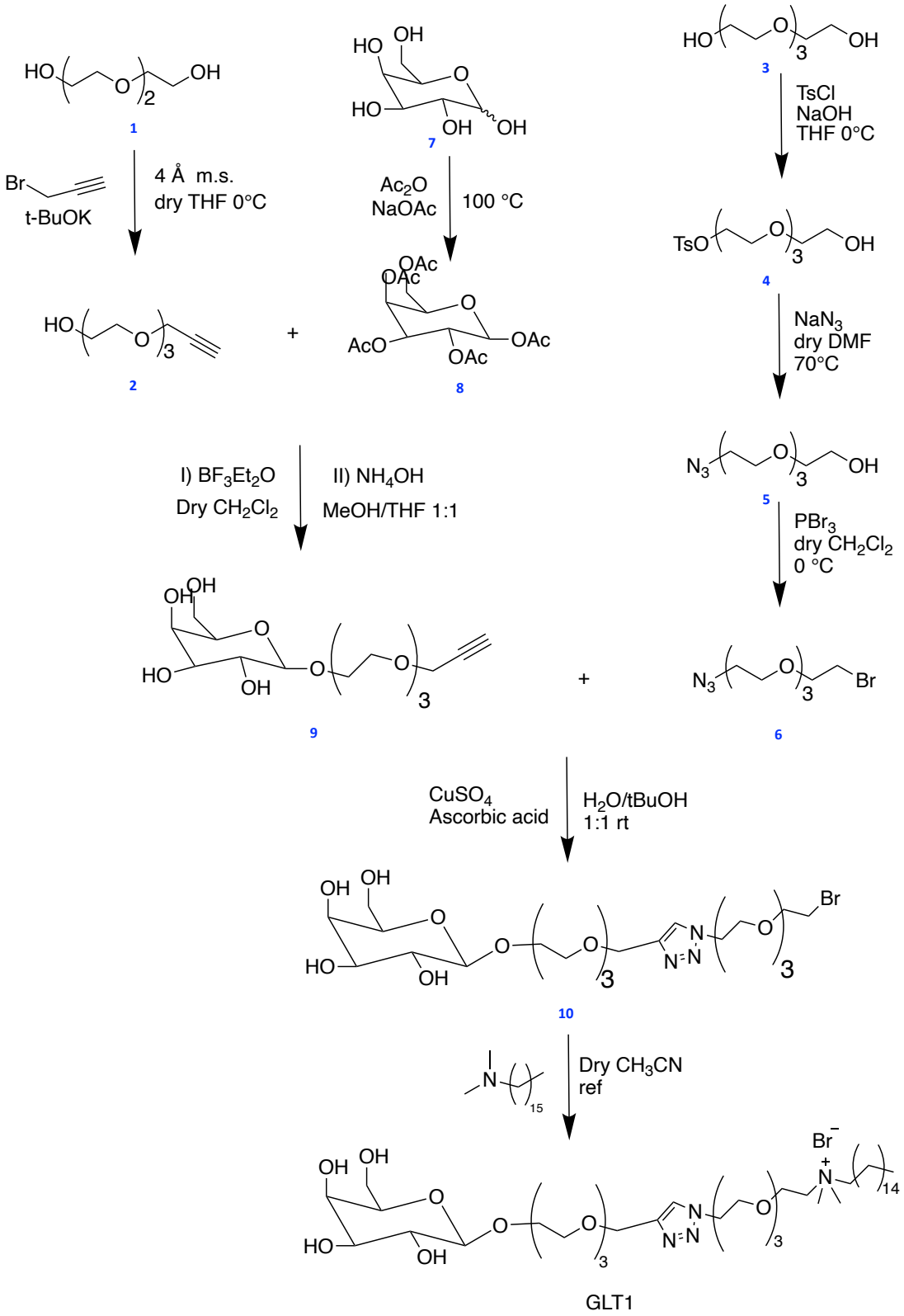

Scheme 1. Synthetic pathway for the preparation of galactosylated amphiphile GLT1.

Compound 2

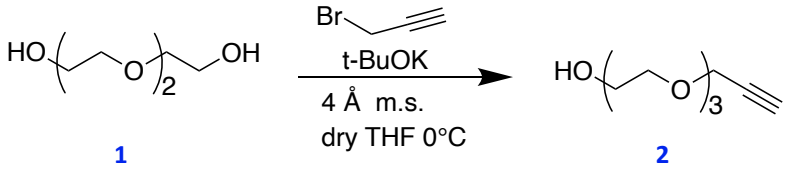

1 2

Triethylene glycol **1** (4.9 g, 32 mmol) was added to a suspension of *t*-BuOK (1.9 g, 17 mmol) in dry THF (75 mL) at 0°C under nitrogen. The mixture was stirred for 30 min at room temperature, then propargyl bromide (1.8 mL, 24 mmol) in dry THF (25 mL) was added dropwise and the reaction was kept under magnetic stirring at room temperature for 14/16 h. Afterwards, the mixture was filtered on celite by eluting with THF. Solvent was removed under reduced pressure and the oily residue was finally purified by chromatography on silica gel (eluent EtOAc, ratio 1:50) to give compound **2** (1.6 g, yield 84%) as a brown oil.

^{1}H-NMR (δ $CDCl_3$, 300 MHz, 298 K) ppm: 4.04 (d, ^{4}JHH = 2.35 Hz, $CH_2C{\equiv}C$); 3.61-3.35 (m, 12H, OCH_2CH_2O); 3.15 (s, 1H, OH); 2.36 (t, ^{4}JHH =2.35 Hz, 1H, C≡CH).

^{13}C-NMR (δ $CDCl_3$, 75 MHz, 298 K) ppm: 79.4; 74.7; 72.4; 70.4; 70.1; 68.8; 61.6; 58.3.

Compound 4

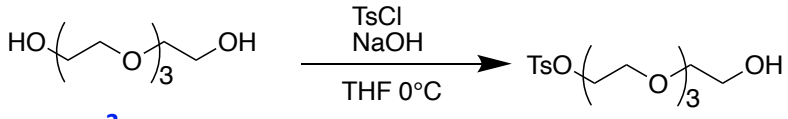

3 4

Aqueous NaOH 5 M (20 mL) was added to a solution of tetraethylene glycol **3** (90 mL, 0.5 mol) in THF (20 mL). The solution was kept under stirring at 0°C overnight, then a solution of *p*-toluenesulfonyl chloride (TsCl, 10 g, 0.05 mol) in THF (70 mL) was added dropwise at 0°C and the reaction mixture was stirred until complete addition of TsCl. THF (200 mL) and brine (1000 mL) were added to the mixture under vigorous stirring. The organic phase was isolated and the solvent removed by rotary evaporator. The residue was dissolved in CH_2Cl_2, washed with brine (10 x 150 mL) and dried over anhydrous Na_2SO_4. After filtration, the solvent was evaporated under reduced pressure to obtain compound **4** (25.3 g, yield 69%) as a pale-yellow oil.

^{1}H-NMR (δCD_3O, 300 MHz, 298 K) ppm:7.78−7.30(m, 4H, CH);4.15 (t,^{3}JHH = 6.50 Hz, 2H, CH_2OH); 3.69-3.57 (m, 14H, CH_2OCH_2, CH_2OH); 2.59 (s, 1H, OH); 2.44 (s, 3H, CH_3).

^{13}C-NMR (δ$CDCl_3$, 75 MHz, 298 K) ppm: 140.8; 138.2; 129.9; 128.0; 72.4; 70.8; 70.7; 70.4; 70.3; 69.3; 68.8; 61.7; 22.3.

Compound 5

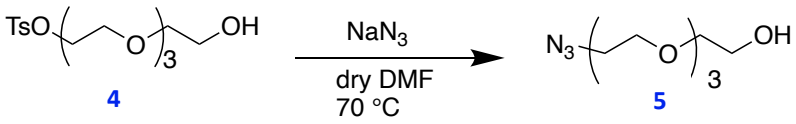

Compound **4** (25 g, 72 mmol) and NaN_3 (7 g, 108 mmol) were dissolved in dry DMF (120 mL) and the mixture was stirred at 70°C for 12 h. The solvent was removed by distillation under high vacuum and the oily residue was dissolved in CH_2Cl_2. After filtration, the solvent was removed under reduced pressure to get compound **5** (30.9 g, yield 80%) without any further purification.

^{1}H-NMR (δ$CDCl_3$, 300 MHz, 298 K) ppm: 3.66−3.58 (m, 14H, CH_2O); 3.38 (t, ^{3}JHH = 6.02 Hz, 2H, CH_2N_3); 2.59 (s, 1H, OH).

^{13}C-NMR (δ$CDCl_3$,75 MHz, 298 K) ppm: 72.5; 70.7; 70.6; 70.4; 70.0; 61.7; 50.7.

Compound 6

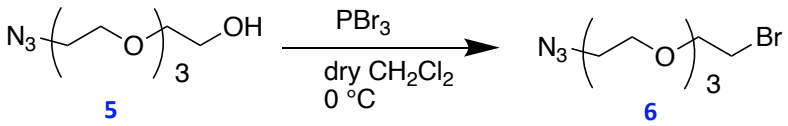

Compound **5** (30.9 g, 14.1 mmol) was dissolved in dry CH_2Cl_2 (250 mL) and PBr_3 (4.4 mL, 47 mmol) in dry CH_2Cl_2 (50 mL) was added dropwise under nitrogen at 0°C. The reaction was stirred overnight at room temperature, then a saturated aqueous solution of $NaHCO_3$ was added and the aqueous phase extracted with CH_2Cl_2. All the organic layers were combined and dried over anhydrous Na_2SO_4. After filtration, the solvent was removed under reduced pressure and the oily residue purified by chromatography on silica gel (eluent $CHCl_3$, ratio 1:40) to obtain compound **6** (21.3 g, yield 86%).

^{1}H-NMR (δ$CDCl_3$, 300 MHz, 298 K) ppm: 3.81 (t, ^{3}JHH = 6.65 Hz, 2H, CH_2CH_2Br); 3.70− 3.65 (m, 10H, OCH_2CH_2O, $CH_2CH_2N_3$); 3.47 (t, ^{3}JHH = 6.65 Hz, 2H, CH_2Br); 3.38 (t, ^{3}JHH = 6.04 Hz, 2H, CH_2N_3).

^{13}C-NMR (δ$CDCl_3$,75 MHz, 298 K) ppm: 71.0; 70.6; 70.5; 70.4; 69.9; 50.5; 30.3.

Compound 8

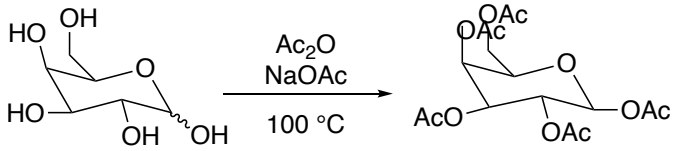

7 8

β-D-galactopyranoside **7** (12.5 g, 70 mmol), acetic anhydride (60 mL, 0.56 mol) and NaOAc (5.6 g, 70 mmol) were mixed and stirred at 100 °C for 20 min, then cooled at room temperature and poured in water (200 mL) under stirring at 0 °C for 1 h. The product was extracted with CH_2Cl_2, then the organic phase was dried over anhydrous Na_2SO_4, filtered and the solvent was removed under reduced pressure. The residue was purified by crystallization from EtOH to get compound **8** (27.4 g, yield 100%) as a pale-yellow oil.

^{1}H-NMR (δ $CDCl_3$, 300 MHz, 298 K) ppm: 5.68 (d,^{3}JHH = 8.3 Hz, 1H, H-1); 5.40 (m, 1H, H-4); 5.31 (t,^{3}JHH = 8.3 Hz, 1H, H-2); 5.09 (dd, ^{3}JHH = 8.3, 3.1 Hz, 1H, H-3); 4.14-4.04 (m, 3H, H5, H-6); 2.14 (s, 3H, CH_3); 2.10 (s, 3H, CH_3); 2.02 (s, 6H, CH_3); 1.97 (s, 3H, CH_3).

^{13}C-NMR (δ $CDCl_3$, 75 MHz, 298 K) ppm: 171.68; 171.46; 171.30; 170.71; 170.32; 93.46; 73.01; 72.15; 69.13; 68.12; 62.36; 22.15; 21.99; 21.87.

Compound 9

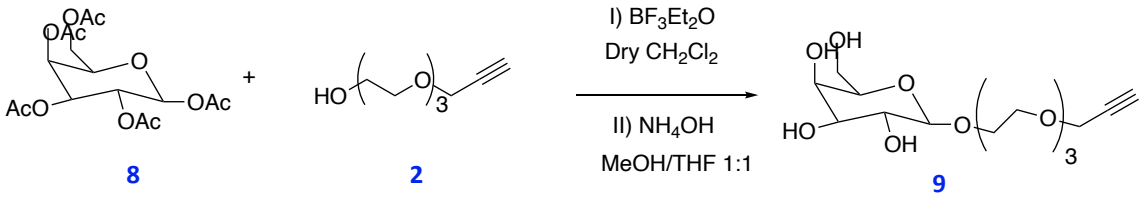

8 2 9

Compound **8** (2.8 g, 7.2 mmol) and compound **2** (1.6 g, 8.5 mmol) were dissolved in dry CH_2Cl_2 (28 mL) under nitrogen. A solution of BF_3Et_2O (1.3 mL, 10.3 mmol) was added dropwise to the mixture at 0 °C and the solution was stirred for 14 h. Then K_2CO_3 (1.6 g) was added to neutralize the solution, the mixture was filtered and the organic phase was washed with water. The aqueous phase was extracted 4 times with CH_2Cl_2, the organic layers were combined and dried over anhydrous Na_2SO_4. After filtration the solvent was removed under reduced pressure and the residue was dissolved in MeOH/THF (161 mL, 1:1). NH_4OH 5 M (57.5 mL) was added and the solution was stirred for 12 h at room temperature. Finally, the solvent was removed under reduced pressure and the residue was purified by chromatography on silica gel (eluent CH_2Cl_2/MeOH, ratio 9:1) to obtain compound **9** (0.52 g, yield 40%).

^{1}H-NMR (δ MeOD, 300 MHz, 298 K) ppm:4.78 (d, J = 1.8 Hz, 1H, H-1); 4.18 (d, J = 2.4 Hz, 2H, $CH_2C{\equiv}C$); 3.84-3.55 (m, 22H, OH, H-2, H-3, H-4, H-5, 2 H-6, $OCO(CH_2CH_2O)_3$); 2.84 (t, J = 2.4 Hz, 1H, C≡CH).
^{13}C-NMR (δ MeOD, 75 MHz, 298 K) ppm: 101.7; 80.5; 75.9; 74.6; 72.5; 72.0; 71.5; 71.4; 71.3; 70.0; 68.6; 67.7; 62.9; 58.9; 52.3.

Compound 10

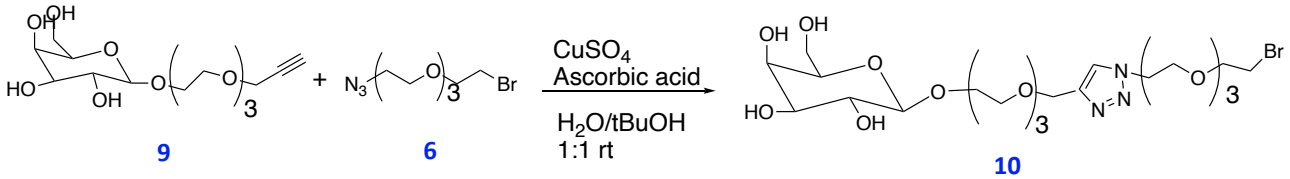

9 6 10

Compound **9** (0.98 g, 2.7 mmol) and compound **6** (0.95 g, 3.4 mmol) were dissolved in H_2O/*t*-BuOH (1:2, 10 mL). Ascorbic acid (14 mg) and $CuSO_4{\cdot}H_2O$ (6 mg) were added and the reaction was stirred at room temperature for 7 days. Then the mixture was cooled to 0 °C and neutralized by an aqueous saturated solution of $NaHCO_3$. The solvent was removed under vacuum and the residue dissolved in MeOH. The solution was filtered and the solvent was removed by rotary evaporator. The residue was purified by chromatography on silica gel (eluent CH_3OH/AcOEt, ratio 15:85) to get compound **10** (1 g, yield 58%).

^{1}H-NMR (δ MeOD, 300 MHz, 298 K) ppm: 8.06 (s, 1H, C=CH-N-N); 4.65 (s, 2H, O-CH2-C(=C)-N=N); 4.60(t, 2H, N=N-N-CH_2-CH_2); 4.26(d, 1H, H-1); 3.91 (t, 2H, N-N-N-CH_2-CH_2); 3.83-3.62 (m, 32H, OH, H-2, H-3, H-4, H-5, 2H-6, $OCO(CH_2CH_2O)_3$); 3.51 (t, 2H, CH_2Br).
^{13}C-NMR (δ MeOD, 75 MHz, 298 K) ppm: 145.6; 126.1; 105.0; 76.7; 74.9; 72.5; 72.3; 71.5; 71.5; 71.4; 71.4; 71.3; 70.7; 70.3; 70.2; 69.5, 64.9; 62.5; 51.4; 31.6

GLT1

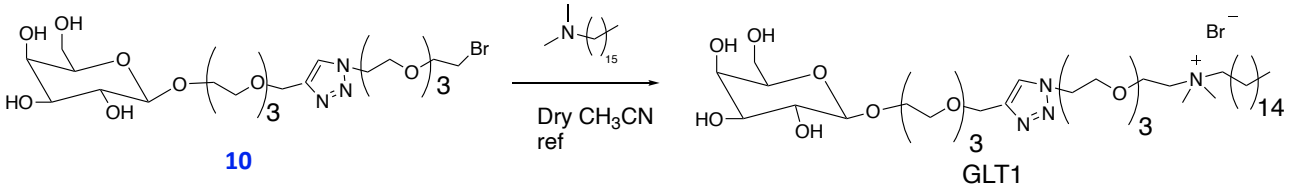

10 GLT1

Compound **10** (1 g, 1.5 mmol) and *N,N*-hexadecyl-dimethyl-ammine (0.8 mL, 2.3 mmol) were dissolved in dry CH_3CN (10 mL). The mixture was heated to reflux for 1 week. Then the solvent was removed under reduced pressure and the residue was dissolved in MeOH and filtered. Finally, the

residue was washed several times with hexane to collect the final product **GLT1** (0.9 g, yield 68%) as a yellow oil.

^{1}H-NMR (δ MeOD, 300 MHz, 298 K) ppm: 8.06 (s, 1H, C=CH-N-N), 4.63 (s, 2H, O-CH_2-C(=C)-N=N); 4.59 (t, 2H, N=N-N-CH_2-CH_2); 4. 25 (d, 1H, H-1); 3.91-3.47 (m, 32H, OH, H-2, H-3, H-4, H-5, 2 H-6, OCO($CH_2CH_2O)_3$); 3.37 (m, 2H, N-CH_2($CH_2)_{13}CH_2CH_3$); 3.12 (m, 6H, N($CH_3)_2$); 1.77 (m, 2H, N-CH_2($CH_2)_{13}CH_2CH_3$); 1.38-1.25 (m, 26H, N($CH_2)_{13}CH_2CH_3$); 0.89 (t, 3H, $CH_2CH_2CH_3$).

^{13}C-NMR (δ MeOD, 75 MHz, 298 K) ppm: 145.8¸ 125.8; 105.1; 76.7; 74.8; 72.4; 71.4; 70.8; 70.3; 70.2; 69.6; 66.8; 65.7; 64.9; 64.3; 62.5; 52.3; 51.3; 33.0; 30.7; 30.6; 30.5; 30.4; 30.3; 27.4; 23.8; 23.6; 14.5

3.4.3. Liposomes preparation

Liposomes were formulated with an unsaturated phosphocholine (DOPC) and cholesterol (Chol) in presence or absence of the cationic amphiphile GLT1.

Liposomes, both empty and RSV loaded, were prepared according to the lipid film hydration protocol, coupled with the freeze-thaw procedure[33] and followed by the extrusion process.[34]

Briefly, a proper amount of lipid components was dissolved in $CHCl_3$ (DOPC and Chol) and MeOH (GLT1) in a round bottom flask, dried by rotary evaporation (Buchi Rotavapor R-200) and then under high vacuum (5h) to remove any traces of organic solvents and to obtain a thin lipid film. For RSV-loaded liposomes, the proper amount of a RSV solution in absolute ethanol was added to the lipid mixture, before the film formation, to have a molar ratio 1:8 RSV/lipids. The film was hydrated with 150 mM phosphate buffer saline solution (PBS) to have a final liposomal suspension 20 mM in total lipid concentration. The suspension was vortex-mixed to completely detach the lipid film from the flask and freeze-thawed five times, from liquid nitrogen to 50°C, to reduce multilamellarity. RSV-loaded liposomal suspensions were sonicated (probe tip sonicator Sonics Vibra-Cell, 3 mm diameter tip) at 40 W (10 cycles of 10 seconds) to improve its entrapment in the lipid bilayer by breaking aggregates that usually it forms in aqueous solutions.[21] Size reduction was carried out by extrusion of liposomal dispersions, ten times (10 mL Lipex Biomembranes) under high pressure through a 100 nm pore size polycarbonate membrane (Whatman Nucleopore) at temperature higher than T_m to obtain small unilamellar vesicles (SUVs).

Finally, liposomes purification from unentrapped RSV was performed by dialysis against PBS under slow magnetic stirring, using a buffer volume equal to 25-times than the sample volume.

During all preparation steps (film formation, extrusion, dialysis) samples were protected from light to avoid the isomerization of *trans*-resveratrol in the less active *cis* isomer.

3.4.4. Physicochemical characterization of liposomes

Size distributions, polydispersity index (PDI) and ζ-potential were determined by Dynamic and Dielectrophoretic Light Scattering (DLS, DELS) measurements using a Malvern Nano-Zetasizer spectrometer equipped with a 5 mV He/Ne laser (λ=632.8 nm) and a thermostated cell holder. Temperature was fixed at 25°C in all the measurements.

Particle size and PDI were measured in backscatter detection, at an angle of 173°, this condition representing a significant advantage because less sensitive to a multiple scattering effects compare to the more conventional 90° configuration and contribution of micrometric larger particles is considerably reduced.[35] The measured intensity autocorrelation function was analyzed by using the cumulant fit.[36] The first cumulant was used to obtain the apparent diffusion coefficients D of the particles, further converted into apparent hydrodynamic diameters, D_h, by using Stokes-Einstein relationship (**Eq. 1**):

$$D_h = \frac{K_b T}{3\pi\eta D} \qquad \textbf{(Eq. 1)}$$

where k_BT is the thermal energy and η is the solvent viscosity.

The ζ-potential of liposome formulations was determined by DELS measurements. Low voltages have been applied to avoid the risk of Joule heating effects. Analysis of the Doppler shift to determine the electrophoretic mobility was done by using phase analysis light scattering (PALS)[37] a method which is especially useful at high ionic strengths, where mobilities are usually low. The mobility μ of the liposomes was converted into ζ-potential using the Smoluchowski relation ζ =μ η/ε, where ε and η are the permittivity and the viscosity of the solution, respectively.

DLS and DELS measurements were performed after dilution of liposomal suspensions to 1 mM in total lipids in PBS or diluted PBS (15 mM), respectively. Data were collected soon after preparation, after the dialysis (for RSV-loaded liposomes) and in the following 14 days (samples stored in the dark at room temperature) to evaluate the stability over time and to highlight any aggregation phenomena.

The data reported for hydrodynamic diameter (D_h), PDI and ζ-potential correspond to the average of at least three different independent experiments.

3.4.4.1. Determination of RSV entrapment efficiency in liposomes

The content of RSV loaded in neutral and galactosylated liposomes was evaluated by UPLC measurements. Chromatographic analyses were carried out by an Aquity^{TM} UPLC H-Class Bio System (Waters, Milford) equipped with a quaternary pump, a sample manager, an autosampler, a column temperature controller and a PDA detector.

Before UPLC measurements, samples were properly diluted with methanol to obtain liposome disruption and the complete solubilization of formulation components. *Trans*-stilbene (TSB) was used as internal standard and then all the samples were filtered on PTFE membranes (4 mm x 0.2 μm; Sartorius) before the injection.

RSV determinations were performed on an Aquity UPLC BEH C18 column (50 x 2.1 mm id, 1.7 μm), equipped with an Aquity UPLC BEH C18 pre-column (5 x 2.1 mm id, 1.7 μm). Chromatographic elution was assessed in gradient mode using a mobile phase consisting of 0.1% (v/v) formic acid in water (phase A), 0.1% (v/v) formic acid in methanol (phase B) and 0.1% (v/v) formic acid in acetonitrile (phase C). The gradient program was: 0 – 2 min from 80 % A, 10 % B and 10 % C to 0 % A, 50 % B and 50 % C; 2 – 8.5 min 0 % A, 50 % B and 50 % C; 8.5 – 9 min from 0 % A, 50 % B and 50 % C to 80 % A, 10 % B and 10 % C. Sample injection volume was 2 μL, flow rate was 0.25 mL/min and column temperature was settled at 40°C. Both RSV and TSB were detected at 306 nm.

Method validation was determined assessing linearity, sensitivity and precision. RSV stock standard solution (305 μM) was prepared in MeOH. Calibration standard solutions in the concentrations range between 0.024 and 305 μM (n = 7) were prepared by diluting the stock standard solution of RSV with a methanol-water (80:20, v/v) mixture. RSV calibration curve was constructed by triple injections of calibration standard solutions. Each concentration level was spiked with TSB 20 μM. Calibration curve obtained was linear over the concentration range studied, with a correlation coefficient of 0.9995.

Limit of Detection (LOD) and Limit of Quantitation (LOQ) calculated for RSV were determined by using a signal-to-noise ratio of 3 and 10, respectively. LOD and LOQ were found to be 0.008 μM and 0.024 μM, respectively.

Precision of the method was evaluated in terms of repeatability and reproducibility. Intra- and inter-day precisions, expressed as relative standard deviation (RSD) of migration time and peak area, were assessed by performing six consecutive injections of the same solution in the same day (RSD < 1 %) and over three days (RSD < 2 %).

The entrapment efficiency (EE%) of RSV in liposomes was calculated using the following equation (**Eq. 2**):

$$EE\ (\%) = \frac{[RSV]_{pd}}{[RSV]_0} \times 100 \qquad \textbf{(Eq. 2)}$$

where $[RSV]_{pd}$ indicates RSV concentration after dialysis and $[RSV]_0$ is the concentration soon after extrusion.

3.4.4.2. *In vitro* release study of RSV from liposomes

The release of RSV from DOPC/Chol and DOPC/Chol/GLT1 liposomes was evaluated by dialysis against PBS (phosphate buffer volume 50-times larger than the sample volume) keeping the systems under constant magnetic stirring. After liposomes purification by dialysis, samples were collected every 1 hour over a period of 24 hours and analyzed by UPLC to study the releasing profile of RSV previously encapsulated. Each liposomal aliquot was diluted with MeOH (1:1 v/v) to break lipid aggregates and to enhance the release of RSV and the resulting solution filtered on PTFE membranes (4 mm x 0.2 µm; Sartorius). To determine the percentage of RSV released over the time, a chromatographic analysis was carried out as described above for the EE% determination.

During the whole process, samples were protected from light to avoid the isomerization of *trans*-resveratrol.

3.4.5. Bacterial strains

Antimicrobial activity of RSV, both free and loaded in liposomes, was examined against two American Type Culture Collection (ATCC) strains of *Staphylococcus aureus:* ATCC 25923 (wild type strain) and ATCC 33591 (methicillin-resistant *Staphylococcus aureus*, MRSA). Both strains were retrieved from the titrated frozen stocks and streaked in fresh Mueller-Hinton (MH) broth, then incubated at 37 °C for 18 h and subcultured on fresh MH agar plates to have fresh colonies and single colonies forming units (CFU).

3.4.6. Evaluation of liposome-bacteria interaction

The binding affinity of neutral and galactosylated liposomes on bacteria strains involved in our study was investigated by DELS measurements, determining the ζ-potential variation of the solution analyzed.

S. aureus and MRSA were grown overnight in MH broth medium, then centrifuged to obtain a bacteria pellet, which was washed 3 times with diluted PBS (15 mM) to remove all traces of culture broth. Afterwards, bacteria suspensions in diluted PBS (15 mM) were diluted to reach the desired final concentration, assessed by optical density (OD) measurements.

Measurements were carried out at 25 °C in 15 mM PBS at different liposomes concentration (0, 0.1, 0.3, 0.5, 0.7, 1 mM in total lipid concentration) in presence or absence of 10^5 CFU/mL bacteria.

3.4.7. *In vitro* biofilm formation and Crystal Violet assay

S. aureus wild type was grown in MH medium supplemented with 0.25 % glucose solution, at 10^7 CFU/mL by serial dilutions, and submerged biofilms were established in flat-bottom 96 well microtiter plate wells (Thermo Scientific, NUNCLONE-Delta surface, Milan, Italy) left growth at 37 °C for 96 h.

The biofilm formation was measured by Crystal Violet (CV) assay.[9] In brief, wells were washed with DPBS to remove nonattached bacteria and stained with 100 μL of 0.1 % CV solution. After 45 min of incubation at room temperature, plates were emptied and extensively washed with distilled water to remove the CV excess. Quantification of biofilm bacteria was assessed by adding 50 μL of 95 % ethanol to the wells to solubilize all biofilm-associated dye and the absorbance at 530 nm was determined by a microplate reader (VICTOR-NIVOTM, Perkin Elmer, Italy).

3.4.8. Demolition assay on *S. aureus* wild type biofilm

The biofilm demolition activity of RSV, both free and loaded in neutral and galactosylated liposomes, has been evaluated on *S. aureus* wild type strain. RSV-loaded liposomes and free RSV (solubilized in DMSO) were sterilized through a 0.22 μm PES filter and diluted with DPBS to have concentrations ranging from 25 μg/mL to 200 μg/mL.

S. aureus biofilm was left to grow for 96 h, as described previously. Then, plates were incubated with different concentration of free or liposome-embedded RSV. On the fifth day, wells were empties, washed with DPBS and then washed again with DPBS before 100 μL of 0.1% CV solution were added. After 45 min at room temperature, plates were emptied and washed with distilled water to remove excess CV. For biofilm quantification, 50 μL of 95% ethanol were added to the wells to solubilize all biofilm-associated dye and the absorbance at 530 nm was determined by a microplate reader (VICTOR-NIVOTM, Perkon Elmer).

3.4.9. Anti-adherence assay

MH agar plates were prepared by spreading 500 μL of *S. aureus* and MRSA overnight (ON) cultures brought to a concentration between 1 x 10^8 and 2 x 10^8 CFU/mL by serial dilution in MH broth, and dried under the sterile flow bench for 15 min. Then, 10 μL of 1.5 μg/mL RSV solution, solubilized in DMSO or loaded in DOPC/Chol/GLT1 liposomes, were dropped on the inoculated agar surface and dried as described above. Furthermore, 10 μL of empty liposomes and DMSO were dropped on control plates. Finally, plates were incubated for 16 h at 37 °C and the anti-adherence activity was evaluated by the naked eye.

For those plates showing a transparent halo, the diameter of area of transparency was measured to estimate the inhibition of bacteria adherence associated to the investigated sample.

3.4.10 Determination of *Minimum Inhibitory Concentration* (MIC)

To assess the Minimum Inhibitory Concentration (MIC) of free RSV (solubilized in DMSO) and RSV loaded in DOPC/Chol/GLT1 liposomes, *S. aureus* and MRSA were grown in 10 mL of MH broth medium ON at 37°C. Then, the ON culture of each bacterium was brought to a concentration of 0.8 x 10^5 - 1.2 x 10^6 bacteria/mL by serial dilutions in MH broth. The final concentration was estimated by measuring the OD at 600 nm. Both diluted cultures were aliquoted in 96 wells/plates (flat bottom, one plate for each strain studied) and the antimicrobial agent was added, in triplicates, at different concentration from 50 μg/mL to 200 μg/mL. Plates were kept ON at 37°C. Afterwards, plates were observed and all the transparent wells, likely corresponding to the MIC values, were plated on fresh MH agar plate kept at 37°C overnight. Finally, MH agar plates were observed and those showing bacterial growth were annotated as MIC.

3.4.11. Cell wall damage assay by propidium iodide uptake

S. aureus and MRSA strains were put in culture for 16 h in chamber slides (μ-Slide VI 0.4 ibiTreat, 80606, IBIDI GmbH, Germany) with free RSV at the respective MIC concentration identified above (200 μg/mL for *S. aureus* and 100 μg/mL for MRSA). The following day, a propidium iodide solution (1 mg/mL) was diluted 1:1000 in each chamber slides well to reach 1 μg/mL final concentration. This dye cannot pass through intact cell membranes but may freely enter cells with compromised cell membranes. After 5 min, samples were analyzed by an Olympus FV1200 confocal laser scanning microscope with 20X air objective with optical pinhole at 1AU and a multiline argon laser at 488 nm, He/Ne ion laser at 543 nm and blue diode laser at 405 nm as excitation sources. Propidium iodide

was acquired using excitation at 515 nm and emission at 615 nm. Confocal images were processed with ImageJ (National Institutes of Health, NIH, https://imagej.nih.gov/ij).

3.4.12. Statistical analysis

All statistical analysis were performed with the support of GraphPad prism version 5.0 and Stata software. Data were analyzed by one-way ANOVA and post hoc Bonferroni comparison tests ($p<0.05$).

3.5. References

[1] M. Vestergaard, H. Ingmer H, Antibacterial and antifungal properties of resveratrol, *Int J Antimicrob Agents*, **2019**, *53* (6), 716.
https://doi.org/10.1016/j.ijantimicag.2019.02.015.

[2] B. Catalgol, S. Batirel, Y. Taga, N.K. Ozer, Resveratrol: French paradox revisited, *Front Pharmacol*, **2012**, *3*, 141.
https:/doi.org/10.3389/fphar.2012.00141.

[3] M.M. Chan, Antimicrobial effect of resveratrol on dermatophytes and bacterial pathogens of the skin, *Biochem Pharmacol*, **2002**, *63* (2), 99.
https://doi.org/10.1016/s0006-2952(01)00886-3.

[4] L. Paulo, S. Ferreira, E. Gallardo, J.A. Queiroz, F. Domingues, Antimicrobial activity and effects of resveratrol on human pathogenic bacteria, *World J. Microbiol. Biotechnol,* **2010**, *26*, 1533.
https://doi.org/10.1007/s11274- 010-0325-7.

[5] H.S. Cho, J.H. Lee, M.H. Cho, J. Lee, Red wines and flavonoids diminish Staphylococcus aureus virulence with anti-biofilm and anti-hemolytic activities, *Biofouling*, **2015**, *31* (1), 1.
https:/doi.org/10.1080/08927014.2014.991319.

[6] D. Hwang, Y.H. Lim, Resveratrol antibacterial activity against Escherichia coli is mediated by Z-ring formation inhibition via suppression of FtsZ expression, *Sci Rep*, **2015**, *5*, 10029.
https:/doi.org/10.1038/srep10029.

[7] K. Lee, J.H. Lee, S.Y. Ryu, M.H. Cho, J. Lee, Stilbenes reduce Staphylococcus aureus hemolysis, biofilm formation, and virulence, *Foodborne Pathog Dis*, **2014**, *11* (9), 710.
https://doi.org/10.1089/fpd.2014.1758.

[8] N. Qin, X. Tan, Y. Jiao, L. Liu, W. Zhao, S. Yang, A. Jia, RNA-Seq-based transcriptome analysis of methicillin-resistant Staphylococcus aureus biofilm inhibition by ursolic acid and resveratrol, *Sci Rep*, **2014**, *4*, 5467.
https://doi.org/10.1038/srep05467.

[9] S. Aiello, L. Pagano, F. Ceccacci, B. Simonis, S. Sennato, F. Bugli, C. Martini, R. Torelli, M. Sanguinetti, A. Ciogli, C.Bombelli, G. Mancini,Mannosyl, glucosyl or galactosyl liposomes to improve resveratrol efficacy against Methicillin Resistant Staphylococcus aureus biofilm, *Col Surfa A*, **2021**, *617*, 126321.
https://doi.org/10.1016/j.colsurfa.2021.126321.

[10] T. Walle, F. Hsieh, M.H. DeLegge, J.E.J. Oatis, U.K. Walle, High absorption but very low bioavailability of oral resveratrol in humans, *Drug Metab Dispos*, **2004**, *32* (12), 1377. https:/doi.org/10.1124/dmd.104.000885.

[11] D.J. Boocock, G.E. Faust, K.R. Patel, A.M. Schinas, V.A. Brown, M.P. Ducharme, T.D. Booth, J.A. Crowell, M. Perloff, A.J. Gescher, W.P. Steward, D.E. Brenner, Phase I dose escalation pharmacokinetic study in healthy volunteers of resveratrol, a potential cancer chemopreventive agent, *Cancer Epidemiol Biomarkers Prev*, **2007**, *16* (6), 1246. https:/doi.org/10.1158/1055-9965.EPI-07-0022.

[12] H.H. Chow, L.L. Garland, C.H. Hsu, D.R. Vining, W.M. Chew, J.A. Miller, M. Perloff, J.A. Crowell, D.S. Alberts, Resveratrol modulates drug- and carcinogen-metabolizing enzymes in a healthy volunteer study, *Cancer Prev Res (Phila*), **2010**, *3* (9), 1168. https:/doi.org/10.1158/1940-6207.CAPR-09-0155.

[13] J.C. Nwabuife, A.M. Pant, T. Govender, Liposomal delivery systems and their applications against Staphylococcus aureus and Methicillin-resistant Staphylococcus aureus, *Adv Drug Deliv Rev*, **2021**, *178*, 113861. https://doi.org/10.1016/j.addr.2021.113861.

[14] M. Monsigny, R. Mayer, A.C. Roche, Sugar-lectin interactions: sugar clusters, lectin multivalency and avidity, *Carbohydr Lett*, **2000**, *4* (1), 35.

[15] N. Sharon, H. Lis, History of lectins: from hemagglutinins to biological recognition molecules, *Glycobiology*, **2004**, *14* (11), 53R. https://doi.org/10.1093/glycob/cwh122.

[16] T.G. Pistole, Interaction of bacteria and fungi with lectins and lectin-like substances, *Annu Rev Microbiol*, **1981**, *35*, 85. https://doi.org/10.1146/annurev.mi.35.100181.000505.

[17] A. Mauceri, S. Borocci, L. Galantini, L. Giansanti, G. Mancini, A. Martino, L. Salvati Manni, C. Sperduto, Recognition of Concanavalin A by Cationic Glucosylated Liposomes, *Langmuir*, **2014**, *30* (38), 11301. https://doi.org/10.1021/la502946t.

[18] G. Bozzuto, A. Molinari, Liposomes as nanomedical devices, *Int J Nanomedicine*, **2015**, *10* (1), 975. https://doi.org/10.2147/IJN.S68861

[19] A. Mauceri, A. Fracassi, M. D'Abramo, S. Borocci, L. Giansanti, A. Piozzi, L. Galantini, A.Martino, V. D'Aiuto, G. Mancini, Role of the hydrophilic spacer of glucosylated amphiphiles included in liposome formulations in the recognition of Concanavalin A, *Coll Surfa B*, **2015**, *136*, 232.
https://doi.org/10.1016/j.colsurfb.2015.09.016
[20] C.V. Iancu, J. Zamoon, S.B. Woo, J. Choe, Crystal structure of a glucose/H^+ symporter and its mechanism of action, *PNAS*, **2013**, *110* (44), 17862.
https://doi.org/10.1073/pnas.1311485110.
[21] C. Bonechi, S. Martini, L. Ciani, S. Lamponi, H. Rebmann, C. Rossi, S. Ristori, Using liposomes as carriers for polyphenolic compounds: the case of trans-resveratrol, *PLoS One*, **2012**, *7* (8), e41438.
https://doi.org/10.1371/journal.pone.0041438.
[22] J. Han, K. Suga, K. Hayashi, Y. Okamoto, H. Umakoshi, Multi-Level Characterization of the Membrane Properties of Resveratrol-Incorporated Liposomes, *J Phys Chem B*, **2017**, *121* (16), 4091.
https://doi.org/10.1021/acs.jpcb.7b00368.
[23] D.G. Villalva, L. Giansanti, A. Mauceri, F. Ceccacci, G. Mancini, Influence of the state of phase of lipid bilayer on the exposure of glucose residues on the surface of liposomes, *Colloids Surf B*, **2017**, *159*, 557.
https://doi.org/10.1016/j. colsurfb.2017.08.025.
[24] E.G. Yanes, S.R. Gratz, A.M. Stalcup, Tetraethylammoniun tetrafluoroborate: a novel electrolyte with a unique role in the capillary electrophoretic separatiaon of polyphenols fround in grape seed extracts, *Analyst*, **2000**, *125*, 1919.
https://doi.org/10.1039/B004530F.
[25] L. Pagano, F. Gkartziou, S. Aiello, B. Simonis, F. Ceccacci, S. Sennato, A. Ciogli, S. Mourtas, I. Spiliopoulou, S.G. Antimisiaris, Resveratrol Loaded in Cationic Glucosylated Liposomes to Treat Staphylococcus Epidermidis Infections, *Chem. Phys. Lipids*, **2022**, *243*, 105174.
https://doi.org/10.1016/j.chemphyslip.2022.105174.
[26] D. E. Koppel, Analysis of Macromolecular Polydispersity in Intensity Correlation Spectroscopy: The Method of Cumulants, *J. Chem. Phys*, **1972**, *57* (11), 4814.
https://doi.org/10.1063/1.1678153.
[27] M. Petaccia, C. Bombelli, F. Paroni Sterbini, M. Papi, L. Giansanti, F. Bugli, M. Sanguinetti, G. Mancini, Liposome-Based Sensor for the Detection of Bacteria, *Sensors Actuators, B Chem.,* **2017**, *248*, 247.
https:/doi.org/10.1016/j.snb.2017.03.124.

[28] S. Sennato, A. Sarra, C. Panella, L. Capria, C. Bombelli, E. Donati, P. Postorino, F. Bordi, Quantification of Particle Number Concentration in Liposomal Suspensions by Laser Transmission Spectroscopy (LTS), *Colloids Surfaces B Biointerfaces,* **2023**, *222*, 113137.
https://doi.org/10.1016/j.colsurfb.2023.113137.
[29] C.V. Montefusco-Pereira, B. Formicola, A. Goes, F. Re, C.A. Marrano, F. Mantegazza, C. Carvalho-Wodarz, G. Fuhrmann, E. Caneva, F. Nicotra, Coupling Quaternary Ammonium Surfactants to the Surface of Liposomes Improves Both Antibacterial 683 Efficacy and Host Cell Biocompatibility, *Eur. J. Pharm. Biopharm,* **2020**, *149*, 12.
https://doi.org/10.1016/j.ejpb.2020.01.013.
[30] R. Sharma, V.K.L. Reddy, G.M. Prashant, V. Ojha, N.P.G. Kumar, Antimicrobial and Anti-Adherence Activity of Various 685 Combinations of Coffee-Chicory Solutions on Streptococcus Mutans: An in-Vitro Study, *J. Oral Maxillofac. Pathol,* **2014**, *18*, 201.
https:/doi.org/10.4103/0973-029X.140749.
[31] M. Rozalski, B. Micota, B. Sadowska, A. Stochmal, D. Jedrejek, M. Wieckowska-Szakiel, B. Rozalska, Antiadherent and 688 Antibiofilm Activity of Humulus Lupulus L. Derived Products: New Pharmacological Properties, *Biomed Res. Int,* **2013**, *2013*, 689.
https:/doi.org/10.1155/2013/101089.
[32] T.K. Swetha, M. Pooranachithra, G.A. Subramenium, V. Divya, K. Balamurugan, S.K. Pandian, Umbelliferone Impedes Bio-691 film Formation and Virulence of Methicillin-Resistant Staphylococcus Epidermidis via Impairment of Initial Attachment and Inter-692 cellular Adhesion, *Front. Cell. Infect. Microbiol,* **2019**, *9*, ID357.
https:/doi.org/10.3389/fcimb.2019.00357.
[32] M. Yokoyama, E. Stevens, M. Laabei, L. Bacon, K. Heesom, S. Bayliss, N. Ooi, A.J. O'Neill, E. Murray, P. Williams, 696 Epistasis Analysis Uncovers Hidden Antibiotic Resistance-Associated Fitness Costs Hampering the Evolution of MRSA, *Genome Biol,* **2018**, *19*, 94.
https://doi.org/10.1186/s13059-018-1469-2.
[33] R.C. Mac Donald, R.I. Mac Donald, Applications of Freezing and Thawing in Liposome Technology. In *Liposome Technology,* G. Gregoriadis, Ed.; CRC Press: Boca Raton, Fla., **1992**.
[34] L.D. Mayer, M.J. Hope, P.R Cullis, Vesicles of Variable Sizes Produced by a Rapid Extrusion Procedure, *BBA – Biomembr*, **1986**, *858*, 161.
https://doi.org/10.1016/0005-2736(86)90302-0.

[35] H. S. Dhadwal, R.R. Ansari, W.V. Meyer, A Fiber - Optic Probe for Particle Sizing in Concentrated Suspensions, *Rev. Sci. Instrum.,* **1991**, *62*, 2963.
https://dx.doi.org/doi:10.1063/1.1142190.
[36] D.E. Koppel, Analysis of Macromolecular Polydispersity in Intensity Correlation Spectroscopy: The Method of Cumulants, *J. Chem. Phys*, **1972**, *57*, 4814.
https:/doi.org/10.1063/1.1678153.
[37] R.J. Hunter, Zeta Potential in Colloid Science Principles and Applications, R.H. Ottewill, R.L. Rowell, 1st edition, Elsevier, **1988.**

4. Agri-food waste extracts encapsulation in liposomes for enhancing their antimicrobial activity

4.1. Introduction

Agri-food industries generate a high amount of by-products and waste, both solids and liquids, from the production, preparation and consumption of foods, representing a serious environmental and economic problem worldwide in terms of pollution, depletion of natural resources and compromised food safety.[1] Therefore, for the last decades it has been necessary to seek new strategies to transform biomass waste into valuable products, with the aim of minimizing waste production and obtaining biomaterials and compounds, which can deliver new solutions to existing problems. In this regard, a circular economy approach on agri-food wastes could represent an important opportunity to create sustainable growth and generate profit.

Citrus fruits and olives represent some of the main foods on which the Mediterranean diet is based, due to the high contents of beneficial nutrients such as vitamins, minerals and dietary fibers. The worldwide production of these two fruits counts for millions of tons per year and consequently high levels of waste and by-products are produced. In particular, in the orange juice industry orange peels often represent a waste whose annual production is estimated to be 32 million tons,[2] whereas the pruning of olive trees in Europe generates 11.8 million tons of biomass.[3]

Both these by-products represent a serious economic and environmental problem for producers. Meanwhile, they contain valuable and valued compounds produced by plants as secondary metabolites and known as phytochemicals.[4]

The major group of bioactive compounds present in citrus peels and olive leaves are polyphenols which, exhibiting positive effects on well-being due to their antioxidant,[5,6] antimicrobial,[7,8] anti-inflammatory,[9] anti-atherogenic[10] and anticancer[11] properties, have gained pivotal attention in many application fields.[12]

Phenolic compounds present in olive leaves[13] and orange peels[14] can be extracted according to different procedures, such as conventional solvent extraction,[15] supercritical fluid extraction,[16] microwave-assisted extraction[17] or ultrasound-assisted extraction (UAE).[18] Among these techniques, UAE is widely recognized as a green and innovative procedure, because it involves reduced operations and relatively low costs, moderate energy consumption and short processing time; in addition, low quantity of water and solvents are generally required.[19] UAE is based on the principle of acoustic cavitation capable of damaging the cell walls of the vegetal matrix, thus favoring the release of bioactive compounds through several mechanisms, such as the collision

between particles and ultrasonic waves or the implosion of solvent bubbles on the surface of the vegetal matrix.[20]

However, most of natural compounds have shown low bioavailability because of intrinsic factors (chemical structure, low water solubility) and extrinsic factors (low stability in biological fluids, extensive phase 1 and phase 2 metabolism, rapid elimination), high sensitivity to environmental conditions (temperature, pH, light, presence of oxygen, enzymatic activity) and poor sensorial characteristics, thus preventing their potential use. To improve their bioavailability a number of nano-encapsulation techniques have been developed.[21] Among various delivery systems, liposomes have shown promising advantages as carriers of bioactive agents due to their ability to encapsulate hydrophilic and hydrophobic compounds, enhanced paracellular and transcellular cargo transport, and their low toxicity and biodegradable nature.[22]

Liposomes can be prepared by sonication technique, a simple green method widely exploited since the 1960s.[23] Sonication acoustic energy is employed to convert large and multilamellar vesicles or vesicle aggregates in smaller unilamellar liposomes, either empty or loaded with a cargo. The effect on the reduction of sizes, lamellarity and polydispersity index are closely related to the methodology specifications such as sonication power and sonication time[24,25] and can be ascribed to the cavitation phenomena which include the formation, growth, and implosive collapse of microbubbles/cavities releasing high energy in the medium.[26] Probe and bath sonication are the two main sonication methods used in liposomes production, besides probe sonication is probably the most widely used method of the two for the preparation of liposomes on small scale, because the sample has not to be warmed above the phase transition temperature due to local heating, and the high energy input can be applied directly into the lipid dispersion to obtain vesicles with suitable features. Nevertheless, the dissipation of energy at the tip results in local overheating and consequently the vessel containing the sample must be immersed in an ice/water bath to avoid lipid degradation, in particular long sonication time (up to 1 hour) can hydrolyse the lipids.[27]

Here we report on an investigation, carried out during my research period abroad spent at the Abertay University of Dundee (Scotland, UK) in collaboration with the research group of the Professor Alberto Fiore, aimed at evaluating the effect of the encapsulation in liposomes on the *in vitro* antimicrobial activity of olive leaves (OLE) and orange peels (OPE) extracts against *Staphylococcus aureus* (NCIMB 9518), *Bacillus subtilis (*ATCC 6051) and *Enterococcus faecalis* (NCIMB 775) as *Gram*-positive bacteria pathogens, and *Escherichia coli (*NCIMB 13302), *Pseudomonas aeruginosa (*NCIMB 9904) and *Klebsiella oxytoca* (NCIMB 12259) as *Gram*-negative.

The best ultrasound-assisted extraction conditions using a sonotrode were established to obtain polyphenols-rich extracts, which were characterized in terms of yield of extraction, total phenolic content and antioxidant capacity. The polyphenolic profiles of extracts were investigated by HPLC-MS analysis.

Liposomes formulated with a natural phospholipid, namely 1,2-dioleoyl-*sn*-glycero-3-phosphocholine (DOPC), and cholesterol (Chol) loaded with olive leaves and orange peels extracts (**Figure 1**) were characterized in terms of particle features, encapsulation efficiency, stability and releasing profile over time.

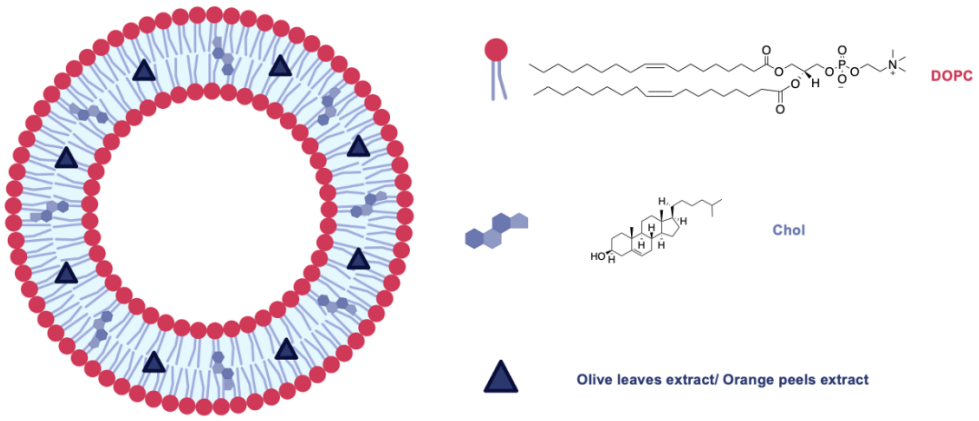

Figure 1. Schematic representation of liposome including plant extracts (created with BioRender.com).

4.2. Results and Discussion

4.2.1. Preparation and characterization of extracts

The optimization of UAE of olive leaves was tuned to obtain polyphenols and antioxidants enriched extracts, screening the effects of ultrasound duration on the yield of extraction and on the total phenolic content (TPC). In particular, the effect of sonication time was investigated keeping the sonicator amplitude constant (100%, 20 kHz frequency) and varying the extraction time up to 25 min.

The extraction was carried out keeping the temperature below 75°C. Actually, though temperature conditions above 75°C can stimulate breaking of matrix bond in addition to mass transfer phenomena, compound solubility and solvent diffusion rate, they can also promote higher degradation rates of the compounds of interest.[28]

Table 1. Values of extraction yield, TPC and technological parameters obtained for OLE at different sonication times.

Time (min)	Power (W)	T_i (°C)	T_f (°C)	ΔT (°C)	Power density (Ws/mL)	Yield (%)	TPC ($mg_{GAE}/g_{extract}$)
5	597	9	25	16	119.6	5.6	102 ± 5
10	540	9	49	40	229.8	6.6	159 ± 9
15	576	9	53	44	360.6	6.6	157 ± 4
20	601	9	62	53	504.4	6.6	155 ± 5
25	569	9	71	62	617.1	7.9	162 ± 2

The results reported in **Table 1** show higher extraction efficiencies and TPC in correspondence of the longest extent of sonication (25 minutes). The temperature reached for this time of sonication was 71°C and any further increment of sonication time yielded a sample temperature higher than 75°C. In particular, the extract obtained at 25 minutes was characterized by an extraction yield of 7.9% and a TPC of 162 $mg_{GAE}/g_{extract}$.

The UAE of orange peels was carried out at the Bio Based Europe Pilot Plant by a pilot scale process. Before UAE, matrix plant was enzymatically treated to break down pectin structure, with the aim to improve the yield of extraction and the polyphenolic content of the extract produced. Although the extraction yield obtained for OPE is quite high, namely 39.4%, its TPC is four times lower than that obtained in the case of OLE.

Table 2. Yield of extraction and antioxidant characterization of OLE and OPE.

Extract	Yield (%)	TPC ($mg_{GAE}/g_{extract}$)	TEAC ($mg_{TE}/g_{extract}$)	DPPH ($mg_{GAE}/g_{extract}$)	FRAP ($mg_{GAE}/g_{extract}$)
OLE	7.9	162 ± 2	140 ± 1	44 ± 1	41 ± 3
OPE	39.4	40 ± 4	83 ± 3	13 ± 2	31 ± 5

The antioxidant capacity of both extracts was assessed by Trolox Equivalent Antioxidant Capacity (TEAC) assay, DPPH radical scavenging assay and Ferric Ability Reducing Power (FRAP).

As reported in **Table 2**, the antioxidant activity evaluated by each assay is higher in the case of OLE than in the case of OPE, in agreement with the results obtained by Folin-Ciocalteu assay.

The determination of TPC and antioxidant capacity is a useful tool to characterize the nature of plant extracts, however it is not sufficient to fully characterize them. Therefore, a HPLC-ESI-TOF-MS analysis was carried out to assess the polyphenolic profile of both extracts.

4.2.2. Identification and quantification of phenolic compounds by HPLC-ESI-TOF-MS

4.2.2.1. Olive leaves extract (OLE)

The polyphenolic profile of OLE was determined by HPLC-ESI-TOF-MS analysis. Thirty-six compounds were identified according to their *m/z* molecular ion and by comparing them with data reported in the literature[29] and with several databases (PubChem, KEGG COMPOUNDS Database), and by the co-elution with commercial standards, when possible. The results are reported in **Table 3**, whereas **Figure 2** shows a representative chromatogram of OLE.

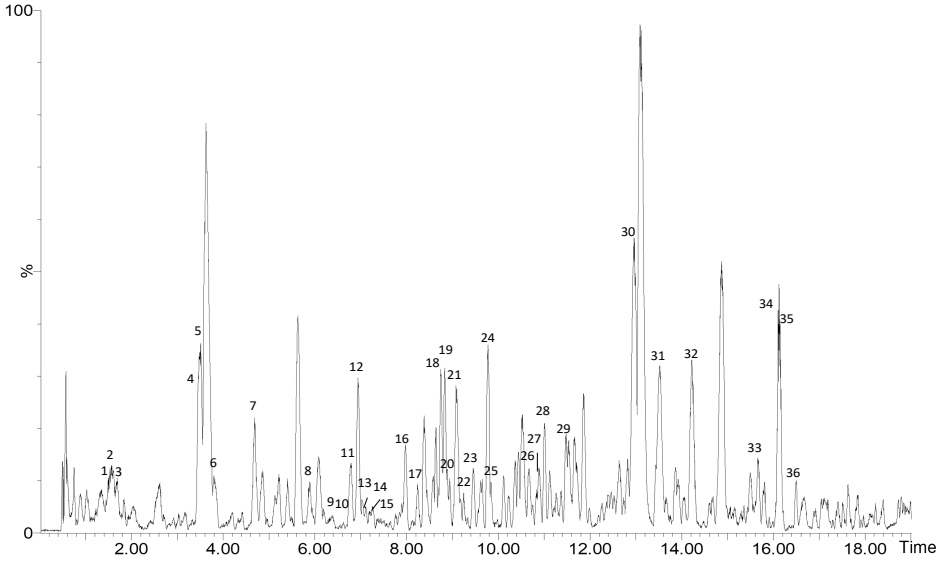

Figure 2. Chromatogram of OLE analyzed by HPLE-ESI-TOF-MS. Numbered peaks (1-36) correspond to the peaks reported in Table 3.

Table 3. Identification and quantification of phenols and antioxidant compounds in OLE by HPLC-ESI-TOF-MS.

Peak	RT (min)	Compound	*m/z* experimental	*m/z* calculated	Molecular Formula	µg/$g_{extract}$
1	1.45	Hydroxytyrosol-hexose	315.1074	315.1080	$C_{14}H_{20}O_8$	3134.3 ± 0.2
2	1.51	Oleoside	389.1064	389.1084	$C_{16}H_{22}O_{11}$	1689.6 ± 0.4
3	1.64	Hydroxytyrosol	153.0546	153.0552	$C_8H_{10}O_3$	2148.9 ± 0.8
4	3.44	Oleoside/secologanoside isomer a	389.1076	389.1084	$C_{16}H_{22}O_{11}$	628.7 ± 0.3
5	3.45	Oleoside/secologanoside isomer b	389.1076	389.1084	$C_{16}H_{22}O_{12}$	1493.0 ± 0.5
6	3.76	Elenolic acid glucoside isomer a	403.1233	403.1240	$C_{17}H_{24}O_{11}$	107.5 ± 0.1
7	4.62	Elenolic acid glucoside isomer b	403.1235	403.1240	$C_{17}H_{24}O_{11}$	635.3 ± 0.1
8	5.84	Luteolin rutinoside isomer a	593.1494	593.1506	$C_{27}H_{30}O_{15}$	75.5 ± 0.1
9	6.35	Elenolic acid glucoside isomer c	403.1230	403.1240	$C_{17}H_{24}O_{11}$	890.4 ± 0.1
10	6.59	Dihydroxyoleuropein isomer a	571.1658	571.1663	$C_{25}H_{32}O_{15}$	162.1 ± 0.1
11	6.72	Luteolin-diglucoside isomer a	609.1458	609.1456	$C_{27}H_{30}O_{16}$	126.6 ± 0.1
12	6.89	Elenolic acid glucoside isomer d	403.1240	403.1240	$C_{17}H_{24}O_{11}$	142.4 ± 0.1
13	7.04	β-Hydroxyverbascoside [Campneoside II] isomer a	639.1914	639.1925	$C_{29}H_{36}O_{16}$	191.4 ± 0.1
14	7.19	β-Hydroxyverbascoside [Campneoside II] isomer b	639.1918	639.1925	$C_{29}H_{36}O_{16}$	280.2 ± 01
15	7.52	Elenolic acid glucoside isomer e	403.1237	403.1240	$C_{17}H_{24}O_{11}$	214.3 ± 0.1
16	8.16	Elenolic acid glucoside isomer f	403.1222	403.1240	$C_{17}H_{24}O_{11}$	112.8 ± 0.1
17	8.35	Demethyloleuropein isomer	525.1597	525.1608	$C_{24}H_{30}O_{13}$	157.0 ± 0.1
18	8.71	Hydroxyoleuropein isomer a	555.1702	555.1714	$C_{25}H_{32}O_{14}$	3366.0 ± 0.2
19	8.79	Hydroxyoleuropein isomer b	555.1702	555.1714	$C_{25}H_{32}O_{14}$	387.3 ± 0.1
20	9.05	Luteolin rutinoside isomer b	593.1497	593.1506	$C_{27}H_{30}O_{15}$	219.2 ± 0.1
21	9.06	Luteolin glucoside isomer a	447.0918	447.0927	$C_{21}H_{20}O_{11}$	356.7 ± 0.1
22	9.26	Oleuropein glucoside isomer a	701.2291	701.2293	$C_{31}H_{42}O_{18}$	69.3 ± 0.1
23	9.43	Oleuropein glucoside isomer b	701.2292	701.2293	$C_{31}H_{42}O_{18}$	61.6 ± 0.1
24	9.62	Hydroxyoleuropein isomer c	555.1723	555.1714	$C_{25}H_{32}O_{14}$	686.8 ± 0.2
25	9.74	Verbascoside isomer a	623.1990	623.1976	$C_{29}H_{36}O_{15}$	351.2 ± 0.2
26	10.72	Oleuropein glucoside isomer c	701.2292	701.2293	$C_{31}H_{42}O_{18}$	717.0 ± 0.1
27	10.86	Oleuropein glucoside isomer d	701.2289	701.2293	$C_{31}H_{42}O_{18}$	1049.2 ± 0.1
28	10.97	Oleuropein glucoside isomer e	701.2301	701.2293	$C_{31}H_{42}O_{18}$	135.9 ± 0.1
29	11.44	Oleuropein glucoside isomer f	701.2296	701.2293	$C_{31}H_{42}O_{18}$	473.2 ± 0.2
30	12.43	Hydro-oleuropein	541.1932	541.1921	$C_{25}H_{34}O_{13}$	7832.1 ± 1.2
31	13.63	Ligstroside aglycone glucuronide	537.1608	537.1608	$C_{25}H_{30}O_{13}$	118.7 ± 0.1
32	14.32	Luteolin	285.0399	285.0399	$C_{15}H_{10}O_6$	253.0 ± 0.1
33	15.77	Ligstroside	523.1822	523.1816	$C_{25}H_{32}O_{12}$	60.5 ± 0.1
34	16.04	Oleuropein aglycone	377.1232	377.1236	$C_{19}H_{22}O_8$	396.4 ± 0.1
35	16.13	Frameroside/2"-epi-frameroside	601.2128	601.2132	$C_{27}H_{38}O_{15}$	182.8 ± 0.1
36	16.20	Oleuroside methyl ether isomer a	553.1922	553.1921	$C_{26}H_{34}O_{13}$	517.6 ± 0.1
		Sum of Oleuropein derivatives				15493.9 ± 0.2
		Sum of phenolic compounds				29517 ± 2

Some of the compounds identified in the sample were classified as phenols, elenolic acid derivatives, secoiridoids and flavonoids. Most of them are glucoside derivatives due to the high polarity of water, employed as extracting solvent.

The amount of each compound in the sample was determined and a total of 29517 μg/$g_{extract}$ of polyphenols was assessed, notably oleuropein derivatives represent the most abundant phenols accounting for 52.5 % of total identified phenols. Among them, hydro-oleuropein with *m/z* 541 is the most abundant compound (7832 μg/$g_{extract}$). Other abundant oleuropein derivatives are hydroxyoleuropein isomers with m/z 555 and oleuropein glucoside isomers with m/z 701 (3753 μg/$g_{extract}$ and 2506 μg/$g_{extract}$ respectively).

Finally, OLE was found to be rich in hydroxytyrosol-hexose (m/z 315), hydroxytyrosol (m/z 153) and oleoside (m/z 389), counting for 3134 μg/$g_{extract}$. All the other less abundant compounds are reported in **Table 3**.

4.2.2.2. Orange peel extract (OPE)

Analogously to OLE, phenolic compounds present in OPE were characterized by HPLC-ESI-TOF-MS analysis. A representative chromatogram of OPE is reported in **Figure 3**.

Table 4 reports the forty-one polar compounds identified in OPE, in good agreement with a previous report;[30] among them only phenolic acids and flavonoids were quantified.

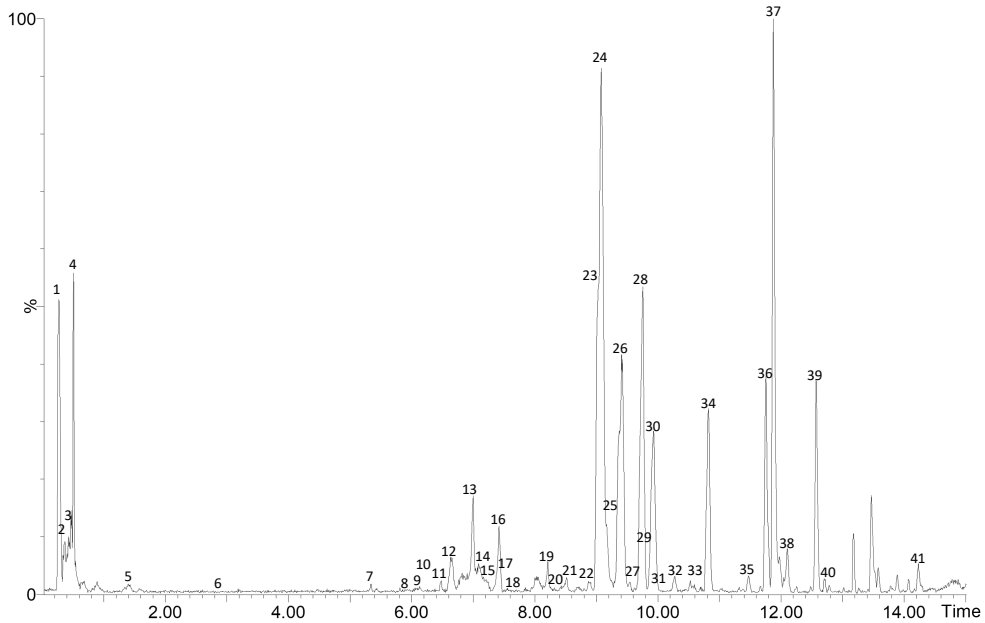

Figure 3. Chromatogram of OPE analyzed by HPLE-ESI-TOF-MS. Numbered peaks (1-41) correspond to the peaks reported in Table 4.

Table 4. Identification and quantification of phenols and antioxidant compounds in OPE by HPLC-ESI-TOF-MS.

Peak	RT (min)	Compound	*m/z* experimental	*m/z* calculated	Molecular formula	µg/$g_{extract}$
1	0.36	Gluconic acid isomer a	195.0499	195.0505	$C_6H_{12}O_7$	-
2	0.39	Citric acid	191.0185	191.0192	$C_6H_8O_7$	-
3	0.43	Gluconic acid isomer b	195.0498	195.0505	$C_6H_{12}O_7$	-
4	0.49	Isocitric acid	191.0183	191.0192	$C_6H_8O_7$	-
5	1.61	Norbergenin	313.0548	313.0560	$C_{13}H_{14}O_9$	144.3± 0.1
6	2.85	Caffeoylglycolic acid methyl ester isomer a	251.0552	251.0556	$C_{12}H_{12}O_6$	1355.0 ± 11.5
7	5.38	Cyranoside A	443.1900	443.1917	$C_{21}H_{32}O_{10}$	729.9 ± 2.0
8	5.88	Caffeoylglycolic acid methyl estrer isomer b	251.0547	251.0556	$C_{12}H_{12}O_6$	1142.3 ± 10.0
9	6.14	Caffeoylmalic acid isomer a	295.0441	295.0454	$C_{13}H_{12}O_8$	1330.3 ± 11.0
10	6.20	Citroside	385.1845	385.1862	$C_{19}H_{30}O_8$	-
11	6.58	Rutin	609.1436	609.1456	$C_{27}H_{30}O_{16}$	< LOQ
12	6.64	Apigenin-di-C-hexoside (Vicenin-2) isomer a	593.1532	593.1506	$C_{27}H_{30}O_{15}$	1114.3 ± 7.1
13	7.00	Apigenin-di-C-hexoside (Vicenin-2) isomer b	593.1534	593.1506	$C_{27}H_{30}O_{15}$	3283 ± 14
14	7.18	Dihydroisorhamnetin 7-rutinoside	625.1798	625.1827	$C_{21}H_{38}O_{21}$	25.1 ± 0.7
15	7.37	Isorhamnetin-3-O-rutinoside isomer a	623.1586	623.1612	$C_{28}H_{32}O_{16}$	50.2 ± 3.1
16	7.51	Isorhamnetin-3-O-rutinoside isomer b	623.1613	623.1612	$C_{28}H_{32}O_{16}$	102.4 ± 2.8
17	7.51	Caffeoylmalic acid isomer b	295.0449	295.0454	$C_{13}H_{12}O_8$	1126.1 ± 10.1
18	7.65	Isorhamnetin-3-O-rutinoside isomer c	623.1597	623.1612	$C_{28}H_{32}O_{16}$	< LOQ
19	8.36	Alpha-Glucosyl Hesperidin	771.2352	771.2348	$C_{34}H_{44}O_{20}$	560.3 ± 2.2
20	8.40	Eriocitrin	595.1657	595.1663	$C_{27}H_{32}O_{15}$	< LOQ
21	8.61	Vitexin-O-pentoside isomer a	563.1392	563.1401	$C_{26}H_{28}O_{14}$	315.3 ± 1.6
22	8.81	Naringin hydrate	597.1835	597.1819	$C_{27}H_{34}O_{15}$	202.8 ± 2.7
23	9.00	Vitexin-O-pentoside isomer b	563.1400	563.1401	$C_{26}H_{28}O_{14}$	467.2 ± 4.7
24	9.08	Limonin 17-β-D-glucopyranoside	649.2471	649.2496	$C_{32}H_{42}O_{14}$	-
25	9.17	Prunin	433.1132	433.1135	$C_{21}H_{22}O_{10}$	1634.9 ± 2.4
26	9.18	Naringenin	271.0599	271.0606	$C_{15}H_{12}O_5$	1473.7 ± 1.2
27	9.35	Naringin 4'-glucoside	741.2255	741.2242	$C_{33}H_{42}O_{19}$	144.2 ± 3.3
28	9.41	Narirutin isomer a	579.1708	579.1714	$C_{27}H_{32}O_{14}$	7319.6 ± 11.8
29	9.55	Kaempferol 3-rhamnoside-7-galacturonide	607.1310	607.1299	$C_{27}H_{28}O_{16}$	89.1 ± 4.4
30	9.75	Narirutin isomer b	579.1722	579.1714	$C_{27}H_{32}O_{14}$	7337.7 ± 57.1
31	9.89	Hesperetin 7-O-glucoside	463.1244	463.1240	$C_{22}H_{24}O_{11}$	174.7 ± 0.9
32	10.24	Hesperidin	609.1849	609.1819	$C_{28}H_{34}O_{15}$	3051.7 ± 25.9
33	10.58	Isorhamnetin-3-O-rutinoside isomer d	623.1661	623.1671	$C_{21}H_{35}O_{21}$	< LOQ
34	10.82	Isoobacunoic acid 17-β-D-glucoside	651.2642	651.2653	$C_{32}H_{44}O_{14}$	-
35	11.38	Pectolinarin	621.1833	621.1819	$C_{29}H_{34}O_{15}$	< LOQ
36	11.79	Didymin isomer a	593.1882	593.1870	$C_{28}H_{34}O_{14}$	579.7 ± 4.0
37	11.88	Nomilin 17-O-β-D-glucopyranoside	693.2768	693.2758	$C_{34}H_{45}O_{15}$	-
38	12.11	Didymin isomer b	593.1869	593.1870	$C_{28}H_{34}O_{14}$	333.8 ± 6.1
39	12.57	Nomilinic acid 17-β-D-glucoside	711.2861	711.2864	$C_{34}H_{48}O_{16}$	-
40	12.71	Obacunone 17-β-D-glucoside	633.2568	633.2547	$C_{32}H_{42}O_{13}$	-
41	14.23	Limonin	469.1854	469.1862	$C_{26}H_{30}O_8$	-
		Sum of phenolic acids				5098 ± 42
		Sum of flavonoids				28977 ± 76
		Sum of total phenolic compounds				34075 ± 118

For what concerns flavonoids, narirutin isomers (m/z 579) are the most abundant phenols in OPE, corresponding to 14658 $\mu g/g_{extract}$; then, in order of abundance, vicenin-2 isomers (m/z 593), hesperidin (m/z 609), prunin (m/z 433) and naringenin (m/z 271) count for 4397 $\mu g/g_{extract}$, 3052 $\mu g/g_{extract}$, 1635 $\mu g/g_{extract}$ and 1474 $\mu g/g_{extract}$, respectively.

For what concerns phenolic acids, the main compounds quantified are caffeoylglycolic acid methyl ester isomers (m/z 251) and caffeoylmalic acid isomers (m/z 295), 2497$\mu g/g_{extract}$ and 2456 $\mu g/g_{extract}$ respectively.

4.2.3. Preparation and characterization of liposomes

4.2.3.1. Preparation of liposomes

With the aim of protecting OLE and OPE from physical and biological degradation and deliver them with high efficiency to the target bacteria, we investigated their inclusion into liposomes formulated with a natural unsaturated phospholipid (DOPC) and cholesterol (Chol), at a 8:2 DOPC/Chol ratio and total lipid concentration of 10 mM. The presence of Chol in the formulation involves a more compact and stable lipid membrane with reduced permeability to water-soluble compounds, thus increasing the retention of the entrapped cargo.[31]

Liposomes were prepared by the thin lipid film hydration method, coupled with a freeze-thaw protocol followed by sonication. In the case of extract loaded liposomes, OLE and OPE were added to lipid mixture thus including the compounds in the thin lipid film.

Unloaded compounds were removed by dialysis from sonicated liposomes.

4.2.3.2. Size and ζ-potential determination

The mean diameter and the polydispersity index (PDI) of empty and loaded DOPC/Chol liposomes were investigated by Dynamic Light Scattering (DLS) analysis, while their ζ-potential was obtained by electrophoretic mobility measurements. The results of the experiments are reported in **Table 5**.

Table 5. Hydrodynamic diameter (D_h), PDI, ζ-Potential and Entrapment Efficiencies (EE%) of empty and loaded liposomes (10 mM in total lipids) in PBS (pH 7.4).

Composition	D_h (nm)	PDI	ζ-Potential (mV)	EE (%)
DOPC/Chol 8.0:2.0	95 ± 1	0.25 ± 0.01	-2.7 ± 0.6	-
DOPC/Chol/OLE 8.0:2.0	96 ± 1	0.21 ± 0.01	-4.5 ± 0.9	29
DOPC/Chol/OPE 8.0.2.0	101 ± 1	0.22 ± 0.01	-5.3 ± 0.5	11

As reported in **Table 5**, all formulations display monomodal size distributions characterized by dimensions ranging between 95 nm and 101 nm. The presence of OPE in liposomes induces a slight increase of hydrodynamic diameter with respect to empty liposomes. This suggests that loaded compounds induce a different organization of lipid membrane, thus modifying its properties.[32]

The PDI values of all the systems, in the range 0.21- 0.25, reveal the homogeneity and uniformity of the investigated liposomes.

The values of ζ-potential of liposomes loaded either with OLE or with OPE are lower with respect to empty liposomes, thus suggesting that the extract compounds are partially localized at the lipid/water interface, changing the net surface charge of liposomes. The difference in ζ-potential values of OLE and OPE loaded liposomes are due to the different nature of encapsulated phenolic compounds and to their amount absorbed at the surface of liposome membrane.

4.2.3.3. Entrapment Efficiency of extracts

The Entrapment Efficiencies (EE%) of OLE and OPE loaded into liposomes were assessed by Folin-Ciocalteu assay. Following this procedure, the amount of total polyphenols entrapped in DOPC/Chol liposomes was evaluated in comparison with their amount present in the free extracts. As reported in **Table 5**, the EE% measured for OLE and OPE was 29% and 11%, corresponding to 302 μg_{GAE}/mL and 40 μg_{GAE}/mL, respectively. Therefore, in the case of OLE, the amount of total polyphenols entrapped into liposomes is more than seven times higher than in the case of OPE. Although the EE% found in the case of OLE might seem low, the quantity of encapsulated phenols is fairly high. On the other hand, the low amount of polyphenols encapsulated into liposomes in the case of OPE could be due to the more hydrophilic nature of the polyphenolic compounds present in OPE.

4.2.3.4. Stability to storage

To investigate the physical stability of empty and loaded liposomes, particle hydrodynamic diameter and PDI values were evaluated by DLS measurements over 28 days of storage at 4°C protected from light sources. As shown in **Figure 4**, size and PDI of liposomes during storage changed only in the case of DOPC/Chol/OPE liposomes. In fact, in this case a progressive increase of dimensions, from 101 nm to 159 nm, and an increment of PDI value were observed. The increase of nanoparticles size could be due to vesicle aggregation phenomena.[33,34]

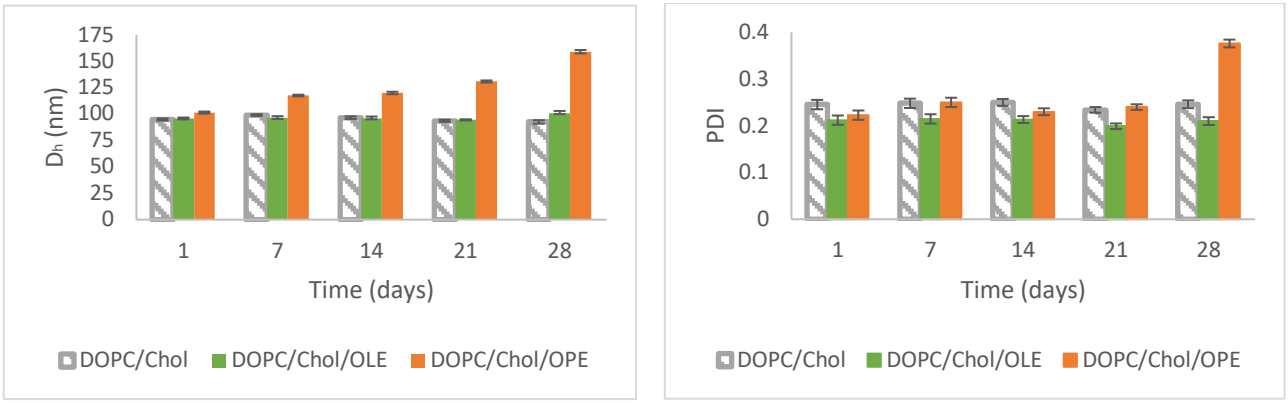

Figure 4. Liposomes particle size diameter (D_h) and PDI values during 28 days of storage at 4°C in the dark.

4.2.3.5. *In vitro* release study

To evaluate the ability of liposomes to act as extract delivery systems, an *in vitro* release study was carried out using dialysis. The release over time of phenolic compounds from DOPC/Chol/OLE and DOPC/Chol/OPE liposomes was evaluated from dialyzed samples by Folin-Ciocalteu assay.

As shown in **Figure 5**, 80:20 DOPC/Chol liposomes release 50% of entrapped polyphenols within 2-3 hours in the case of OLE and within 3-4 hours in the case of OPE. In both cases, the release of cargo from liposomes is slow during the first hour, then an increase of the releasing rate is observed, especially in the case of OLE loaded liposomes.

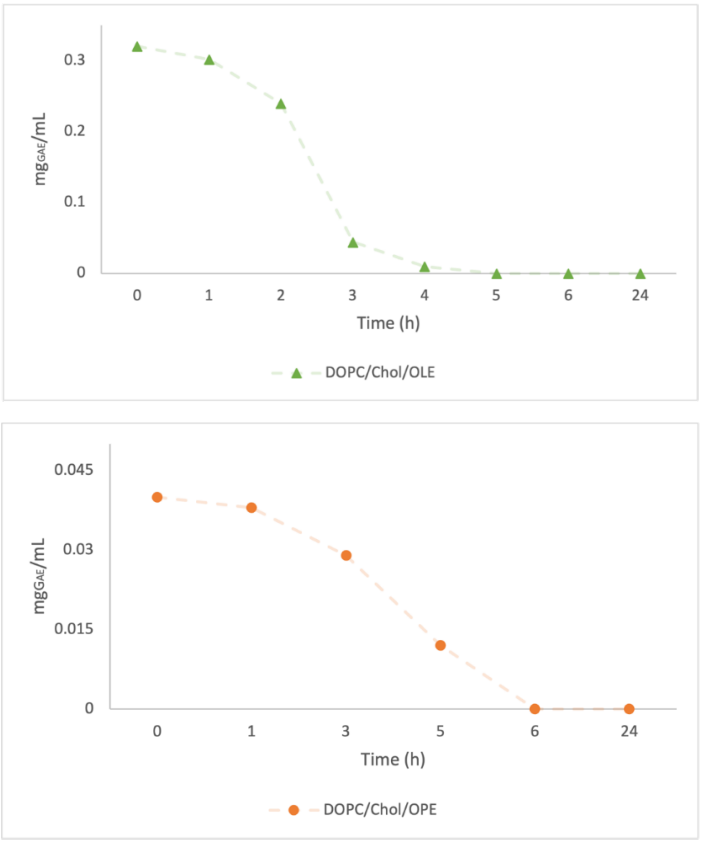

Figure 5. *In vitro* forced release of OLE (green triangles) and OPE (orange dots) from DOPC/Chol liposomes.

4.2.4. Antimicrobial activity

In the present study the antimicrobial activity of OLE and OPE, either free or loaded in DOPC/Chol liposomes, was investigated by the broth macrodilution method.

Firstly, the antimicrobial activity of free OLE and OPE was screened against six different bacteria pathogens, three *Gram*-positive and three *Gram*-negative strains. The tested microorganisms showed a variable susceptibility to OLE and OPE as reported in **Table 6**.

Table 6. Susceptibility of bacteria pathogen strains to OLE and OPE.

	Gram-positive			*Gram*-negative		
Extract	*S. aureus* NCIMB 9518	*E. faecalis* NCIMB 775	*B. subtilis* ATCC 6051	*E. coli* NCIMB 13302	*K. oxytoca* NCIMB 12259	*P. aeruginosa* NCIMB 9904
OLE	+	-	-	-	-	-
OPE	-	-	+	-	-	-

+ effective - not effective

Both OLE and OPE did not show any antimicrobial activity against bacteria pathogens belonging to the screened *Gram*-negative strains. However, it is worth of note that generally the treatment of *Gram*-negative bacterial infections is more difficult because of the presence of active efflux pumps,

of the production of antibiotic degrading enzymes and of some additional resistance mechanisms to antibiotics due to the structure of the outer membrane of these bacteria, composed by lipopolysaccharide and proteins; all these factors influence and reduce their susceptibility to various antimicrobial drugs.[35,36]

On the other hand, OLE was found to be selectively effective against a *Gram*-positive pathogen strain, namely *S. aureus* (NCIMB 9518), with a MIC value of 7 mg/mL corresponding to 1.135 mg_{GAE}/mL (as assessed by Folin-Ciocalteu assay) and OPE showed an antimicrobial activity against *B. subtilis* (ATCC 6051) with a MIC value of 10 mg/mL corresponding to 0.403 mg_{GAE}/mL (as assessed by Folin-Ciocalteu assay). In both cases, MBC values were not determined because it was considered not relevant and useful to test extract concentrations higher than 10 mg/mL.

Liposomes can protect polyphenols from chemical and biological degradation,[37] further they can be a useful tool to deliver them efficiently to a specific tissue or cell target, also eluding specific mechanisms of resistance,[38] therefore we investigated the antimicrobial activity of OLE and OPE included into DOPC/Chol liposomes.

Because we ascribe the antimicrobial activity of the extracts to the polyphenols and we cannot quantify their total amount when encapsulated, we assumed as reasonable to report MIC and MBC values of both free (see above) and encapsulated extracts as milligrams of Gallic Acid equivalents per milliliter (mg_{GAE}/mL) to have values useful for the comparison.

OLE loaded in liposomes showed an antimicrobial activity with a final MIC value of 0.113 mg_{GAE}/mL; experimentally we couldn't determine MBC, we evaluated that it is higher than 0.151 mg_{GAE}/mL, which was the highest concentration testable. Therefore, by comparing the MIC values of OLE tested in free form and loaded in liposomes, it is worth of note that the encapsulation of OLE in liposomes showed a positive effect on the activity against *S. aureus* by increasing the antimicrobial activity of OLE encapsulated by ~ 10 times. This great effect could be related to the surface polarity of liposomes, which enhances the interaction with bacteria membrane surface. This could lead to the better diffusion and interaction of the active compounds released from the lipid bilayer across the bacterial cell walls, favoring their permeability and affecting bacteria organelles, eventually resulting in the inhibition of bacterial growth.[39] Therefore, the inclusion of OLE polyphenols in liposomes not only increases their solubility in biological fluids, their bioavailability at the target sites and the protective effect from internal and external degradation by retarding chemical reactions,[40,41] it also improves their antimicrobial activity.

On the other hand, the inclusion of OPE in DOPC/Chol liposomes did not show the same beneficial effect observed for OLE in terms of antimicrobial activity against *B. subtilis* (ATCC 6051). In fact, it was not possible to assess MIC and MBC values of encapsulated OPE, that are certainly higher than the highest testable concentration (0.025 mg_{GAE}/mL) in our experimental conditions. This is due to the EE% obtained for DOPC/Chol/OPE liposomes corresponding to 11% of total OPE polyphenols, which was not sufficient to achieve any inhibitory effects.

The activity of DOPC/Chol empty liposomes was evaluated against both bacterial strains responsive to the action of OLE and OPE. In both cases, there was no evidence of antimicrobial activity due to empty liposomes.

4.3. Conclusions

Olive leaves and orange peels are good sources of phenolic compounds with high benefits to human health due to their antioxidant, antibacterial and antiproliferative activities.

In this work we obtained extracts from olive leaves and orange peels, rich in polyphenolic compounds, by UAE using a food-grade solvent, such as water. Extracts were characterized in terms of total phenolic content and antioxidant capacity, moreover their polyphenolic profile was investigated by HPLC-MS analysis.

The efficient encapsulation of extracts into liposomes formulated with a natural phospholipid (DOPC) and cholesterol, beside enhancing the solubility, stability and the bioavailability of the loaded phenols, proved to improve their antimicrobial activity. In particular, the encapsulation of OLE in DOPC/Chol liposomes enhances its antibacterial activity against *S. aureus* by an order of magnitude.

4.4. Experimental Materials and Methods

4.4.1. Materials

Olive leaves from *Olea europaea* and orange peels from *Citrus sinensis* were provided by Bidah-Chaumel (Lorquì, Murcia, Spain) as dry materials. Gallic acid (purity 97%), trolox ((±)-6-hydroxy-2,5,7,8-tetramethylchromane-2-carboxylic acid (purity ≥ 97%), trichloroacetic acid, hydroxytyrosol, oleuropein, apigenin-7-glucoside, rutin, luteolin, vanillic acid, quercetin, chlorogenic acid, ferulic acid, Folin & Ciocalteu's phenol reagent, phosphate-buffered saline (PBS; 0.01 M phosphate buffer, 0.0027 M KCl, 0.137 M NaCl, pH 7.4, at 25 °C), cellulose dialysis membrane (D9527-100FT, molecular weight cut off = 14 kDa) and cholesterol (purity 99%) were purchased from Sigma-Aldrich. Sodium carbonate (purity ≥ 98%) was purchased by Fluka Chemie. 1,2-dioleoyl-*sn*-glycero-3-phosphocholine (DOPC) was purchased from Avanti Polar Lipids (Alabaster, AL, USA). ABTS (2,2'-Azino-bis (3-ethylbenzothiazoline-6-sulfonic acid) diammonium salt, purity ≥ 98%) and potassium persulfate were purchased from Roche Diagnostic GmbH. DPPH (2,2-diphenyl-1-picrylhydrazyl, purity 95%) was purchased from Alfa Aesar. Iron (III) chloride hexahydrate (purity 97%), Muller Hinton Broth (CM 0405) and Muller Hinton Agar (CM 0337) were purchased from Thermo Fisher Scientific. Chloroform, methanol, ethanol, acetic acid, acetonitrile and water were HPLC grade and were purchased from Merk KGaA.

4.4.2. Ultrasound-assisted extraction

4.4.2.1. Olive leaves extract (OLE)

OLE was obtained by ultrasound-assisted extraction, using a UIP2000hdT (20KHz, 2000W) ultrasonicator (Hielschier) settled with the ultrasound generator, transducer and radial sonotrode (RS4d40L4, d=40 mm) in a batch process. Dried olive leaves were grinded to a fine powder that was suspended into a cylinder filled with chilled water (4-6°C), at 1:50 (w/v) sample:water ratio. The cylinder was immersed in an ice bath to keep temperature below 75°C during sonication process. The extraction process was carried out taking into consideration the influence of the extraction time (from 5 to 25 minutes) and acoustic parameters (amplitude, total power (W), energy transferred (W x s) and power density (W x s/mL)) on the yield of extraction and on the TPC. The extract was filtered with a strainer and centrifuged (Hermle Z323K) at 8000 rpm at 4°C for 15 min. Finally, the

supernatants were protected from light and stored under refrigeration (-20°C) until spray drying process.

4.4.2.2. Orange peels extract (OPE)

OPE was produced at Bio Based Europe Pilot Plant on a pilot scale trial process in the framework of the European Project Shealthy (Horizon 2020 - grant number 817936). 70 kg of powdered dried orange peels in 600 L of water were enzymatically treated using 400 mL of Pectinex ULTRA SP-L at 30°C for 24 h. Afterwards, the ultrasound assisted extraction was performed by an UIP2000hdT (20KHz, 2000W) ultrasonicator (Hielschier) apparatus settled with the ultrasound generator, transducer and cascatrode (CS4d40L3, d=40 mm). The slurry was recirculated over sonicator at 10°C for 12 h. The residual solid matrix was removed via decanter, while the liquid extract was subjected to different filtration processes: microfiltration (0.45 μm), ultrafiltration (10 kDa), nanofiltration (0.15-0.30 kDa) and sterile filtration (PES 0.2 μm). Finally, the extract produced was stored at -20°C until spray drying process.

4.4.3. Spray-Drying process

250 mL aliquots of each extract were spray dried by a Büchi Mini Spray Dryer B-290, using the following parameters: inlet temperature 170-180 °C, aspirator 100%, pump 20%, flow 40-60%. For each sample, the yield of extraction was determined as the percentage ratio between the weight of the dry extract residue and that of the plant material used in the extraction process (**Eq. 1**):

$$R(\%) = \frac{g_{spray-dried\ extract}}{g_{plant\ material}} \times 100 \qquad \textbf{(Eq. 1)}$$

The final spray-dried extracts were stored at -20°C before use.

4.4.4. Total Phenolic Content (TPC)

The TPC of the extracts was determined by Folin-Ciocalteu assay, following the procedure reported by de Falco et al.[42]

Briefly, Folin-Ciocalteu (FC) reagent was diluted with water (1/10 v/v) and protected from light; then 540 μL of diluted FC reagent and 432 μL of 7.5 % (w/v) Na_2CO_3 solution were added to 27 μL of sample (concentration ranging from 0.4 mg/mL to 10 mg/mL) and incubated at 50°C for 5 minutes. Finally, the absorbance was measured at 760 nm using a spectrophotometer (Thermo GENESYS™

10UV UV-Vis) and readings were performed in triplicate. The TPC was calculated using Gallic Acid as reference standard (calibration curve 15.3-500 μg/mL) and expressed in milligrams of Gallic Acid equivalents (GAE) per gram of dry extract ($mg_{GAE}/g_{extract}$).

4.4.5. Determination of antioxidant capacity

4.4.5.1. Trolox Equivalent Antioxidant Capacity (TEAC assay)

TEAC assay was used to evaluate the antioxidant capacity of OLE and OPE according to the procedure reported by de Falco et al.[42]

Briefly, ABTS radical cation ($ABTS^{\bullet+}$) was generated by reacting 7 mM ABTS and 140 mM potassium persulfate leaving the solutions overnight at 4°C in the dark, then the aqueous solution of $ABTS^{\bullet+}$ was diluted to obtain an absorbance of 0.700-0.750 at 734 nm. 1 mL of $ABTS^{\bullet+}$ solution was then added to 100 μL of sample (concentration ranging from 0.4 mg/mL to 2.0 mg/mL). The mixture was kept at room temperature for 150 s and the absorbance was measured at 734 nm.

Readings were assessed in triplicate and were used to determine the % of inhibition according to the following equation (**Eq. 2**):

$$\%\ inhibition = \left(1 - \frac{Abs_{sample}}{Abs_{control}}\right) \times 100 \qquad \textbf{(Eq. 2)}$$

where Abs_{sample} is the absorbance of the sample in the presence of $ABTS^{\bullet+}$ and $Abs_{control}$ is the absorbance of $ABTS^{\bullet+}$ solution alone.

Trolox, a water-soluble analogue of vitamin E, was used as reference standard and a calibration curve (3.90-62.6 μg/mL) was made plotting the percentage of $ABTS^{\bullet+}$ inhibitions as a function of micrograms (μg) of Trolox added.

% of inhibition of extract samples were finally expressed as milligrams of Trolox equivalents (TE) per gram of dry extract ($mg_{TE}/g_{extract}$).

4.4.5.2. DPPH radical-scavenging assay

The scavenging activity of OLE and OPE on DPPH free radical was measured according to the following procedure.[43,44] 1 mM DPPH stock solution in methanol was prepared and diluted with methanol to obtain a DPPH working solution characterized by an absorbance of 0.800-0.900 at

517 nm. Extract analyses were carried out by adding 1 mL DPPH working solution to 20 µL of extract (concentration ranging from 2 mg/mL to 10 mg/mL). The mixture was incubated 10 minutes at room temperature and the absorbance was measured at 517 nm. All analysis were carried out in triplicate and the percentage of inhibition was calculated as reported in equation **Eq. 3**:

$$\% \, inhibition = \left(1 - \frac{Abs_{sample}}{Abs_{\text{control}}}\right) \times 100 \qquad \textbf{(Eq. 3)}$$

where Abs_{sample} is the absorbance of the sample in the presence of DPPH and $Abs_{control}$ is the absorbance of the DPPH solution.

Gallic Acid was used as reference standard and a calibration curve (5.0-150 µg/mL) was made plotting the percentage of DPPH inhibitions as a function of micrograms (µg) of Gallic Acid added.

% of inhibition of extract samples were finally expressed as milligrams of Gallic Acid equivalents (GAE) per gram of dry extract ($mg_{GAE}/g_{extract}$).

4.4.5.3. Ferric reducing ability power

Antioxidant capacity of OLE and OPE was also assessed evaluating their ferric reducing ability, following the procedure reported by Benzie et al., slightly modified.[45] In particular, i) a 300 mM sodium acetate buffer solution, adjusted to pH 3.6 with acetic acid, ii) a 10 mM ferrous-TPTZ (2,4,6-tris(2-pyridyl)-s-triazine) complex solution in 40 mM HCl, and iii) a 20 mM $FeCl_3 \bullet 6H_2O$ solution were prepared. FRAP reagent was prepared by mixing 25 mL of sodium acetate buffer with 2.5 mL of ferrous-TPTZ solution and 2.5 mL of $FeCl_3 \bullet 6H_2O$ solution. To perform the assay 900 µL of FRAP reagent were added to 100 µL of sample (sample concentration ranging from 0.2 mg/mL to 2 mg/mL) and the mixture was allowed to react for 4 minutes at room temperature. The absorbance was then measured at 517 nm in triplicate. Gallic Acid was used as reference standard (calibration curve 0.025-0.40 µg/mL) and results were expressed as milligrams of Gallic Acid equivalents (GAE) per gram of dry extract ($mg_{GAE}/g_{extract}$).

4.4.6. Determination of OLE phenolic profile by HPLC-ESI-TOF-MS analysis

The phenolic composition of OLE was determined according to the method previously described by Talhaoui et al. slightly modified.[46,47] The equipment consists of an ACQUITY (Water Corporation, Milford, MA, USA) UPLC system coupled with a time-of-flight analyzer (TOF) (Water Corporation, Milford, MA, USA). Phenolic compounds were separated by a Poroshell 120 EC-C18 analytical

column (4.6 x 100 mm, 2.7 mm) from Agilent Technologies, under the following conditions: column temperature 25°C, flow rate 0.8 mL min^{-1}, injection volume 2.5 µL. The mobile phases were water with 1% acetic acid (phase A) and acetonitrile (phase B), changing the solvent gradient as it follows: 0 min, 5% B; 4 min, 9% B; 7 min, 12% B; 8 min, 15% B; 9 min, 16% B; 14 min, 20% B; 15 min, 22% B; 18 min, 28% B; 19 min, 30% B; 20 min, 31% B; 24 min, 40% B; 28 min, 100% B; 31 min, 100% B; 33 min, 5% B. Mass spectrometer was equipped with an interface with electrospray ionization (ESI) source operating in negative mode. Operational conditions were: capillary voltage, 2300 kV; source temperature, 100°C; cone gas flow, 40 L/h; desolvatation temperature, 500°C; desolvatation gas flow, 11.000 L/h; scan range, *m/z* 50-1500. MassLynx 4.1 (Water Corporation, Milford, MA, USA) software was used to process acquired data.

The quantification of phenolic compounds in the extracts was performed by using five different standards, namely, hydroxytyrosol, apigenin-7-glucoside, rutin, luteolin and oleuropein. Their calibration curves were assessed in the range of 1-250 µg/mL at eight concentrations.

4.4.7. Determination of OPE phenolic profile by HPLC-ESI-TOF-MS analysis

The analysis on OPE were assessed according to the procedure previously stated by Verni et al.[48] The analysis was carried out by an ACQUITY UPLC system (Waters Corporation, Milford, MA, United States) coupled to an electrospray ionization (ESI) source operating in the negative mode and a time-of-flight (TOF) mass detector (Waters Corporation, Milford, MA, United States) following these conditions: capillary voltage, 2300 kV; source temperature, 100 °C; cone gas flow, 40 L/Hr; desolvatation temperature, 500 °C; desolvatation gas flow, 11,000 L/h; scan range, *m/z* 50–1500. The compounds of interest were separated on an ACQUITY UPLC BEH Shield RP18 column (1.7 µm, 2.1 mm x 100 mm; Waters Corporation, Milford, MA, United States) at 40 °C. The elution gradient was carried out using water containing 1% acetic acid (phase A) and acetonitrile (phase B), and applied as follows: 0 min, 1% B; 2.3 min, 1% B; 4.4 min, 7% B; 8.1 min, 14% B; 12.2 min, 24% B; 16 min, 40% B; 18.3 min, 100% B, 21 min, 100% B; 22.4 min, 1% B; 25 min, 1% B. The sample volume injected was 2 µL and the flow rate used was 0.6 mL/min. The compounds were monitored at 280 nm. Integration and data elaboration were performed using MassLynx 4.1 software (Waters Corporation, United States). For the quantification of phenolic compounds, solutions of ferulic acid, chlorogenic acid, vanillic acid, catechin, rutin and quercetin in methanol: water 1:1 (v/v) were prepared and used as standards. The calibration curves were elaborated by using the peak areas of

each standard measured by HPLC at different concentrations from LOQ (0.14-1.57 µg/mL) to 250 µg/mL.

4.4.8. Preparation of liposomes

Liposomes, both empty and extract loaded, were formulated with a natural unsaturated phospholipid (DOPC, 6.28 mg/mL) and cholesterol (Chol, 0.77 mg/mL). Empty and loaded liposomes were prepared according to the Thin-Layer Evaporation method combined with the sonication protocol reported.[27] In particular, the proper amount of lipid components (DOPC and Chol) was dissolved in chloroform, while the dry extracts (OLE or OPE, 7.05 mg/mL) were dissolved in methanol to obtain a final ratio lipids:extract 1:1 (w/w). All the components were mixed in a round bottom flask, dried by rotary evaporation and then under a flux of nitrogen to remove all trace of solvents obtaining a thin lipid film, which was hydrated with a phosphate buffer saline solution (PBS 150mM) to give a suspension of liposomes 10 mM in total lipids concentration (DOPC 8 mM and Chol 2 mM), then vortex-mixed to completely detach the film from flask wall. The resulting multilamellar vesicles were freeze-thawed five times from liquid nitrogen to 50°C and then were subjected to 15 minutes of sonication (Model Q55, Sonica Sonicator) in pulsed mode (3 minutes ON and 3 minutes OFF) at an amplitude of 20% of full power. Finally, to remove the metallic particles sheddered from the tip and the larger lipid particles, the suspensions were centrifuged at 14.000 rpm for 10 minutes. The removal of unentrapped extract was performed by dialysis in PBS (buffer volume 25-times the total volume of the sample) by changing the diffusate buffer every 30 min over 2 h and keeping the system slowly stirred throughout.

4.4.9. Physicochemical characterization of liposomes

4.4.9.1. Size and ζ-potential measurements

Size distributions, polydispersity index (PDI) and ζ-potential were determined by Dynamic and Dielectrophoretic Light Scattering (DLS, DELS) measurements using a Malvern Zetasizer Nano ZS equipped with a 5 mV He/Ne laser (λ = 632.8 nm) and a thermostated cell holder. Temperature was set at 25°C in all the measurements.

Particle size and PDI were measured in the backscatter detection at an angle of 173°. The measured autocorrelation function was analysed by using the cumulant fit. The first cumulant was used to obtain the apparent diffusion coefficients (D) of the nanoparticles, further converted into apparent hydrodynamic diameters (D_h) by using Stokes-Einstein relation (**Eq. 4**):

$$D_h = \frac{K_b T}{3\pi\eta D} \quad \textbf{(Eq. 4)}$$

where $k_B T$ is the thermal energy and η is the solvent viscosity.

Before the measurements, suspensions of liposomes were diluted to 1 mM in total lipid concentration in PBS 150 mM and then analysed by DLS.

The ζ-potential of liposomes was determined by DELS measurements. Low voltages have been applied to avoid the risk of Joule heating effects. Analysis of the Doppler shift to assess the electrophoretic mobility was done by using phase analysis light scattering (PALS),[49] a method which is especially useful at high ionic strengths, where mobility is usually low. The mobility μ of the liposomes was converted into a ζ-potential using the Smoluchowski relation ζ =μ η/ε, where ε and η are the permittivity and the viscosity of the solution, respectively.

Liposome suspensions were diluted to 1 mM in total lipid concentration in diluted PBS (15 mM) to assess DELS measurements.

All data reported of hydrodynamic diameter, PDI and ζ-potential correspond to the average of three different measurements.

4.4.9.2. Evaluation of liposomes stability

The stability of extract loaded and empty liposomes was evaluated by checking vesicles size and PDI over 28 days of storage at 4°C, protecting samples from light sources. Measurements were performed as described in the above section.

4.4.9.3. Entrapment Efficiency determination

The Entrapment Efficiency (EE%) of OLE and OPE into liposomes was determined by Folin-Ciocalteu assay. In particular, the content of total phenolic compounds was assessed on the extracts loaded into liposomes and compared with the amount measured in the spray dried extracts. The suspensions of liposomes were properly diluted with methanol (1:1 v/v) to break lipid aggregates thus triggering the release of loaded phenolic compounds. The assay was carried out also on empty liposomes diluted with methanol (1:1 v/v) to assess the contribution to the Folin-Ciocalteu assay due to lipid components. Absorbance was measured at 760 nm and readings were performed in triplicate. The results were expressed as micrograms of Gallic Acid equivalents (μg_{GAE}).

Finally, the entrapment efficiency was calculated as follows (**Eq. 5**):

$$EE\% = \frac{(\mu g_{GAE})_{loaded\ liposome} - (\mu g_{GAE})_{empty\ liposome}}{(\mu g_{GAE})_{dry\ extract}}\ x\ 100 \qquad \textbf{(Eq. 5)}$$

where $(\mu g_{GAE})_{loaded\_liposome}$, $(\mu g_{GAE})_{empty\_liposome}$ and $(\mu g_{GAE})_{dry\_extract}$ are respectively the micrograms of Gallic Acid equivalents obtained for extract loaded liposomes, empty liposomes and spray dried extract unentrapped.

4.4.9.4. *In vitro* release of extracts from liposomes

The release of phenolic compounds from OLE and OPE loaded liposomes was determined by dialysis method (PBS volume 50-times the total volume of the sample). Samples were collected every 1 hour over a period of 24 hours and analysed by Folin-Ciocalteu assay (Gallic Acid used as reference standard, calibration curve 10-2000 μg/mL) to study the releasing profile of the polyphenols encapsulated. All the collected liposomal aliquots were analysed after dilution with MeOH (1:1 v/v) to break the lipid aggregates and to enhance the release of phenolic compounds entrapped. Then, the assay was assessed as described above. The phenolic content still encapsulated in liposomes was determined at a specific time and expressed as micrograms of Gallic Acid equivalents per milliliters (μg_{GAE}/mL).

4.4.10. *In vitro* antimicrobial activity

4.4.10.1. Bacterial strains

Antimicrobial activity assessment of OLE and OPE, both free and loaded in liposomes, was evaluated against different bacteria strains: *Staphylococcus aureus* (NCIMB 9518), *Bacillus subtilis (*ATCC 6051) and *Enterococcus faecalis* (NCIMB 775) as *Gram*-positive, as well as *Escherichia coli (*NCIMB 13302), *Pseudomonas aeruginosa (*NCIMB 9904) and *Klebsiella oxytoca* (NCIMB 12259) as *Gram*-negative.

4.4.10.2 Determination of *Minimum Inhibitory Concentration* (MIC) and *Minimum Bactericidal Concentration* (MBC)

The broth macrodilution method was used to measure quantitatively the *in vitro* activity of OLE and OPE, both free and loaded in liposomes, against the selected bacteria strains. As described in the Clinical and Laboratory Standards Institute (CLSI) guidelines,[50] an overnight culture of each bacterial strain was prepared in Muller Hinton Broth (MHB) and incubated at 37°C. Briefly, a series of 10 tubes

with MHB was prepared with various concentration of extract, either free or loaded in liposomes. The tubes were then inoculated with a standardized suspension of the test microorganisms. Strains were prepared for testing by adjusting the turbidity of each microbial culture to reach an optical density comparable to that of a 0.5 M McFarland standard solution. These resulted in suspensions containing approximately 1-2 x 10^8 CFU/mL. After incubation at 37°C for 24 h, the MIC was deduced from the first tube of the series in which no bacterial growth occurred (no turbidity, no deposit of bacterial products). Growth inhibition in each test tube was compared to the growth control (positive control, free treatment test tube). The test tube in which bacterial growth was not detected were streaked on Muller Hinton Agar (MHA) plates. Petri Dishes were then incubated at 37°C for 24h and the MBC was deduced from the lowest concentration at which no culture was observed on MHA plates. The experiments were repeated until three consistent results were achieved.

4.5. References

[1] S. Corrado, S. Sala, Food waste accounting along global and European food supply chains: State of the art and outlook, *Waste Management*, **2018**, *79*, 120.
https://doi.org/10.1016/j.wasman.2018.07.032

[2] U. Michael-Igolima, S. J. Abbey, A. O. Ifelebuegu, E. U. Eyo, Modified Orange Peel Waste as a Sustainable Material for Adsorption of Contaminants, *Materials*, **2023**, *16* (3), 1092.
https://doi.org/10.3390/ma16031092

[3] J. Berbel, A. Posadillo, Review and Analysis of Alternatives for the Valorisation of Agro-Industrial Olive Oil By-Products. *Sustainability*, **2018**, *10* (1), 237.
https://doi.org/10.3390/su10010237

[4] W. Peschel, F. Sánchez-Rabaneda, W. Diekmann, A. Plescher, I. Gartzía, D. Jiménez, R. Lamuela-Raventós, S. Buxaderas, C. Codina, An Industrial approach in the search of natural antioxidants from vegetable and fruit wastes, *Food Chemistry*, **2006**, *97*, 137.
https://doi.org/10.1016/j.foodchem.2005.03.033

[5] I. Kafantaris, D. Stagos, B. Kotsampasi, A. Hatzis, A. Kypriotakis, K. Gerasopoulos, S. Makri, N. Goutzourelas, C. Mitsagga, I. Giavasis, K. Petrotos, S. Kokkas, P. Goulas, V. Christodoulou, D. Kouretas, Grape pomace improves performance, antioxidant status, fecal microbiota and meat quality of piglets, *Animal*, **2018**, *12* (2), 246.
https://doi.org/10.1017/S1751731117001604

[6] R. Briante, M. Patumi, S. Terenziani, E. Bismuto, F. Febbraio, R. Nucci, *Olea europaea* L. Leaf Extract and Derivatives: Antioxidant Properties, *Journal of Agricultural* and *Food Chemistry,* **2002**, *50* (17), 4934.
https://doi.org/10.1021/jf025540p

[7] H. Kumar, K. Bhardwaj, N. Cruz-Martins, E. Nepovimova, P. Oleksak, D. S. Dhanjal, S. Bhardwaj, R. Singh, C. Chopra, R. Verma, P. P. Chauhan, D. Kumar, K. Kuca Applications of Fruit Polyphenols and Their Functionalized Nanoparticles Against Foodborne Bacteria: A Mini Review, *Molecules,* **2021**, *26*, 3447.
https://doi.org/10.3390/molecules26113447

[8] M. Miklasińska-Majdanik, M. Kępa, R. D. Wojtyczka, D. Idzik, T. J. Wąsik, Phenolic Compounds Diminish Antibiotic Resistance of *Staphylococcus Aureus* Clinical Strains, *International Journal of Environmental Research and Public Health,* **2018**, *15 (10)*, 2321.
https://doi.org/10.3390/ijerph15102321

[9] R. Direito, J. Rocha, B. Sepodes, M. Eduardo-Figueira, Phenolic Compounds Impact on Rheumatoid Arthritis, Inflammatory Bowel Disease and Microbiota Modulation, *Pharmaceutics* **2021**, *13* (2), 145.
https://doi.org/10.3390/pharmaceutics13020145
[10] F. Visioli, C. Galli, Antiatherogenic components of olive oil, *Current Atherosclerosis Reports*, **2001**, *3*, 64.
https://doi.org/10.1007/s11883-001-0012-0
[11] R. Sirianni, A. Chimento, A. De Luca, I. Casaburi, P. Rizza, A. Onofrio, D. Iacopetta, F. Puoci, S. Andò, M. Maggiolini, V. Pezzi, Oleuropein and hydroxytyrosol inhibit MCF-7 breast cancer cell proliferation interfering with ERK1/2 activation, *Molecular Nutrition & Food Research*, **2010**, *54*, 833.
https://doi.org/10.1002/mnfr.200900111
[12] L. L. D. R. Osorio, E. Flórez-López, C. D. Grande-Tovar, The Potential of Selected Agri-Food Loss and Waste to Contribute to a Circular Economy: Applications in the Food, Cosmetic and Pharmaceutical Industries, *Molecules*, **2021**, *26* (2), 515.
https://doi.org/10.3390/molecules26020515
[13] A. P. Pereira, I. C. Ferreira, F. Marcelino, P. Valentão, P. B. Andrade, R. Seabra, L. Estevinho, A. Bento, J. A. Pereira, Phenolic Compounds and Antimicrobial Activity of Olive (*Olea europaea* L. *Cv.* Cobrançosa) Leaves, *Molecules*, **2007**, *12* (5), 1153.
https://doi.org/10.3390/12051153
[14] C. Mitsagga, K. Petrotos, I. Giavasis, Antimicrobial Properties of Lyophilized Extracts of Olive Fruit, Pomegranate and Orange Peel Extracts against Foodborne Pathogenic and Spoilage Bacteria and Fungi In Vitro and in Food Matrices, *Molecules*, **2021**, *26* (22), 7038.
https://doi.org/10.3390/molecules26227038
[15] C. Liyana-Pathirana, F. Shahidi, Optimization of extraction of phenolic compounds from wheat using response surface methodology, *Food Chemistry*, **2005**, *93* (1) 47.
https://doi.org/10.1016/j.foodchem.2004.08.050
[16] L. T. Danh, R. Mammucari, P. Truong, N. Foster, Response surface method applied to supercritical carbon dioxide extraction of *Vetiveria zizanioides* essential oil, *Chemical Engineering Journal*, **2009**, *155* (3), 617.
https://doi.org/10.1016/j.cej.2009.08.016

[17] Z. Lianfu, L. Zelong, Optimization and comparison of ultrasound/microwave assisted extraction (UMAE) and ultrasonic assisted extraction (UAE) of lycopene from tomatoes, *Ultrasonics Sonochemistry*, **2008**, *15* (5), 731.
https://doi.org/10.1016/j.ultsonch.2007.12.001
[18] F. Chemat, N. Rombaut, A. Sicaire, A. Meullemiestre, A. Fabiano-Tixier, M. Abert-Vian, Ultrasound assisted extraction of food and natural products. Mechanisms, techniques, combinations, protocols and applications. A review, *Ultrasonics Sonochemistry*, **2017**, *34*, 540.
https://doi.org/10.1016/j.ultsonch.2016.06.035
[19] F. Chemat, N. Rombaut, A. Meullemiestre, M. Turk, S. Perino, A. Fabiano-Tixier, M. Abert-Vian, Review of Green Food Processing techniques. Preservation, transformation, and extraction, *Innovative Food Science & Emerging Technologies*, **2017**, *41*, 357.
https://doi.org/10.1016/j.ifset.2017.04.016
[20] B.K. Tiwari, Ultrasound: A clean, green extraction technology, *Trends in Analytical Chemistry*, **2015**, *71*, 100.
https://doi.org/10.1016/j.trac.2015.04.013
[21] M. Vinceković, M. Viskić, S. Jurić, J. Giacometti, D. B. Kovačević, P. Putnik, F. Donsì, F. J. Barba, A. R. Jambrak, Innovative technologies for encapsulation of Mediterranean plants extracts, *Trends in Food Science & Technology*, **2017**, *69*, 1.
https://doi.org/10.1016/j.tifs.2017.08.001
[22] M. Yogesh, A. K. Krishn, S. C. Bhupesh, G. Jitendra, G. Reena, A Review on Novel Herbal Drug Delivery System and its Application, *Current Traditional Medicine*, **2023**, *9* (2).
https://dx.doi.org/10.2174/2215083808666220428092638
[23] C. Huang, Studies on phosphatidylcholine vesicles. Formation and physical characteristics, *Biochemistry*, **1969**, *8* (1), 344.
https://doi.org/10.1021/bi00829a048
[24] J. Pereira-Lachataignerais, R. Pons, P. Panizza, L. Courbin, J. Rouch, O. López, Study and formation of vesicle systems with low polydispersity index by ultrasound method, *Chemistry and Physics of Lipids*, **2006**, *140* (1-2), 88.
https://doi.org/10.1016/j.chemphyslip.2006.01.008
[25] E. S. Richardson, W. G. Pitt, D. J. Woodbury, The Role of Cavitation in Liposome Formation, *Biophysical Journal*, **2007**, *93* (12), 4100.
https://doi.org/10.1529/biophysj.107.104042

[26] S. P. Wrenn, S. M. Dicker, E. F. Small, N. R. Dan, M. Mleczko, G. Schmitz, P. A. Lewin, Bursting Bubbles and Bilayers, *Theranostics*, **2012**, *2* (12), 1140.
https://www.thno.org/v02p1140.htm // doi:10.7150/thno.4305
[27] V. Torchlin, V. Weissing, Liposomes: A Practical Approach, 2nd edition, Oxford University Press, **2003**.
[28] C. Carrera, A. Ruiz-Rodríguez, M. Palma, C. G. Barroso, Ultrasound assisted extraction of phenolic compounds from grapes, *Analytica Chimica Acta*, **2012**, *732*, 100.
https://doi.org/10.1016/j.aca.2011.11.032
[29] B. Martín-García, S. De Montijo-Prieto, M. Jiménez-Valera, A. Carrasco-Pancorbo, A. Ruiz-Bravo, V. Verardo, A.M. Gómez-Caravaca, Comparative Extraction of Phenolic Compounds from Olive Leaves Using a Sonotrode and an Ultrasonic Bath and the Evaluation of Both Antioxidant and Antimicrobial Activity, *Antioxidants*, **2022**, *11* (3), 558.
https://doi.org/10.3390/antiox11030558
[30] M. d. C. Razola-Díaz, E. J. Guerra-Hernández, C. Rodríguez-Pérez, A. M. Gómez-Caravaca, B. García-Villanova, V. Verardo, Optimization of Ultrasound-Assisted Extraction via Sonotrode of Phenolic Compounds from Orange By-Products. *Foods*, **2021**, *10* (5), 1120.
https://doi.org/10.3390/foods10051120
[31] G. Bozzuto, A. Molinari, Liposomes as nanomedical devices, *International Journal of Nanomedicine*, **2015**, *10* (1), 975.
https://doi.org/10.2147/IJN.S68861)
[32] C. Bonechi, A. Donati, G. Tamasi, A. Pardini, H. Rostom, G. Leone, S. Lamponi, M. Consumi, A. Magnani, C. Rossi, Chemical characterization of liposomes containing nutraceutical compounds: Tyrosol, hydroxytyrosol and oleuropein, *Biophysical Chemistry*, **2019**, *246*, 25.
https://doi.org/10.1016/j.bpc.2019.01.002
[33] V. Janbandhu Nitesh, M. Mogre Ranjan, Comparative Physical and Chemical Stability Studies of Orlistat Liposomal Drug Delivery Systems, *Asian Journal of Pharmaceutics*, **2018**, *12* (03), S971.
https://doi.org/10.22377/ajp.v12i03.2636
[34] A. Praveen, M. Aqil, S. S. Imam, A. Ahad, T. Moolakkadath, F. J. Ahmad, Lamotrigine encapsulated intra-nasal nanoliposome formulation for epilepsy treatment: Formulation design, characterization and nasal toxicity study, *Colloids and Surfaces B: Biointerfaces*, **2019**, *174*, 553.
https://doi.org/10.1016/j.colsurfb.2018.11.025

[35] J. M. Pagès, L. Amaral, Mechanisms of drug efflux and strategies to combat them: Challenging the efflux pump of Gram-negative bacteria, *Biochimica et Biophysica Acta (BBA) - Proteins and Proteomics*, **2009**, *1794* (5), 826.
https://doi.org/10.1016/j.bbapap.2008.12.011
[36] L. Kakoullis, E. Papachristodoulou, P. Chra, G. Panos, Mechanisms of Antibiotic Resistance in Important Gram-Positive and Gram-Negative Pathogens and Novel Antibiotic Solutions, *Antibiotics*, **2021**, *10* (4), 415.
https://doi.org/10.3390/antibiotics10040415
[37] T. Lian, RJ. Ho, Trends and developments in liposome drug delivery systems, *J Pharm Sci*., **2001**, *90* (6), 667.
https://doi.org/10.10002/jps.1023
[38] H. Pinto-Alphandary, A. Andremont, P. Couvreur, Targeted delivery of antibiotics using liposomes and nanoparticles: research and applications, *International Journal of Antimicrobial Agents*, **2000**, *13* (3), 155.
https://doi.org/10.1016/S0924-8579(99)00121-1
[39] S. M. McAllister, H. O. Alpar, M. R. Brown, Antimicrobial properties of liposomal polymyxin B, *Journal of Antimicrobial Chemotherapy*, **1999**, *43* (2), 203.
https://doi.org/10.1093/jac/43.2.203
[40] P. Labuschagne, Impact of wall material physicochemical characteristics on the stability of encapsulated phytochemicals: A review, *Food Research International*, **2018**, *107*, 227.
https://doi.org/10.1016/j.foodres.2018.02.026
[41] M. J. Aliaño-González, J. Gabaston, V. Ortiz-Somovilla, E. Cantos-Villar, Wood Waste from Fruit Trees: Biomolecules and Their Applications in Agri-Food Industry. *Biomolecules*, **2022**, *12* (2), 238.
https://doi.org/10.3390/biom12020238
[42] B. de Falco, A. Fiore, R. Bochicchio, M. Amato, V. Lanzotti, Metabolomic analysis by UAE-GC MS and antioxidant activity of *Salvia hispanica* (L.) seeds grown under different irrigation regimes, *Industrial Crops and Products*, **2018**, *112*, 584.
https://doi.org/10.1016/j.indcrop.2017.12.030
[43] M. Blois, Antioxidant Determinations by the Use of a Stable Free Radical, *Nature*, **1958**, *181*, 1199.
https://doi.org/10.1038/1811199a0

[44] W. Brand-Williams, M. E. Cuvelier, C. Berset, Use of a free radical method to evaluate antioxidant activity, *Food Science and Technology*, **1995**, *28* (1), 25.
https://doi.org/10.1016/S0023-6438(95)80008-5
[45] I. F. F. Benzie, J. J. Strain, The Ferric Reducing Ability of Plasma (FRAP) as a Measure of "Antioxidant Power": The FRAP Assay, Analytical Biochemistry, **1996**, *239* (1), 70.
https://doi.org/10.1006/abio.1996.0292
[46] N. Talhaoui, A. M. Gómez-Caravaca, L. León, R. De la Rosa, A. Segura-Carretero, A. Fernández-Gutiérrez, Determination of phenolic compounds of 'Sikitita' olive leaves by HPLC-DAD-TOF-MS. Comparison with its parents 'Arbequina' and 'Picual' olive leaves, *Food Science and Technology*, **2014**, *58* (1), 28.
https://doi.org/10.1016/j.lwt.2014.03.014
[47] A. Starzyńska-Janiszewska, C. Fernández-Fernández, B. Martín-García, V. Verardo, A. M. Gómez-Caravaca, Solid State Fermentation of Olive Leaves as a Promising Technology to Obtain Hydroxytyrosol and Elenolic Acid Derivatives Enriched Extracts. *Antioxidants*, **2022**, *11* (9), 1693.
https://doi.org/10.3390/antiox11091693
[48] M. Verni, E. Pontonio, A. Krona, S. Jacob, D. Pinto, F. Rinaldi, V. Verardo, E. Díaz-de-Cerio, R. Coda, C. G. Rizzello, Bioprocessing of Brewers' Spent Grain Enhances Its Antioxidant Activity: Characterization of Phenolic Compounds and Bioactive Peptides. *Frontiers in Microbiology*, **2020**, *11*, 1831.
https://doi.org/10.3389/fmicb.2020.01831
[49] R. J. Hunter, Zeta Potential in Colloid Science. Principles and Applications, 1st edition, Elsevier, **1988**
[50] CLSI. Methods for Dilution Antimicrobial Susceptibility Tests for Bacteria That Grow Aerobically; Approved Standard - Tenth Edition. CLSI document M07-A10. Wayne, PA: Clinical Laboratory Standards Institute; **2015**.

5. Olive leaves valorization, from by-product to a valuable source of new antimicrobial tools

5.1. Introduction

Olea europaea tree*,* belonging to *Oleaceae* family and *Olea* genus, is one of the most emblematic fruit trees of the whole Mediterranean area. Since antiquity, in fact, olive trees have been cultivated to produce olive oil and compounds suitable for beneficial and curative purposes[1] owing to the presence of polyphenolic bioactive compounds identified in many tree components such as wood, leaves and olive fruit.

Olea europaea leaves, produced in high amount during the harvesting of olive fruit and the pruning of olive trees, are a valuable source of biocompounds characterized by antioxidant, anti-inflammatory and antimicrobial properties[2] with potential applications in pharmaceutical, nutraceutical, food and cosmetic fields.[3] These molecules are secondary metabolites produced by plants as a defense mechanism against pathogens, parasites, herbivores and many stress triggers. Moreover, the amounts produced are strictly related to the kind of cultivar considered, the state of soil hydration and the meteorological condition of plants growth.

Therefore, the recovery and re-use of this by-product, which constitutes an economic and environmental problem for olive trees producers, can represent an example of circular economy with the aim of valorizing biomass waste and residues into valuable products to reduce waste production to a minimum.

Nowadays, commercial applications of olive leaves are mostly limited to folk medicine,[2] and although many efforts have been made to extend their use from traditional to pharmaceutical applications, their recovery for application in modern medicine is limited by several challenges, in particular the complex composition in active molecules of their extracts, as well as the stability and bioavailability of these molecules.

Generally, the study of therapeutic and pharmacological properties of plant extracts is reduced to the identification of the main bioactive compound, to identify a candidate that can be used for drug development. Nevertheless, botanical extract activity is often due to the combined action of different molecules present in the extract, that can be synergic or antagonistic.[4-6]

Olive leaves are abundant in phenolic compounds such as Oleuropein, Hydroxytyrosol, Verbascoside, Apigenin-7-glucoside, Luteolin-7-glucoside, Maslinic acid, Oleacin and Oleocanthal.[7,8]

These compounds are potent antioxidants with anti-inflammatory, anti-tumor, hepatoprotective, neuroprotective and antiviral properties for human health.[9]

In particular, olive leaves extracts have been proven to possess antimicrobial activity against many bacteria species, both *Gram*-positive and *Gram*-negative, such as *Escherichia coli*, *Pseudomonas aeruginosa*, *Staphylococcus aureus*, *Bacillus subtilis*, *Klebsiella pneumoniae*, *Listeria monocytogens* and *Salmonella*.[10-15]

Therefore, olive leaves extracts could represent a valid alternative to the use of conventional antibiotics especially in the treatment of infections caused by antibiotic-resistant pathogens. In fact, the combined action of different biocompounds present in these extracts, through different cellular mechanisms of action, could reduce the development of bacterium resistance representing an alternative route to the treatment of infections with pharmaco-resistance.

From a circular economy perspective, this work aims to recover and valorize olive leaves, biowaste of the olive-oil chain, to obtain products with antibacterial activity, which can provide new tools against the drug resistance acted by bacteria.

Olive leaves extracts (OLEs) were prepared by ultrasound-assisted extraction using different mixture of green solvents, such as water and ethanol. The extracts produced were characterized in terms of yield of extraction, total phenolic content, and antioxidant capacity. The main phenols present in the extracts were identified and quantified by UPLC-PDA-MS analysis. Afterwards, dry extracts and the main polyphenols identified were loaded in liposomes, with the aim to improve their pharmacokinetic properties. In fact, phenolic compounds usually show low solubility, poor permeability, instability, rapid elimination, susceptibility to environmental factors and low bioavailability at target sites.[16] In the following study, liposomes were formulated with a natural phospholipid, namely 1,2-dioleoyl-*sn*-glycero-3-phosphocholine (DOPC), and cholesterol (Chol) in the presence or in the absence of a cationic galactosylated amphiphile (GLT1) (**Chart 1**).

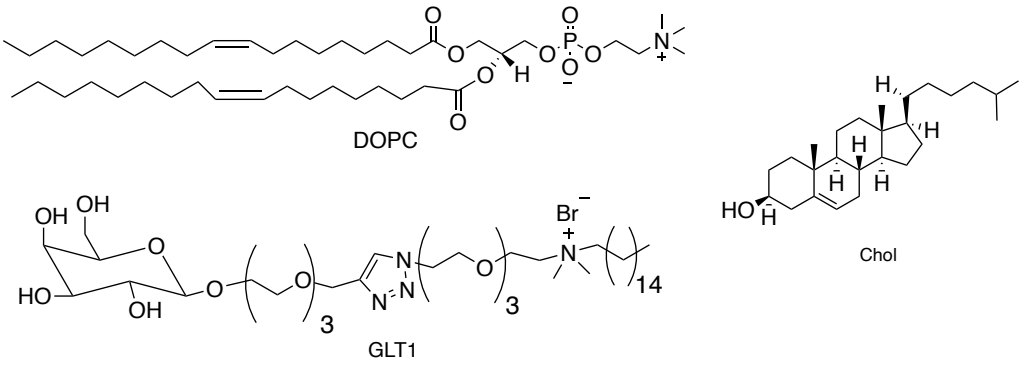

Chart 1. Lipid components of liposomes developed.

Liposomes were characterized in terms of dimensions, polydispersity index, ζ-potential and entrapment efficiency. Moreover, liposomes stability over time and at different pH was evaluated, as well as the forced release of entrapped polyphenols over time.

Finally, the antimicrobial activity of the extracts and the main polyphenols identified, free and loaded in neutral or galactosylated liposomes, was investigated against two strains of *Staphylococcus aureus*: ATCC 25923 (wild type strain) and ATCC 33591 (methicillin-resistant strain, MRSA).

5.2. Results and Discussion

5.2.1. Preparation of Olive leaves extracts

Olea europaea leaves owned to "*Frantoio*" cultivar, one of the most widespread in Italy, were picked up in Montelibretti in November 2020, during the olives harvest period due to the large amount of biomass waste produced by the olive-oil industry.

The sampling concerned olive trees not subjected to any pest treatment, thereby avoiding any form of contamination. Immediately after sampling, olive leaves were washed, dried, frozen by liquid nitrogen and grinded. Once shredded, olive leaves were freeze-dried to decrease their content of water, corresponding to a 50% weight loss in the samples.

Bioactive compounds from olive leaves were extracted using water and ethanol in different ratio; these green solvents, in addition to being biocompatibility, are capable to produce extracts rich in polyphenols.

The extractions were carried out for 45 min at 40°C, according to preliminary studies that have identified this extraction time as the optimal one.

Three different extracts were produced using 100% water, ethanol/water 50:50 (v/v) and ethanol/water 80:20 (v/v) as extracting solvents, and they were named OLE100, OLE50 and OLE20, respectively.

OLEs were characterized in terms of yield of extraction, total phenolic content and antioxidant activity (TEAC) (**Table 1**).

Table 1. Yield of extraction, total phenolic content and antioxidant activity of OLEs.

Extract	Yield of extraction (%)	Total Phenolic Content (mg_{GAE}/g_{leaves})	TEAC t_{1min} ($mmol_{TE}/g_{leaves}$)	TEAC t_{4min} ($mmol_{TE}/g_{leaves}$)
OLE100	33 ± 1	17.9 ± 0.6	0.16 ± 0.02	0.17 ± 0.03
OLE50	40 ± 2	24 ± 3	0.28 ± 0.02	0.31 ± 0.03
OLE20	41 ± 1	26.7 ± 0.8	0.34 ± 0.03	0.39 ± 0.05

5.2.2. Yield of extraction

With the aim to determine the yield of extraction for OLE100, OLE50 and OLE20, OLEs were freeze-dried after ethanol removal by rotary evaporation.

Consequently, the dry extracts obtained are more stable, less degradable and easier to handle compared to the liquid extracts.

For each sample, the yield of extraction (%) has been calculated as the percentage ratio between the weight of the freeze-dried extract and the weight of the olive leaves used in the extraction process.

According to the data reported in **Table 1**, the yields of extraction for the hydroalcoholic extracts are comparable to each other and higher than that of the aqueous extract.

5.2.3. Total Phenolic Content by Folin-Ciocalteu assay

Total phenolic content (TPC) of OLE100, OLE50 and OLE20 was evaluated by Folin-Ciocalteu assay, using Gallic Acid as reference standard. This assay is convenient, quite easy to perform and reproducible, in fact it is widely used in the literature for the determination of total phenols in plants extracts.[17]

The assay is carried out employing the Folin & Ciocalteu's phenol reagent composed by a mixture of sodium tungstate (Na_2WO_4), sodium molibdate (Na_2MoO_4), chloridric acid, phosphoric acid and water. In Folin-Ciocalteu assay alkaline conditions (pH ≈ 10) are necessary to deprotonate phenolic compounds and trigger an electron transfer process from the phenolate anions to the FCR.

TPC is expressed as Gallic Acid equivalents and results are reported as milligrams of Gallic Acid per gram of olive leaves extracted (mg_{GAE}/g_{leaves}).

According to the results showed in **Table 1**, the TPC increases by increasing the percentage of ethanol present in the extracting solvent, ranging from 17.9 mg_{GAE}/g_{leaves} for OLE100 to 26.7 mg_{GAE}/g_{leaves} for OLE20. The results obtained are consistent with those reported in the literature.[18,19]

It is worth to highlight that although the extraction yields for OLE50 and OLE20 are comparable, the TPC is higher for OLE20, suggesting that a greater extraction yield does not directly result in a higher TPC.

5.2.4. Antioxidant capacity by TEAC assay

The antioxidant capacity was evaluated by TEAC assay based on the reaction between the $ABTS^{\bullet+}$ and the polyphenols contained in OLEs.

$ABTS^{\bullet+}$ is obtained by the oxidation of 2,2'-azino-bis(3-ethylbenzothiazoline-6-sulphonic acid) with potassium persulfate; it is a stable radical cation and a blue-green chromophore with a maximum of absorbance at 734 nm. However, $ABTS^{\bullet+}$ absorption at 734 nm decreases in presence of antioxidant compounds able to quench it through a direct reduction by electron transfer or by

hydrogen atom transfer. Therefore, this assay is widely used to evaluate the antioxidant properties of many compounds, food or plant matrices.[20]

Trolox, a water-soluble analogue of vitamin E, is used in TEAC assay as reference standard and the antioxidant capacity of olive leaves extracts was determined at two different reaction times (1 min and 4 min), following an end-point procedure reported in the literature. Results, expressed as millimol of Trolox equivalents per gram of olive leaves extracted ($mmol_{TE}/g_{leaves}$) in **Table 1**, displayed that the extract prepared using the highest percentage of ethanol in the extraction solvent shows the highest antioxidant capacity, which in detail doubles going from OLE100 to OLE20, with a similar trend to that recorded for the TPC.

5.2.5. Identification and quantification of phenolic compounds by UPLC-PDA-MS

OLEs were analyzed by UPLC-PDA-MS using a C18 column, thermostatically controlled at 40°C, and a mobile phase composed by water and acetonitrile, both acidified with 0.1% formic acid.

A mixture of analytical standards consisting of different compounds, which can be found in *Olea europaea* leaves, has been prepared and analyzed (**Figure 1**) to compare the chromatogram obtained for the analytical standards with those of OLE100, OLE50 and OLE20.

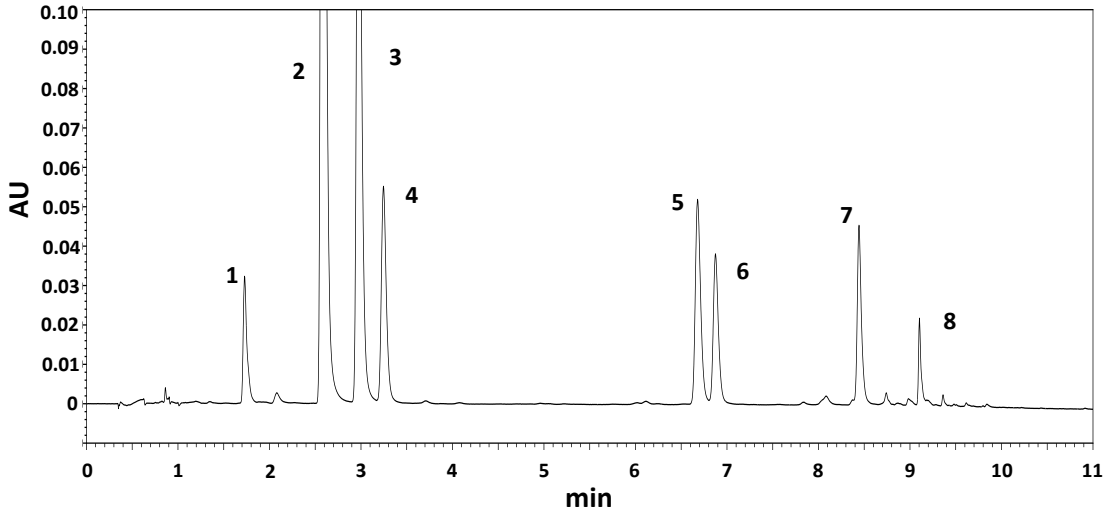

Figure 1. Chromatographic profile of the standards mixture used for the identification of phenols in the extracts, detection at 280 nm: 1) Hydroxytyrosol, 2) Tyrosol, 3) 4-Hydroxy-phenylacetic acid, 4) Vanillic acid, 5) Luteolin-7-glucoside, 6) Verbascoside, 7) Apigenin-7-glucoside, 8) Oleuropein.

The chromatographic profiles of OLE100, OLE50 and OLE20 are reported in **Figure 2.**

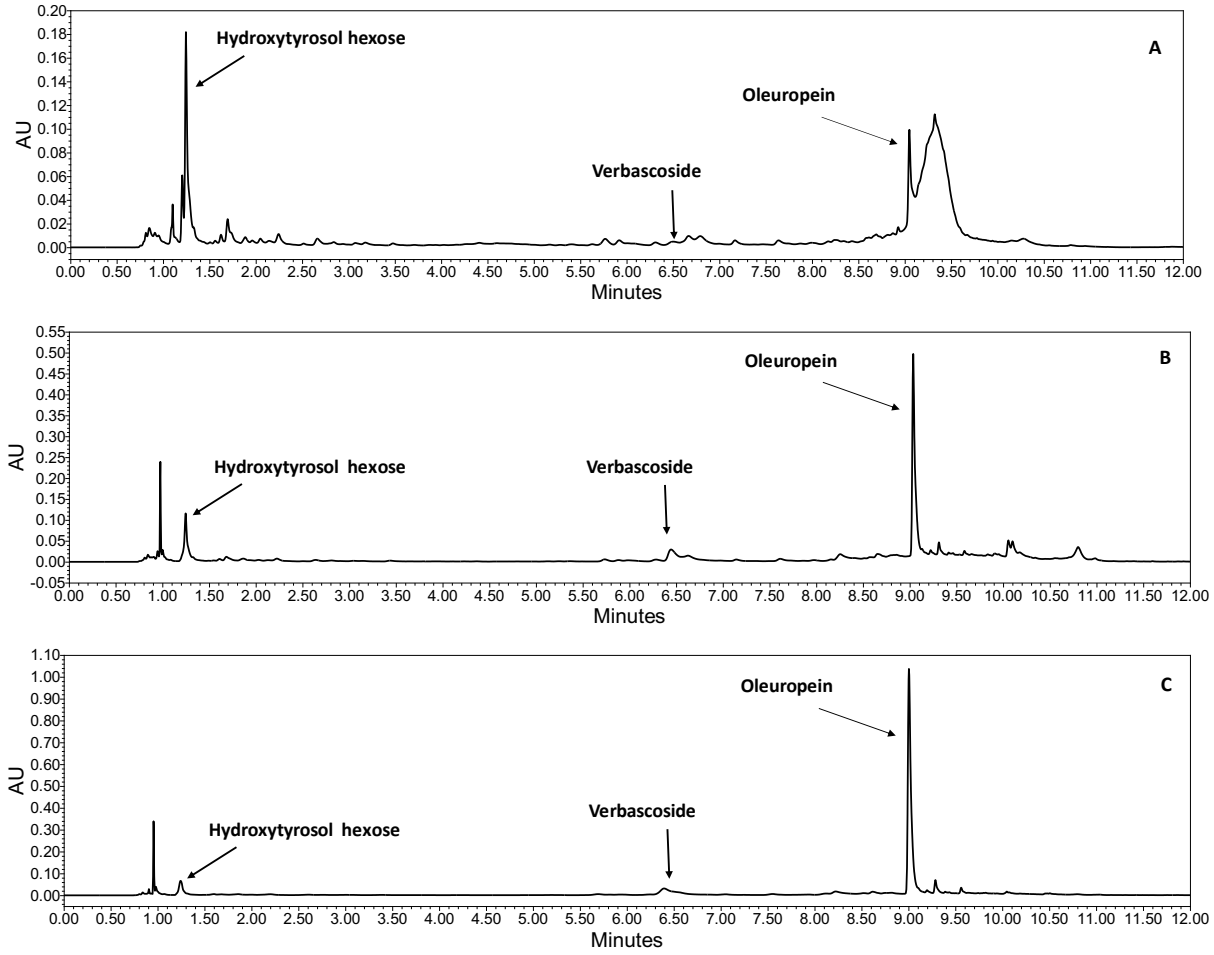

Figure 2. Chromatographic profiles of (A) OLE100, (B) OLE50 and (C) OLE20, detection at 280 nm.

The UPLC analysis assessed on OLEs, by comparison of UV spectra, mass spectra and retention times with those of the analytical reference standards, allowed the detection of Oleuropein and Verbascoside in all samples.

In detail, Oleuropein is the most abundant polyphenol present in the extracts OLE50 and OLE20, and one of the most abundant in OLE100, whereas Verbascoside is one of the least abundant components in all OLEs produced, despite it has been detected in all of them.

Hydroxytyrosol was not identified as such in OLEs, but as an adduct with a six carbon atoms sugar. ESI-MS analysis of OLEs in negative scanning mode showed that this compound is present as two structural isomers, both characterized by a molecular ion $[M-1]^-$ with *m/z* 315 (molecular formula $C_{14}H_{20}O_8$) but featuring different retention times (RT) (**Figure 3**). The presence of this type of compounds in olive leaves is already known in the literature.[22,23] In the following paragraphs these

two isomers will be identified as Hydroxytyrosol-hexose "*isomer a*" (RT = 1.29 min) and "*isomer b*" (RT = 1.56 min).

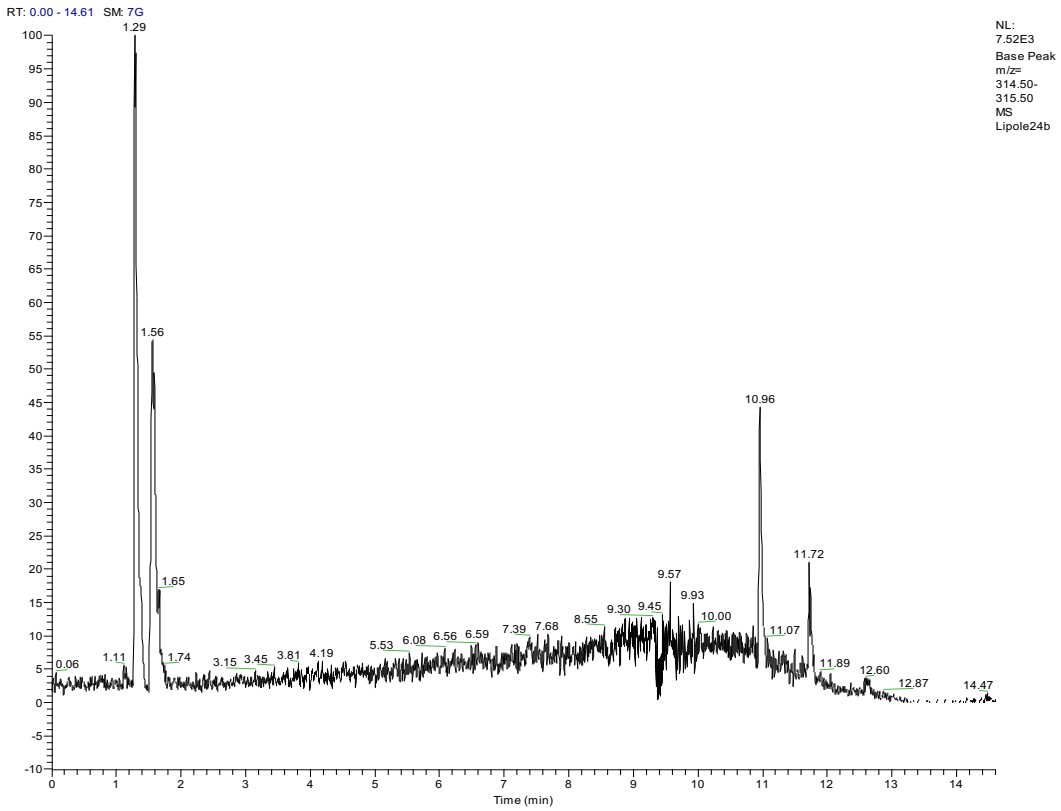

Figure 3. ESI-MS detection in negative scanning mode for *m/z* = 315, analysis performed on OLE20.

UV-Vis spectra recorded for compounds detected in OLEs are reported in **Figure 4**.

Since Hydroxytyrosol-hexose *isomer a* and *isomer b* show identical UV-Vis absorption spectra, only one is reported for both isomers. In fact, the glycosidic bound between the sugar moiety and one of the phenolic hydroxyl groups or the ethanolic one does not modify the UV spectra of the molecules.

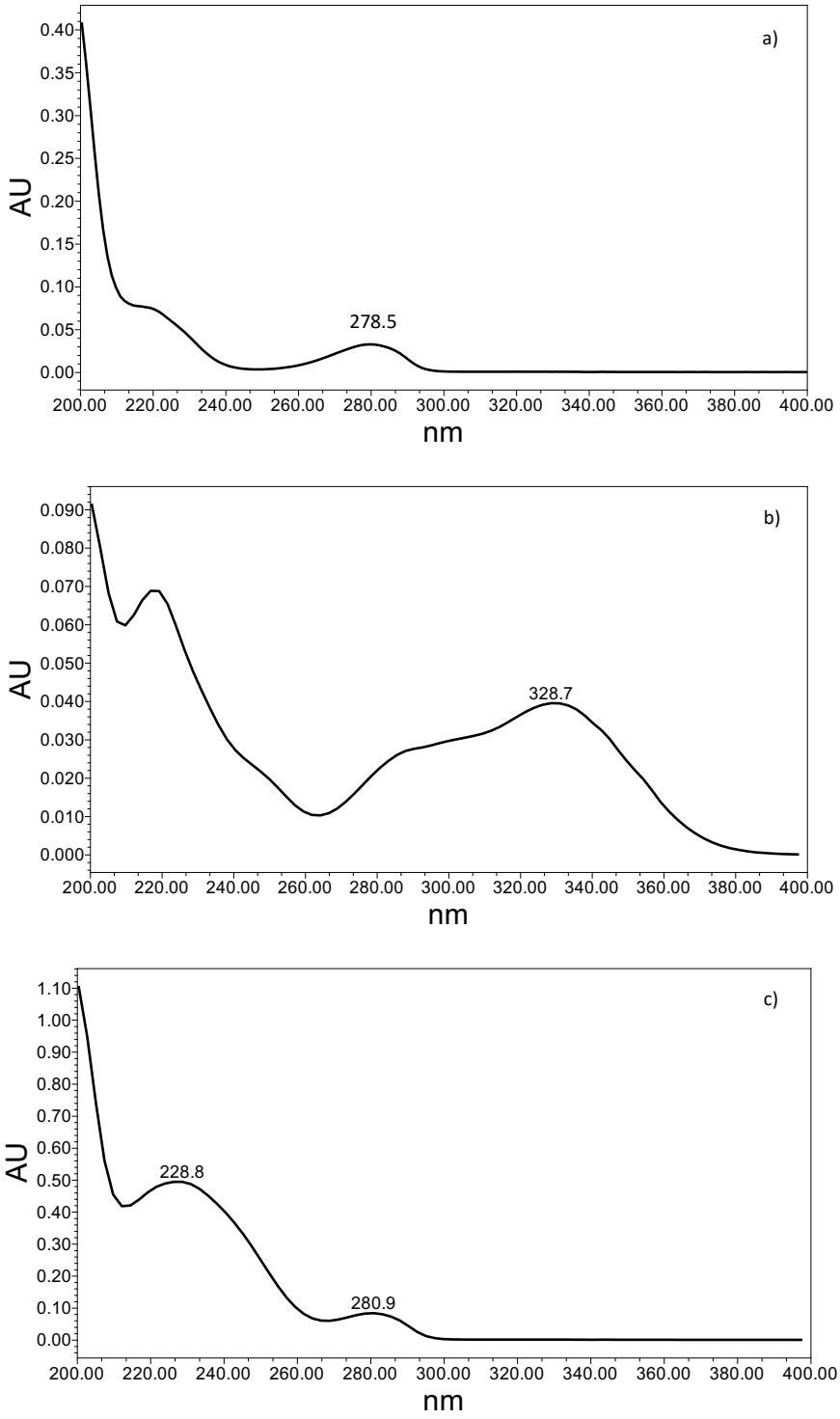

Figure 4. UV-Vis spectra of (a) Hydroxytyrosol-hexose *isomer a* and *isomer b*, (b) Verbascoside and (c) Oleuropein.

Figures 5-**7** show the mass spectra recorded in negative mode for Hydroxytyrosol-hexose *isomer a* and *isomer b* (molecular ions $[M\text{-}H]^-$ *m/z* = 315, identical mass spectra, only one is reported), Verbascoside ($[M\text{-}H]^-$ *m/z* = 623) and Oleuropein ($[M\text{-}H]^-$ *m/z* = 539).

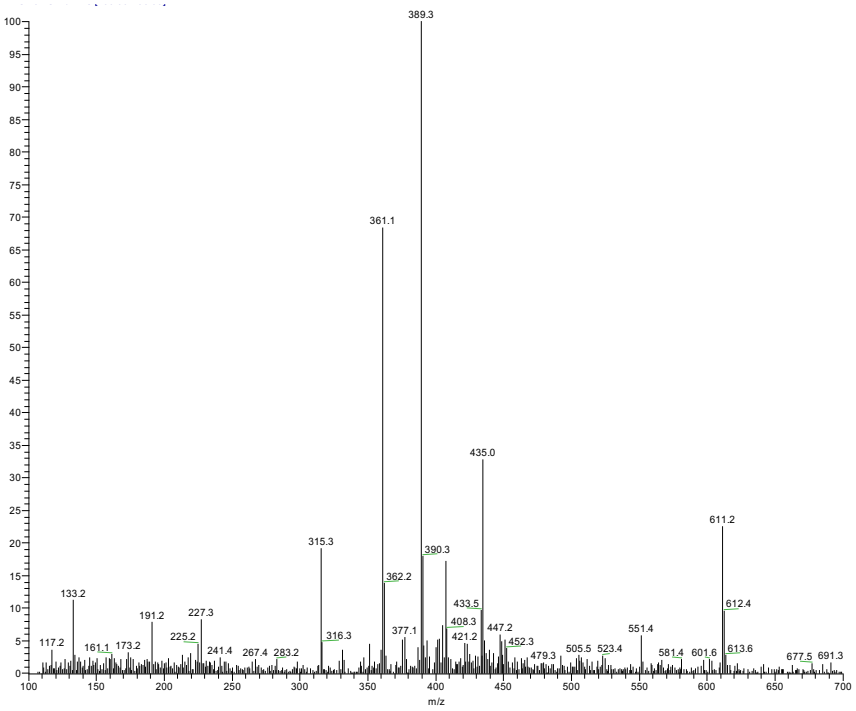

Figure 5. Mass spectrum of Hydroxytyrosol-hexose *isomer a* and *isomer b*, molecular ion $[M-H]^-$ *m/z* = 315.

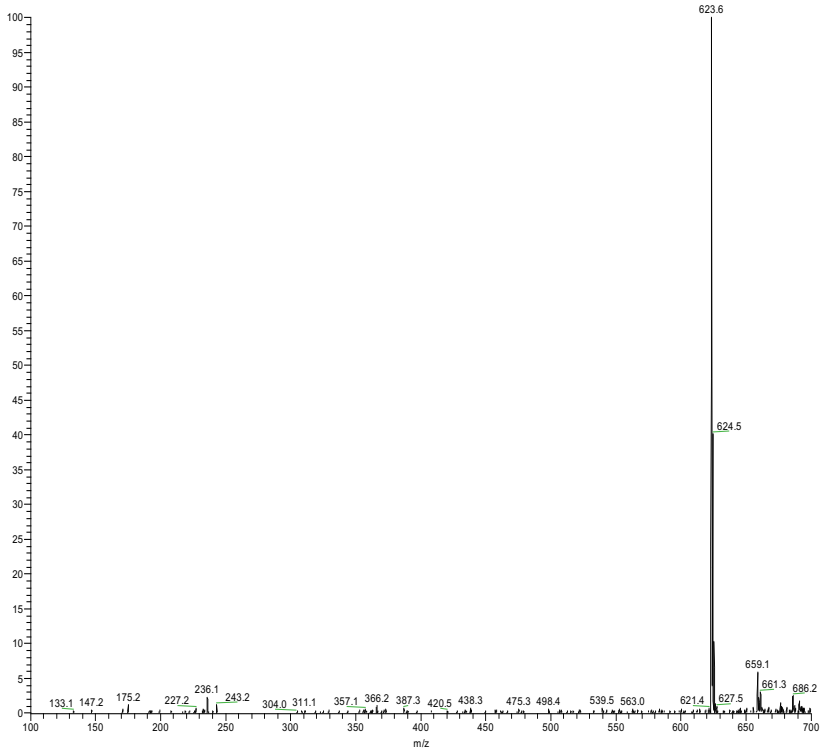

Figure 6. Mass spectrum of Verbascoside, molecular ion $[M-H]^-$ *m/z* = 623.

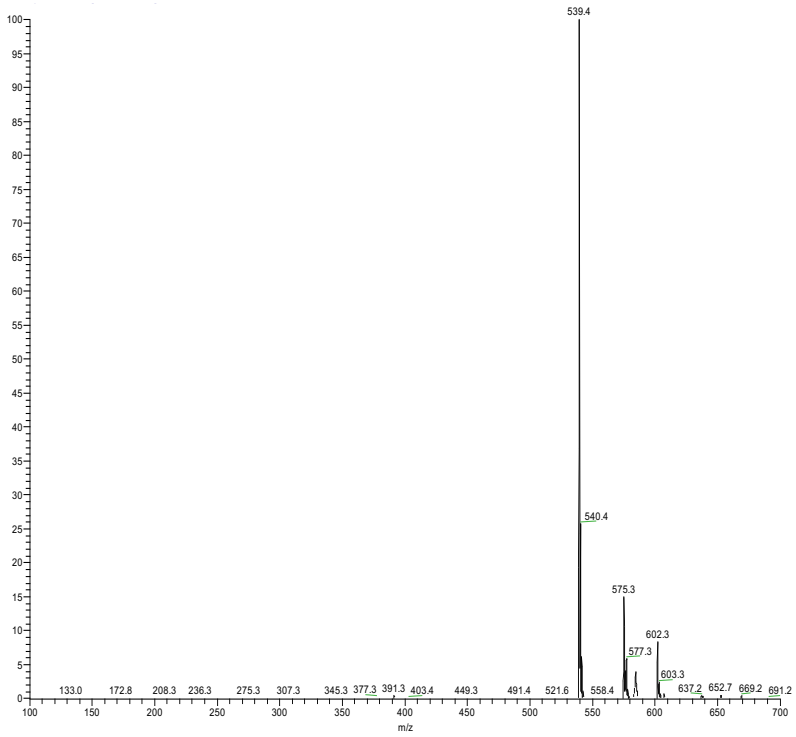

Figure 7. Mass spectrum of Oleuropein, molecular ion $[M-H]^-$ *m/z* = 539.

The amounts of Hydroxytyrosol *isomer a* and *isomer b*, Verbascoside and Oleuropein in OLEs were assessed by UPLC-PDA analysis by external calibration method. The calibration curves were obtained using the corresponding analytical standards, though in the case of the two glycosylated Hydroxytyrosol isomers it was used, as analytical standard, Hydroxytyrosol as such.

In **Table 2**, the collected results are reported as milligrams of compound per milliliter of extract ($mg/mL_{extract}$), milligrams of compound per gram of olive leaves extracted (mg/g_{leaves}) and milligrams of compound per gram of dry extract ($mg/g_{dry\_extract}$).

From the data reported in **Table 2**, it is worth noting that among the compounds identified Oleuropein is the most abundant one in all the extracts. In particular, its quantity increases as a function of the percentage of ethanol present in the extracting solvent, going from 24.1 $mg/g_{dry\_extract}$ for OLE100 to 324.1 $mg/g_{dry\_extract}$ for OLE20.

Instead, Verbascoside is the least abundant in both the hydroalcoholic extracts and it is not quantifiable (< LOQ) in OLE100.

Besides, Hydroxytyrosol-hexose *isomer a* and *isomer b* are present in all OLEs in comparable amounts.

Table 2. Amounts of Hydroxytyrosol-hexose *isomer a* and *isomer b*, Verbascoside and Oleuropein in OLEs produced.

	Compound	$mg/mL_{extract}$	mg/g_{leaves}	$mg/g_{dry\_extract}$
OLE100	Hydroxytyrosol-hexose *isomer a*	0.04 ± 0.01	0.7 ± 0.1	1.6 ± 0.1
	Hydroxytyrosol-hexose *isomer b*	0.10 ± 0.01	2.1 ± 0.2	5.0 ± 0.4
	Verbascoside	< LOQ	< LOQ	< LOQ
	Oleuropein	0.5 ± 0.1	10.2 ± 2.6	24.1 ± 4.0
OLE50	Hydroxytyrosol-hexose *isomer a*	0.05 ± 0.01	1.1 ± 0.1	2.8 ±0.2
	Hydroxytyrosol-hexose *isomer b*	0.08 ± 0.01	1.6 ± 0.2	4.1 ± 0.3
	Verbascoside	0.0112 ± 0.0002	0.224 ± 0.004	0.62 ±0.01
	Oleuropein	3.0 ± 0.8	60.5 ± 15.6	155.4 ± 34.4
OLE20	Hydroxytyrosol-hexose *isomer a*	0.03 ± 0.1	0.8 ± 0.1	2.6 ± 0.1
	Hydroxytyrosol-hexose *isomer b*	0.05 ± 0.02	1.2 ± 0.2	3.9 ± 0.1
	Verbascoside	0.0090 ± 0.0002	0.179 ± 0.004	0.47 ± 0.03
	Oleuropein	3.7 ± 0.9	95.2 ± 26.8	324.1 ± 115.7

5.2.6. Liposomes preparation

Liposome as delivery systems of Hydroxytyrosol (HOTyr), Verbascoside (VERB), Oleuropein (OLEUR) and OLEs were formulated with an unsaturated natural phospholipid (DOPC) and cholesterol (Chol) in presence or absence of the cationic galactosylated amphiphile GLT1 (**Chart 1**), with the aim to enhance their solubility in water, stability in biological fluids and bioavailability at the target sites.[16] The inclusion of cholesterol in the lipid mixture enhances the stability of the lipid bilayer through the *bilayer-tightening effect* inducing a dense packing and increasing the orientation order of lipid chains. This leads to a more compact structure with reduced permeability to water soluble molecules and increased retention of entrapped cargo.[24] Moreover, cholesterol was added to improve the lipid bilayer stability, mostly in presence of GLT1 because of its detergent properties and ability to destabilize the lipid bilayer leading to the formation of micellar aggregates.[25]

The presence of GLT1 as cationic amphiphile into lipid bilayer should enhance the electrostatic interactions with the negatively charged bacterial membrane cells, moreover it could further improve the interaction between liposomes and bacteria thanks to a possible specific interaction between its sugar moiety, exposed on liposomal surface, and lectins or sugar protein transporters, that as it is known bacteria express on their cellular membrane.[26,27]

Liposomes, 10 mM in total lipids concentration, were prepared in 150 mM phosphate buffer saline solution (PBS) according to the thin lipid film hydration method combined with a freeze-thaw

protocol and an extrusion process, thus obtaining unilamellar vesicles of suitable dimensions (~100 nm). HOTyr, VERB, OLEUR and OLEs were entrapped inside the lipid bilayer by passive loading, using a molar ratio [phenol]/ [total lipids] equal to 1/8 for polyphenols encapsulation and a weight ratio (dry extract)/ (total lipids) corresponding to 1/1 for OLEs encapsulation.

Unentrapped HOTyr, VERB and OLEUR and OLEs were finally removed by dialysis in PBS.

5.2.7. Liposomes characterization

Hydrodynamic diameter (D_h), polydispersity index (PDI), ζ-potential and Entrapment Efficiency (EE%) were investigated for all liposomes developed.

Liposomes particle size distribution and polydispersity index were investigated by dynamic light scattering (DLS) measurements. Results reported in **Table 3** and **Table 4** show a narrow size distribution for all liposomes with a diameter between 79 nm and 120 nm and a good PDI (0.09-0.20) according to the extrusion protocol adopted.

Table 3. Physicochemical features of empty and HOTyr, VERB and OLEUR loaded liposomes (10 mM in total lipids) in PBS (pH 7.4).

Formulation	Composition	D_h (nm)	PDI	ζ-potential (mV)	EE (%)	[mM]#
1	DOPC/Chol 8.0:2.0	119 ± 2	0.10 ± 0.02	-3 ± 2	-	-
1a	DOPC/Chol/HOTyr* 8.0:2.0:1.25	107 ± 2	0.09 ± 0.02	-1 ± 5	62 ± 3	0.78 ± 0.02
1b	DOPC/Chol/VERB* 8.0:2.0:1.25	109 ± 2	0.09 ± 0.02	-5 ± 5	98 ± 2	1.23 ± 0.02
1c	DOPC/Chol/OLEUR* 8.0:2.0:1.25	100 ± 2	0.12 ± 0.01	-10 ± 1	73 ± 2	0.92 ± 0.01
2	DOPC/Chol/GLT1 7.0:2.0:1.0	94 ± 2	0.12 ± 0.01	16 ± 1	-	-
2a	DOPC/Chol/GLT1/HOTyr* 7.0:2.0:1.0:1.25	94 ± 1	0.11 ± 0.01	13 ± 3	57 ± 2	0.71 ± 0.02
2b	DOPC/Chol/GLT1/VERB* 7.0:2.0:1.0:1.25	111 ± 2	0.20 ± 0.01	12 ± 2	98 ± 2	1.23 ± 0.02
2c	DOPC/Chol/GLT1/OLEUR* 7.0:2.0:1.0:1.25	79 ± 1	0.14 ± 0.01	14 ± 3	75 ± 5	1.0 ± 0.1

*[Phenol]/ [total lipids] ratio at the beginning of the preparation is 1/8. #Encapsulated polyphenol concentration.

Table 4. Physicochemical features of OLEs loaded liposomes (10 mM in total lipids) in PBS (pH 7.4).

Formulation	Composition	D_h (nm)	PDI	ζ-potential (mV)	EE (%)
1d	DOPC/Chol/OLE100* 8.0:2.0	102 ± 1	0.18 ± 0.01	-10 ± 1	26 ± 4
1e	DOPC/Chol/OLE50* 8.0:2.0	111 ± 1	0.18 ± 0.01	-10 ± 5	32 ± 5
1f	DOPC/Chol/OLE20* 8.0:2.0	120 ± 1	0.20 ± 0.01	-10 ± 5	43 ± 7
2d	DOPC/Chol/GLT1/OLE100* 7.0:2.0:1.0	93 ± 1	0.15 ± 0.01	10 ± 2	36 ± 6
2e	DOPC/Chol/GLT1/OLE50* 7.0:2.0:1.0	94 ± 1	0.16 ± 0.01	10 ± 3	51 ± 7
2f	DOPC/Chol/GLT1/OLE20* 7.0:2.0:1.0	119 ± 1	0.20 ± 0.01	9 ± 1	57 ± 13

*OLE/total lipids ratio at the beginning of the preparation is 1/1 (w/w).

In particular, it is worth to highlight the slight reduction in size for galactosylated formulations compared to the neutral ones, both in the case of the single biomolecule encapsulation and in the case of OLEs encapsulation, due to the arrangement caused by GLT1 within the DOPC/Chol bilayer. The only exception is represented by liposomes of formulation **2f**, which show similar dimensions to the liposomes of the corresponding formulation lacking GLT1 (**1f**). Moreover, liposomes of these two formulations, **1f** and **2f**, are characterized by the highest values of hydrodynamic diameters between all formulations studied, probably due to the different composition in polyphenols of OLE20 respect to the others OLEs, which can arrange in a different way into the lipid bilayer after their entrapment.

Furthermore, OLEUR encapsulation in neutral and galactosylated liposomes induced a decrease in average size of liposomes compared to the reference empty formulations. In fact, either these liposomes (**1c** and **2c**) are characterized by the lowest values of hydrodynamic diameters between all formulations studied. This behavior may suggest that OLEUR changes the normal conformation of both lipid bilayer developed.[28]

With the aim to investigate the surface charge of liposomes, ζ-potential values were determined by electrophoretic mobility measurements, using the phase analysis light scattering (PALS). According to the results reported, DOPC/Chol empty liposomes feature a small negative ζ-potential value due to the exposure of the phosphocholine phosphate groups, though the net charge of the zwitterionic

phospholipid polar head is zero. The inclusion of HOTyr, VERB and OLEUR or OLEs in DOPC/Chol liposomes induced a slight decrease of ζ-potential values, becoming more negative, probably due to the localization of biocompounds loaded at the membrane surfaces, which could be able to interact with the polar headgroups of DOPC through the formation of hydrogen bonds.[29]

Instead, DOPC/Chol/GLT1 based liposomes, empty and loaded, exhibit a positive and quite high ζ-potential, with a slight decrease in value when single biocompounds or OLEs are entrapped, thus reducing the probability of aggregation phenomena accountable for the physical instability of liposomes.[31] Moreover, the positive ζ-potential values recorded represent an indirect evidence of the GLT1 inclusion within the lipid bilayer.

The loaded content of HOTyr, VERB and OLEUR was evaluated by UPLC measurements soon after extrusion and soon after dialysis. Liposomes were diluted with a methanolic solution to break lipid aggregates and to enhance the release of loaded compounds.

The Entrapment Efficiency (EE%) was defined as the percentage ratio between the polyphenol concentration measured after the purification by dialysis and the polyphenol concentration measured after the extrusion step. According to the results reported in **Table 3**, all liposomes feature quite high entrapment efficiencies, with no significant differences between neutral and galatacosylated liposomes. In particular, the highest EE % values were recorded for Verbascoside loaded in both types of liposomes (**1b** and **2b**).

Regarding OLEs loaded liposomes, the entrapment efficiencies were assessed by Folin-Ciocalteu assay. According to this procedure, the total amount of polyphenols encapsulated in neutral and galactosylated liposomes was evaluated after the purification by dialysis and compared to the amount present in the unencapsulated extracts. Liposomal suspensions were diluted with a methanolic solution to break lipid aggregates and to enhance the release of entrapped polyphenols. Based on the results reported in **Table 4**, there is a slight increase of EE% values for all OLEs loaded in galactosylated liposomes (**2d-2f**) compared to the neutral ones (**1d-1f**).

Furthermore, the EE% and the relative amount of the main polyphenols of OLE100, OLE50 and OLE20 encapsulated in neutral (**1d-1f**) and galactosylated (**2d**-**2f**) liposomes were evaluated by UPLC measurements, results are reported in **Table 5** and **Table 6**.

Compared to the quantitative analysis assessed on unencapsulated OLEs (see **Table 2**), the relative ratio between polyphenols in free OLEs and loaded in liposomes is only slightly modified, with the exception of VERB for which its relative encapsulated amount was not detectable (<LOQ). It has to be note that olive leaves and consequently OLEs are already poor in VERB content.

Table 5. Entrapment efficiencies (EE%) of HOTyr-hexose *isomer a* and *isomer b*, VERB and OLEUR entrapped in OLE loaded liposomes.

	EE (%)					
Compound	**1d**	**2d**	**1e**	**2e**	**1f**	**2f**
HOTyr-hexose *isomer a*	61	63	66	73	65	76
HOTyr-hexose *isomer b*	53	57	57	65	49	66
VERB	nd	nd	nd	nd	nd	nd
OLEUR	68	72	61	72	48	70

1 = DOPC/Chol liposomes; **2** = DOPC/Chol/GLT1 liposomes;
d = OLE100; **e** = OLE50; **f** = OLE20; nd = not determined.

Table 6. Relative amounts (μg/mL) of HOTyr-hexose *isomer a* and *isomer b*, VERB and OLEUR entrapped in OLE loaded liposomes.

	[μg/mL]					
Compound	**1d**	**2d**	**1e**	**2e**	**1f**	**2f**
HOTyr-hexose *isomer a*	3.69 ± 0.01	3.72 ± 7.72	4.05 ± 0.02	4.1 ± 10.1	3.24 ± 0.01	3.58 ± 7.89
HOTyr-hexose *isomer b*	7.56 ± 0.02	7.72 ± 0.02	9.72 ± 0.06	10.13 ± 0.03	6.36 ± 0.03	7.89 ± 0.08
VERB	nd	nd	nd	nd	nd	nd
OLEUR	56.5 ± 0.3	39.3 ± 0.4	294.2 ± 2.2	336.2 ± 0.8	406.6 ± 1.5	621.8 ± 4.9

1 = DOPC/Chol liposomes; **2** = DOPC/Chol/GLT1 liposomes; **d** = OLE100; **e** = OLE50; **f** = OLE20; nd = not determined.

5.2.8. Storage stability

To assess storage stability of liposomes over time at 4°C, their particles hydrodynamic diameter and PDI were analyzed for 90 days. Experiments were carried out on neutral and galactosylated OLEUR loaded liposomes (**1c**-**2c**) and OLEs loaded liposomes (**1d**-**1f** and **2d**-**2f**). Formulations **1c** and **2c** were selected since OLEUR is the most abundant polyphenol quantified in OLEs.

Results reported in **Table 7** showed the great physical stability for both OLEUR loaded liposomes, **1c** and **2c**, highlighting no changes in dimensions and PDI during all the storage time investigated.

OLEs loaded DOPC/Chol liposomes (**1d**-**1f**) result to be less stable of the corresponding DOPC/Chol/GLT1 liposomes (**2d**-**2f**), with a slight increase in dimensions and PDIs during storage. Except for liposomes **2f**, which experienced an increment in size and PDI values up to 90 days, all the others cationic galactosylated liposomes did not highlighted any evidence of instability during their storage, this is in accordance with their quite high ζ-potential, which reduce the probability of aggregation phenomena.

Table 7. Stability over time of liposomes under investigation.

DOPC/Chol based liposomes				DOPC/Chol/GLT1 based liposomes			
Formulation	**Time (day)**	**D_h (nm)**	**PDI**	**Formulation**	**Time (day)**	**D_h (nm)**	**PDI**
1c	1	100 ± 2	0.12 ± 0.01	**2c**	1	79 ± 1	0.14 ± 0.01
	30	102 ± 1	0.13 ± 0.01		30	81 ± 1	0.13 ± 0.01
	60	102 ± 1	0.13 ± 0.02		60	81 ± 1	0.15 ± 0.01
	90	102 ± 1	0.14 ± 0.01		90	81 ± 2	0.14 ± 0.01
1d	1	100 ± 1	0.23 ± 0.01	**2d**	1	91 ± 1	0.15 ± 0.01
	30	99 ± 1	0.29 ± 0.02		30	93 ± 1	0.14 ± 0.01
	60	104 ± 1	0.29 ± 0.02		60	95 ± 1	0.15 ± 0.01
	90	99 ± 3	0.23 ± 0.07		90	92 ± 1	0.12 ± 0.02
1e	1	100 ± 2	0.10 ± 0.01	**2e**	1	90 ± 1	0.12 ± 0.01
	30	107 ± 2	0.17 ± 0.02		30	89 ± 2	0.12 ± 0.02
	60	110 ± 2	0.20 ± 0.02		60	92 ± 1	0.18 ± 0.02
	90	125 ± 1	0.27 ± 0.01		90	93 ± 1	0.16 ± 0.02
1f	1	111 ± 2	0.13 ± 0.01	**2f**	1	110 ± 1	0.21 ± 0.01
	30	112 ± 1	0.17 ± 0.01		30	114 ± 3	0.19 ± 0.01
	60	118 ± 3	0.20 ± 0.01		60	117 ± 3	0.18 ± 0.01
	90	136 ± 1	0.26 ± 0.01		90	133 ± 4	0.25 ± 0.01

1 = DOPC/Chol based liposomes; **2** = DOPC/Chol/GLT1 based liposomes; **c** = OLEUR; **d** = OLE100; **e** = OLE50; **f** = OLE20.

5.2.9. Liposomes pH stability

Since liposomes are thermodynamically unstable systems, lipid vesicles could undergo degradation or aggregation under environmental shock conditions, such as pH variation.

In particular, as regards polyphenols loaded liposomes, pH is a noticeable factor affecting the polyphenols position inside the lipid bilayer. In acidic environment, phenolic hydroxyl groups are protonated, and consequently polyphenols tend to locate in the hydrophobic region of liposome, while in alkaline environment polyphenols are deprotonated and they prefer to interact with polar headgroups at the lipid bilayer–water interface.[31]

In the case of a potential oral administration *in vivo* liposomes experience significant pH variation of the environment around them, therefore the stability of OLEUR and OLEs loaded liposomes to pH variations was evaluated by DLS measurements checking vesicles size and PDI at different pH. To this purpose, the pH of liposomes solution was adjusted by adding aqueous solution of HCl or NaOH to mimic those of human digestive system, in particular pH 5-7 for mouth, pH 1-5 for stomach, pH

6-7.5 for small intestine and pH 5-8 for colon. For these specific values of pH, vesicles size and PDI of liposomes were checked after a time corresponding to that of the physiological transit in the tract of the digestive system we are mimicking. All data collected at different pH values were compared to those obtained at pH = 7.4 (reference value), corresponding to the physiological pH of blood. According to the results reported in **Table 8**, liposomes incubation at different pH does not affect significant changes in dimension and PDI values underlining their great stability to pH variation.

Table 8. pH stability of liposomes under investigation.

DOPC/Chol liposomes				DOPC/Chol/GLT1 liposomes			
Formulation	**pH**	**D_h (nm)**	**PDI**	**Formulation**	**pH**	**D_h (nm)**	**PDI**
	2.9	96 ± 1	0.11 ± 0.01		2.9	84 ± 1	0.12 ± 0.01
	5.7	96 ± 1	0.09 ± 0.01		5.7	84 ± 1	0.12 ± 0.01
1c	6.4	96 ± 1	0.11 ± 0.01	**2c**	6.4	85 ± 1	0.13 ± 0.01
	7.4	94 ± 1	0.11 ± 0.02		7.4	87 ± 1	0.15 ± 0.01
	8.1	94 ± 1	0.10 ± 0.03		8.1	84 ± 1	0.12 ± 0.01
	2.9	104± 1	0.31 ± 0.01		2.9	89 ± 1	0.16 ± 0.01
	5.7	101 ± 2	0.12 ± 0.01		5.7	91 ± 1	0.15 ± 0.01
1d	6.4	98 ± 1	0.13 ± 0.02	**2d**	6.4	90 ± 1	0.18 ± 0.01
	7.4	100 ± 1	0.17 ± 0.01		7.4	92 ± 1	0.19 ± 0.01
	8.1	95 ± 1	0.23 ± 0.01		8.1	88 ± 2	0.17 ± 0.01
	2.9	112 ± 1	0.22 ± 0.01		2.9	92 ± 1	0.15 ± 0.01
	5.7	98 ± 1	0.16 ± 0.01		5.7	92 ± 1	0.16 ± 0.01
1e	6.4	97 ± 1	0.15 ± 0.01	**2e**	6.4	92 ± 1	0.15 ± 0.01
	7.4	103 ± 1	0.17 ± 0.01		7.4	94 ± 1	0.16 ± 0.01
	8.1	109 ± 2	0.18 ± 0.01		8.1	93 ± 1	0.17 ± 0.01
	2.9	123 ± 2	0.22 ± 0.02		2.9	115 ± 2	0.16 ± 0.01
	5.7	118 ± 1	0.21 ± 0.01		5.7	117 ± 1	0.16 ± 0.01
1f	6.4	121 ± 2	0.22 ± 0.01	**2f**	6.4	115 ± 1	0.17 ± 0.01
	7.4	120 ± 1	0.20 ± 0.01		7.4	119 ± 1	0.20 ± 0.01
	8.1	117 ± 3	0.21 ± 0.01		8.1	116 ± 2	0.17 ± 0.01

1 = DOPC/Chol liposomes; **2** = DOPC/Chol/GLT1 liposomes; **c** = OLEUR; **d** = OLE100; **e** = OLE50; **f** = OLE20.

5.2.10. *In vitro* release study

With the aim to evaluate the releasing profiles of OLEUR and OLEs from liposomes, an *in vitro* study was assessed by dialysis method.

The release of OLEUR from liposomes of formulations **1c** and **2c** was examined by UPLC analysis, determining the percentage of OLEUR leakage over a period of 24 h (**Figure 8**).

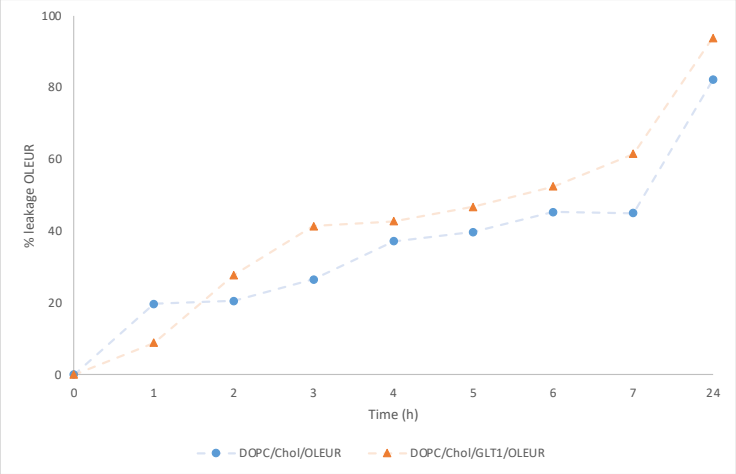

Figure 8. Leakage of OLEUR from DOPC/Chol liposomes (light blue dots) and DOPC/Chol/GLT1 liposomes (orange triangles) under forced release condition.

Both release curves highlighted a similar trend characterized by a progressive release during the first 7 h, and after 24 h a final OLEUR leakage of ~ 90% and ~ 80% from DOPC/Chol/GLT1 and DOPC/Chol liposomes was observed respectively. The higher percentage of OLEUR leakage from DOPC/Chol/GLT1 liposomes may be related to the detergent properties and destabilizing capacity of GLT1, which could induce a higher release of OLEUR from the DOPC/Chol/GLT1 lipid bilayer compared to DOPC/Chol lipid bilayer.

The *in vitro* release study of phenolic compounds of OLE100, OLE50 and OLE20 from neutral (**1d**-**1f**) and galactosylated (**2d**-**2f**) liposomes was evaluated over time by Folin-Ciocalteu assay, determining the total phenolic content still encapsulated in liposomes over a period of 24 h.

As shown in **Figures 9**-**11**, the release of ~ 50% of polyphenols occurred in the first 3-4 hours for all extract loaded liposomes, with a complete cargo release whitin 5-6 hours from DOPC/Chol liposomes and 7-24 hours from DOPC/Chol/GLT1 liposomes.

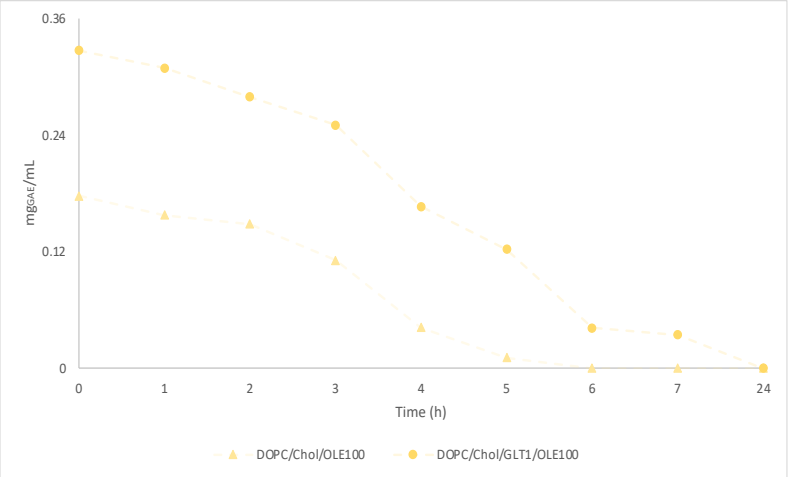

Figure 9. Total phenolic content still encapsulated in DOPC/Chol/OLE100 liposomes (light yellow triangles) and DOPC/Chol/GLT1/OLE100 liposomes (yellow dots) over time under forced release condition.

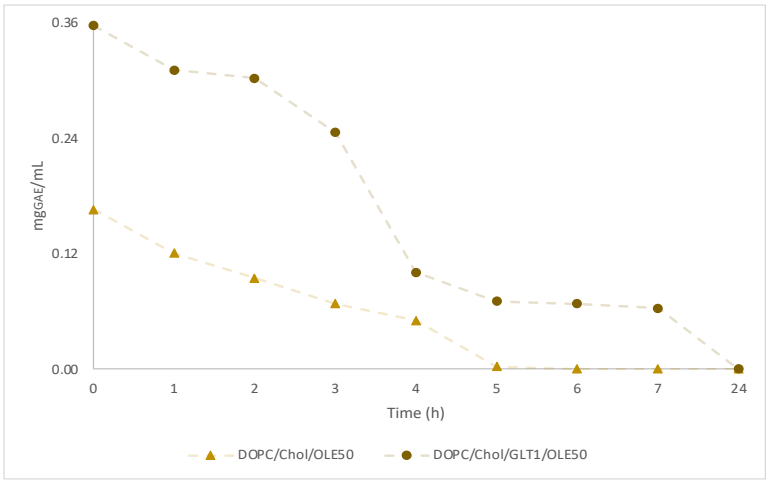

Figure 10. Total phenolic content still encapsulated in DOPC/Chol/OLE50 liposomes (light brown triangles) and DOPC/Chol/GLT1/OLE50 liposomes (brown dots) over time under forced release condition.

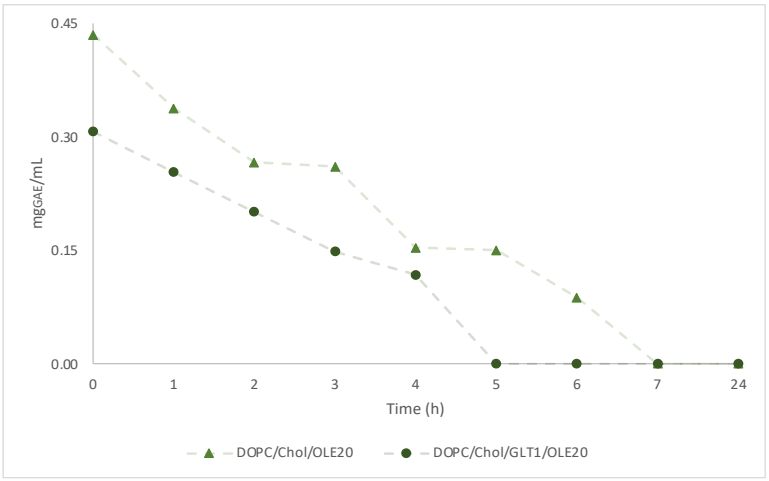

Figure 11. Total phenolic content still encapsulated in DOPC/Chol/OLE20 liposomes (light green triangles) and DOPC/Chol/GLT1/OLE20 liposomes (green dots) over time under forced release condition.

Furthermore, HOTyr-hexose *isomer a* and *isomer b* and OLEUR release from OLEs loaded DOPC/Chol (**1d**-**1f**) and DOPC/Chol/GLT1 (**2d**-**2f**) liposomes was assessed by UPLC analysis to quantify the specific amount of the single polyphenol still loaded inside liposomes at a specific time. As already mentioned, VERB, due to its low content in all the extracts under investigation, was not detectable (<LOQ) after encapsulation.

Figures 12-17 show the results collected for HOTyr (*isomer a* and *isomer b)* and OLEUR release from each extract loaded liposome studied.

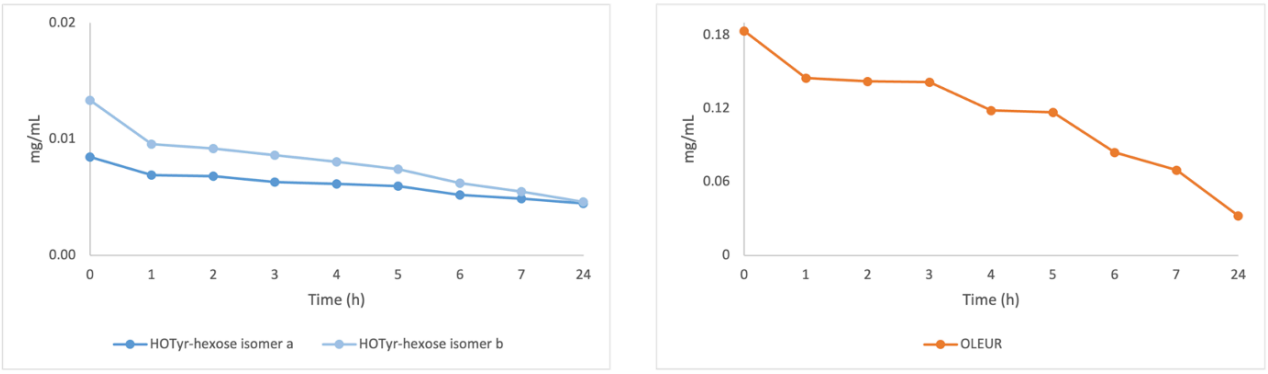

Figure 12. HOTyr-hexose (*isomer a* and *isomer b*) and OLEUR amounts still encapsulated in DOPC/Chol/OLE100 (**1d**) liposomes over time under forced release condition.

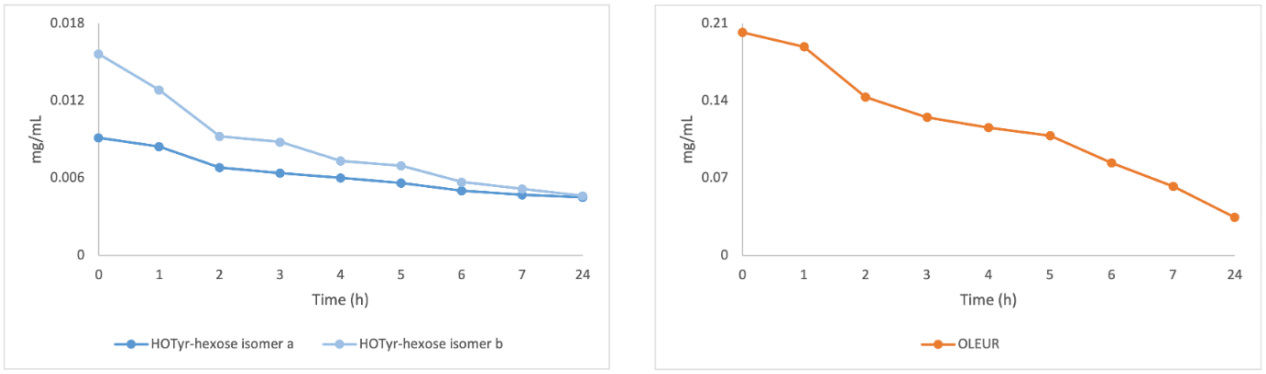

Figure 13. HOTyr-hexose (*isomer a* and *isomer b*) and OLEUR amounts still encapsulated in DOPC/Chol/GLT1/OLE100 (**2d**) liposomes over time under forced release condition.

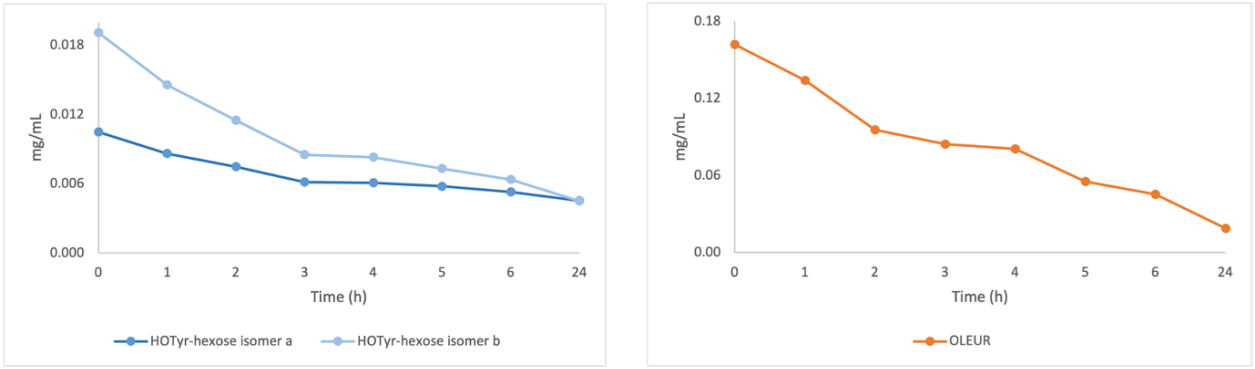

Figure 14. HOTyr-hexose (*isomer a* and *isomer b*) and OLEUR amounts still encapsulated in DOPC/Chol/OLE50 (**1e**) liposomes over time under forced release condition.

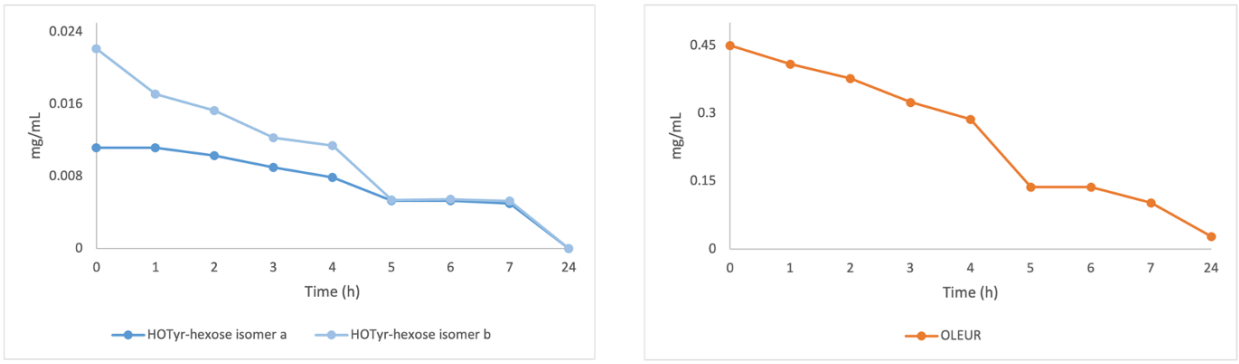

Figure 15. HOTyr-hexose (*isomer a* and *isomer b*) and OLEUR amounts still encapsulated in DOPC/Chol/GLT1/OLE50 (**2e**) liposomes over time under forced release condition.

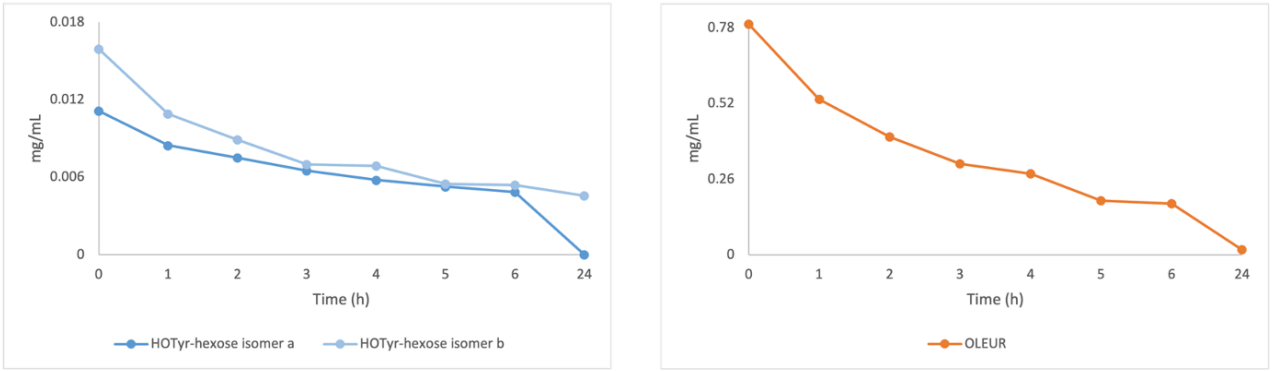

Figure 16. HOTyr-hexose (*isomer a* and *isomer b*) and OLEUR amounts still encapsulated in DOPC/Chol/OLE20 (**1f**) liposomes over time under forced release condition.

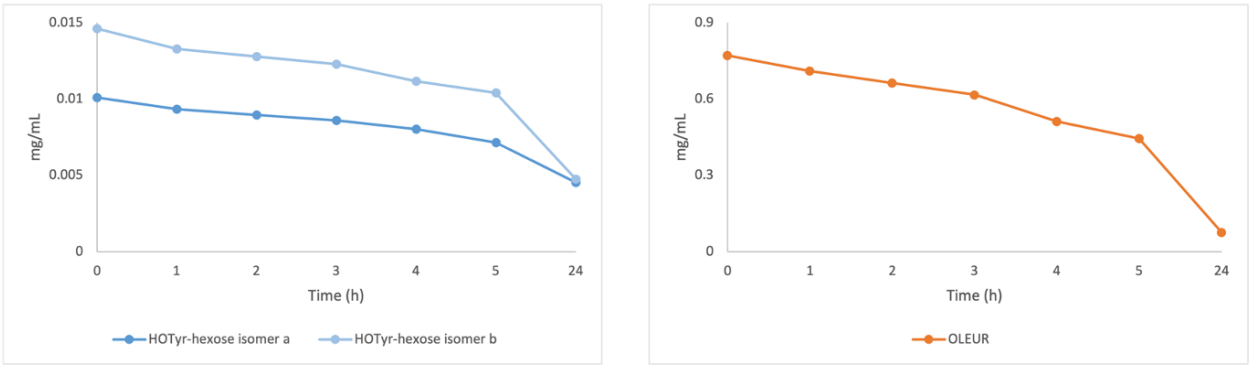

Figure 17. HOTyr-hexose (*isomer a* and *isomer b*) and OLEUR amounts still encapsulated in DOPC/Chol/GLT1/OLE20 (**2f**) liposomes over time under forced release condition.

Due to the higher sensitivity of UPLC analysis compared to the Folin-Ciocalteu assay, it is worth of noting that the forced release is not complete after 5-7 hours, indeed small quantity of biomolecule investigated (HOTyr-hexose isomers and OLEUR) are still present in the liposomes after 24 hours.

5.2.11. Antimicrobial activity

The antimicrobial activity of HOTyr, VERB, OLEUR and OLEs in free form and loaded in neutral or galactosylated liposomes was investigated against two strains of *Staphylococcus aureus*, ATCC 25923 (wild type strain) and ATCC 33591 (MRSA, methicillin-resistant strain), determining the *Minimum Inhibitory Concentration* (MIC) and the *Minimum Bactericidal Concentration* (MBC) according to the microdilution method.

MIC is defined as the lowest concentration of an antimicrobial agent that under defined *in vitro* conditions prevents the appearance of visible growth of microorganism within a determined period, whilst MBC is known as the lowest concentration able to destroy the 99.9% of microorganisms tested.

The molecular structures of the single polyphenols under investigation are reported in **Chart 2**.

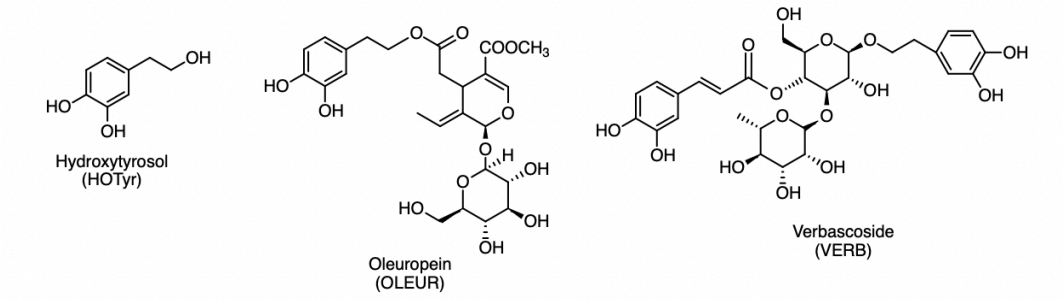

Chart 2. Molecular structures of polyphenols under investigation.

All the polyphenols investigated possess interesting biological properties: HOTyr has been one of the most widely studied polyphenol in the last years due to its anti-inflammatory, anti-thrombotic, anti-cancer, antioxidant and antimicrobial properties;[32,33] VERB is a phenylpropanoid glycoside highly widespread in the plant kingdom featuring antimicrobial, anti-inflammatory, anti-cancer, antioxidant, healing and neuroprotective properties;[34] OLEUR belongs to the secoiridoids family with anti-inflammatory, antioxidant, hepatoprotective, neuroprotective, antiviral properties and antimicrobial activity affecting both *Gram*-positive and *Gram*-negative bacteria.[35,36]

The antimicrobial activity of Hydroxytyrosol as such was evaluated because of the lack of Hydroxytyrosol hexose isomers as reference standards.

To determine MIC and MBC values of investigated antimicrobials, the experiments were conducted on bacteria cells at 8 x 10^5 CFU/mL diluted in Mueller-Hinton (MH) broth. The antimicrobial was added, at specific concentrations, to the target bacteria in a 96 well plate and after 24 h of incubation at 37°C the bacteria growth was evaluated analyzing the suspension turbidity. In fact, at the end of the incubation time, if the broth in the well become cloudy or a layer of cells is formed at the bottom, it means that bacterial growth has occurred, and the antimicrobial tested has not been active at the evaluated concentration. Instead, if the broth in the well appears clear and transparent, it must be transferred on MH agar plates and incubated at 37°C for 24 h. Finally, the lowest concentration of the antimicrobial tested in which bacteria growth did not occur in the well but occur after transfer on MH agar plate is defined as MIC, whilst the lowest concentration of the antimicrobial tested in which bacteria did not growth both in the well and on MH agar plate is defined as MBC.

Gentamicin was tested as control against both bacteria strains at a concentration of 5 μg/mL showing a bactericidal effect against ATCC 25923 strain and an inhibitory effect on ATCC 33591 strain, as already reported in the literature.

MIC and MBC values of HOTyr, VERB and OLEUR tested in free form against both bacteria strains are reported in **Table 9**, results are expressed as micrograms of compound per milliliter (μg/mL) and as absolute concentration (μM).

Table 9. Antimicrobial activity of HOTyr, VERB and OLEUR free on ATCC 25923 and ATCC 33591.

	S. aureus wild type (ATCC 25923)				MRSA (ATCC 33591)			
Compound	**MIC (μg/mL)**	**MIC (μM)**	**MBC (μg/mL)**	**MBC (μM)**	**MIC (μg/mL)**	**MIC (μM)**	**MBC (μg/mL)**	**MBC (μM)**
HOTyr	18	117	20	130	19	123	21	136
VERB	48	77	51	82	37	59	51	82
OLEUR	75	138	90	167	84	155	94	174

VERB is resulted to be the most active polyphenol among those tested with MICs of 77 μM against *S. aureus* wild type and 59 μM against MRSA, thus highlighting a higher inhibitory activity against the resistant strain compared to the wild type one. Instead, MBC value of VERB for both bacteria strains was 82 μM.

Although OLEUR is the most abundant polyphenol identified in our extracts, it is the least active among those investigated, with MIC value of 138 μM against the wild type strain and 155 μM against the resistant strain.

HOTyr shows an intermediate antimicrobial activity between VERB and OLEUR, which resulted higher on the wild type strain compared to MRSA (MIC = 117 μM and MBC = 130 μM for *S. aureus* wild type, MIC = 123 μM and MBC = 136 μM for MRSA).

MIC and MBC values of OLE100, OLE50 and OLE20 in free form are reported in **Table 10**, expressed as milligrams of dry extract per milliliter ($mg_{extract}$/mL).

Table 10. Antimicrobial activity of OLEs on ATCC 25923 and ATCC 33591.

	S. aureus wild type (ATCC 25923)		MRSA (ATCC 33591)	
Extract	**MIC ($mg_{extract}$/mL)**	**MBC ($mg_{extract}$/mL)**	**MIC ($mg_{extract}$/mL)**	**MBC ($mg_{extract}$/mL)**
OLE100	0.24	0.29	0.24	0.31
OLE50	0.15	0.18	0.14	0.18
OLE20	0.18	0.19	0.16	0.18

According to the results in **Table 10**, the hydroalcoholic extracts OLE50 and OLE20 show a higher activity than the aqueous extract OLE100, with quite similar MIC and MBC values. In particular, MIC values recorded in both cases are lower against ATCC 33591 than ATCC 25923, suggesting a higher inhibitory effect on the resistant strain than on the wild type. Instead, MBC values of OLE50 and OLE20 are mainly the same for both bacteria strains investigated.

Though OLE100 is the least active extract investigated, its antimicrobial activity is higher than that expected for its OLEUR content (6.5 times less abundant than in OLE50 and 13.5 times less abundant than in OLE20, see **Table 2**), nevertheless its content of HOTyr-hexose *isomer a* and *isomer b* is essentially the same as OLE20 and OLE50, therefore this probably contribute to partially decreasing the loss of antimicrobial activity of OLE100.

It is worth to note that the concentrations at which OLEs were active correspond to amounts of HOTyr-hexose *isomer a* and *isomer b*, VERB and OLEUR considerably lower than those of MIC and

MBC determined for the individual compounds, hence highlighting a possible synergistic effect between the bioactive compounds inside the extracts tested. For example, if we consider OLE50, its MIC value is 0.15 $mg_{extract}$/mL against ATCC 25923, the concentration of OLEUR present in this amount of OLE20 is 23.3 μg/mL, which is 3.2 times lower than the MIC found for free OLEUR (75 μg/mL). Similar consideration can be made for all the other compounds identified and investigated.

Afterwards, the effect of encapsulation in DOPC/Chol and DOPC/Chol/GLT1 liposomes on OLEUR antimicrobial activity was evaluated. OLEUR was selected since it is the most abundant polyphenol present in our extracts. MIC and MBC values of OLEUR loaded in both formulations are reported in **Table 11** and results are expressed both as micrograms of compound per milliliter (μg/mL) and as absolute concentration (μM).

Table 11. Antimicrobial activity of OLEUR free and loaded in liposomes on ATCC 25923 and ATCC 33591.

		S. aureus wild type (ATCC 25923)				MRSA (ATCC 33591)			
Compound	**Formulation**	**MIC (μg/mL)**	**MIC (μM)**	**MBC (μg/mL)**	**MBC (μM)**	**MIC (μg/mL)**	**MIC (μM)**	**MBC (μg/mL)**	**MBC (μM)**
OLEUR	-	75	139	90	167	84	155	94	174
	1c	111	205	131	242	115	213	131	242
	2c	107	198	129	239	129	233	146	270

1 = DOPC/Chol liposomes; **2** = DOPC/Chol/GLT1; - = OLEUR in free form.

The inclusion of OLEUR in DOPC/Chol and DOPC/Chol/GLT1 liposomes did not highlight any improvement in terms of antimicrobial activity for both bacteria, in fact higher MIC and MBC values were obtained compared to those collected for OLEUR tested in free form. In particular, OLEUR loaded in both types of liposomes, **1c** and **2c**, proved to be more active against the wild type strain compared to MRSA. Regarding the relative antimicrobial activity showed by OLEUR in a specific type of liposome on the two bacteria strains, OLEUR loaded in neutral liposomes has a higher activity against MRSA respect to *S. aureus* wild type, on the contrary OLEUR loaded in galactosylated liposomes showed the opposite behavior.

Nevertheless, considering all the beneficial effects deriving from the inclusion of OLEUR in liposomes on its pharmacokinetics features (stability, release profile, bioavailability etc.), the higher values of MIC and MBC determined for OLEUR after encapsulation should not be considered as a negative result.

Finally, the effect of inclusion in DOPC/Chol and DOPC/Chol/GLT1 liposomes on the antimicrobial activity of OLEs has been also investigated determining their MIC and MBC values against the two selected *S. aureus* strains.

Because we ascribe the antimicrobial activity of OLEs to the polyphenols present in the extracts and we cannot quantify their total amount when encapsulated, we assumed as reasonable to report MIC and MBC values of both free and encapsulated extracts as micrograms of Gallic Acid equivalents per milliliter (μg_{GAE}/mL, assessed by Folin-Ciocalteau) to have values useful for the comparison. Results obtained are reported in **Table 12** and **Table 13**.

Table 12. Antimicrobial activity of OLEs free and loaded in liposomes on ATCC 25923.

		S. aureus wild type (ATCC 25923)			
Extract	**Formulation**	**MIC ($mg_{extract}$/mL)**	**MIC (μg_{GAE}/mL)**	**MBC ($mg_{extract}$/mL)**	**MBC (μg_{GAE}/mL)**
OLE100	-	0.24	12.8	0.29	15.4
	1d	n.d.	30.5	n.d.	31.2
	2d	n.d.	8	n.d.	8.2
OLE50	-	0.15	9.3	0.18	11.2
	1e	n.d.	34.4	n.d.	41.9
	2e	n.d.	10.8	n.d.	14.1
OLE20	-	0.18	11.7	0.19	12.4
	1f	n.d.	36	n.d.	37.6
	2f	n.d.	8.6	n.d.	9.6

1 = DOPC/Chol liposomes; **2** = DOPC/Chol/GLT1 liposomes;
d = OLE100; **e** = OLE50; **f** = OLE20; - = OLE in free form; n.d. = not determined.

Table 13. Antimicrobial activity of OLEs free and loaded in liposomes on ATCC 33591.

		MRSA (ATCC 33591)			
Extract	**Formulation**	**MIC ($mg_{extract}$/mL)**	**MIC (μg_{GAE}/mL)**	**MBC ($mg_{extract}$/mL)**	**MBC (μg_{GAE}/mL)**
OLE100	-	0.24	12.8	0.31	16.6
	1d	n.d.	34.8	n.d.	35.5
	2d	n.d.	8.5	n.d.	8.9
OLE50	-	0.14	8.7	0.18	11.2
	1e	n.d.	75.5	n.d.	78.2
	2e	n.d.	10.8	n.d.	11.2
OLE20	-	0.16	10.4	0.18	11.7
	1f	n.d.	57.3	n.d.	58.9
	2f	n.d.	8.9	n.d.	9.1

1 = DOPC/Chol liposomes; **2** = DOPC/Chol/GLT1 liposomes;
d = OLE100; **e** = OLE50; **f** = OLE20; - = OLE in free form; n.d. = not determined.

OLEs inclusion in neutral liposomes (**1d**-**1f**) did not lead to any improvement in terms of antimicrobial activity against both bacteria strains, hence resulting in higher MIC and MBC values than those collected for OLEs in free form.

As regards galactosylated liposomes, we obtained comparable or slightly increased antimicrobial activity for all loaded OLEs with respect to the free ones, without any substantial differences in MIC and MBC values among the bacteria strains investigated.

In particular, the encapsulation in galactosylated liposomes displayed a positive effect on the antimicrobial activity of OLE100 and OLE20, while any improvement was observed for OLE50 activity, though it is not as detrimental as in the case of OLEs encapsulation in neutral liposomes.

OLEs antimicrobial activity improvement assessed after encapsulation in DOPC/Chol/GLT1 liposomes is probably related to the presence of GLT1 inside the lipid bilayer, which should be able to enhance the interaction between liposomes and bacteria on one side through the electrostatic interaction of cationic liposomes with the negatively charged bacteria, and on the other according to the interaction between galactose residues exposed on liposome surface and lectins or sugar transporters expressed by bacterial membrane. This could lead to the better diffusion and interaction of the active compounds released from the lipid bilayer across the bacterial cell walls, which coupled with the synergistic effect of OLEs polyphenols released leads to an increase in antimicrobial activity.

The activity of DOPC/Chol and DOPC/Chol/GLT1 empty liposomes was also evaluated against both bacterial strains and in both cases there was no evidence of antimicrobial activity caused by the lipidic components of liposomes.

5.3. Conclusion

The investigation carried out in this chapter represents an example of circular economy approach toward the valorization of agri-food waste, such as *Olea europaea* leaves, a biowaste of the olive-oil chain, which were used to produce extracts with antibacterial activity.

Olea europaea leaves extracts were prepared by ultrasound-assisted extraction using different mixture of green extracting solvents such as water and ethanol. All extracts were found to be rich in Hydroxytyrosol-hexose isomers and Oleuropein.

The dry extracts and the main polyphenolic constituents were loaded in liposomes to enhance their solubility, stability and bioavailability. Liposomes were formulated with natural lipids, DOPC and cholesterol, in presence or absence of a synthetic galactosylated amphiphile (GLT1) added to the formulation to enhance the interaction with bacteria cells involved in the study. Liposomes produced have shown suitable physicochemical features, and good stability at different pH values and in storage condition.

OLEs have exhibited good antimicrobial activity against two strains of *Staphylococcus aureus*, ATCC 25923 (wild type strain) and ATCC 33591 (Methicillin-resistant strain, MRSA), highlighting a possible synergistic effect between the bioactive compounds inside the extracts tested.

Encapsulation of OLEs in DOPC/Chol/GLT1 liposomes have displayed comparable or slightly increased antimicrobial activity on both bacteria strains with respect to that of free extracts.

5.4. Experimental Materials and Methods

5.4.1. Materials

5.4.1.1. Reagents, standards and solvents

1,2-dioleoyl-*sn*-glycero-3-phosphocholine (DOPC) was purchased from Avanti Polar Lipids (Alabaster, AL, USA). Cholesterol (Chol, purity = 99%), hydroxytyrosol (4-dihydroxyphenylethanol, purity ≥ 98%), oleuropein ((2*S*,3*E*,4*S*)-3-Ethylidene-2-(β-D-glucopyranosyloxy)-3,4-dihydro-5-(methoxycarbonyl)-2*H*-pyran-4-acetic acid 2-(3,4-dihydroxyphenyl) ethyl ester, purity ≥ 80%), verbascoside (purity ≥ 99%), trolox ((±)-6-Hydroxy-2,5,7,8-tetramethylchromane-2-carboxylic acid, purity ≥ 97%), ABTS (2,2'-Azino-bis(3-ethylbenzothiazoline-6-sulfonic acid) diammonium salt, purity ≥ 98%), Folin & Ciocalteu's phenol reagent were purchased from Sigma-Aldrich. Gallic acid (purity ≥ 98%), 4-hydroxy-phenilacetic acid (purity ≥ 98%), sodium carbonate (purity ≥ 98%) were purchased from Fluka Chemie. Phosphate-buffered saline (PBS; 0.01 M phosphate buffer, 0.0027 M KCl, 0.137 M NaCl, pH 7.4, at 25 °C, prepared by dissolving 1 tablet in 200 mL of deionized water), cellulose dialysis membrane (D9527-100FT, molecular weight cut off= 14 kDa) were purchased from Sigma-Aldrich.

All the solvents used were HPLC grade: chloroform ($CHCl_3$, Merck KGaA), methanol (MeOH, VWR Chemicals), ethanol (EtOH, VWR Chemicals), formic acid (Merck KGaA), acetonitrile (VWR Chemicals) and water (H_2O, VWR Chemicals).

All the materials used for the antimicrobial assays were purchased from Fisher Scientific (Milan, Italy).

The galactosylated amphiphile GLT1 was synthesized according to the procedure previously described in **Chapter 3**.

5.4.1.2 Plant materials

Olive leaves from *Olea Europaea*, cultivar "Frantoio", were picked up in Montelibretti, a small village placed in the north-east of Rome (N 42° 12' 3.301'' W 12° 68' 7.907''), during the olives harvest period, from trees not subjected to any pest treatments. Afterward, olive leaves were frozen with liquid nitrogen, triturated with mortar and pestle, and freeze-dried until obtaining a stable weight over time. Finally, grinded leaves were stored at -80°C until further experiments.

5.4.2. Preparation of Olive leaves extracts (OLEs)

Aqueous and hydroalcoholic extracts from olive leaves grinded were obtained by ultra-sound assisted extraction. In particular, 500 milligrams of olive leaves were extracted with 10 mL of different mixture of solvents: H_2O (100%), EtOH/H_2O (50:50 v/v) and EtOH/H_2O (80:20 v/v), obtaining three different extracts identified as OLE100, OLE50 and OLE20 respectively.

The ultrasound-assisted extraction was carried out for 45 minutes at 40°C using a bath sonicator (Elmasonic S 30 H). Afterwards, the extracts were centrifuged (UNIVERSAL 320R, Hettich) at 4000 rpm for 10 minutes at 20°C to remove the insoluble part, the supernatants produced were analyzed both spectrophotometrically and chromatographically, and finally stored for a maximum of two weeks at -20°C (**Figure 18**).

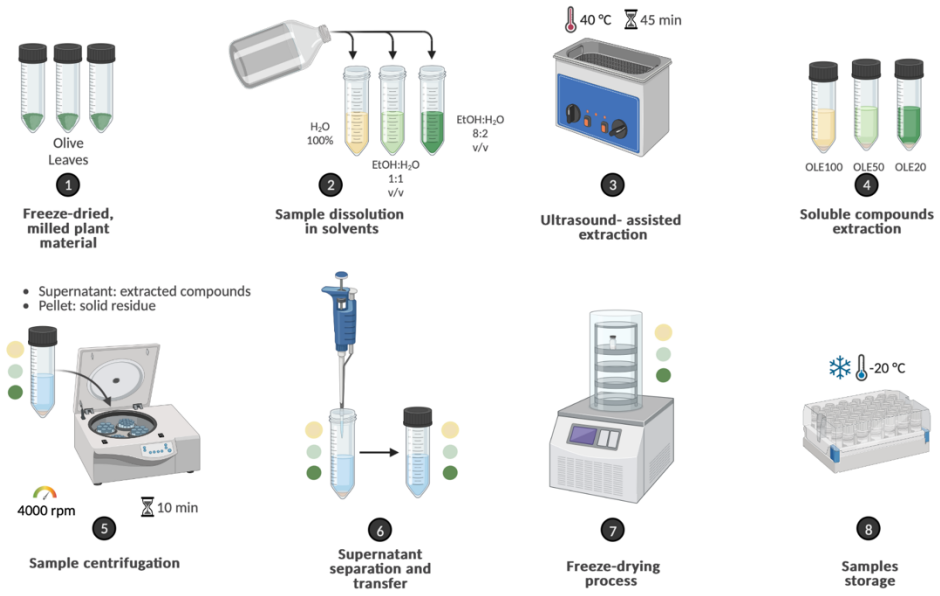

Figure 18. Graphical representation of olive leaves extraction process (created with BioRender.com).

5.4.2.1. Freeze-drying process

With the aim to preserve the extracts as longer as possible, extraction solvents were removed by lyophilization. In particular, ethanol was removed from OLE50 and OLE20 under vacuum by rotary evaporator, then the extracts OLE100, OLE50 and OLE20 were freeze-dried using a FreeZone 7740030 (LabConco Corporation).

For each extract, the yield of extraction (R%) has been calculated as follows:

$$R(\%) = \frac{g_{freeze-dried\ extract}}{g_{dry\ matter}} \times 100 \qquad \textbf{(Eq. 1)}$$

Where $g_{freeze\text{-}dried\ extract}$ corresponds to the amount of dry extract obtained by lyophilization and $g_{dry\ matter}$ corresponds to the amount of olive leaves used for the extraction.

5.4.3. Chemical characterization of OLEs

OLEs were characterized by UV-Vis spectrophotometry to evaluate the total phenolic content by Folin-Ciocalteu assay and the antioxidant activity by TEAC assay. Moreover, the identification and quantification of the main polyphenols in OLE100, OLE50 and OLE20 were assessed by UPLC-MS-PDA analysis.

5.4.3.1. Total Phenolic Content

The total phenolic content of OLE100, OLE50 and OLE20 was determined by Folin-Ciocalteau assay according to the following procedure.[18,37]

Initially, a calibration curve was created preparing a set of different solution of Gallic Acid, used as reference standard, with known concentration ranging from 0.025 mg/mL to 2.0 mg/mL. Then, 10 µL of each Gallic Acid solution was mixed with 50 µL of Folin-Ciocalteau reagent, 150 µL of 2% (w/v) Na_2CO_3 and the volume was made up to 1 mL with water. After 2h of incubation in the dark at 25°C, the absorbance was measured at 760 nm using a spectrophotometer (Shimadzu UV-2401PC). All the absorbance values recorded were plotted as a function of the Gallic Acid concentration, as shown by the calibration curve reported in **Figure 19**.

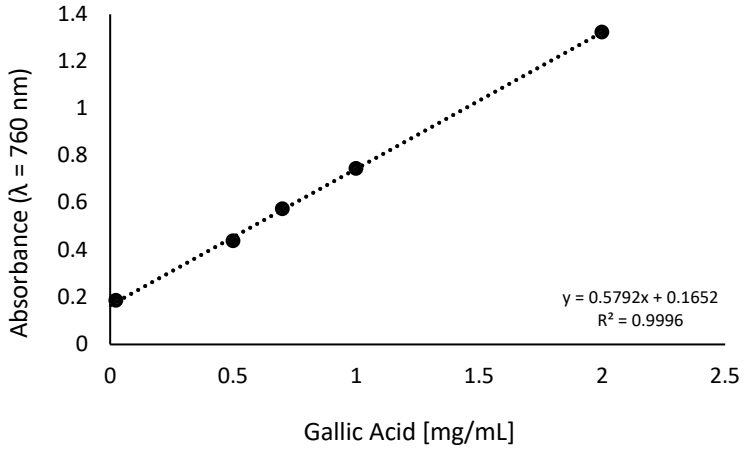

Figure 19. Gallic acid calibration curve.

The total phenolic content of the extract was obtained mixing 10 µL of OLE100, OLE50 or OLE20 with 50 µL of Folin-Ciocalteau reagent, 150 µL of 2% (w/v) Na_2CO_3 and bringing the final volume of the solution to 1 mL with water. After 2 h of incubation in the dark at 25°C, the absorbance was measured at 760 nm by a spectrophotometer. The total phenolic content of each extract was determined using the calibration curve and the results were expressed as milligrams of Gallic Acid equivalents per gram of extracted olive leaves (mg_{GAE}/g_{leaves}).

5.4.3.2. Antioxidant Capacity

Trolox equivalent antioxidant capacity (TEAC) assay was performed with the aim to evaluate the antioxidant capacity of OLE100, OLE50 and OLE20. The reduction process of $ABTS^{\bullet+}$ to ABTS by reaction with antioxidant compounds (**Figure 20**) can be followed by UV-Vis spectroscopy.[21]

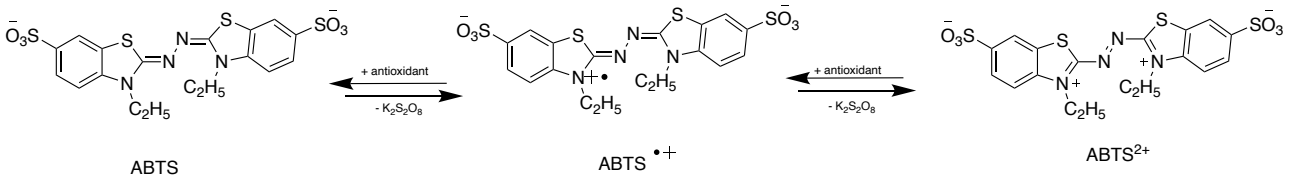

Figure 20. Chemical reactions involved in TEAC assay.

Briefly, ABTS radical cation ($ABTS^{\bullet+}$) was produced by reacting 7 mM ABTS solution with 2.45 mM potassium persulfate ($K_2S_2O_8$), keeping the mixture under stirring in the dark at room temperature for 16-18 h before use.

Trolox, a water-soluble analogue of vitamin E, was used as reference standard, to obtain a calibration curve. Different volumes (1, 1.5, 2, 3, 4, 5 µL) of 3.8 mM Trolox solution in EtOH were added to 980 µL of EtOH and 20 µL of $ABTS^{\bullet+}$, previously prepared. For each solution the absorbance (Abs) was measured at 734 nm by a spectrophotometer at different times after the addition of Trolox: 0 minutes (t_0, before adding Trolox), 1 minute (t_1) and 4 minutes (t_4). The percentage of $ABTS^{\bullet+}$ inhibition for the different concentration of Trolox was evaluated according to the following equation:

$$\%_{\text{inhibition}} = \frac{A_0 - A_t}{A_0} \times 100 \qquad \textbf{(Eq. 2)}$$

Where A_0 is the Abs recorded for $ABTS^{\bullet+}$ in absence of Trolox and A_t is the Abs recorded after 1 min or 4 min of reaction. Then, the obtained values of percentage of inhibition were plotted as a function of μmol of added Trolox, as shown in **Figure 21** and **Figure 22**.

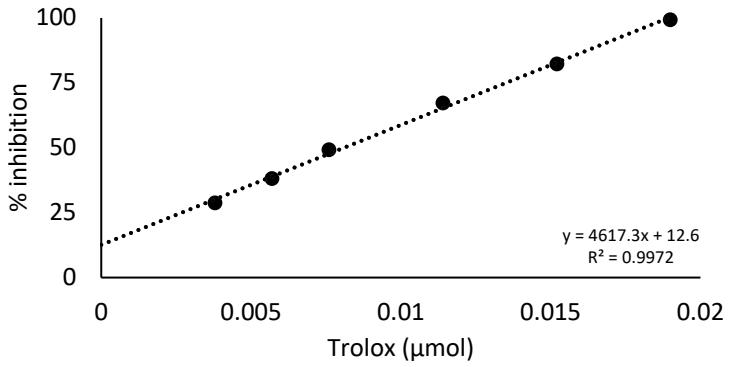

Figure 21. Trolox calibration curve after 1 min of reaction (t_1).

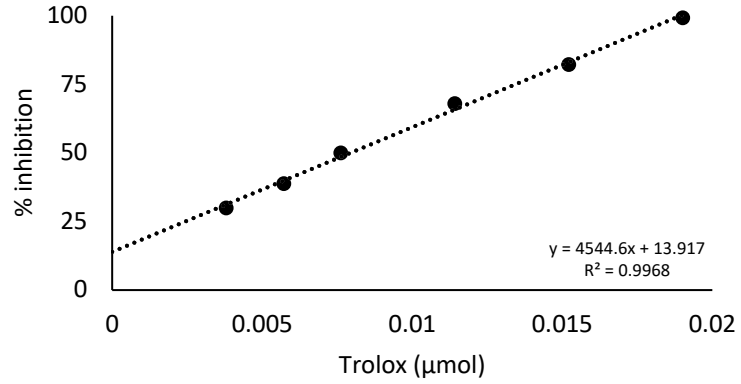

Figure 22. Trolox calibration curve after 4 min of reaction (t_4).

According to the procedure above, different volumes (10, 8, 6, 4, 2 μL) of each OLEs were added to 980 μL of EtOH and 20 μL of $ABTS^{\bullet+}$. For each solution the absorbance was measured at 734 nm at different times (t_0, t_1 and t_4). The percentage of inhibition of $ABTS^{\bullet+}$ triggered by the antioxidant compounds present in the extracts was determined using **Eq. 2**. Results obtained were finally expressed as mmol of Trolox equivalents per gram of extracted olive leaves ($mmol_{TE}$ /g_{leaves}).

5.4.3.3. UPLC-PDA-MS method

Chromatographic characterization of OLEs to identify the main phenolic compounds present in the extracts has been assessed by UPLC Acquity™ H-Class Bio (Waters, Milford) set up with a solvent mixing system, an autosampler, a thermostatically controlled column and a PDA detector, directly

coupled with an ion trap mass spectrometer (LXQ-MS System, Thermo Scientific). To carry out the analysis, an Acquity UPLC HSS T3 column (1.8 µm, 150 × 2.1 mm id; Waters, Milford) was employed using as mobile phases water (0.1% (v/v) formic acid, phase A) and acetonitrile (0.1% (v/v) formic acid, phase B) eluted according to the following gradient: 0-3 min from 85% phase A and 15% phase B to 82% phase A and 18% phase B; 3-6.5 min from 82% phase A and 18% phase B to 77% phase A and 23& phase B; 6.5-10 min from 77% phase A and 23% phase B to 40% phase A and 60% phase B; 10-11 min from 40% phase A and 60% phase B to 100% phase B until the minutes 22. Flow rate was 0.4 mL/min and volume of injection was 2 µL. The diode array detector recorded the spectra between 200 nm and 400 nm. The MS operated in ESI negative ionization mode using the following parameters: capillary temperature 275°C; capillary voltage -10 V; spray voltage 3.60 kV; sheath gas flow 10 units; auxiliary gas flow 5 units. The instrument acquired data in the range m/z 100-700.

5.4.3.3.1. UPLC-PDA validation method

The UPLC method previously described has been validated in terms of linearity, sensitivity and precision. The LOD and LOQ were determined for each compound detected by gradual dilutions of the stock solutions. For each analyte, the LOD was defined as the concentration able to record a chromatographic peak with S/N>3. The LOQ was determined as the amount of compound able to record a signal with S/N>10. LOD and LOQ obtained for Hydroxytyrosol, Verbascoside and Oleuropein are reported in the **Table 13**.

Table 13. LOD and LOQ values obtained for Hydroxytyrsol, Verbascoside and Oleuropein.

Compound	**LOD** (mg/mL)	**LOQ** (mg/mL)
Hydroxytyrosol	0.00011	0.00033
Verbascoside	0.00010	0.00036
Oleuropein	0.00038	0.00114

5.4.3.3.2. Quantification of phenolic compounds by UPLC-PDA analysis

The quantification of the main phenolic compounds in OLEs was assessed by external calibration method. The calibration curves were obtained analyzing standard solutions at different concentration (at least 6) in triplicate: Hydroxytyrosol 0.00011-1.1 mg/mL, Verbascoside 0.00036-0.84 mg/mL, Oleuropein 0.0038-1.9 mg/mL.

All the results have shown good results in terms of linearity compared to the analytical concentration and the R^2 factor recorded were ≥ 0.9993.

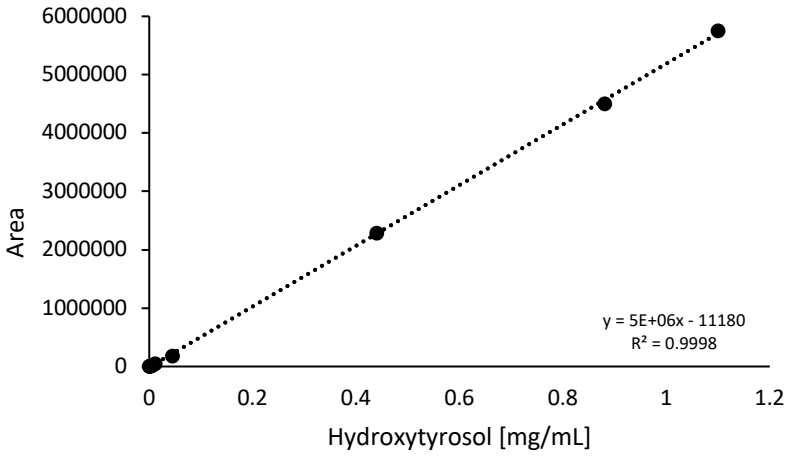

Figure 23. Hydroxytyrosol calibration curve.

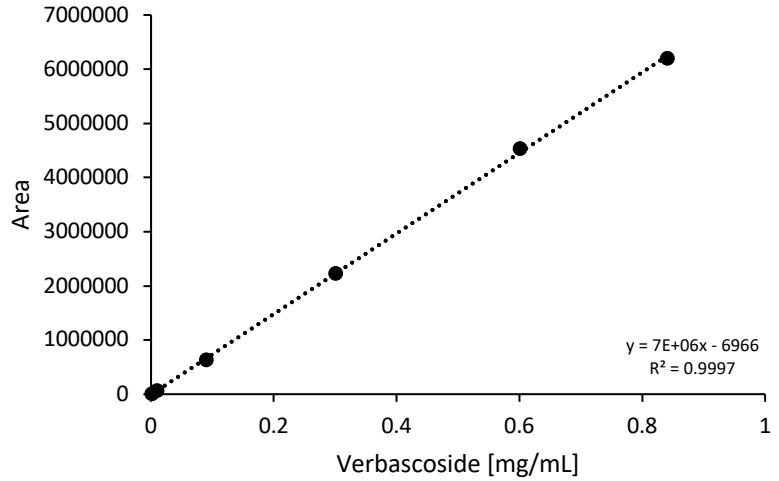

Figure 24. Verbascoside calibration curve.

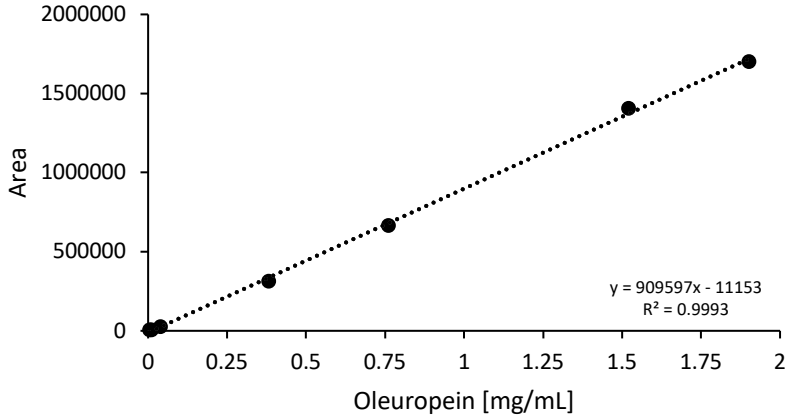

Figure 25. Oleuropein calibration curve.

A solution containing Hydroxytyrosol, Verbascoside and Oleuropein was analyzed for the repeatability tests. Analyses were carried out on the same day (repeatability intra-day) and on three days (repeatability inter-day) in a replicate of six times. The precision obtain has been expressed as relative standard deviation and in both cases the error recorded is lower than 2%.

5.4.4. Liposomes preparation

Empty neutral and galactosylated liposomes (**Table 14**), were prepared according to the lipid film hydration protocol, coupled with the freeze-thaw procedure and followed by an extrusion process,[38] as reported in **Figure 26**.

Table 14. Composition of empty liposomes (10 mM in total lipids).

Formulation	Composition	Lipids (mM)
1	DOPC/Chol	8.0:2.0
2	DOPC/Chol/GLT1	7.0:2.0:1.0

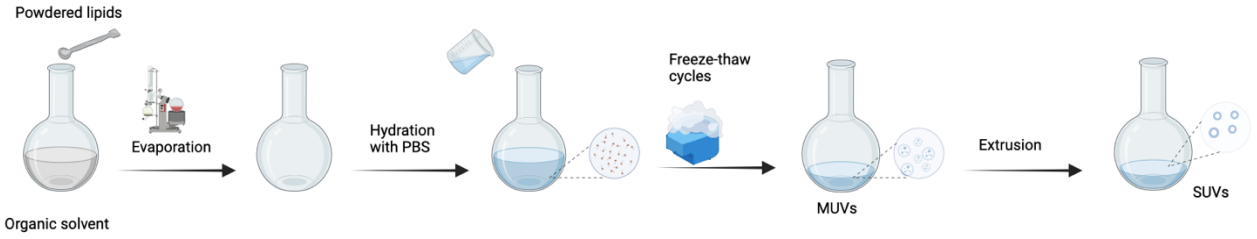

Figure 26. Graphical representation of empty liposomes preparation according to the Thin Layer Evaporation method (created with BioRender.com).

Briefly, a proper amount of lipid components was dissolved in $CHCl_3$ (DOPC and Chol) and MeOH (GLT1) in a round bottom flask, dried by rotary evaporation (BUCHI Rotavapor R-200) and then under high vacuum (5h) to remove any traces of organic solvents and to obtain a thin lipid film. Then, the film was hydrated with a phosphate buffer saline (PBS, 150 mM) solution to give a liposomal suspension 10 mM in total lipids. The aqueous suspension was vortex-mixed to completely detach the lipid film from the flasks and the obtained multilamellar vesicles (MLVs) were freeze-thawed five times, from liquid nitrogen to 50°C. Size reduction of MLVs was carried out by extrusion (10 mL Genizer LLC) of liposomal dispersions, ten times under high pressure through a polycarbonate membrane with pore size of 100 nm (Whatman Nucleopore) at temperature higher than T_m to obtain small unilamellar vesicles (SUVs).

5.4.4.1. Preparation of loaded liposomes

HOTyr, VERB, OLEUR and OLEs were loaded in neutral and galactosylated liposomes according to the procedure reported in paragraph **5.4.5** and represented in **Figure 27**.

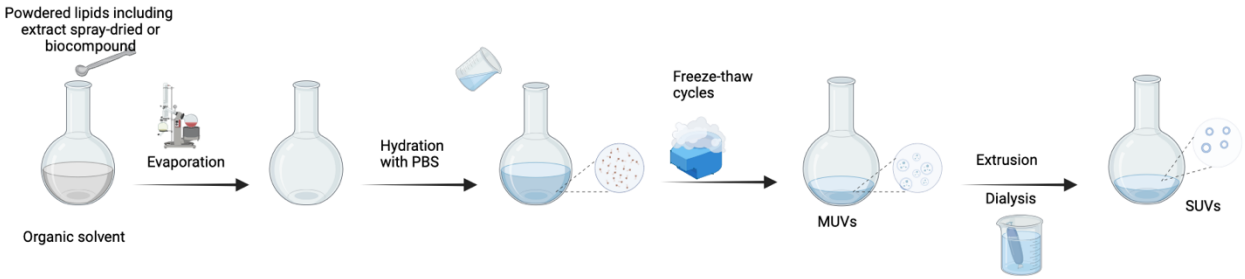

Figure 27. Preparation of neutral and galactosylated loaded liposomes following the Thin Layer Evaporation procedure (created with BioRender.com).

In this case though HOTyr, VERB, OLEUR and OLEs were dissolved in methanol and added to the lipid mixture before the film formation.

HOTyr, VERB and OLEUR were added to the lipid mixture to have a 1:8 polyphenol/lipids molar ratio (**Table 15**), while OLEs were added with a weight ratio (total lipids)/ (dry extract) equal to 1/1 (w/w) (**Table 16**).

Finally, liposomes purification from unentrapped polyphenols was performed by dialysis against PBS using a buffer volume equal to 25-times the total volume of the sample, under slow magnetic stirring.

Table 15. Composition of HOTyr, VERB and OLEUR loaded liposomes investigated.

Formulation	Compound [1.25 mM]	Composition*	Lipids (mM)
1a	HOTyr		
1b	VERB	DOPC/Chol	8.0:2.0
1c	OLEUR		
2a	HOTyr		
2b	VERB	DOPC/Chol/GLT1	7.0:2.0:1.0
2c	OLEUR		

*[total lipids]/[phenol] ratio at the beginning of the preparation is 8:1

Table 16. Composition of OLEs loaded liposomes investigated.

Formulation	Extract	Composition*	Lipids (mM)
1d	OLE100		
1e	OLE50	DOPC/Chol	8.0:2.0
1f	OLE20		
2d	OLE100		
2e	OLE50	DOPC/Chol/GLT1	7.0:2.0:1.0
2f	OLE20		

*[total lipids]/[OLE] ratio at the beginning of the preparation is 1:1 (w/w)

5.4.5. Physicochemical characterization of liposomes

5.4.5.1. Size and ζ-potential measurements

Size distributions, polydispersity index (PDI) and ζ-potential were determined by Dynamic and Dielectrophoretic Light Scattering (DLS, DELS) measurements using a Malvern Zetasizer Nano ZS equipped with a 5 mV He/Ne laser (λ=632.8 nm) and a thermostated cell holder.

Temperature was set at 25°C for all the measurements.

Particle size and PDI were measured through the backscatter detection at an angle of 173°. The measured autocorrelation function was analyzed by using the cumulant fit. The first cumulant was used to obtain the apparent diffusion coefficients D of the particles, further converted into apparent hydrodynamic diameters, D_h, by using Stokes-Einstein equation:

$$D_h = \frac{K_b T}{3\pi\eta D} \qquad \textbf{(Eq. 3)}$$

where $k_B T$ is the thermal energy and η is the solvent viscosity.

The ζ-potential of liposome formulations was determined by DELS measurements. Low voltages have been applying to avoid the risk of Joule heating effects. Analysis of the Doppler shift to determine the electrophoretic mobility was done by using phase analysis light scattering (PALS)[39] a method which is especially useful at high ionic strengths, where mobilities are usually low. The mobility μ of the liposomes was converted into ζ-potential using the Smoluchowski relation ζ =μ η/ε, where ε and η are the permittivity and the viscosity of the solution, respectively.

All liposomal suspensions were diluted to 1 mM in total lipids with PBS (150 mM) and diluted PBS (15 mM) to assess DLS and DELS measurements respectively.

5.4.5.2. Assessment of stability

Stability of OLEUR and OLEs loaded neutral and galatcosylated liposomes was evaluated during 90 days of storage at 4°C protected from light sources, determining vesicles size and PDI, as previously described, to highlight any aggregation phenomena related to the physical instability of liposomes. The stability of OLEUR and OLEs loaded liposomes was also investigated at different pH, modified by adding to the sample appropriate volumes of HCl and NaOH aqueous solutions. The pH was set at the same values of pH present in the digestive systems, such as mouth (pH 5-7), stomach (pH 1-5), small intestine (pH 6-7.5) and colon (pH 5-8). The average particle diameter and PDI were evaluated after incubation of liposomes at pH 5.7 for 1-3 min (mimicking mouth), at pH 2.9 for 30 min-3 h (mimicking stomach), at pH 6.4 for 3 h (mimicking intestine) and at pH 8.1 for 24 h (mimicking colon). Results were compared with those obtained at pH 7.4 in PBS.[40]

5.4.5.3. Entrapment Efficiency (EE%) determination of Hydroxytyrosol, Verbascoside and Oleuropein in liposomes

The content of HOTyr, VERB and OLEUR loaded in neutral and galactosylated liposomes was evaluated by UPLC-PDA analysis, according to the procedure described below.

Before UPLC measurements, liposomes were properly diluted with methanol to obtain their disruption and the complete solubilization of loaded compounds. All samples were then filtered on PTFE membranes (4 mm x 0.2 µm; Sartorius) before injection.

An Acquity UPLC HSS T3 column (1.8 µm, 150 × 2.1 mm id; Waters, Milford) was employed using as mobile phases water (0.1% (v/v) formic acid, phase A) and acetonitrile (0.1% (v/v) formic acid, phase B) eluted according to the following gradient: 0-3 min from 85% phase A and 15% phase B to 82% phase A and 18% phase B; 3-6.5 min from 82% phase A and 18% phase B to 77% phase A and 23& phase B; 6.5-10 min from 77% phase A and 23% phase B to 40% phase A and 60% phase B; 10-11 min from 40% phase A and 60% phase B to 100% phase B until the minutes 22. The optimum flow rate was 0.4 mL/min while the injection volume was 2 µL. The detection wavelength was set at 320 nm for VERB and 280 nm for HOTyr and OLEUR.

According to the calibration curve reported in **Figures 23-25**, the entrapment efficiency (EE%) of the phenol loaded in liposomes was calculated using the following equation:

$$EE\ (\%) = \frac{[Compound]_{pd}}{[Compound]_0} \times 100 \qquad \textbf{(Eq. 4)}$$

where $[Compound]_{pd}$ indicates HOTyr, VERB or OLEUR concentration after the purification by dialysis and $[Compound]_0$ corresponds to their concentration soon after extrusion.

5.4.5.4. Entrapment Efficiency (EE%) determination of OLEs in liposomes

The amount of OLEs polyphenols encapsulated in liposomes was determined by Folin-Ciocalteu assay, evaluating the amount of polyphenolic compounds entrapped within the lipid vesicles compared to the amount measured in the extracts in free form. Following the procedure reported above (paragraph **5.4.3.1.**), a calibration curve using Gallic Acid as reference standard was set up. The assay was carried out on dry free extracts, after dissolution in the respective extracting solvent, at the same concentration used in liposomes preparation, thus corresponding to an entrapment efficiency of 100%. In particular, 10 µL of OLE were mixed with 50 µL of Folin-Ciocalteau reagent and 150 µL of 2% (w/v) Na_2CO_3, then the final volume was made up to 1 mL with water. After 2 h of incubation in the dark at 25°C, the absorbance was measured at 760 nm by a spectrophotometer. The total phenolic content was expressed as micrograms equivalents of Gallic Acid (μg_{GAE}) in the free dry extract. Furthermore, the assay was carried out on the liposomal formulations properly diluted with methanol (1:1 v/v) to break the lipid aggregated and to the enhance the release of phenolic compounds loaded. In this case, 20 µL of liposomal formulation were mixed with 50 µL of Folin-Ciocalteau reagent, 150 µL of 2% (w/v) Na_2CO_3 and the final volume was made up to 1 mL with water. After 2 h of incubation in the dark at 25°C, the absorbance was measured at 760 nm by a spectrophotometer. The total phenolic content was expressed as micrograms of Gallic Acid equivalents (μg_{GAE}) in the loaded liposomal formulation analyzed. Finally, the assay was also assessed on empty liposomes diluted with methanol (1:1 v/v) to highlight the contribution to the assay due to the lipidic components of liposomes: 20 µL of liposomal formulation were mixed with 50 µL of Folin-Ciocalteau reagent, 150 µL of 2% (w/v) Na_2CO_3 and the final volume was made up to 1 mL with water. After 2 h of incubation in the dark at 25°C, the absorbance was measured at 760 nm by a spectrophotometer. The total phenolic content was expressed as micrograms of gallic acid equivalents (μg_{GAE}) in the empty liposomal formulation analyzed. The entrapment efficiency was calculated as follows:

$$EE(\%) = \frac{(\mu g_{GAE})_{loaded\ liposome} - (\mu g_{GAE})_{empty\ liposome}}{(\mu g_{GAE})_{dry\ extract\ unentrapped}} \times 100 \qquad \textbf{(Eq. 5)}$$

Where $(\mu g_{GAE})_{\text{loaded liposome}}$ corresponds to micrograms of Gallic Acid equivalents of the dry extract entrapped in liposome, $(\mu g_{GAE})_{\text{empty liposome}}$ corresponds to micrograms of Gallic Acid equivalents of the empty formulation, and $(\mu g_{GAE})_{\text{dry extract unentrapped}}$ corresponds to micrograms of Gallic Acid equivalents present in the dry extract unentrapped.

5.4.5.5. Entrapment Efficiency (EE%) of Hydroxytyrosol isomers, Verbascoside and Oleuropein encapsulated in OLEs loaded liposomes

The amount of the main polyphenols identified in OLEs, such as HOTyr *isomer a* and *isomer b*, VERB and OLEUR, was determined after OLEs encapsulation in both neutral and galactosylated liposomes, according to the UPLC-PDA analysis procedure described above (paragraph **5.4.4.3.2.**).

According to the calibration curve reported in **Figures 23-25**, the entrapment efficiency (EE%) of the phenol entrapped in liposomes was calculated using the following equation:

$$EE\ (\%) = \frac{[Compound]_{pd}}{[Compound]_0} \times 100 \qquad \textbf{(Eq. 6)}$$

where $[Compound]_{pd}$ indicates the concentration of HOTyr *isomer a* and *isomer b*, VERB or OLEUR entrapped from OLEs in liposome determined after the dialysis purification, and $[Compound]_0$ corresponds to the concentration determined soon after the extrusion process.

5.4.5.6. *In vitro* release study of Oleuropein from liposomes

The release of OLEUR from DOPC/Chol and DOPC/Chol/GLT1 liposomes was evaluated by dialysis against PBS (phosphate buffer volume 50-times the total volume of the sample) keeping the systems under stirring. After liposomes purification by dialysis, corresponding to the initial time (t_0), samples were collected every 1 hour over a period of 24 hours and analyzed by UPLC to study the releasing profile of OLEUR from liposomes. All the collected liposomal aliquots were analyzed by UPLC after dilution with MeOH (1:1 v/v) and filtration by PTFE membranes (4 mm x 0.2 µm; Sartorius), to break lipid aggregates and to enhance the release of OLEUR.

The percentage of released OLEUR over time was determined by chromatographic analyses carried out as described above.

5.4.5.7. *In vitro* release study of OLEs from liposomes

The release of phenolic compounds from OLEs loaded neutral and galatcosylated liposomes was determined by dialysis method in PBS, buffer volume 50-times the total volume of liposome samples. Samples were collected every 1 hour over a period of 24 hours and analyzed by Folin-Ciocalteu assay to study the releasing profile of the total phenolic content encapsulated. All the collected liposomal aliquots were analyzed after dilution with MeOH (1:1 v/v) to break the lipid aggregates and to enhance the release of phenolic compounds entrapped. Then, the assay was assessed as described above. The phenolic content still encapsulated in liposomes was determined at a specific time and expressed as micrograms of Gallic Acid equivalents per milliliter (μg_{GAE}/mL) by using Gallic Acid as reference standard, calibration curve 10-2000 μg/mL.

Moreover, the release of the main phenols found in OLE100, OLE50 and OLE20 (HOTyr *isomer a* and *isomer b*, VERB and OLEUR) and entrapped in DOPC/Chol and DOPC/Chol/GLT1 liposomes was investigated by UPLC analysis, assessed as described above, to determine the amount still encapsulated in liposomes at a specific time. Results collected were expressed as milligrams of compound per milliliter (mg/mL).

5.4.6. Antimicrobial activity

Determination of *Minimum Inhibitory Concentration* (MIC) and *Minimum Bactericidal Concentration* (MBC)

The *in vitro* antimicrobial activity of HOTyr, VERB, OLEUR and OLEs, free and loaded in liposomes, was determined through the microdilution method[41] against two strains of *Staphylococcus aureus*: ATCC 25923 (wild type strain) and ATCC 33591 (Methicillin-resistant strain, MRSA).

In microdilution tests, microorganisms are tested for their ability to produce visible growth in a broth containing different concentration of an antimicrobial agent. Therefore, the lowest concentration of an antimicrobial agent that under defined *in vitro* conditions prevents the appearance of visible growth of microorganism within a defined period is defined as MIC. Instead, MBC is defined as the lowest concentration of an antimicrobial agent required to kill a bacterium over a fixed period such as 24 h.

Both bacteria strains were retrieved from frozen stocks and streaked on a fresh Mueller-Hinton (MH) agar plate, then incubated at 37 °C overnight. Afterwards, few CFU of fresh *S. aureus* wild type or MRSA were grown in 10 mL of MH broth medium overnight at 37°C. Then, the inoculum prepared above was diluted in MH broth to give a final organism density of 3-7 x 10^5 CFU/mL, corresponding

to an absorbance of 0.0001 at 600 nm. Both diluted cultures were aliquoted in a 96 wells/plate flat bottom and the antimicrobial agent was added, in triplicates, at different concentrations. Then, 96 wells/plates were incubated overnight at 37°C. At the end of the incubation period, plates were checked and all the transparent wells, likely corresponding to the MIC values, were plated on fresh MH agar plate kept at 37°C overnight. Finally, MH agar plates were observed and those showing bacterial growth were annotated as MIC, instead those plates showing nonbacterial growth were annotated as MBC.

5.5. References

[1] M.M. Özcan, B. Matthäus, A review: benefit and bioactive properties of olive (*Olea europaea* L.) leaves, *Eur Food Res Technol*, **2017**, *243*, 89.
https://doi.org/10.1007/s00217-016-2726-9

[2] F.S. Markhali, J.A. Teixeira, C.M.R. Rocha, Olive Tree Leaves—A Source of Valuable Active Compounds, *Processes*, **2020**, *8* (9), 1177.
https://doi.org/10.3390/pr8091177

[3] L.L.D.R. Osorio, E. Flórez-López, C.D. Grande-Tovar, The Potential of Selected Agri-Food Loss and Waste to Contribute to a Circular Economy: Applications in the Food, Cosmetic and Pharmaceutical Industries, *Molecules*, **2021**, *26* (2), 515.
https://doi.org/10.3390/molecules26020515

[4] H. Wagner, G. Ulrich-Merzenich, Synergy research: approaching a new generation of phytopharmaceuticals, *Phytomedicine*, **2009**, *16* (2-3), 97.
https://doi.org/10.1016/j.phymed.2008.12.018

[5] H.A. Junio, A.A. Sy-Cordero, K.A. Ettefagh, J.T. Burns, K.T. Micko, T.N. Graf, S.J. Richter, R.E. Cannon, N.H. Oberlies, N.B. Cech, Synergy-directed fractionation of botanical medicines: a case study with goldenseal (Hydrastis canadensis), *J Nat Prod*, **2011**, *74* (7), 1621.
https://doi.org/10.1021/np200336g

[6] G. Ulrich-Merzenich, D. Panek, H. Zeitler, H. Vetter, H. Wagner, Drug development from natural products: exploiting synergistic effects, *Indian J Exp Biol*, **2010**, *48* (3), 208.

[7] O. Benavente-García, J. Castillo, J. Lorente, A. Ortuño, J.A. Del Rio, Antioxidant activity of phenolics extracted from Olea europaea L. leaves, *Food Chem,* **2000,** 68 (4), 457.
https://doi.org/10.1016/S0308-8146(99)00221-6.

[8] L. Karygianni, M. Cecere, A. Argyropoulou, E. Hellwig, A.L. Skaltsounis, A. Wittmer, J.P. Tchorz, A. Al-Ahmad, Compounds from Olea europaea and Pistacia lentiscus inhibit oral microbial growth, *BMC Complement Altern Med*, **2019**, *19* (1), 51.
https://doi.org/10.1186/s12906-019-2461-4.

[9] M.M. Rahman, M.S. Rahaman, M.R. Islam, F. Rahman, F.M. Mithi, T. Alqahtani, M.A. Almikhlafi, S.Q. Alghamdi, A.S. Alruwaili, M.S. Hossain, M. Ahmed, R. Das, T.B. Emran, M.S. Uddin, Role of Phenolic Compounds in Human Disease: Current Knowledge and Future Prospects, *Molecules*, **2021**, *27* (1), 233.
https://doi.org/10.3390/molecules27010233.

[10] D. Markin, L. Duek, I. Berdicevsky, In vitro antimicrobial activity of olive leaves, *Mycoses*, **2003**, *46* (3-4), 132.
https://doi.org/10.1046/j.1439-0507.2003.00859.x.
[11] A.N. Sudjana, C. D'Orazio, V. Ryan, N. Rasool, J. Ng, N. Islam, T.V. Riley, K.A Hammer, Antimicrobial activity of commercial Olea europaea (olive) leaf extract, *Int J Antimicrob Agents*, **2009**, *33* (5), 461.
https://doi.org/10.1016/j.ijantimicag.2008.10.026.
[12] O. Lee, B.Y. Lee, Antioxidant and antimicrobial activities of individual and combined phenolics in Olea europaea leaf extract, *Bioresource technology*, **2010**, *101*, 3751.
https://doi.org/10.1016/j.biortech.2009.12.052.
[13] N.R. El-sayed, R. Samir, M. Jamil, L. Abdel-Hafez, M.A. Ramadan, Olive Leaf Extract Modulates Quorum Sensing Genes and Biofilm Formation in Multi-Drug Resistant *Pseudomonas aeruginosa*, *Antibiotics*, **2020**, *9* (9), 526.
https://doi.org/10.3390/antibiotics9090526
[14] V. Šimat, D. Skroza, G. Tabanelli, M. Čagalj, F. Pasini, A.M. Gómez-Caravaca, C. Fernández-Fernández, M. Sterniša, S. Smole Možina, Y. Ozogul, I. Generalić Mekinić, Antioxidant and Antimicrobial Activity of Hydroethanolic Leaf Extracts from Six Mediterranean Olive Cultivars, *Antioxidants*, **2022**, *11* (9), 1656.
https://doi.org/10.3390/antiox11091656.
[15] I. Ben-Amor, M. Musarra-Pizzo, A. Smeriglio, M. D'Arrigo, R. Pennisi, H. Attia, B. Gargouri, D. Trombetta, G. Mandalari, M.T. Sciortino, Phytochemical Characterization of *Olea europea* Leaf Extracts and Assessment of Their Anti-Microbial and Anti-HSV-1 Activity, *Viruses*, **2021**, *13* (6), 1085.
https://doi.org/10.3390/v13061085.
[16] L. Zheng, J. Hong, X. Changmou, G. Liwei, A review: Using nanoparticles to enhance absorption and bioavailability of phenolic phytochemicals, *Food Hydrocolloids*, **2015**, *43*, 153.
https://doi.org/10.1016/j.foodhyd.2014.05.010.
[17] I.G. Munteanu, C. Apetrei, Analytical Methods Used in Determining Antioxidant Activity: A Review, *Int J Mol Sci*, **2021**, *22* (7), 3380.
https://doi.org/10.3390/ijms22073380.
[18] M. Herrero, T.N. Temirzoda, A. Segura-Carretero, R. Quirantes, M. Plaza, E. Ibañez, New possibilities for the valorization of olive oil by-products,*J Chromatogr A*, **2011**, *1218* (42), 7511.
https://doi.org/10.1016/j.chroma.2011.04.053.

[19] D. Cifá, M. Skrt, P. Pittia, C. Di Mattia, N. Poklar Ulrih, Enhanced yield of oleuropein from olive leaves using ultrasound-assisted extraction, *Food Sci Nutr*, **2018**, *6* (4), 1128. https://doi.org/10.1002/fsn3.654.

[20] D. Huang, B. Ou, R.L. Prior, The chemistry behind antioxidant capacity assays, *J Agric Food Chem*, **2005**, *53* (6), 1841. https://doi.org/10.1021/jf030723c.

[21] R. Re, N. Pellegrini, A. Proteggente, A. Pannala, M. Yang, C. Rice-Evans, Antioxidant activity applying an improved ABTS radical cation decolorization assay, *Free Radic Biol Med*, **1999**, *26* (9-10), 1231. https://doi.org/10.1016/s0891-5849(98)00315-3.

[22] N. Talhaoui, A. M. Gómez-Caravaca, L. León, R. De la Rosa, A. Segura-Carretero, A. Fernández-Gutiérrez, Determination of phenolic compounds of 'Sikitita' olive leaves by HPLC-DAD-TOF-MS Comparison with its parents 'Arbequina' and 'Picual' olive leaves, *LWT - Food Science and Technology*, **2014**, *58* (1), 28. https://doi.org/10.1016/j.lwt.2014.03.014.

[23] R. Pennisi, I. Ben Amor, B. Gargouri, H. Attia, R. Zaabi, A.B. Chira, M. Saoudi, A. Piperno, P. Trischitta, M.P. Tamburello, Analysis of Antioxidant and Antiviral Effects of Olive (*Olea europaea* L.) Leaf Extracts and Pure Compound Using Cancer Cell Model, *Biomolecules,* **2023**, *13*, 238. https://doi.org/10.3390/biom13020238.

[24] Bozzuto G, Molinari A., Liposomes as nanomedical devices, *Int J Nanomedicine*, **2015**, *10* (1), 975. https://doi.org/10.2147/IJN.S68861

[25] A. Mauceri, S. Borocci, L. Galantini, L. Giansanti, G. Mancini, A. Martino, L. Salvati Manni, C. Sperduto, Recognition of Concanavalin A by Cationic Glucosylated Liposomes, *Langmuir,* **2014,** *30* (38), 11301. https://doi.org/10.1021/la502946t.

[26] N. Sharon, H. Lis, Lectins as cell recognition molecules, *Science*, **1989**, *246* (4927), 227. https://doi.org/10.1126/science.2552581.

[27] C.V. Iancu, J. Zamoon, S.B. Woo, A. Aleshin, J.Y. Choe , Crystal structure of a glucose/H+ symporter and its mechanism of action, *Proc Natl Acad Sci U S A*, **2013**, *110* (44) 17862. https://doi.org/10.1073/pnas.1311485110.

[28] C. Bonechi, A. Donati, G. Tamasi, A. Pardini, H. Rostom, G. Leone, S. Lamponi, M. Consumi, A. Magnani, C. Rossi, Chemical characterization of liposomes containing nutraceutical compounds: Tyrosol, hydroxytyrosol and oleuropein, *Biophysical Chemistry*, **2019**, *246*, 25. https://doi.org/10.1016/j.bpc.2019.01.002.

[29] R. González-Ortega, L. Šturm, M. Skrt *et al,* Liposomal Encapsulation of Oleuropein and an Olive Leaf Extract: Molecular Interactions, Antioxidant Effects and Applications in Model Food Systems. *Food Biophysics*, **2021**, *16*, 84.
https://doi.org/10.1007/s11483-020-09650-y.

[30] S. Bhattacharjee, DLS ans zeta potential- What they are and what they are not?, *J Contr Rel*, **2016**, *235*, 337.
https://doi.org/10.1016/j.jconrel.2016.06.017.

[31] L. Movileanu, I. Neagoe, M.L. Flonta, Interaction of the antioxidant flavonoid quercetin with planar lipid bilayers, *Int J Pharm*, **2000**, *205* (1-2), 135.
https://doi.org/10.1016/s0378-5173(00)00503-2.

[32] M. Bertelli, A. K. Kiani, S. Paolacci, E. Manara, D. Kurti, K. Dhuli, V. Bushati, J. Miertus, D. Pangallo, M. Baglivo, T. Beccari, S. Michelini, Hydroxytyrosol: A natural compound with promising pharmacological activities*, J Biotech*, **2020**, *309*, 29.
https://doi.org/10.1016/j.jbiotec.2019.12.016.

[33] E. Medina, A. de Castro, C. Romero, M. Brenes, Comparison of the concentrations of phenolic compounds in olive oils and other plant oils: correlation with antimicrobial activity, *J Agric Food Chem*, **2006**, *54* (14), 4954.
https://doi.org/10.1021/jf0602267.

[34] K. Alipieva, L. Korkina, I.E. Orhan, M.I. Georgiev, Verbascoside-a review of its occurrence, (bio)synthesis and pharmacological significance, *Biotechnol Adv*, **2014**, *32* (6), 1065.
https://doi.org/10.1016/j.biotechadv.2014.07.001.

[35] S. Burgalassi, E. Zucchetti, E. Birindelli, S. Tampucci, P. Chetoni, D. Monti, Ocular Application of Oleuropein in Dry Eye Treatment: Formulation Studies and Biological Evaluation, *Pharmaceuticals*, **2021**, *14* (11), 1151.
https://doi.org/10.3390/ph14111151.

[36] S.H. Omar, Oleuropein in olive and its pharmacological effects, *Sci Pharm*, **2010**, *78* (2), 133.
https://doi.org/10.3797/scipharm.0912-18.

[37] V.L. Singleton, R. Orthofer, R.M. Lamuela-Raventos, Analysis of Total Phenols and Other Oxidation Substrates and Antioxidants by Means of Folin-Ciocalteu Reagent, *Methods in Enzymology,* **1999**, *299*, 152.
http://dx.doi.org/10.1016/S0076-6879(99)99017-1.
[38] M.R.I. MacDonald, Liposome Technology 2nd Ed, 2nd ed., CRC Press, Bosca Raton Florida, **1992**.
[39] R.J. Hunter, Zeta Potential in Colloid Science Principles and Applications, R.H. Ottewill, R.L. Rowell, 1st edition, Elsevier, **1988**.
[40] M. Huang, J. Wang, C. Tan, Liposomal co-delivery strategy to improve stability and antioxidant activity of trans-resveratrol and narigenin, *Int J Food Sci Tech*, **2022**, *57* (5), 2701.
https://doi.org/10.1111/ijfs.15486.
[41] Determination of minimum inhibitory concentrations (MICs) of antibacterial agents by broth dilution, Clinical Microbiology and Infection, **2003**, *9* (8), 9.
https://doi.org/10.1046/j.1469-0691.2003.00790.x.

6. Hydroxytyrosol oleate, how structure affects the antimicrobial activity

6.1. Introduction

The investigation here reported was triggered by the results collected in **Chapter 5** on the antimicrobial activity showed by Hydroxytyrosol (HOTyr, **Figure 1**).

HOTyr is one of the major polyphenolic compounds identified in extra-virgin olive oil, but it was also found to be particularly abundant in the by-products generated by the olive oil supply chain, such as olive leaves and olive mill wastewater. HOTyr can be recovered from these waste products using environmentally and economically sustainable technologies[1] and reused to take on new life in different application fields, according to a circular economy approach.

In olive products and by-products, HOTyr is present mainly as secoiridoid derivatives together with minor amounts of its free form, which is produced as a result of endogenous β-glucosidase hydrolytic activity releasing it from secoiridoids such as oleuropein and its aglycone form.[2]

HOTyr displays a wide range of biological activities including antioxidant, cardio-protective, hypotensive, hypoglycemic, anticancer, anti-inflammatory and antimicrobial effects.[3] Based on these attractive functions, an increasing number of research groups have focused their efforts both on synthesizing HOTyr and on recovering it from agri-food waste and by-products.[4] However, HOTyr pharmacokinetic properties are unfavorable, because it shows low oral bioavailability and fast elimination in humans, mainly due to its hydrophilic character, thus preventing its potential therapeutic use.[5,6]

Therefore, the esterification of polyphenols, by acylation of one of their hydroxyl functions with a fatty acid (saturated, mono, or polyunsaturated), through the production of the so called "phenolipids" or "lipophenols", is a convenient method to improve their pharmacokinetics properties. In this perspective, phenolipid derivatives of HOTyr with different acyl chain lengths (short (C2), medium (C12) and long (C16 and C18)) have been synthesized to increase HOTyr lipophilicity,[7-9] and consequently to modify its solubility without affecting its biological properties, hence opening up new opportunities for potential application in pharmaceutical and food industries.

Among all HOTyr derived phenolipids studied in the literature, Hydroxytyrosol oleate (HOTyrOL, **Figure 1**) is one of the most interesting. It is a synthetic fatty ester obtained by acylation of HOTyr ethanolic hydroxyl group with oleic acid (C18:1), thus preserving unaltered the catechol moiety of

HOTyr which is mainly responsible for its biological activities,[10] endowed with a significant lipophilicity (log K_{OW} (HOTyrOL) > 3.3 vs log K_{OW} (HOTyr) = 0.809).[11]

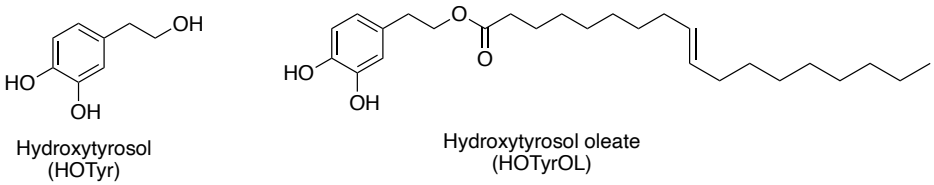

Figure 1. Molecular structure of Hydroxytyrosol and Hydroxytyrosol oleate.

HOTyrOL can be considered as a surfactant due to its amphiphilic structure characterized by the hydrophilic head derived from HOTyr and the hydrophobic tail provided by the oleic acid.

Therefore, dispersed HOTyrOL molecules in aqueous solution may aggregate and form micelles when the concentration of surfactant molecules is higher than their *critical micelle concentration* (*cmc*), which is defined as the concentration of surfactants in free form in equilibrium in solution with surfactants in aggregated form. Micelles take form by orienting the hydrophobic portions of surfactants toward the core of the micelle and hydrophilic head groups toward the external aqueous phase (**Figure 2**, a). Moreover, the amphiphilic nature and the molecular features of HOTyrOL make it an excellent candidate as component of lipid bilayers in liposomes production (**Figure 2**, b).

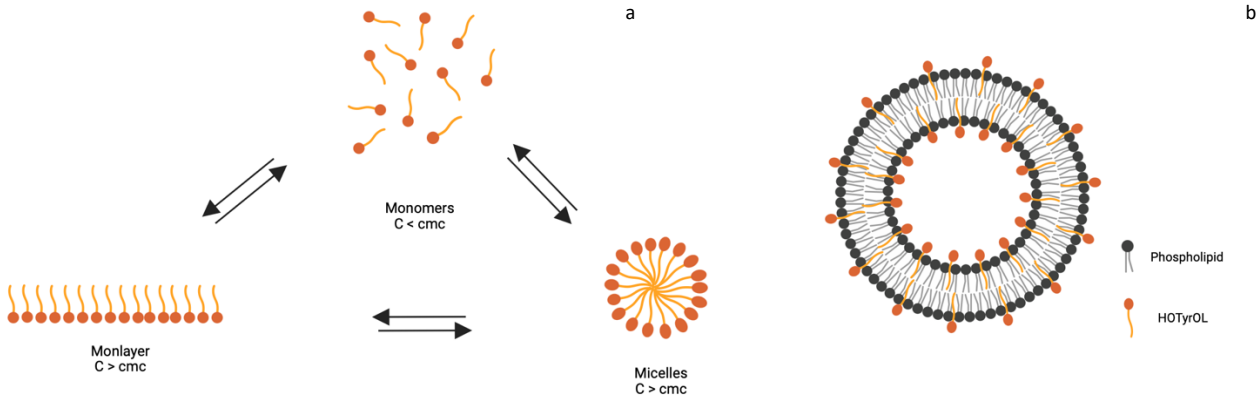

Figure 2. Surfactants in aqueous solution can exist in different aggregate forms depending on their concentration (a) and can be used for liposomes development (b) (created with BioRender.com).

Although HOTyrOL appears to have antioxidant, antitumor, and antiproliferative properties with higher or comparable effect to HOTyr,[11] HOTyrOL antimicrobial activity was found to be lower than HOTyr against *S. aureus* according to a previous study reported in the literature.[12]

Thereby, in this chapter the antimicrobial activity of HOTyrOL free and in liposomes was investigated against two strains of *Staphylococcus aureus*: ATCC 25923 (wild type strain) and ATCC 33591 (methicillin-resistant strain, MRSA).

The amphiphilic nature of HOTyrOL was highlighted determining its *cmc* by Dynamic Light Scattering and simulating the formation of HOTyrOL micelle by Molecular Dynamics Simulations.

HOTyrOL based liposomes formulated with natural phospholipids (DOPC, DPPC, DMPC), in presence and in the absence of cholesterol or a synthetic cationic amphiphile, were characterized in terms of dimensions, polydispersity index, ζ-potential and stability over time.

6.2. Results and Discussion

6.2.1. HOTyrOL *cmc* determination

Dynamic Light Scattering (DLS) is a technique well suited to determine the *cmc* of surfactants, representing a valid alternative to methodology based on conductivity, surface tension and fluorescence measurements.[13-15]

The determination of HOTyrOL *cmc* by DLS measurements was performed in water measuring the intensity of scattered light (expressed in kilo counts per second, k_{cps}) by HOTyrOL solutions with concentration ranging from $2x10^{-3}$ µM to 5 µM (**Figure 3**).

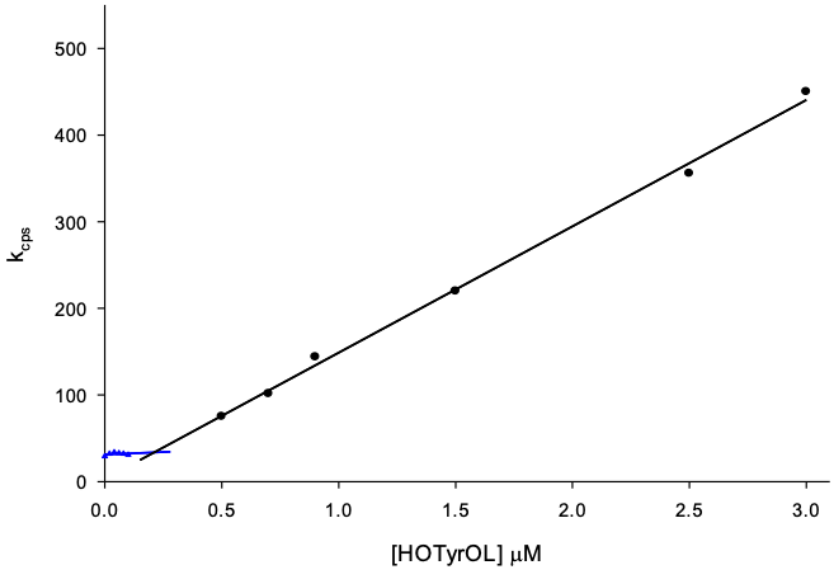

Figure 3. Plot of intensity of scattered light (k_{cps}) as a function of HOTyrOL concentration (µM).

As shown in **Figure 3**, the intensity of scattered light detected for HOTyrOL concentrations below the *cmc* is approximately constant and corresponds to that of deionized water. Once HOTyrOL concentration reaches the *cmc*, micelles start to be formed in solution and the light is scattered. At this point the intensity of scattered light linearly increases with increasing HOTyrOL concentration. HOTyrOL *cmc* is obtained by the intersection of the two linear fits and corresponds to $(2.2 \pm 0.2) \times 10^{-7}$ M.

6.2.2. Molecular Dynamics Simulations

Molecular Dynamics (MD) simulations were used to investigate the formation of HOTyrOL micelles starting from a random orientation of the monomers.

In the first 4 ns of MD simulation, HOTyrOL molecules form a worm-like structure with the alkyl chains oriented toward the inner region of the aggregate and the hydroxytyrosol head group exposed on the surface of the aggregate. The worm-like aggregate is stable for the remaining 96 ns of MD simulation (**Figure 4**), suggesting that for concentration above its *cmc* HOTyrOL tend to form micellar aggregates with a cylindrical shape rather than spherical micelles.

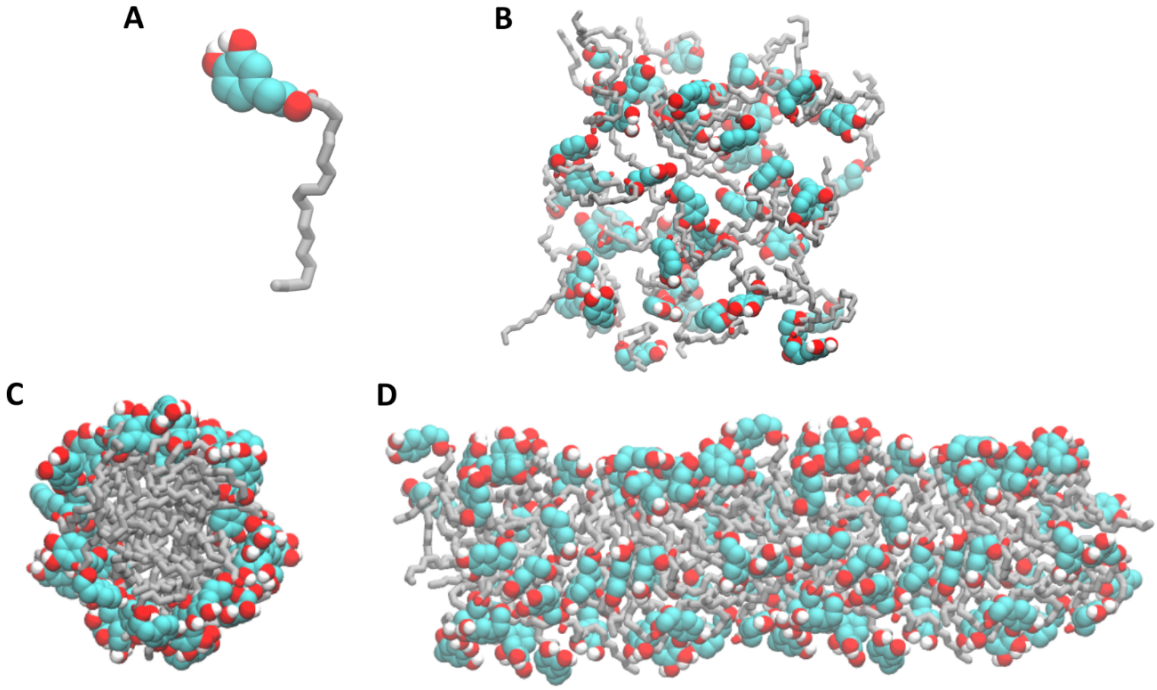

Figure 4. **A)** Structure of HOTyrOL. The hydroxytyrosol head group of surfactant molecule is represented in van der Walls and the acyl chain is represented in licorice. The carbon atoms of head group are colored in turquoise whereas the carbon atoms of acyl chain are colored in gray and the oxygen atoms are colored in red. For clarity, only the hydrogen bound to oxygen atoms are represented. **B)** Initial configuration of the simulated system. The water molecules are not represented for clarity. **C-D)** Snapshot of aggregate of HOTyrOL at the end of 100 ns of molecular dynamics simulation.

6.2.3. Liposomes preparation and characterization

The development of HOTyrOL based liposomes has involved the preparation of several liposomal formulations employing different lipids, both natural and synthetic (**Chart 1**).

Liposomes 10 mM in total lipids (**Table 1**) were prepared in 150 mM phosphate buffer saline solution (PBS) according to the thin lipid film hydration method combined with a freeze-thaw protocol to reduce their lamellarity, and followed by an extrusion process, thus obtaining unilamellar vesicles of suitable dimensions (~100 nm).

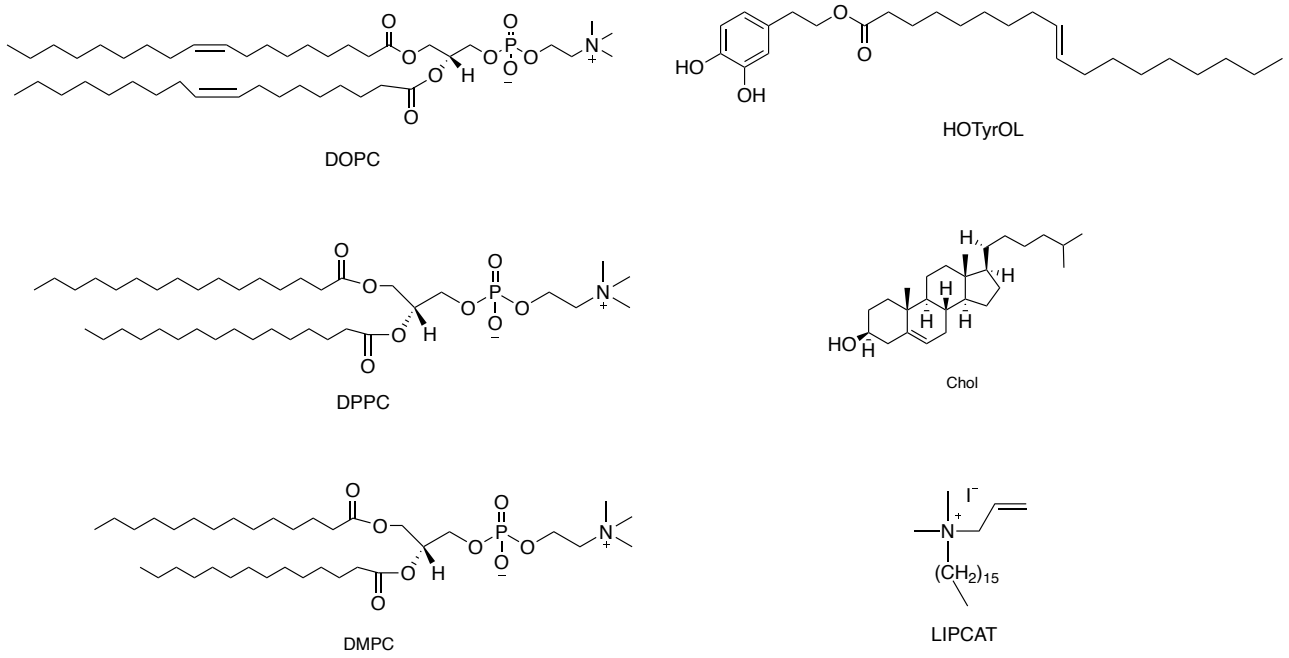

Chart 1. Lipid components of HOTyrOL based liposomes developed.

Table 1. Physicochemical features of liposomes (10 mM in total lipids) in PBS (pH 7.4).

Formulation	Composition	D_h (nm)	PDI	ζ-potential (mV)
F1	DOPC/Chol/HOTyrOL 7.0:2.0:1.0	116 ± 2	0.14 ± 0.01	-3.0 ± 0.2
F2	DOPC/HOTyrOL 8.0:2.0	95 ± 3	0.13 ± 0.01	-8 ± 3
F3	DPPC/Chol/HOTyrOL 7.0:2.0:1.0	110 ± 3	0.08 ± 0.01	-8 ± 2
F4	DPPC/HOTyrOL 8.0:2.0	104 ± 3	0.06 ± 0.01	-17 ± 1
F5	DMPC/Chol/HOTyrOL 7.0:2.0:1.0	119 ± 4	0.06 ± 0.01	-14 ± 2
F6	DMPC/HOTyrOL 8.0:2.0	96 ± 2	0.08 ± 0.02	-14 ± 2
F7	DPPC/LIPCAT/HOTyrOL 7.0:2.0:1.0	94 ± 1	0.04 ± 0.01	42 ± 2
F8	DPPC/HOTyrOL/LIPCAT 7.0:2.0:1.0	95 ± 1	0.11 ± 0.01	29 ± 2

Firstly, HOTyrOL based liposomes were formulated with natural phospholipids having different alkyl chain lengths, namely 1,2-dioleoyl-*sn*-glycero-3-phosphocholine (C18:1, DOPC), 1,2-dipalmitoyl-*sn*-glycero-3-phosphocholine (C16:0, DPPC) and 1,2-dimyristoyl-*sn*-glycero-3-phosphocholine (C14:0, DMPC), in presence or absence of cholesterol (Chol). Cholesterol was added inside lipid bilayer to obtain liposomes with a more compact and stable structure, inducing a dense packing and increased orientation order of lipid chains.[16]

Afterwards, in the perspective of promoting the interaction between liposomes and bacteria cells involved in our study, we formulated liposomes with DPPC, as natural phospholipid, and HOTyrOL in the presence of the synthetic cationic amphiphile LIPCAT (**Chart 1**) added at different molar ratios. In fact, the inclusion of LIPCAT within the lipid bilayer provides liposomes positively charged, thus enhancing the electrostatic interactions between liposomes and bacteria cells, which display an overall negative charge on their cell wall. In this regard, we decided to formulate HOTyrOL based cationic liposome employing DPPC and LIPCAT since a previous study reported in the literature showed how DPPC/LIPCAT liposomes are particularly able to interact with *S. aureus*.[17]

Liposomes particle size distribution and polydispersity index (PDI) were investigated by DLS measurements. Results reported in **Table 1**, showed a narrow size distribution for all liposomes developed with a diameter between 94 nm and 119 nm and good PDI values (0.04-0.14), in accordance with the extrusion protocol adopted.

ζ-potential values were determined by Dielectrophoretic Light Scattering (DELS) measurements, using the Phase Analysis Light Scattering (PALS). According to the results showed in **Table 1**, all liposomes of formulations **F1**-**F6** exhibit negative ζ-potential values, probably due to the exposure of the hydroxytyrosol moieties of HOTyrOL on liposomes surface and to the phosphocholine phosphate groups of DOPC/DPPC/DMPC used. In particular, ζ-potential value decreases, becoming more negative, by decreasing the length of alkyl chain of phospholipids used. This evidence may be related to the fact that liposomes formulated with lipids characterized by shorter acyl chains expose the hydroxytyrosol residue moiety of HOTyrOL more externally from the lipid bilayer.

On the other hand, cationic liposomes **F7** and **F8** exhibited high positive ζ-potential values, +42 mV and +29 mV respectively, due to the presence of LIPCAT in the lipid bilayer.

Lastly, cationic liposomes without HOTyrOL were formulated with DPPC and LIPCAT, added to the formulations at different molar ratios, to estimate the potential contribution of LIPCAT to the biological activity of liposomes under investigation.

As in the case of liposomes **F7** and **F8,** a narrow size distribution, good PDI and high positive ζ-potential values were obtained for formulations **F9** and **F10**, as reported in **Table 2**.

Table 2. Physicochemical features of cationic liposomes (10 mM in total lipids) in PBS (pH 7.4).

Formulation	Composition	D_h (nm)	PDI	ζ-potential (mV)
F9	DPPC/LIPCAT 8.0:2.0	108 ± 1	0.04 ± 0.02	37 ± 2
F10	DPPC/LIPCAT 9.0:1.0	102 ± 1	0.08 ± 0.02	26 ± 1

The final concentration of lipid components in liposomes **F1**-**F10** was quantified by ^{1}H NMR analysis, the results obtained for all liposomes **F1**-**F10** confirmed approximatively the initial formulated lipid molar ratios used for liposomes production. This analysis was particularly useful for the dosage of HOTyrOL, when loaded in liposomes, in the antimicrobial experiments reported below.

6.2.3.1. **Liposomes storage stability**

The storage stability for liposomes **F1**-**F8**, at 4°C and protected from light, was investigated for 28 days through the determination of particles diameter and PDI values by DLS measurements.

Data reported in **Table 3** displayed an excellent stability during storage conditions for liposomes **F1**-**F7**, while liposomes of formulation **F8** showed an increment in dimensions and PDI starting from the first week of storage. In particular, it was observed the presence of a second and third population, with dimensions around 1000 nm and 5000 nm respectively, evidencing an unexpected physical instability for **F8** due to aggregation phenomena (**Figure 5**).

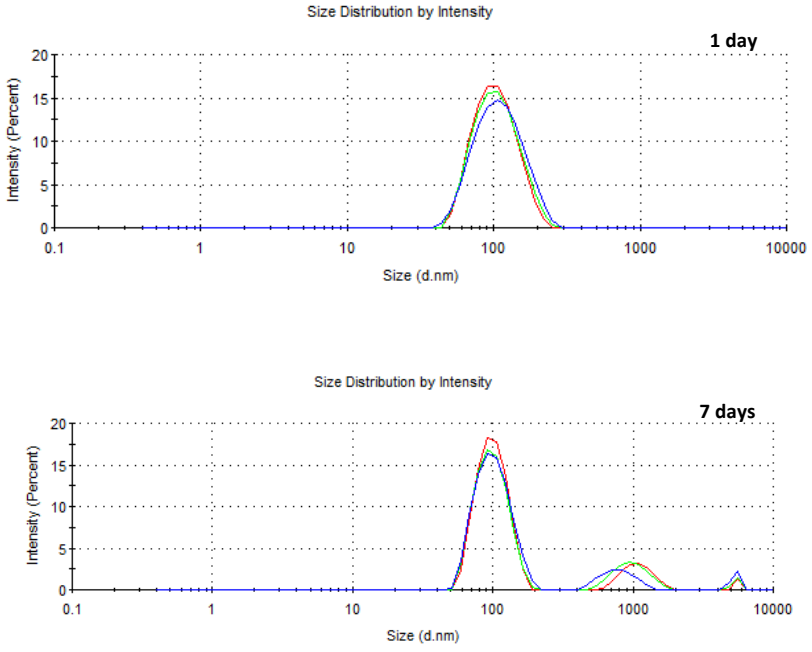

Figure 5. Variation on size distribution of formulation **F8** over time.

Table 3. Stability over time of HOTyrOL based liposomes developed.

Formulation	Time (day)	D_h (nm)	PDI	Formulation	Time (day)	D_h (nm)	PDI
	1	116 ± 2	0.14 ± 0.01		1	95 ± 3	0.13 ± 0.01
	7	121 ± 3	0.17 ± 0.01		7	97 ± 2	0.11 ± 0.02
F1	14	122 ± 1	0.18 ± 0.01	**F2**	14	98 ± 2	0.11 ± 0.01
	21	120 ± 2	0.15 ± 0.01		21	97 ± 2	0.12 ± 0.02
	28	122 ± 2	0.15 ± 0.01		28	103 ± 1	0.14 ± 0.01
	1	110 ± 3	0.08 ± 0.01		1	104 ± 3	0.06 ± 0.01
	7	106 ± 1	0.06 ± 0.02		7	101 ±2	0.07 ± 0.01
F3	14	109 ± 1	0.07 ± 0.02	**F4**	14	100 ± 2	0.06 ± 0.02
	21	110 ± 1	0.05 ± 0.02		21	101 ± 1	0.10 ± 0.02
	28	111 ± 1	0.13 ± 0.01		30	109 ± 1	0.11 ± 0.02
	1	119 ± 4	0.06 ± 0.01		1	96 ± 2	0.08 ± 0.02
	7	120 ± 2	0.06 ± 0.01		7	95 ± 2	0.08 ± 0.02
F5	14	123 ± 1	0.09 ± 0.01	**F6**	13	98 ± 1	0.07 ± 0.01
	21	121 ± 1	0.07 ± 0.02		21	99 ± 1	0.08 ± 0.01
	28	125 ± 1	0.12 ± 0.02		30	98 ± 1	0.09 ± 0.02
	1	94 ± 1	0.04 ± 0.01		1	99 ± 1	0.14 ± 0.02
	7	94 ± 1	0.05 ± 0.01		7	129 ± 1	0.43 ± 0.02
F7	14	94 ± 1	0.06 ± 0.02	**F8**	14	n.d.	n.d.
	21	96 ± 1	0.07 ± 0.01		21	n.d.	n.d.
	28	97 ± 3	0.05 ± 0.01		28	n.d.	n.d.

n.d. = not determined

6.2.4. Antimicrobial activity

The antimicrobial activity of HOTyrOL and HOTyrOL based liposomes was investigated against two strains of *Staphylococcus aureus*, ATCC 25923 (wild type strains) and ATCC 33591 (MRSA), determining the *Minimum Inhibitory Concentration* (MIC) and the *Minimum Bactericidal Concentration* (MBC) according to the microdilution method, as previously described in **Chapter 5**.

MIC and MBC values of HOTyrOL against both *S. aureus* strains are reported in **Table 4** and are expressed as micrograms of compound per milliliter (μg/mL) and as absolute concentration (μM); MIC and MBC values of HOTyr, previously determined and discussed in **Chapter 5**, are also reported.

Table 4. Antimicrobial activity of HOTyr and HOTyrOL on ATCC 25923 and ATCC 33591.

Compound	*S. aureus* wild type (ATCC 25923)				MRSA (ATCC 33591)			
	MIC (μg/mL)	**MIC (μM)**	**MBC (μg/mL)**	**MBC (μM)**	**MIC (μg/mL)**	**MIC (μM)**	**MBC (μg/mL)**	**MBC (μM)**
HOTyr	18	117	20	130	19	123	21	136
HOTyrOL	31	74	42	100	42	99	49	116

According to the results expressed as absolute concentration, HOTyrOL highlighted greater antimicrobial activity on ATCC 25923 (*S. aureus* wild type strain, MIC = 74 μM and MBC = 100 μM) compared to ATCC 33591 (MRSA, MIC = 99 μM and MBC = 116 μM). Furthermore, the antimicrobial effect exerted by HOTyrOL resulted higher than that showed by HOTyr against both bacteria strains investigated. The increased activity displayed by HOTyrOL could be due to its higher lipophilic nature with respect to HOTyr, which improves its stability to oxygen[18] and probably its passage through bacterial membranes, finally contributing to the enhancement of HOTyrOL functionality.[19]

These results encouraged us to investigate the antimicrobial activity of HOTyrOL as a component of the lipid bilayer in liposomes against *S. aureus* wild type and MRSA strains.

The dosage of HOTyrOL to perform the antimicrobial experiments was assessed by ^{1}H NMR analysis. However, it has to be noted that due to its amphiphilic nature, HOTyrOL inside a lipid bilayer is oriented (see **Figure 2, b**) both towards the aqueous core of the liposomes and towards the aqueous medium in which liposomes are dispersed (external lipid bilayer-water interface). Therefore, HOTyrOL concentrations tested is theoretically half than those initially dosed.

Table 5. Antimicrobial activity of HOTyrOL in liposomes against ATCC 25923 and ATCC 33591.

Formulation	*S. aureus* wild type (ATCC 25923)		MRSA (ATCC 33591)	
	MIC (μM)	**MBC (μM)**	**MIC (μM)**	**MBC (μM)**
F1	n.a.	n.a.	n.a.	n.a.
F2	n.a.	n.a.	n.a.	n.a.
F3	n.a.	n.a.	n.a.	n.a.
F4	n.a.	n.a.	n.a.	n.a.
F5	n.a.	n.a.	n.a.	n.a.
F6	n.a.	n.a.	n.a.	n.a.
F7	n.d.	47	n.d.	47
F8	n.a.	n.a.	275	n.d.

n.a. = no activity; n.d. = not determined

Neutral formulations **F1**-**F6** did not display any antimicrobial effect against both bacteria strains and consequently it was not possible to identify MIC and MBC values (**Table 5**), despite in our

experimental conditions the highest testable amount of HOTyrOL, embedded within the lipid bilayers, was tested.

Afterwards, the antimicrobial activity of cationic formulations **F7**-**F8** (**Table 5**), containing different molar ratio of the cationic lipid LIPCAT and HOTyrOL, was evaluated to highlight if the absence of activity showed by formulations **F1**-**F6** was due to the lack of electrostatic interaction between neutral liposomes and bacteria strains investigated. In this respect, as already mentioned above, in the literature is reported that DPPC/LIPCAT liposomes are particularly able to interact with *S. aureus* bacteria strain.[17]

Based on the results reported in **Table 5**, an antimicrobial activity was observed for both cationic formulations **F7** and **F8**, but some important considerations must be made.

Even though HOTyrOL in liposomes **F7** proved to be active against *S. aureus* wild type and MRSA (MBC value = 47 μM against both bacteria strains), the activity evidenced was due to the high concentration of LIPCAT present in liposomes **F7** corresponding to 20 μM. In fact, the same antimicrobial activity was observed for liposomes of formulation **F9**, which were formulated without HOTyrOL but with the same amount of LIPCAT present in formulation **F7** (see **Table 2**), implying how actually the effect observed was related to the presence of LIPCAT and not to HOTyrOL.

Instead, liposomes of formulation **F10**, lacking in HOTyrOL and formulated with a molar ratio of LIPCAT halved compared to that of formulation **F9** (see **Table 2**), did not highlight any antimicrobial effect on both bacteria strains. Consequently, the antimicrobial activity observed for cationic liposomes of formulation **F8**, containing the same amount of LIPCAT present in formulation **F10**, should be attributed exclusively to the presence of HOTyrOL.

In particular, liposomes of formulation **F8** experienced an inhibitory effect only on the growth of MRSA strain with a MIC value of 275 μM, while any bactericidal effect was observed on MRSA and any kind of activity was not even evidenced on *S. aureus* wild type.

However, the inhibitory effect observed on MRSA by liposomes of formulation **F8** was not completely reproducible, because half of the antimicrobial tests assessed showed no effect on the growth of MRSA. These results are probably due to the instability of liposomes of formulation **F8,** which, as previously discussed, are not completely stable over time. Therefore, the inhibitory effect observed in some cases on MRSA might be related to the activity of HOTyrOL in free form, released from the vesicles after aggregation of liposomes.

Thereby, the results obtained by investigating the *in vitro* antimicrobial activity of HOTyrOL suggest how the molecular structure of HOTyrOL can influence its biological activity depending on the form in which it is administrated. The HOTyrOL hydrophobic tail provided by the oleic acid makes HOTyrOL more active than HOTyr, thanks to its improved lipophilic features which probably enhance its passage through bacterial membranes. Furthermore, HOTyrOL hydrophobic tail makes it an excellent component for producing stable liposomes. Unfortunately, most of the HOTyrOL based liposomes produced are so stable that HOTyrOL is not released, thus suppressing its antibacterial action and indirectly proving that HOTyrOL internalization in bacteria cell is necessary to exert its antimicrobial effect.

6.3. Conclusions

HOTyrOL showed excellent antimicrobial activity against two strains of *Staphylococcus aureus*, ATCC 25923 (wild type strain) and ATCC 33591 (methicillin-resistant strain, MRSA), which resulted higher than that of HOTyr, thanks to its highest lipophilicity.

However, the same antimicrobial activity was not observed when HOTyrOL was loaded in liposomes formulated with natural phospholipids, such as DOPC, DPPC and DMPC, in presence or absence of cholesterol or a synthetic cationic amphiphile.

Although we did not collect any satisfying results regarding the antimicrobial activity of the liposomal formulation investigated against the bacteria strains involved in our study, the results collected have highlighted great stability for the neutral formulation **F1**-**F6**, opening to their possible use as antioxidant additives. In fact, HOTyrOL based liposomes expose catechol residues on their external surface, which possess powerful antioxidant properties.

6.4. Experimental Materials and methods

6.4.1. Materials

HOTyrOL has been kindly provided by the Professor Roberta Bernini of the Department of Agriculture and Forests Sciences at the University of Tuscia (Viterbo, Italy), which has been synthesized according to the procedure reported in the literature.[20]

Natural phospholipids 1,2-dioleoyl-*sn*-glycero-3-phosphocholine (C18:1, DOPC), 1,2-dipalmitoyl-*sn*-glycero-3-phosphocholine (C16:0, DPPC) and 1,2-dimyristoyl-*sn*-glycero-3-phosphocholine (C14:0, DMPC) were purchased from Avanti Polar Lipids (Alabaster, AL, USA).

The cationic amphiphile allyl-hexadecyl-dimethyl-ammonium iodide (LIPCAT) has been previously synthetized in the laboratory where this thesis was carried out according to the procedure reported in the literature.[21]

Cholesterol (Chol, purity 99%), 4-Methylbenzophenone, phosphate-buffered saline tablet (PBS; 0.01 M phosphate buffer, 0.0027 M KCl, 0.137 M NaCl, pH 7.4, at 25 °C, prepared by dissolving 1 tablet in 200 mL of deionized water), cellulose dialysis membrane (D9527-100FT, molecular weight cut off= 14 kDa), chloroform ($CHCl_3$), water (H_2O) and chloroform-d ($CDCl_3$)were purchased from Sigma-Aldrich.

DMSO was purchased from Romil (pure chemistry).

All the materials used for the antimicrobial assays were purchased from Fisher Scientific (Milan, Italy).

6.4.2. Characterization of the amphiphile HOTyrOL

6.4.2.1. Determination of the critical micelle concentration (*cmc*)

The *cmc* was determined using a Malvern Nano-Zetasizer equipped with a 4 mW He-Ne laser operating at a wavelength of 632.8 nm.[13] The scattered light was detected at an angle of 173°, an optical arrangement that maximizes the detection of scattered light while maintaining signal quality. This provides the exceptional sensitivity that is required for measuring the size of entities such as nanoparticles and polymer micelles, at low concentrations.

Different solutions ranging from $2x10^{-3}$ µM to 5 µM were prepared by dilution of an aqueous solution of HOTyrOL 1 mM. Measurements were carried out in a polystyrene cell at 25°C in triplicates.

6.4.2.2. Molecular Dynamics Simulation

The initial configuration of the simulated system was built by placing 50 molecules of HOTyrOL with a random orientation and 2823 water molecules in a cubic box of 4.92×4.92×4.92 nm^3.

The molecular dynamics simulations were performed using GROMACS package (version 2020.5)[22] with the CHARMM36[23] to describe the bonding and non-bonding interactions of the surfactant molecules. Water was modelled with the TIP3P model.[24] Non-bonding interactions were calculated using a cut-off of 1.2 nm. The particle mesh Ewald (PME) method was applied to the long-range electrostatic interactions. The systems were energy minimized and equilibrated at 298 K and 1 bar by using the velocity-rescale thermostat[25] and Parrinello-Rahman barostat.[26]

The system was simulated for 100 ns.

6.4.3. Liposomes preparation

Liposomes were prepared according to the lipid film hydration protocol, coupled with the freeze-thaw procedure and followed by an extrusion process (**Table 6**).

Table 6. Composition of liposomes (10 mM in total lipids) investigated.

Formulation	Composition	Lipids (mM)
F1	DOPC/Chol/HOTyrOL	7.0:2.0:1.0
F2	DOPC/HOTyrOL	8.0:2.0
F3	DPPC/Chol/HOTyrOL	7.0:2.0:1.0
F4	DPPC/HOTyrOL	8.0:2.0
F5	DMPC/Chol/HOTyrOL	7.0:2.0:1.0
F6	DMPC/HOTyrOL	8.0:2.0
F7	DPPC/LIPCAT/HOTyrOL	7.0:2.0:1.0
F8	DPPC/HOTyrOL/LIPCAT	7.0:2.0:1.0
F9	DPPC/LIPCAT	8.0:2.0
F10	DPPC/LIPCAT	9.0:1.0

Briefly, a proper amount of lipid components was dissolved in $CHCl_3$ in a round bottom flask, dried by rotary evaporation (BUCHI Rotavapor R-200) and then under high vacuum for 5h to remove any traces of organic solvents and to obtain a thin lipid film. Then, the film was hydrated with 150 mM phosphate buffer saline solution (PBS) to give a liposomal suspension 10 mM in total lipids. The

aqueous suspension was vortex-mixed to completely detach the lipid film from the flasks and the obtained multilamellar vesicles (MLVs) were freeze-thawed five times, from liquid nitrogen to 50°C. Size reductions of MLVs were carried out by extrusion (10 mL Genizer LLC) of liposomal dispersions, ten times under high pressure through a 100 nm pore size polycarbonate membrane (Whatman Nucleopore) at temperature higher than T_m to obtain small unilamellar vesicles (SUVs).

All liposomes were purified by dialysis against PBS using a buffer volume equal to 25-times the total volume of the sample, under slow magnetic stirring.

6.4.4. Physicochemical characterization of liposomes

6.4.4.1. Size and ζ-potential measurements

Size distributions, polydispersity index (PDI) and ζ-potential were determined by Dynamic and Dielectrophoretic Light Scattering (DLS, DELS) measurements using a Malvern Nano-Zetasizer equipped with a 5 mV He/Ne laser (λ=632.8 nm) and a thermostated cell holder.

Temperature was set at 25°C in all the measurements.

Particle size distribution and PDI were measured in backscatter detection of scattered light at an angle of 173°. The measured autocorrelation function was analyzed by using the cumulant fit. The first cumulant was used to obtain the apparent diffusion coefficients D of the particles, further converted into apparent hydrodynamic diameters, D_h, by using Stokes-Einstein relationship:

$$D_h = \frac{K_b T}{3\pi\eta D} \qquad \textbf{(Eq. 1)}$$

where k_BT is the thermal energy and η is the solvent viscosity.

The ζ-potential of liposome formulations was determined by DELS measurements, applying low voltages to avoid the risk of Joule heating effects. Analysis of the Doppler shift to determine the electrophoretic mobility was done by using phase analysis light scattering (PALS)[28] a method which is especially useful at high ionic strengths, where mobilities are usually low. The mobility μ of the liposomes was converted into ζ-potential using the Smoluchowski relation ζ =μ η/ε, where ε and η are the permittivity and the viscosity of the solution, respectively.

All liposomal suspensions were diluted to 1 mM in total lipids in PBS (150 mM) to assess DLS measurements and in diluted PBS (15 mM) to perform DELS measurements.

6.4.4.2. Assessment of stability

Liposomes stability was evaluated during 28 days of storage at 4°C protected from light sources determining vesicles size and PDI, as previously described, to highlight any aggregation phenomena related to the physical instability of liposomes.

6.4.4.3. Determination of liposome composition by NMR analysis

The concentration of lipid components in **F1**-**F10** formulations was quantified by ^{1}H NMR analysis; NMR spectra were recorded at 27°C on a Bruker AVANCE 600 NMR spectrometer operating at the proton frequency of 600.13 MHz.

Briefly, 1 mL of the liposome solution was freeze dried and the residues was solubilized in 0.9 mL of $CDCl_3$. 100 μL of an internal standard (IS) were added (IS final concentration in the sample 1mM). The solution was then filtered to remove inorganic salts present in PBS buffer. 4-Methylbenzophenone was chosen as IS since it provides well-separated signals without any interference with the signals of the liposome constituents in the NMR spectra. In particular, for quantitative purposes, the multiplet signal, two hydrogens, at 7.730-7.716 ppm of 4-methylacetophenone was selected as reference signal because it did not overlap with the other signals. The signals used for quantification of lipid components in **F1**-**F10** formulations were identified by comparison with reference samples of the constituents alone in $CDCl_3$.

6.4.5. Antimicrobial activity

Determination of *Minimum Inhibitory Concentration* (MIC) and *Minimum Bactericidal Concentration* (MBC)

The *in vitro* antimicrobial activity of HOTyrOL free and as lipid component in liposomes, was determined through the microdilution method[29] by determining the *Minimum Inhibitory Concentration* (MIC) and the *Minimum Bactericidal Concentration* (MBC) against two strains of *Staphylococcus aureus*: ATCC 25923 (wild type strain) and ATCC 33591 (methicillin-resistant strain, MRSA).

In microdilution tests, microorganisms are tested for their ability to produce visible growth in a broth containing different concentration of an antimicrobial agent. Therefore, the lowest concentration of an antimicrobial agent that under defined *in vitro* conditions prevents the appearance of visible growth of microorganism within a defined period is defined as MIC. Instead,

MBC is defined as the lowest concentration of an antimicrobial agent required to kill a bacterium within the same period.

Both bacteria strains were retrieved from frozen stocks and streaked on a fresh Mueller-Hinton (MH) agar plate, then incubated at 37 °C overnight. Afterwards, few CFU of fresh *S. aureus* wild type or MRSA were grown in 10 mL of MH broth medium overnight at 37°C. Then, the inoculum prepared above was diluted in MH broth to give a final organism density of 3-7 x 10^5 CFU/mL, corresponding to an absorbance of 0.0001 at 600 nm. Both diluted cultures were aliquoted in a 96 wells/plate flat bottom and the antimicrobial agent was added, in triplicates, at different concentrations. Then, 96 wells/plates were incubated overnight at 37°C. At the end of the incubation period, plates were checked and all the transparent wells, likely corresponding to the MIC values, were plated on fresh MH agar plate and kept at 37°C overnight. Finally, MH agar plates were observed and those showing bacterial growth were annotated as MIC, instead those plates showing nonbacterial growth were annotated as MBC.

6.5. References

[1] A. Romani, P. Pinelli, F. Ieri, R. Bernini, Sustainability, Innovation, and Green Chemistry in the Production and Valorization of Phenolic Extracts from Olea europaea L, *Sustainability*, **2016**, *8* (10), 1002.
https://doi.org/10.3390/su8101002

[2] M. Robles-Almazan, M. Pulido-Moran, J. Moreno-Fernandez, C. Ramirez-Tortosa, C. Rodriguez-Garcia, J. L. Quiles, M.C. Ramirez-Tortosa, Hydroxytyrosol: Bioavailability, toxicity, and clinical applications, *Food Res Inter*, **2018**, *105*, 654.
https://doi.org/10.1016/j.foodres.2017.11.053.

[3] M. Bertelli, A.K. Kiani, S. Paolacci, E. Manara, D. Kurti, K. Dhuli, V. Bushati, J. Miertus, D. Pangallo, M. Baglivo, T. Beccari, S. Michelini, Hydroxytyrosol: A natural compound with promising pharmacological activities, *J Biotech,* **2020**, *309*, 29.
https://doi.org/10.1016/j.jbiotec.2019.12.016.

[4] R. Capasso, A. Evidente, S. Avolio, F. Solla, A highly convenient synthesis of hydroxytyrosol and its recovery from agricultural waste waters, *J Agric Food Chem*, **1999**, *47* (4), 1745.
https://doi.org/:10.1021/jf9809030.

[5] M. Navarro, F. J. Morales, Effect of hydroxytyrosol and olive leaf extract on 1,2-dicarbonyl compounds, hydroxymethylfurfural and advanced glycation endproducts in a biscuit model, *Food Chem*, **2017**, *217*, 602.
https://doi.org/10.1016/j.foodchem.2016.09.039

[6] G. Corona, D. Vauzour, A. Amini, J. P.E. Spencer, The Impact of Gastrointestinal Modifications, Blood-Brain Barrier Transport, and Intracellular Metabolism on Polyphenol Bioavailability: An Overview, Editor(s): Ronald Ross Watson, Victor R. Preedy, Sherma Zibadi, Polyphenols in Human Health and Disease, Academic Press, **2014**, *44*, 591.
https://doi.org/10.1016/B978-0-12-398456-2.00044-X.

[7] D. Tofani, V. Balducci, T. Gasperi, S. Incerpi, A. Gambacorta, Fatty Acid Hydroxytyrosyl Esters: Structure/Antioxidant Activity Relationship by ABTS and in Cell-Culture DCF Assays, *J Agri Food Chem,* **2010,** *58* (9), 5292.
https://doi.org/10.1021/jf1000716

[8] G. Fernandez-Bolanos, O. Lopez, J. Fernandez-Bolanos, G. Rodriguez-Gutierrez, Hydroxytyrosol and Derivatives: Isolation, Synthesis, and Biological Properties, *Current Organic Chemistry*, **2008**, *12*(6), 442.
https://dx.doi.org/10.2174/138527208784083888
[9] J.G. Fernandez-Bolanos, O. Lopez, M.A. Lopez-Garcia, A. Marset, Biological properties of hydroxytyrosol and its derivatives, In Olive Oil Constituents, Quality, Health Properties and Bioconversions, *InTech*, **2012**, 375.
http://dx.doi.org/10.5772/30743
[10] S. Bulotta, M. Celano, S.M. Lepore, T. Montalcini, A. Pujia, D. Russo, Beneficial effects of the olive oil phenolic components oleuropein and hydroxytyrosol: focus on protection against cardiovascular and metabolic diseases, *J Transl Med*, **2014**, *12*, 219.
https://doi.org/10.1186/s12967-014-0219-9.
[11] A. Procopio, C. Celia, M. Nardi, M. Oliverio, D. Paolino, G. Sindona, Lipophilic hydroxytyrosol esters: fatty acid conjugates for potential topical administration, *J Nat Prod*, **2011**, *74* (11), 2377.
https://doi.org/10.1021/np200405s
[12] M. Ghalandari, M. Naghmachi, M. Oliverio, M. Nardi, H.R.G Shirazi, O. Eilami, Antimicrobial effect of Hydroxytyrosol, Hydroxytyrosol Acetate and Hydroxytyrosol Oleate on Staphylococcus Aureus and Staphylococcus Epidermidis, *ELECTRON J GEN MED*, **2018**, *15* (4), em46. https://doi.org/10.29333/ejgm/85686.
[13] O. Topel, B. Acar Çakır, L. Budama, N. Hoda, Determination of critical micelle concentration of polybutadiene-block-poly(ethyleneoxide) diblock copolymer by fluorescence spectroscopy and dynamic light scattering, *J Molec Liquids*, **2013**, *177*, 40.
https://doi.org/10.1016/j.molliq.2012.10.013
[14] K.S. Birdi, Handbook of Surface and Colloid Chemistry, 3rd edition Press, **2008**. https://doi.org/10.1201/9781420007206
[15] Y. Nakahara, T. Kida, Y. Nakatsuji, M. Akashi, New fluorescence method for the determination of the critical micelle concentration by photosensitive monoazacryptand derivatives, *Langmuir*, **2005**, *21* (15), 6688.
https://doi.org/10.1021/la050206
[16] G. Bozzuto, A. Molinari, Liposomes as nanomedical devices, *Int J Nanomedicine*, **2015**, *10* (1), 975.
https://doi.org/10.2147/IJN.S68861

[17] M. Petaccia, C. Bombelli, F. Paroni Sterbini, M. Papi, L. Giansanti, F. Bugli, M. Sanguinetti, G. Mancini, Liposome-based sensor for the detection of bacteria, *Sensors and Actuators B: Chemical*, **2017**, *248*, 247.
https://doi.org/10.1016/j.snb.2017.03.124
[18] G. Pereira-Caro, B. Sarriá, A. Madrona, J. L. Espartero, M. E. Escuderos, L. Bravo, R. Mateos, Digestive stability of hydroxytyrosol, hydroxytyrosyl acetate and alkyl hydroxytyrosyl ethers, *Int J Food Sci Nutr*, **2012**, *63* (6), 703.
https://doi.org/10.3109/09637486.2011.652943
[19] Z. Bouallagui, M. Bouaziz, S. Lassoued, Hydroxytyrosol Acyl Esters: Biosynthesis and Activities, *Appl Biochem Biotechnol,* **2011***, 163*, 592.
https://doi.org/10.1007/s12010-010-9065-2
[20] R. Bernini, M. S. Gilardini Montani, N. Merendino, A. Romani, F. Velotti, Hydroxytyrosol-Derived Compounds: A Basis for the Creation of New Pharmacological Agents for Cancer Prevention and Therapy, *J Med Chem*, **2015**, *58* (23), 9089.
https://doi.org/10.1021/acs.jmedchem.5b00669
[21] M. Petaccia, D. Gradella Villalva, L. Galantini, C. Bombelli, L. Giansanti, G. Cerichelli, G. Mancini, Evaluation of the effects of hydrophilic probes on membrane permeability and stability, *Colloids and Surfaces A*, **2015**, *468*, 246.
https://doi.org/10.1016/j.colsurfa.2014.12.051
[22] S. Páll, A. Zhmurov, P. Bauer, M. Abraham, M. Lundborg, A. Gray, B. Hess, E. Lindahl, Heterogeneous parallelization and acceleration of molecular dynamics simulations in GROMACS, *J Chem Phys*, **2020**, *153* (13),134110.
https:/doi.org/10.1063/5.0018516.
[23] J.B. Klauda, R.M. Venable, J.A. Freites, J.W. O'Connor, D.J. Tobias, C. Mondragon-Ramirez, I. Vorobyov, A.D.J. MacKerell, R.W. Pastor, Update of the CHARMM all-atom additive force field for lipids: validation on six lipid types, *J Phys Chem B*, **2010**, *114* (23), 7830.
https://doi.org/10.1021/jp101759q.
[24] W. L. Jorgensen, J. Chandrasekhar, J. D. Madura, R. W. Impey, M. L. Klein; Comparison of simple potential functions for simulating liquid water. *J. Chem. Phys*. **1983**, *79* (2), 926. https://doi.org/10.1063/1.445869.

[25] G. Bussi, D. Donadio, M. Parrinello, Canonical sampling through velocity rescaling, *J. Chem. Phys*, **2007**, *126*, 14101.
https://doi.org/10.1063/1.2408420.
[26] M. Parrinello, A. Rahman, Polymorphic transitions in single crystals: A new molecular dynamics method, *J. Appl. Phys*, **1981**, *52* (12), 7182.
https://doi.org/10.1063/1.328693
[27] M.R.I. MacDonald, Liposome Technology, 2nd edition, CRC Press, Bosca Raton Florida, **1992**.
[28] R.J. Hunter, Zeta Potential in Colloid Science Principles and Applications, 1st edition, Elsevier, **1988.**
[29] Determination of minimum inhibitory concentrations (MICs) of antibacterial agents by broth dilution, Clinical Microbiology and Infection, **2003**, *9* (8), 9.
https://doi.org/10.1046/j.1469-0691.2003.00790.x.

7. Concluding remarks

The results presented in this thesis have contributed to improve our knowledge about the multifold aspects of the antimicrobial activity possessed by plant derived polyphenols, focusing on the effect that the encapsulation in liposomes triggers on their antimicrobial activity.

Plants polyphenols involved in our works have shown a notable antimicrobial activity for the treatment of bacterial infections caused by different *Staphylococcus aureus* strains, both as planktonic and biofilm forming bacteria, which can be resistant to antibiotics, able to develop biofilms, and consequently responsible for many infections associated with high mortality rates.

Some of the polyphenols investigated in this thesis were recovered from biomass waste, representing, from the perspective of a circular economy model, an excellent example of converting waste into valuable products with antimicrobial activity.

Interesting results have been obtained by the encapsulation of the polyphenols investigated in liposomes, in particular we observed the enhancement of *trans*-resveratrol anti-biofilm property and the antimicrobial activity improvement of polyphenols extracted from olive leaves.

Among all liposomes developed and functionalized with *ad hoc* amphiphiles able to enhance the interaction with target bacteria cells, cationic galactosylated liposomes have shown excellent affinity for *S. aureus* strains. The establishment of strong interactions between cationic galactosylated liposomes and bacteria is probably accountable of the great results obtained on the improved antimicrobial activity of encapsulated polyphenols under investigation.